Targeted inhibiton of tumor growth and angiogenesis

The printing of this thesis was financially supported by:

J.E. Jurriaanse Stichting, Rotterdam, The Netherlands

Utrecht Institute for Pharmaceutical Sciences, Utrecht, The Netherlands

Pfizer B.V., Capelle aan de IJssel, The Netherlands

Cristal Delivery B.V., Utrecht, The Netherlands

Lipoid GmbH, Ludwigshafen, Germany

Targeted inhibition of tumor growth and angiogenesis
Roy van der Meel
Ph.D. Thesis, with a summary in Dutch
Department of Pharmaceutics, Utrecht Insitute for Pharmaceutical Sciences (UIPS),
Faculty of Science, Utrecht University, The Netherlands
May 2013
ISBN: 978-94-6203-377-1

brandberry

Cover design and layout by Jeroen Dekker, Brandberry.nl

Printed by CPI Wöhrmann Print Service

Targeted inhibition of tumor growth and angiogenesis

Doelgerichte remming van
tumorgroei en angiogenese

(met een samenvatting in het Nederlands)

Proefschrift

ter verkrijging van de graad van doctor aan de Universiteit Utrecht op gezag van de rector magnificus, prof.dr. G.J. van der Zwaan, ingevolge het besluit van het college voor promoties in het openbaar te verdedigen op maandag 17 juni 2013 des middags te 2.30 uur

door

Roy van der Meel

geboren op 24 juni 1984 te Sliedrecht

Promotoren:	Prof.dr. W.E. Hennink Prof.dr. G. Storm
Co-promotoren:	Dr. R.J. Kok Dr. R.M. Schiffelers

" You can't always get what you want, but if you try sometimes,
you just might find, you get what you need."

The Rolling Stones - You Can't Always Get What You Want, 1969

Voor mijn ouders

Table of contents

Chapter 1
General introduction

1. Cancer treatment

Cancer is the leading cause of death in the world responsible for 7.6 million deaths (13% of total) in 2008 [1]. Cancer is a collective term for a variety of complex diseases that are defined by unregulated cell growth. Development of malignant neoplasms is characterized by a series of processes termed "the hallmarks of cancer" [2]. These hallmarks of cancer, enabled by the genomic instability of tumor cells and the inflammation state of the malignant tumor, include continuous growth pathway signaling, reprogrammed energy metabolism, evasion of growth suppression and the immune system, escaping apoptosis, unlimited replication, activation of angiogenesis, invasive behavior and metastasis [2].

Equally complex as the development is the treatment of cancer. Ideally, anti-cancer therapy kills cancer cells without affecting healthy tissues to a large extent. Whether anti-cancer therapy can be effective, mainly relies on the disease state at the time of diagnosis and is mainly based on (combinations of) surgical removal of the tumor, radiotherapy and chemotherapy. Systemically administered chemotherapy acts by prevention of DNA replication or mitosis and has therefore some selectivity towards fast proliferating cells, like tumor cells. However, other fast replicating cells such as cells in the bone marrow, digestive tract and hair follicles are also affected by chemotherapy causing (dose-limiting) side-effects.

Over the years, increased understanding of processes involved in malignant transformation and tumor development has resulted in the identification of relevant molecular targets in cancer. Molecular targeted therapeutics such as monoclonal antibodies (mAb) and kinase inhibitors (KI) are new classes of anti-cancer drugs that more selectively interfere with cancer-related cellular pathways [3-4]. Because of their specificity, molecular targeted anti-cancer therapeutics possess a more favorable balance between efficacy and toxicity, which has resulted in the routine clinical use of mAb and KI for anti-cancer therapy over the last 15 years.

The two main targets of current molecular targeted therapeutics are direct inhibition of tumor survival and proliferation pathways, and interference with tumor angiogenesis. Tumor angiogenesis is the growth of new blood vessels from pre-existing ones and is necessary for tumors to obtain nutrients and oxygen in order to grow beyond 1-2 mm^3. Inhibition of angiogenesis is an attractive strategy for anti-cancer therapy because it is applicable to a broad range of solid tumor types and tumor-induced blood vessels are readily accessible in contrast to the tumor cells themselves [5-6].

The ErbB or HER family of receptor tyrosine kinases is one of the most well studied signaling networks that contribute to tumor development and growth. Specific inhibitors have been developed such as the mAbs cetuximab (anti-epidermal growth factor receptor, EGFR), trastuzumab (anti-HER2), and KI such as erlotinib, gefitinib (anti-EGFR) and lapatinib (anti-EGFR/HER2) while many more are

currently undergoing clinical evaluation [7]. A critical cellular signaling network involved in the promotion of tumor angiogenesis is the family of vascular endothelial growth factor (VEGF) receptors. Angiogenesis inhibitors aimed at inhibition of VEGF-induced signaling include the mAb bevacizumab (anti-VEGF) and the KI sunitinib (multi-targeted including VEGFR-2) [8]. Despite their specificity, favorable efficacy and toxicity profile, many molecular targeted therapeutics could still be improved by shifting their tissue distribution profile [9]. Increasing their concentration at the target site while reducing concentrations in non-target tissues may further augment their applicability.

2. Drug targeting and delivery for cancer therapy

Targeted drug delivery is an approach that employs colloidal drug delivery systems (DDS) for the improvement of pharmacokinetic properties and biodistribution of (therapeutic) molecules. Molecules can either be dissolved, encapsulated or dispersed in DDS, or covalently coupled with degradable or non-degradable linkers [10]. DDS in the submicrometer range loaded with drugs designed to improve therapeutic outcome and to increase safety in patients are nowadays termed nanomedicines. A wide range of DDS have been developed for the generation of nanomedicines including liposomes, conjugates of drug with water-soluble polymer or monoclonal antibodies, polymeric micelles and nanoparticles, dendrimers and albumin nanoparticles [11]. Liposomes are vesicular structures with an aqueous core surrounded by a (phospho)lipid bilayer that were discovered nearly half a century ago [12]. The broad experience and numerous technological advances made in the field of liposome research have resulted in the translation of liposomes from concept to clinically accepted platform with a number of liposomal nanomedicines on the market and many more in the pipeline [13].

In the field of oncology, nanomedicines offer many potential advantages for the delivery of anti-cancer drugs:

- Better pharmacokinetic profile and spatial localization in the body,
- Increased therapeutic index by more selective delivery of therapeutics at the pathological target site (e.g. tumor) and/or by lowering drug-exposure to healthy tissues,
- Flexible engineering of the DDS composition and surface to reduce interactions with proteins in the blood to increase circulation time, attachment of targeting ligands to increase target specificity or to generate stimuli-responsive nanomedicine,
- Potential to deliver multiple therapeutics in one DDS for combination therapy,
- Development of DDS loaded with imaging agents and therapeutics (theranostics) for image-guided drug delivery [14-16].

When developing nanomedicines, important issues regarding the biocompatability and biodegradability of DDS should be taken into consideration. At the same time, altering the pharmacokinetic profile and spatial localization of a drug due to encapsulation in a DDS can also induce unwanted side-effects such as palmar-plantar erythrodysesthesia or hand-foot syndrome.

Regarding the field of nanomedicine, targeting indicates the design of therapeutically active DDS with the intention to preferentially localize in diseased tissue. This is fundamentally distinct from molecular targeted drugs (discussed in the previous section) which are designed to specifically interact with a protein but not for spatial localization and can distribute throughout the body [17].

Targeted drug delivery using nanomedicines is achieved via three strategies. *Passive targeting* or improved delivery refers to the increased accumulation of nanomedicines in tumors compared to administered free anti-cancer drug due to the physicochemical properties of the DDS and the influence of (patho)physiological processes in the circulation and tumor site (Fig. 1). Encapsulation of anti-cancer drugs in DDS can improve their solubility and stability while coating the outer surface of the DDS with hydrophilic polymers such as polyethylene glycol (PEG) provides "stealth"

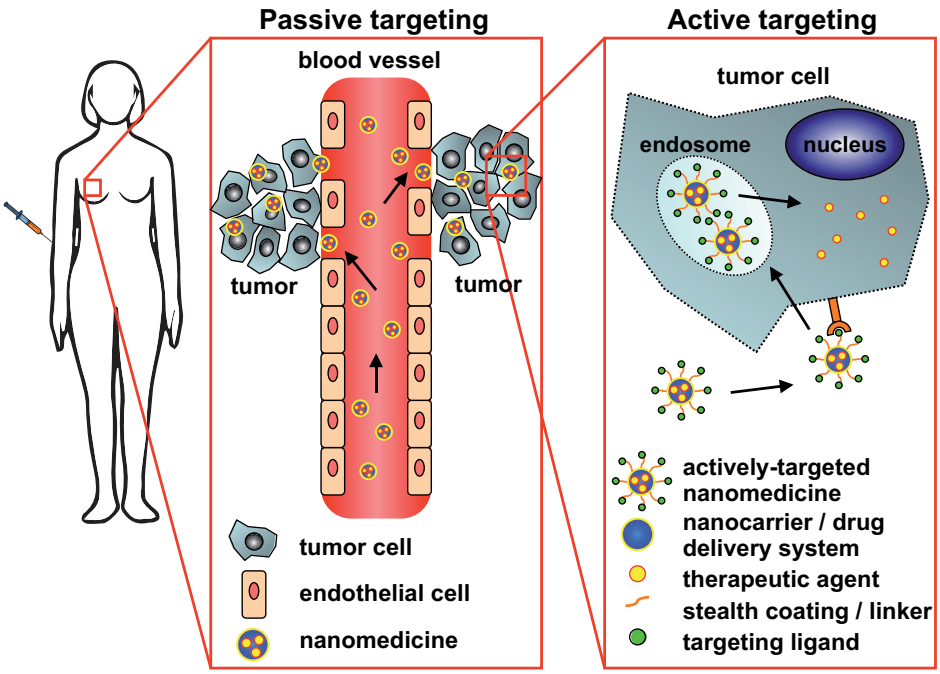

Figure 1. Targeted drug delivery to tumors. *Passive targeting* of nanomedicines is accomplished by virtue of their ability to extravasate out of the leaky tumor vasculature in combination with inefffective lymphatic drainage, also knows as the enhanced permeability and retention (EPR) effect. *Active targeting* is realized by functionalizing nanomedicines with targeting ligands that recognize tumor cell markers to increase cell specificity and uptake.

properties and reduces interactions with blood proteins. This leads to increased circulation times by inhibition of opsonization and subsequent clearance of the DDS by the mononuclear phagocyte system (MPS) [18]. In addition, solid tumors are characterized by poorly developed leaky vasculature and impaired lymphatic drainage allowing for extravasation and detainment of nanomedicines in tumor tissue. This phenomenon is known as the enhanced permeability and retention (EPR) effect and is arguably the most important aspect of improved drug delivery by DDS [19-20]. Secondly, *Active Targeting* (also referred to as ligand-targeting or receptor-mediated targeting) indicates the attachment of targeting moieties to the outer surface of DDS that interact with overexpressed proteins on tumor cells for increased target specificity and therapeutic effect (Fig. 1). It is increasingly accepted that actively-targeted nanomedicines display similar pharmacokinetics and biodistribution profiles as passively-targeted nanomedicines [21-22]. However, the advantages of active targeting such as increased cellular uptake and improved tumor retention times become apparent after the nanomedicine has arrived at the tumor. Additionally, active targeting can be applied for the intracellular delivery of drugs that are unable or inefficient in passing cellular membranes and targeting of drug resistant tumors or the tumor blood supply. Finally, *Triggered Drug Release* is based on nanomedicines that release therapeutics upon internal or external stimuli such as pH, heat or light [23]. The first (passively) targeted nanomedicines were approved in the nineties and a few dozen are nowadays in routine clinical use. It is estimated that approximately 250 nanomedicines are in (pre) clinical development [24-25].

3. Targeted anti-cancer therapy with Nanobodies

Twenty years ago it was discovered that in addition to conventional antibodies, camelids have unique circulating heavy-chain only antibodies (HcAb) [26]. The antigen binding part of HcAbs is a single variable domain (VHH) termed Nanobody (Nb) (Fig. 2). Nbs offer many advantages when compared to monoclonal antibodies (mAb) or derived fragments for therapeutic purposes:

- Nbs are smaller (15 kDa) than mAb (150 kDa), Fab (60 kDa) or scFv (30 kDa) and can therefore recognise uncommon epitopes,
- Better solubility due to their hydrophilicity,
- More stable in harsh conditions,
- Relatively straightforward to produce in bacteria and yeast,
- Similar specificity and affinity towards their target antigen [27-29].

Although the small size of Nbs allows effective tissue penetration, it also results in short serum half-life due to rapid renal clearance.

Several strategies have been employed to increase the circulation time of Nbs in order to improve therapeutic efficacy. For example, the production of trivalent, bispecific

Nbs consisting of two Nbs directed at EGFR and one at mouse serum albumin fused together greatly enhanced circulation times and effectively inhibited tumor growth in a xenograft model [30-31]. Another method includes the development of a multivalent system by conjugation of multiple Nbs to a liposome [32]. Indeed, modification of DDS with Nbs that serve as targeting ligands is an excellent manner to improve the delivery of anti-cancer drugs [33]. Additionally, due to the intrinsic therapeutic activity of Nbs, coupling of Nbs to DDS loaded with drugs is a promising approach for anticancer combination therapy [34-35].
Over the last few years, an increasing number of scientific publications has reported

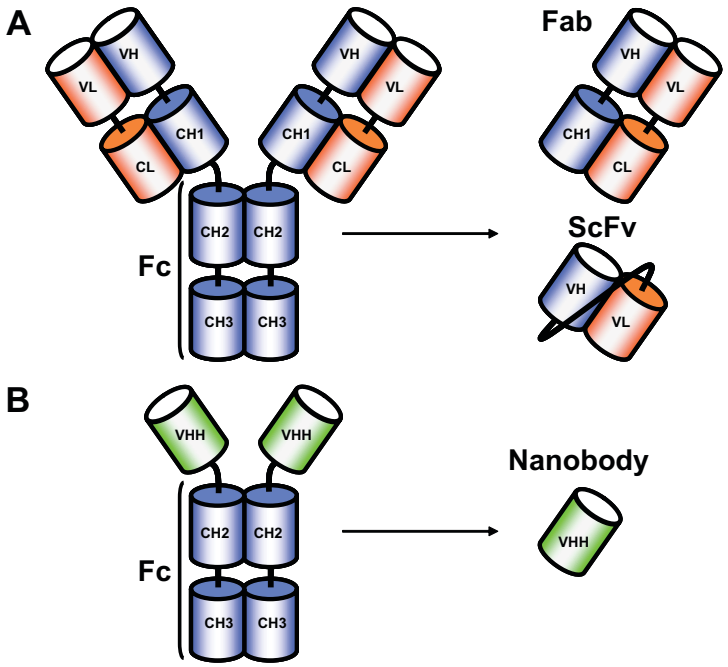

Figure 2. Schematic representation of a conventional (**A**), a camelid heavy chain only antibody (**B**) and their respective antigen-binding fragments. The antigen-binding site of the antibodies or fragments is indicated by white surfaces. Fragment, crystallizable (Fc) region, variable domain light chain (VL), constant domain light chain (CL), variable domain heavy chain (VH), constant domain heavy chain (CH), variable domain of a heavy chain only antibody (VHH or Nanobody).

on the isolation of Nbs directed at targets that are involved in a broad range of diseases. Several Nbs are currently undergoing clinical evaluation for treatment of thrombosis, rheumatoid arthritis, infections and bone metastases [36-37]. The combination of intrinsic therapeutic activity, antigen binding specificity and affinity, relative ease of manipulation, handling and production make Nbs attractive molecules for employment as targeting moieties in actively-targeted nanomedicine

approaches.

4. RNA interference

RNA interference (RNAi) is a conserved mechanism in eukaryotes in which small non-coding RNAs regulate gene expression in cells. Gene regulation by RNAi is vital for cell division, cell differentiation, genome maintenance and protection [38]. RNAi was discovered 15 years ago after the observation that introduction of double stranded RNA induced silencing of gene expression in worms, which was awarded with a Nobel Prize [39]. Gene expression by RNAi and related mechanisms is regulated by small regulating RNAs such as short interfering RNAs (siRNA) [38]. Silencing of genes by siRNA (Fig. 3) is initiated when long double stranded RNA or short hairpin RNA is introduced in the cytoplasm. It is then cleaved by the enzyme DICER into siRNA. Alternatively, synthetic siRNA can be introduced in the cell. One strand of the siRNA (guide strand) is loaded onto an Argonaute

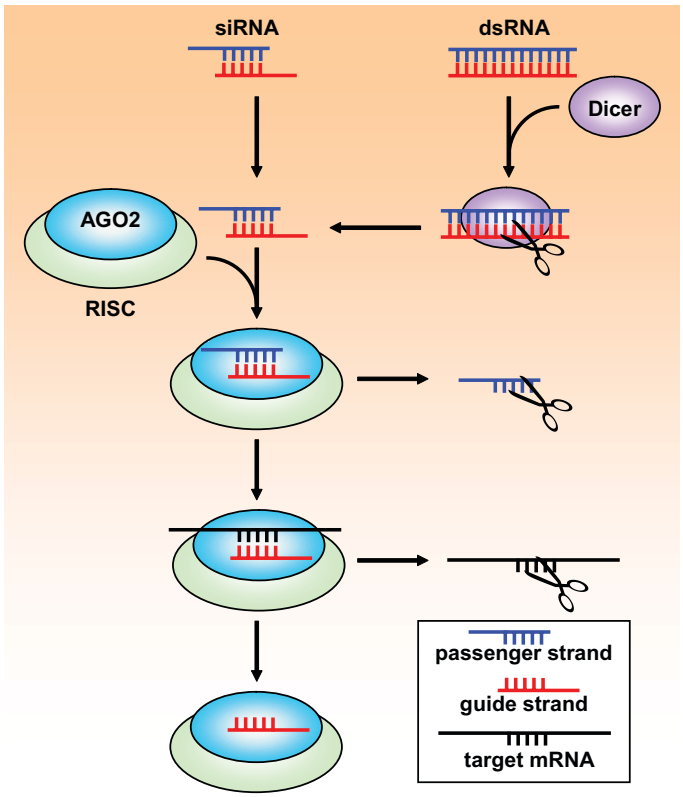

Figure 3. The RNA interference mechanism. Introduction of long double-stranded RNA (dsRNA) or short-interfering RNA (siRNA) in the cytoplasm can eventually silence genes by degradation of target mRNA complementary to the siRNA guide strand (see main text for explanantion).

protein (AGO2) in the RNA-induced silencing complex (RISC). The non-guide strand (passenger strand) is cleaved by Argonaute and discarded. The activated RISC uses the guide strand to scan for complementary messenger RNA (mRNA) which is cleaved upon binding to the complex. The cleaved mRNA is released and the RISC-siRNA complex can be recycled to degrade additional target mRNA [38].
RNAi has become a widely employed valuable research tool as it can be used to specifically and efficiently silence genes of interest, and it can be utilized for high-throughput screening. In theory, small regulatory RNAs can be designed to inhibit the expression of virtually any gene. In combination with the relatively facile production, the utilization of the RNAi mechanism by synthesized small RNAs has an incredible potential therapeutic range and offers the possibility of personalized medicine. However, so far clinical translation of small RNA therapeutics is hampered by the physicochemical properties of the small RNA molecules. Small RNAs can not pass cellular membranes by spontaneous diffusion due to their size and negative charge. In addition, these molecules exhibit short circulation times because of rapid renal clearance and degradation by nucleases. Therefore, much effort has been made to design DDS that protect small therapeutic RNAs against enzymatic cleavage and that are suitable for their cytosolic delivery into target cells [40]. Recently, the therapeutic potential of RNAi in humans was reported for the first time in melanoma patients. Intermediate results from a phase I study demonstrated that treatment with actively-targeted polymeric nanoparticles loaded with siRNA resulted in reduced target mRNA and protein levels in tumor biopsies [41].

5. Aims and outline

This thesis focuses on two main strategies for the development of an effective and targeted anti-cancer treatment. The first strategy describes the development of an actively-targeted nanomedicine that inhibits the proliferation of tumor cells by blocking growth factor signaling cascades. The second strategy consists of an RNAi-mediated approach for the inhibition of tumor angiogenesis. **Chapter 2** provides a concise overview of the current status of actively-targeted nanomedicines that have progressed into clinical trials. The different nanomedicines are described and (pre)clinical data is discussed to evaluate the evidence for added benefits of conjugating targeting ligands to these systems. A scoring table was prepared that summarizes the main research outcomes and characteristics of each evaluated nanomedicine, and the chapter is concluded with a discussion and future prospects of actively-targeted nanomedicines in clinical settings. The development of a tumor-targeted dual-active nanomedicine is described in **Chapter 3**. Anti-EGFR Nb-liposomes were loaded with the anti-IGF-1R kinase inhibitor AG538 for simultaneous inhibition of two signaling pathways involved in tumor cell proliferation. These loaded

Nb-liposomes or Nanobullets were evaluated with regards to their interactions with EGFR-positive tumor cells. In addition, their ability to block the activation of targeted cellular pathways and resulting inhibition of tumor cell proliferation were studied. In **Chapter 4**, the anti-tumor efficacy of the Nanobullets was further explored. Nanobullet-induced inhibition of key proliferation and survival pathway activation and resulting effects on cell proliferation were evaluated in a panel of tumor cell lines. In addition, anti-tumor effects were assessed in two human tumor xenograft models in mice. The Rho GTPase signaling network as a target for anti-cancer therapy is outlined in **Chapter 5**. The role of Rho GTPases in cellular processes that contribute to tumor angiogenesis and invasion is discussed. Moreover, therapeutic strategies to interfere with Rho GTPase signaling are described. **Chapter 6** investigates the function of the Rho GTPase Rac1 in angiogenesis using RNAi. The effects on VEGF-induced angiogenesis of Rac1 knockdown in endothelial cells were assessed by functional assays *in vitro*. The feasibility of siRNA-mediated knockdown of Rac1 to inhibit angiogenesis *in vivo* was explored by a functional assay and a tumor model in mice. **Chapter 7** summarizes this thesis and discusses the described findings and conclusions.

References

1. Ferlay, J., Shin, H.R., Bray, F., Forman, D., Mathers, C., Parkin, D.M., GLOBOCAN 2008 v2.0, Cancer Incidence and Mortality Worldwide: IARC CancerBase No. 10, http://globocan.iarc.fr, Retrieved 04-02-2013.
2. Hanahan, D., Weinberg, R.A., Hallmarks of cancer: the next generation, Cell, 144 (2011) 646-674.
3. Scott, A.M., Wolchok, J.D., Old, L.J., Antibody therapy of cancer, Nat Rev Cancer, 12 (2012) 278-287.
4. Zhang, J., Yang, P.L., Gray, N.S., Targeting cancer with small molecule kinase inhibitors, Nat Rev Cancer, 9 (2009) 28-39.
5. Weis, S.M., Cheresh, D.A., Tumor angiogenesis: molecular pathways and therapeutic targets, Nat Med, 17 (2011) 1359-1370.
6. Carmeliet, P., Jain, R.K., Molecular mechanisms and clinical applications of angiogenesis, Nature, 473 (2011) 298-307.
7. Yarden, Y., Pines, G., The ERBB network: at last, cancer therapy meets systems biology, Nat Rev Cancer, 12 (2012) 553-563.
8. Olsson, A.K., Dimberg, A., Kreuger, J., Claesson-Welsh, L., VEGF receptor signalling - in control of vascular function, Nat Rev Mol Cell Biol, 7 (2006) 359-371.
9. Altintas, I., Schiffelers, R.M., Kok, R.J., Targeted Delivery of Kinase Inhibitors: A Nanomedicine Approach for Improved Selectivity in Cancer, Curr Signal Transd T, 6 (2011) 267-278.
10. Petros, R.A., DeSimone, J.M., Strategies in the design of nanoparticles for therapeutic applications, Nat Rev Drug Discov, 9 (2010) 615-627.
11. Duncan, R., Gaspar, R., Nanomedicine(s) under the microscope, Mol Pharm, 8 (2011) 2101-2141.
12. Bangham, A.D., Standish, M.M., Watkins, J.C., Diffusion of univalent ions across the lamellae of swollen phospholipids, J Mol Biol, 13 (1965) 238-252.
13. Allen, T.M., Cullis, P.R., Liposomal drug delivery systems: From concept to clinical

applications, Adv Drug Deliv Rev, 65 (2013) 36-48.
14. Davis, M.E., Chen, Z.G., Shin, D.M., Nanoparticle therapeutics: an emerging treatment modality for cancer, Nat Rev Drug Discov, 7 (2008) 771-782.
15. Peer, D., Karp, J.M., Hong, S., Farokhzad, O.C., Margalit, R., Langer, R., Nanocarriers as an emerging platform for cancer therapy, Nat Nanotechnol, 2 (2007) 751-760.
16. Jain, R.K., Stylianopoulos, T., Delivering nanomedicine to solid tumors, Nat Rev Clin Oncol, 7 (2010) 653-664.
17. Kamaly, N., Xiao, Z., Valencia, P.M., Radovic-Moreno, A.F., Farokhzad, O.C., Targeted polymeric therapeutic nanoparticles: design, development and clinical translation, Chem Soc Rev, 41 (2012) 2971-3010.
18. Knop, K., Hoogenboom, R., Fischer, D., Schubert, U.S., Poly(ethylene glycol) in drug delivery: pros and cons as well as potential alternatives, Angew Chem Int Ed Engl, 49 (2010) 6288-6308.
19. Matsumura, Y., Maeda, H., A new concept for macromolecular therapeutics in cancer chemotherapy: mechanism of tumoritropic accumulation of proteins and the antitumor agent smancs, Cancer Res, 46 (1986) 6387-6392.
20. Fang, J., Nakamura, H., Maeda, H., The EPR effect: Unique features of tumor blood vessels for drug delivery, factors involved, and limitations and augmentation of the effect, Adv Drug Deliv Rev, 63 (2011) 136-151.
21. Lammers, T., Kiessling, F., Hennink, W.E., Storm, G., Drug targeting to tumors: principles, pitfalls and (pre-) clinical progress, J Control Release, 161 (2012) 175-187.
22. Bae, Y.H., Park, K., Targeted drug delivery to tumors: myths, reality and possibility, J Control Release, 153 (2011) 198-205.
23. Ganta, S., Devalapally, H., Shahiwala, A., Amiji, M., A review of stimuli-responsive nanocarriers for drug and gene delivery, J Control Release, 126 (2008) 187-204.
24. Svenson, S., Clinical translation of nanomedicines, Current Opinion in Solid State and Materials Science.
25. Etheridge, M.L., Campbell, S.A., Erdman, A.G., Haynes, C.L., Wolf, S.M., McCullough, J., The big picture on nanomedicine: the state of investigational and approved nanomedicine products, Nanomedicine, 9 (2013) 1-14.
26. Hamers-Casterman, C., Atarhouch, T., Muyldermans, S., Robinson, G., Hamers, C., Songa, E.B., Bendahman, N., Hamers, R., Naturally occurring antibodies devoid of light chains, Nature, 363 (1993) 446-448.
27. Altintas, I., Kok, R.J., Schiffelers, R.M., Targeting epidermal growth factor receptor in tumors: from conventional monoclonal antibodies via heavy chain-only antibodies to nanobodies, Eur J Pharm Sci, 45 (2012) 399-407.
28. Roovers, R.C., van Dongen, G.A., van Bergen en Henegouwen, P.M., Nanobodies in therapeutic applications, Curr Opin Mol Ther, 9 (2007) 327-335.
29. Muyldermans, S., Baral, T.N., Retamozzo, V.C., De Baetselier, P., De Genst, E., Kinne, J., Leonhardt, H., Magez, S., Nguyen, V.K., Revets, H., Rothbauer, U., Stijlemans, B., Tillib, S., Wernery, U., Wyns, L., Hassanzadeh-Ghassabeh, G., Saerens, D., Camelid immunoglobulins and nanobody technology, Vet Immunol Immunopathol, 128 (2009) 178-183.
30. Tijink, B.M., Laeremans, T., Budde, M., Stigter-van Walsum, M., Dreier, T., de Haard, H.J., Leemans, C.R., van Dongen, G.A., Improved tumor targeting of anti-epidermal growth factor receptor Nanobodies through albumin binding: taking advantage of modular Nanobody technology, Mol Cancer Ther, 7 (2008) 2288-2297.
31. Roovers, R.C., Laeremans, T., Huang, L., De Taeye, S., Verkleij, A.J., Revets, H., de Haard, H.J., van Bergen en Henegouwen, P.M., Efficient inhibition of EGFR signaling and of tumour growth by antagonistic anti-EFGR Nanobodies, Cancer Immunol Immunother, 56 (2007) 303-317.
32. Oliveira, S., Schiffelers, R.M., van der Veeken, J., van der Meel, R., Vongpromek, R., van Bergen En Henegouwen, P.M., Storm, G., Roovers, R.C., Downregulation of EGFR by a

novel multivalent nanobody-liposome platform, J Control Release, 145 (2010) 165-175.
33. Altintas, I., Heukers, R., van der Meel, R., Lacombe, M., Amidi, M., van Bergen En Henegouwen, P.M., Hennink, W.E., Schiffelers, R.M., Kok, R.J., Nanobody-albumin nanoparticles (NANAPs) for the delivery of a multikinase inhibitor 17864 to EGFR overexpressing tumor cells, J Control Release, 165 (2013) 110-118.
34. van der Meel, R., Oliveira, S., Altintas, I., Haselberg, R., van der Veeken, J., Roovers, R.C., van Bergen en Henegouwen, P.M., Storm, G., Hennink, W.E., Schiffelers, R.M., Kok, R.J., Tumor-targeted Nanobullets: Anti-EGFR nanobody-liposomes loaded with anti-IGF-1R kinase inhibitor for cancer treatment, J Control Release, 159 (2012) 281-289.
35. Talelli, M., Oliveira, S., Rijcken, C.J., Pieters, E.H., Etrych, T., Ulbrich, K., van Nostrum, R.C., Storm, G., Hennink, W.E., Lammers, T., Intrinsically active nanobody-modified polymeric micelles for tumor-targeted combination therapy, Biomaterials, 34 (2013) 1255-1260.
36. Bartunek, J., Barbato, E., Heyndrickx, G., Vanderheyden, M., Wijns, W., Holz, J.B., Novel Antiplatelet Agents: ALX-0081, a Nanobody Directed towards von Willebrand Factor, J Cardiovasc Transl Res, (2013).
37. Ablynx N.V., Ablynx's product portfolio, http://www.ablynx.com/en/research-development/pipeline/, Retrieved 25-02-2013.
38. Jinek, M., Doudna, J.A., A three-dimensional view of the molecular machinery of RNA interference, Nature, 457 (2009) 405-412.
39. Fire, A., Xu, S., Montgomery, M.K., Kostas, S.A., Driver, S.E., Mello, C.C., Potent and specific genetic interference by double-stranded RNA in Caenorhabditis elegans, Nature, 391 (1998) 806-811.
40. Whitehead, K.A., Langer, R., Anderson, D.G., Knocking down barriers: advances in siRNA delivery, Nat Rev Drug Discov, 8 (2009) 129-138.
41. Davis, M.E., Zuckerman, J.E., Choi, C.H., Seligson, D., Tolcher, A., Alabi, C.A., Yen, Y., Heidel, J.D., Ribas, A., Evidence of RNAi in humans from systemically administered siRNA via targeted nanoparticles, Nature, 464 (2010) 1067-1070.

Chapter 2
Actively-targeted nanomedicines in the clinic: current status

Roy van der Meel[a*], Laurens J.C. Vehmeijer[a*], Robbert J. Kok[a], Gert Storm[a,b], Ethlinn V.B. van Gaal[a,c]

[a] Department of Pharmaceutics, Utrecht Institute for Pharmaceutical Sciences (UIPS), Faculty of Science, Utrecht University, Universiteitsweg 99, 3584 CG Utrecht, The Netherlands
[b] Department of Targeted Therapeutics, MIRA Institute for Biomedical Technology and Technical Medicine, University of Twente, Enschede, The Netherlands
[c] Cristal Delivery B.V., Padualaan 8, 3584 CH Utrecht, The Netherlands

[*] These authors contributed equally to this work

Submitted for publication

Abstract

Since the introduction of the first nanomedicine on the market about 20 years ago, a number of nanomedicines have become part of treatment regimens in the clinic. These nanomedicines are all considered to be passively-targeted as they rely solely on their physicochemical properties and the (patho)physiological processes in the body for their biodistribution and targeting capability. At the same time, many preclinical studies have reported on nanomedicines exposing targeting ligands, also known as actively-targeted nanomedicines, yet none of these have been approved at this moment. In the present review, we provide a concise overview of 12 actively-targeted particulate nanomedicines that have progressed into clinical trials. The potential of each nanomedicine is discussed based on available (pre)clinical data. Main conclusions of these analyses are that (a) actively-targeted nanomedicines have proven to be safe and efficacious in pre clinical models; (b) the vast majority of actively-targeted nanomedicines is generated for the treatment of cancer; (c) contribution of targeting ligands to the nanomedicine efficacy is not unambiguously proven and (d) targeting ligands often do not increase localization of the nanomedicine within the target tissue, but rather provide benefits in terms of target cell internalization and target tissue retention. Increased understanding of the *in vivo* fate and interactions of the targeted nanomedicines with proteins and cells in the human body is mandatory to rationally advance the clinical translation of actively-targeted nanomedicines. Future perspectives for active-targeting approaches include the delivery of drugs that are unable or inefficient in passing cellular membranes, treatment of drug resistant tumors, targeting of the tumor blood supply and the generation of targeted vaccines.

Graphical abstract

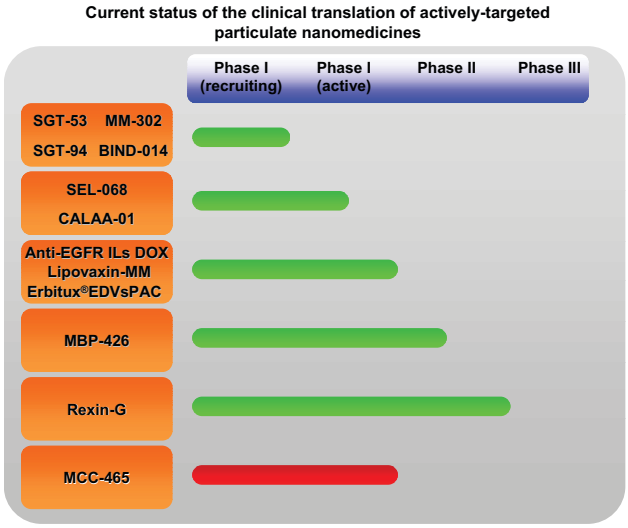

1. Introduction

Nanomedicine is the science and application of nanotechnology for diagnosis, monitoring, prevention, treatment and understanding of disease to ultimately gain clinical benefit [1]. The focus of the current review is on targeted nanomedicines developed to generate therapeutics that are more effective and/or less harmful to patients compared to conventional drugs. Interdisciplinary pioneering research over the last few decades that focused on colloidal systems, polymer chemistry and antibody technology, has led to the introduction of the term "nanomedicine"[2], and has facilitated the rapid evolvement of the drug targeting and delivery field and subsequent clinical translation of targeted nanomedicines [3-5]. The exploitation of particulate nanocarriers (PNC) (Box 1) for targeted drug delivery may have many beneficial features: (1) improve unfavorable pharmacokinetics and tissue distribution of many drugs, (2) increase therapeutic efficacy by achieving higher accumulation of a drug in the target tissue, (3) reduce (dose-limiting) adverse effects by minimizing drug exposure to non-target tissues, (4) feasibility of combination therapy by targeted delivery of multiple therapeutic agents in one nanomedicine, (5) generation of theranostics for image-guided drug delivery by encapsulation of imaging probes and therapeutic agents in one system and (6) ability to manipulate the PNC surface with a range of molecules such as targeting moieties for increased target specificity or polymers to reduce interactions with plasma proteins and blood cells to improve circulation kinetics. Targeted nanomedicines, either marketed or under development, are designed for the treatment of a broad range of indications such as infections [6], cardiovascular diseases [7], central nervous system diseases [8] and inflammatory diseases [9]. The primary emphasis is however on the development of nanomedicines for the treatment of (mostly solid) malignancies [10-12]. All currently marketed nanomedicines can be considered as passively-targeted nanomedicines (PTNM) (Box 1). These PTNM are devoid of targeting ligands and their pharmacokinetic properties and biodistribution rely solely on physicochemical properties of the PNC and subsequent interactions in the circulation and at tissue sites including the site of disease. Actively-targeted nanomedicines (ATNM) (Box 1) are equipped with targeting ligands to increase target specificity. Whereas several PTNM have reached the clinic since the 1990s, only a small number of ATNM have progressed into (early) clinical evaluation and none of them have thus far been approved for clinical use [13]. The aim of this review is to specifically evaluate the evidence for added benefits of conjugating targeting ligands to particulate nanomedicines based on analysis of available (pre)clinical data and the current status of those formulations that have succeeded in reaching clinical evaluation (Table 1). The aim is not to provide a complete (historical) overview and/or perspectives of nanomedicines in general (reviewed elsewhere [3, 5, 13-17]). The ATNM discussed in this review

are defined by three components: *the particulate nanocarrier*, *targeting ligands* and *therapeutic agent*. This review therefore does not discuss other nanomedicines such as PTNM [13], antibody-drug conjugates (ADC) [18-19] and stimuli-responsive nanomedicines [20]. The review consists of an objective presentation of available evidence for target localization, safety and efficacy of the ATNM. Based on these data, a scoring table was prepared which summarizes the main characteristics and research outcomes of the evaluated nanomedicines (Table 2).

Box 1. Definitions

Particulate nanocarrier

Particulate nanocarriers (PNC) are submicrometer size delivery vehicles designed to improve the pharmacokinetic and biodistribution profiles of molecules. These molecules can be adsorbed, entrapped or dissolved in PNC via non-covalent interactions or via degradable or non-degradable covalent linkers [15]. Nanomedicines discussed in this review are defined as PNC developed to deliver therapeutic agents to sites of disease. Over the last few decades, many PNC have been developed for the delivery of therapeutics including liposomes, polymer-drug conjugates, micelles, polymeric nanoparticles, dendrimers and albumin nanoparticles. Currently, a few dozen first generation nanomedicines are routinely used in the clinic and it is estimated that approximately 250 nanomedicines are under (pre)clinical investigation [13, 16].

PEGylation

Polyethylene glycol (PEG) is a hydrophilic polymer that has been widely used for the development of drug-polymer conjugates because it can improve protein solubility, stability and pharmacokinetic parameters [122-123]. In addition, coating the surface of PNC with PEG provides "stealth" properties by inhibiting blood protein adsorption. This effect inhibits subsequent clearance of PNC from the circulation by the mononuclear phagocyte system (MPS). The discovery that PEGylation could greatly enhance the circulation time of NCs such as polymeric nanoparticles [124] and liposomes [125-126] has greatly advanced the clinical translation of nanomedicines. Although the majority of therapeutic PNC clinically approved or under evaluation contains PEG, several issues regarding PEGylation remain such as decrease of drug release and cell uptake ("PEG dilemma") [127], activation of the complement system [128] and accelerated blood clearance of consecutive administered doses [129-130].

EPR effect

The enhanced permeability and retention (EPR) effect was discovered by Maeda and colleagues [131] and describes the phenomenon that macromolecules

accumulate in tumors over time. Tumor vasculature is characterized by poorly developed leaky vasculature containing inter-endothelial gaps which allow for the extravasation of PNC. In addition, tumors often fail to drain extravasated PNC due to an impaired lymphatic system [132]. The EPR effect is exploited by most anti-cancer nanomedicines as it is expected to increase the therapeutic efficacy of chemotherapeutics due to the relative improvement in tumor accumulation of PNC compared to small molecules.

Passive and active targeting

In the field of nanomedicine, targeting refers to the design of therapeutic PNC with the intention of increased accumulation at sites of disease in the body. This is fundamentally different from molecularly targeted drugs that are intended to specifically interact with a certain protein, but have not been designed to localize at specific sites in the body [5]. Passive targeting primarily concerns anti-cancer nanomedicines that accumulate in tumors due to a combination of the physicochemical properties of the PNC and subsequent prolonged circulation half life, extravasation from the blood circulation and the pathophysiology of the tumor contributing to the EPR effect. Active targeting (also described as ligand-targeting or receptor-mediated targeting) involves the attachment of ligands to the surface of PNC that bind to proteins overexpressed on diseased cells. Although in theory this can potentially improve PNC target specificity and improve therapeutic activity, it is believed that in the case of many pathologies, actively-targeted nanomedicines are subjected to the same physiological localization as passively-targeted nanomedicines and therefore have comparable biodistribution and accumulation profiles. However, targeting ligands may offer advantages at in terms of target cell uptake once arrived at the target site. Although it has recently been debated if the terms "passive" and "active" targeting are correctly representing the real-life situation [111, 133], we have decided for the sake of clarity to use the terms "passively-targeted nanomedicines" (PTNM) and "actively-targeted nanomedicines" (ATNM) to distinguish between nanomedicines equipped with or devoid of targeting ligands, respectively, as both terms were originally intended. A third targeting strategy based on stimuli-responsive PNC referred to as triggered drug release is currently receiving much attention but is beyond the scope of this manuscript (for review see [20]).

2. Actively-targeted nanomedicines (ATNM) under clinical evaluation

Up to date, 12 particulate ATNM have progressed into clinical trials (Table 1). These systems include lipid- and polymer-based delivery vehicles, a retroviral vector and bacterially-derived minicells (Figure 1).

Table 1. Overview of actively-targeted nanomedicines undergoing clinical evaluation

Product name	Company	Approx. size (nm)	Payload	Ligand	Target	Clinical indication	Clinical phase
Lipid-based nanomedicines							
MBP-426	Mebiopharm	50-200	Oxaliplatin	Protein	Transferrin receptor	Metastatic gastric, gastro esophageal junction, esophageal adenocarcinoma	Phase Ib/II
SGT-53	SynerGene Therapeutics	90	p53 plasmid DNA	Antibody fragment (scFv)	Transferrin receptor	Solid tumors	Phase I
SGT-94	SynerGene Therapeutics	90	RB94 plasmid DNA	Antibody fragment (scFv)	Transferrin receptor	Solid tumors	Phase I
MM-302	Merrimack Pharmaceuticals	75-110	Doxorubicin	Antibody fragment (scFv)	ErbB2 (HER2)	Breast cancer	Phase I
Lipovaxin-MM	Lipotek		Melanoma antigens and IFNγ	Single domain antibody (dAb) fragment (VH)	DC-SIGN	Melanoma vaccine	Phase I
anti-EGFR ILs-DOX	University Hospital Basel	85	Doxorubicin	Antibody fragment (Fab')	EGFR	Solid tumors	Phase I
MCC-465	Mitsubishi Pharma Corporation	140	Doxorubicin	Antibody fragment (F(ab)'2)	Not characterized	Advanced gastric cancer	Phase I (discontinued)
Polymer-based nanomedicines							
BIND-014	BIND Biosciences	100	Docetaxel	Small molecule	Prostate specific membrane antigen	Solid tumors	Phase II
CALAA-01	Calando Pharmaceuticals	50-70	RRM2 siRNA	Protein	Transferrin receptor	Solid tumors	Phase I
SEL-068	Selecta Biosciences	150-250	Nicotine antigen, T-helper cell peptide, TLR agonist	Small molecule	Antigen presenting cells	Smoking cessation vaccine	Phase I
MiniCell							
Erbitux®EDVsPAC	EnGeneIC	400	Paclitaxel	Antibody	EGFR	Solid tumors	Phase I
Retroviral vector							
Rexin-G	Epeius Biotechnologies	100	Cytocidal dominant negative cyclin-G1 DNA construct	Small molecule	Collagen	Sarcoma, osteosarcoma, pancreatic cancer	Phase II

2.1 Lipid-based nanomedicines

Originally discovered by Bangham and colleagues [21], liposomes were one of the first PNC utilized for the generation of nanomedicines. Liposomes are vesicular structures which consist of an aqueous core surrounded by a lipid bilayer. Doxorubicin (DOX) encapsulated in long-circulating PEGylated liposomes (Doxil®/Caelyx) was the first PTNM to gain clinical approval [22]. The lipid-based nanomedicines discussed in this review feature either liposomes or formulations based on liposomes such as lipoplexes.

2.1.1 MBP-426

MBP-426 (Mebiopharm) is a liposome loaded with oxaliplatin (L-OHP) currently undergoing phase Ib/II trials for treatment of second line gastric, gastroesophageal or esophageal adenocarcinomas in combination with leucovorin and fluorouracil [23]. The liposome is conjugated to transferrin (Tf) for tumor targeting. Platinum binds irreversibly to plasma proteins and erythrocytes and encapsulation of L-OHP in PNC can reduce these interactions thereby improving tumor accumulation and circulation time [24]. Initial studies with empty PEGylated liposomes showed increased Tf-specific cell association and internalization in Tf-overexpressing murine colon carcinoma (Colon 26) cells of Tf-PEG-liposomes compared to non-targeted formulations [25]. Tf-PEG-liposomes loaded with L-OHP (EC_{50} 8 μg/mL L-OHP) were more cytotoxic compared to PEG-liposomes devoid of Tf (EC_{50} 18 μg/mL L-OHP) in Colon 26 cells. The cytotoxicity of L-OHP encapsulated in Tf-PEG liposomes could be inhibited by adding an excess of free Tf, indicating that the cytotoxic effects were mediated by Tf-specific delivery [26]. Studies in mice bearing Colon 26 tumors revealed similar plasma clearance values and biodistribution for actively and passively-targeted and L-OHP-loaded PEG-liposomes indicating that the conjugation of Tf did not influence circulation times or uptake by the mononuclear phagocyte system. Although biodistribution for the passive- and active-targeted formulation was similar, L-OHP concentration in tumors 72 h after injection was ~2.5 times higher in mice treated with L-OHP encapsulated in Tf-PEG-liposomes when compared to PEG-liposomes [26]. Tf-PEG-liposomes loaded with L-OHP significantly suppressed tumor growth compared to L-OHP encapsulated in passively-targeted liposomes [26]. Based on these results, Mebiopharm further developed this formulation for clinical evaluation. The original formulation was optimized and N-glutaryl-phosphatidylethanolamine (NGPE) is used to couple Tf. The use of NGPE causes the liposome to collapse in environments with low pH such as the endosome. In this way, MBP-426 releases L-OHP upon receptor mediated endocytosis and endosomal localization. In mice bearing human pancreas xenograft tumors, additive tumor growth inhibiting effects were observed when MBP-426

treatment was combined with either gemcitabine or erlotinib [27]. Phase I studies in 39 patients with advanced solid or metastatic solid tumors revealed thrombocytopenia as dose limiting toxicity and a dose of 226 mg/m^2 was recommend for further studies [28-29]. Results of phase Ib trials in 9 patients reported 170 mg/m^2 (versus free L-OHP 85 mg/m^2) as recommended dose for phase II studies and potential activity was observed in two L-OHP-resistant patients [23, 30].

2.1.2 SGT-53 and SGT-94

SGT-53 (SynerGene Therapeutics) is a nanomedicine developed for the treatment of solid tumors. The formulation consists of cationic lipids that are complexed with plasmid DNA encoding wild-type p53 tumor suppressor protein. SGT-53 is targeted to the Tf receptor (TfR) on tumor cells via a single-chain antibody fragment (scFv) to achieve intracellular delivery of the plasmid DNA [31]. Initial formulations contained Tf as targeting ligand [32] but the scFv has a smaller size than the Tf molecule and it allows large scale recombinant production and stricter quality control [33]. TfRscFv-lipoplexes were shown to associate specifically with head and neck and prostate tumor cells [31]. Using reporter assays and Western blotting it was demonstrated that transfection of tumor cells by TfRscFv-lipoplexes resulted in functional exogenous p53 expression *in vitro* and *in vivo* [31, 33]. Importantly, in a mouse tumor metastasis model treatment with TfRscFv-p53-lipoplexes combined with docetaxel (DTXL) resulted in a significant increase in survival compared to non-targeted p53-lipolexes combined with DTXL [31]. Although these results were promising, rapid clearance of the TfRscFv-lipoplexes was observed. A sterically stabilized PEGylated lipoplex was designed to optimize circulation times *in vivo* [34]. Although PEGylation of the lipoplexes resulted in reduced transfection efficiency *in vitro*, in a human xenograft prostate tumor model it was demonstrated that the targeted PEGylated lipoplexes induced approximately 7-fold more protein expression in tumors 96 h after treatment than non-PEGylated targeted lipoplexes, indicating the importance of lipoplex stability and circulation time [34]. SGT-53 is now undergoing phase Ib trials to evaluate the safety of combinational therapy with DTXL and to establish a recommended dose for further studies [35].

SGT-94 utilizes the same TfR-targeted platform as SGT-53 but its cargo consists of the gene that encodes the tumor suppressor protein RB94 [36]. RB94 has broad anti-tumor activity and up to date no cytotoxicity with normal human cells or tumor cell resistance to RB94 has been observed [37-39]. *In vitro* cytotoxicity studies revealed that Tf-decorated RB94 lipoplexes increased chemosensitization of human bladder cancer cells 30-fold to gemcitabine and >55-fold to cisplatin compared to passively-targeted formulations. Treatment of normal human endothelial cells did not result in significant sensitization which indicates that Tf-mediated tumor cell specificity

[36]. RB94 protein expression was detected in tumors derived from mice injected with Tf-RB94-lipoplexes and TfRscFv-RB94-lipoplexes but not in mice injected with control formulations. Importantly, no detectable RB94 expression in the liver was observed as determined by Western Blotting (WB), immunohistochemistry and DNA PCR [36]. In efficacy studies with mice bearing human bladder carcinoma xenografts, treatment of mice with TfRscFv-RB94-lipoplexes combined with gemcitabine significantly inhibited tumor growth compared to passively-targeted RB-94-lipoplexes and gemcitabine, and targeted formulations with a control vector combined with gemcitabine [36]. SGT-94 has entered phase I trials to evaluate its safety and maximum tolerated dose and to find evidence of RB94 expression in tumors after systemic administration [40].

2.1.3 MM-302

MM-302 (Merrimack Pharmaceuticals) is a HER2-targeted nanomedicine that consists of PEGylated liposomes loaded with DOX and has progressed into phase I trials [41]. Active tumor targeting is achieved by the attachment of HER2-targeted scFv antibody fragments to the surface of the liposomes [42-45]. Since the first reports on HER2-targeted immunoliposomes (ILs) loaded with DOX emerged [46-47], many parameters of the formulation have been optimized such as liposomal composition, antibody construct and conjugation method [43]. These early studies have described the increase in HER2-positive ($HER2^+$) cell binding and internalization of anti-HER2 liposomes compared to control liposomes. Increased cell association could be reversed by addition of free anti-HER2 antibody fragments confirming HER2-mediated interactions of the ATNM. In addition, a HER2-negative cell line did not show detectable uptake of anti-HER2 liposomes [46-47]. Importantly, biodistribution studies *in vivo* revealed that active targeting by conjugation of anti-HER2 antibody fragments did not increase radiolabeled liposomal tumor accumulation [48]. At the same time, gold-labeled anti-HER2 liposomes localized intracellularly while passively-targeted liposomes primarily distributed to the extracellular tumor stroma. In a HER2-negative xenograft model the intratumoral distribution of targeted and passively-targeted liposomes was similar indicating that both formulations accumulate in the tumor but anti-HER2 ILs associated directly with tumor cells [48]. Pharmacokinetic (PK) studies in rats showed comparable circulation times for HER2-targeted ILs and control formulations indicating that the presence of an antibody fragment on the liposomes did not alter clearance rates or induced accelerated clearance after multiple doses [43, 49]. Anti-tumor efficacy of anti-HER2 ILs-DOX has been extensively evaluated in multiple studies in four different human $HER2^+$ breast cancer xenograft models. Although liposomal formulations varied between studies with regards to PEGylation, antibody

fragment and conjugation method, pooled results of all eight studies demonstrate that treatment with anti-HER2 ILs-DOX significantly inhibited tumor growth when compared to PEGylated liposomal DOX (PLD). In one of the xenograft studies, anti-HER2 ILs-DOX demonstrated cure rates up to 50% [43, 49]. Additionally, anti-HER2 ILs-DOX treatment also showed superior efficacy in a xenograft model when compared to combination treatment with either free DOX or PLD and trastuzumab. In a xenograft model expressing low levels of HER2, treatment with anti-HER2 ILs-DOX and PLD induced only modest anti-tumor effects, confirming anti-HER2 ILs-DOX *in vivo* selectivity and the requirement of a receptor density

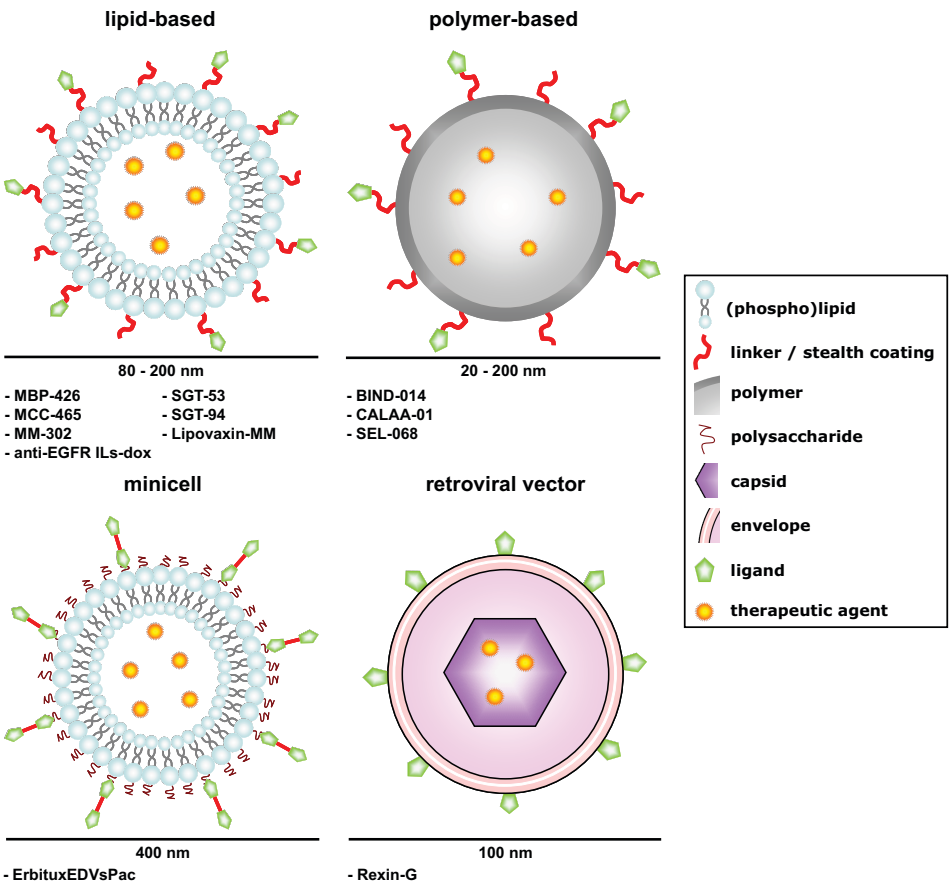

Figure 1. Overview of clinically relevant ATNM. The discussed actively-targeted nanomedicines (ATNM) are defined by three components: the particulate nanocarrier (PNC), targeting ligands and therapeutic agent. Utilized PNC include lipid- and polymer based nanocarriers, bacterially-derived minicells and a retroviral vector. Targeting ligands conjugated to PNC include antibodies or antibody fragments, protein (transferrin) or small molecules. Therapeutically active cargo of the ATNM includes chemotherapeutics, small interfering RNA, plasmid DNA or antigens and adjuvants.

or activity threshold for effective drug delivery [43, 49]. These studies have resulted in an optimized formulation used for clinical evaluation that consists of the anti-HER2 scFv F5 conjugated to PEG-PE micelles which are incorporated into PLD [42-45]. The last few years, updates were presented at conferences on the progress of MM-302 including cardiosafety, efficacy and PK studies in preclinical models [50-52]. Recently, preliminary data of the ongoing phase I trials were presented. So far, 34 patients with $HER2^+$ advanced breast cancer have enrolled of which 12 patients achieved stable disease and two patients have achieved partial response. MM-302 is tolerable in patients up to 50 mg/m^2 and plasma pharmacokinetics are similar to passively-targeted PLD [53].

2.1.4 anti-EGFR ILs-DOX

Generated by the same original developers as MM-302, ILs loaded with DOX that target epidermal growth factor receptor (EGFR) overexpressing tumors via coupling of Fab' fragments of the anti-EGFR mAb cetuximab have also progressed into clinical trials [54]. *In vitro* studies showed superior cell association and internalization of anti-EGFR ILs-DOX compared to passively-targeted control formulations. For example, quantitative studies performed with pH-sensitive-loaded liposomes demonstrated ~30-fold more EGFR-positive cell internalization of anti-EGFR ILs compared to non-targeted PEGylated liposomes. In addition, cytotoxicity studies in EGFR-positive MDA-MB-468 cells showed that anti-EGFR ILs-DOX were 29-fold more effective than PLD [55]. Studies in rats showed similar pharmacokinetics of actively-targeted and passively-targeted liposomal DOX indicating that conjugation of antibody fragments did not alter liposomal stability or circulation time [56]. As observed with MM-302, biodistribution studies in mice showed no differences in tumor accumulation for EGFR-targeted liposomes and passively-targeted formulations. However, cellular uptake of anti-EGFR liposomes loaded with a fluorescent dye was 6-fold higher when compared to passively-targeted liposomes in tumor cells derived from mice [56]. In two EGFR-overexpressing tumor xenograft models, anti-EGFR ILs-DOX significantly inhibited tumor growth when compared to PLD [56]. Interestingly, in a drug resistant tumor xenograft model anti-EGFR ILs-DOX could significantly inhibit tumor growth when compared to PLD, suggesting that anti-EGFR ILs-DOX can overcome multidrug resistance [57]. In a recently finished phase I trial [58], 26 patients with EGFR-overexpressing advanced solid tumors were enrolled and treated with escalating doses of anti-EGFR ILs-DOX. One patient showed complete response, one partial response and ten patients had stable disease lasting 2 – 12 months. A recommended dose of 50 mg DOX per m^2 was recommended for phase II trials [59].

2.1.5 MCC-465

MCC-465 (Mitsubishi Tanabe Pharma) is a DOX-loaded PEGylated liposome targeted to tumor cells via the conjugation of F(ab')2 of the human GAH antibody [60]. Although its target antigen has not been characterized, selective binding of GAH antibody was demonstrated as staining of viable tumor tissues and tissue sections stained positively while no staining was observed on non-cancerous tissues [61-62]. Confocal microscopy studies showed that fluorescently labeled GAH-conjugated ILs loaded with DOX internalized in human stomach cancer cells via GAH-mediated interactions, as the addition of free GAH in combination with GAH-ILs-DOX prevented cell uptake. Passively-targeted control formulations were hardly internalized by the tumor cells [60-61]. In a pulse-chase assay *in vitro*, GAH-ILs-DOX induced significantly stronger dose-dependent cytotoxicity in human gastric tumor cells compared to PLD. No significant cytotoxicity of GAH-ILs-DOX was observed in human endothelial cells. The anti-tumor efficacy of GAH-ILs-DOX in various human xenograft models in mice was significantly higher than non-targeted control PLD [60-63]. No significant anti-tumor efficacy was observed in xenograft studies with GAH-negative cell lines and it was suggested that GAH-ILs-DOX can overcome DOX resistance of tumor cells [60, 62]. Results from a phase I study indicated that MCC-465 was well tolerated and a dose of 32.5 mg/m^2 in an equivalent amount of DOX was recommended for phase II studies. No anti-tumor effects were observed but stable disease was observed in 10 of 18 patients [64]. Recent updates on MCC-465 are not available and it is uncertain whether development is discontinued.

2.1.6 Lipovaxin-MM

Lipovaxin-MM (Lipotek) is a lipid-based vaccine for immunotherapy of malignant melanoma. Lipovaxin-MM does not directly target melanoma cells, but instead its strategy is based on delivering melanoma antigens to dendritic cells (DC) which in turn activate tumor-specific CD8$^+$ cytotoxic T cells (CTL) [65]. The melanoma antigens in Lipovaxin-MM are derived from the membrane fraction of lysed MM200 melanoma cells. MM200 plasma derived membrane vesicles are isolated and subsequently fused with liposomes containing cytokines such as interferon-gamma (IFN-γ) or lipopolysaccharide (LPS) that provide a DC "danger" or maturation signal. The vaccine is targeted to DCs via engraftment of the domain antibody DMS5000 which is highly specific for DC-specific intracellular adhesion molecule 3-grabbing non-integrin (DC-SIGN) [65-66]. In proof of concept studies, cell association of DC-targeted vaccines *in vitro* was 4 to 8-fold higher than non-targeted control formulations. This effect could be reversed by pre-incubation of the cells with free targeting ligand demonstrating specific interactions of the ATNM.

DC-targeting *in vivo* was demonstrated by determining the number fluorescent-positive cells in a draining lymph node after injection with targeted and passively-targeted formulations. DC-targeted vesicles induced 4-fold more fluorescent cells than passively-targeted formulations [67]. In addition, in a B16-OVA melanoma model immunization of mice with targeted vaccines induced strong CTL responses in splenic T cells, induced protective immunity against tumors and could inhibit tumor growth [67]. According to the patent application, Lipovaxin-MM used for studies in non-human primates consists of 4 pre-mix components (MM200 membrane vesicles, lyophilized liposomes, IFN-γ and DMS5000) that are formulated prior to administration [66]. Treatment of macaques with Lipovaxin-MM resulted in production of vaccine-specific antibodies but it is not certain if this effect is caused specifically by the antigens as a passively-targeted control was not included in this study [66]. A phase I study in melanoma patients to determine adverse events, immunogenicity and efficacy of Lipovaxin-MM was recently completed but results have not yet been made available [68].

2.2 Polymer-based nanomedicines

The potential of polymers for drug delivery was demonstrated in the 1970s [69-70]. Polymer-based PNC such as polymeric nanoparticles are produced by self-assembly or cross-linking of polymeric building blocks to obtain nanoparticles with favorable physicochemical characteristics.

2.2.1 BIND-014

BIND-014 (BIND Biosciences) is a polymeric nanoparticle developed for the treatment of solid tumors. BIND-014 is composed of poly(d,l-lactide) (PLA) and PEG block copolymers to form a hydrophobic core for the encapsulation of DTXL, and a hydrophilic surface for prolonged circulation [71]. The ATNM is targeted to prostate-specific membrane antigen (PSMA) expressing cells using the small-molecule S,S-2-[3-[5-amino-1-carboxypentyl]-ureido]-pentanedioic acid (ACUPA) as targeting ligand [71-72]. PSMA is expressed by prostate tumor cells and additionally, by the neovasculature of other types of solid tumors but not on normal vasculature [73]. BIND-014 was developed by a novel strategy in which a library was composed of more than 100 self-assembling nanoparticles to obtain a single ATNM with optimized physicochemical properties [71, 74-75]. Initial *in vitro* studies performed with the PSMA-targeting RNA aptamer A10 [76] as targeting ligand demonstrated a 77-fold increase in cell association of PSMA-targeted formulations compared to passively-targeted formulations. No cell association to PSMA-negative cells was observed for either of the formulations [77]. In mice bearing human PSMA-positive prostate xenograft tumors, targeted poly(lactic-co-glycolic acid)

(PLGA)-based nanoparticles delivered 3.77-fold more chemotherapeutic agent to tumors compared to passively-targeted control nanoparticles after 24 h [78]. PSMA-targeted nanoparticles loaded with DTXL were significantly more cytotoxic *in vitro* compared to control DTXL nanoparticles without targeting ligand. In xenograft studies, ATNM loaded with DTXL significantly inhibited tumor growth and increased survival compared to passively-targeted DTXL nanoparticles [79]. In later pre-clinical studies, optimized BIND-014 treatment caused significant tumor growth inhibition in a mouse xenograft prostate tumor model compared to non-targeted controls. In contrast, no difference in anti-tumor effect was observed in PSMA-negative xenograft models [71]. BIND-014 is currently undergoing a phase I clinical trial to determine the safety in patients with advanced or metastatic cancer [80]. Interim data in 3 patients demonstrated that DTXL plasma levels are two orders of magnitude higher when administered as BIND-014 compared to solvent-based DTXL. Preliminary signs of BIND-014 anti-tumor efficacy were observed in two patients [71]. Phase II studies to evaluate the safety and efficacy of BIND-014 in patients with metastatic castration-resistant prostate cancer or as second-line therapy for patients with lung cancer were recently announced [81-82].

2.2.2 CALAA-01

CALAA-01 (Calando Pharmaceuticals) is a polymeric nanoparticle for siRNA-mediated treatment of solid tumors. This nanomedicine based on the RONDEL™ platform, which consists of four components that are mixed together and self-assemble into nanoparticles prior to administration: a linear cyclodextrin-containing polymer (CDP) backbone, adamantane-conjugated polyethylene glycol (AD-PEG), Tf-conjugated AD-PEG (Tf-PEG-AD) and siRNA [83]. CALAA-01 induces knockdown of the M2 subunit of ribonucleotide reductase (RRM2), which catalyzes the formation of deoxyribonucleotides from ribonucleotides for DNA synthesis [84-85]. Tf-nanoparticles were shown to associate with HeLa cells in a ligand density-dependent manner and cell uptake studies in the presence of free Tf demonstrated TfR-mediated cell internalization [86]. A multimodality imaging approach revealed no differences in tumor accumulation and tissue distribution between ATNM and PTNM siRNA formulations [87]. However, using reporter assays it was shown that Tf-targeted nanoparticles did exhibit enhanced transfection efficiency in tumor bearing mice compared to non-targeted formulations [87]. Increased inhibition of tumor growth in mice by Tf-siRNA-nanoparticles compared to passively-targeted formulations was demonstrated in a mouse model of metastatic Ewing's sarcoma [88]. In addition, in mice bearing head and neck cancer xenografts, CALAA-01 treatment reduced RRM2 mRNA and protein levels resulting in significant inhibition of tumor growth compared to nanoparticles with control siRNA [89]. Multiple systemic

doses of CALAA-01 in non-human primates were well-tolerated and no significant signs of toxicity were observed at siRNA doses up to 8 mg/kg [90]. Phase I trials evaluating CALAA-01 are ongoing [91] and early results in three patients with solid tumors showed dose-dependent intracellular localization in tumor cells but not in the adjacent epidermis. Decreased protein expression of RRM2 in the tumor was observed in at least one patient, suggesting evidence for RNAi in humans [92].

2.2.3 SEL-068

SEL-068 (Selecta Biosciences) is a nicotine vaccine developed for treatment of tobacco dependence [93]. The self-assembling synthetic polymeric nanoparticle [74] contains encapsulated toll-like receptor agonist to reduce the production of inflammatory cytokines, encapsulated universal T-helper cell peptide to evoke T-cell responses and nicotine covalently conjugated to the surface of the nanoparticle as a B-cell antigen [94-95]. Administration of SEL-068 in mice and cynomolgus monkeys induced high titers of anti-nicotine antibodies with high affinity [94-95]. In this way, addictive effects of smoking are counteracted by largely preventing nicotine in the circulation to cross the blood brain barrier and bind to nicotine receptors. Although SEL-068 is currently undergoing phase I clinical trials to evaluate the safety in smokers and non-smokers [96], available and/or accessible data is largely limited to conference abstracts and the website of Selecta Biosciences.

2.3 Minicells

A relatively new NC platform utilizes bacterially derived minicells for drug delivery. Minicells are bacterial cells of approximately 400 nm, devoid of a nucleus and produced by mutants in which genes responsible for cell division have been inactivated [97].

2.3.1 Erbitux®EDVsPAC

Targeted minicells for the treatment of solid tumors are under development by EnGeneIc. A wide range of chemotherapeutic drugs can be incorporated in the minicells, including DOX, paclitaxel (PAC) and cisplatin [98]. Additionally, minicells can be loaded in a similar fashion with siRNA or with plasmid DNA encoding short hairpin RNA (shRNA) [99]. Tumor targeting of minicells is achieved by bispecific antibodies which recognize both the O-polysaccharide component of the lipopolysaccharide present on the minicell surface and a cell surface receptor overexpressed on tumor cells such as EGFR [97]. Cell specific association, uptake and toxicity of EGFR-targeted minicells loaded with DOX ($^{EGFR}minicells_{DOX}$) was demonstrated in EGFR-expressing MDA-MB-468 human breast cancer cells [98]. In several human tumor xenograft models *in vivo* (breast, lung, ovarian, lung, leukemia),

		MBP-462 [25-26]	SGT-53 [31,33-34]	SGT-94 [36]	MM-302 [46-49]	Lipovaxin-MM [67]	Anti-EGFR ILs-DOX [55-56]	MCC-465 [60-62]	BIND-014 [71,77-79]	CALAA-01 [86-87,92,134]	SEL-068	Erbitux®EDVsPAC [98-99]	Rexin-G [104-105, 135]
cellular studies	Cell associaiation[a]	+	+	*	+	+	+		+	+		+	
	Competition[b]	+	+	*	+	+		+	+	+			
	Target specificity[c]		+	+	+		+	+	+			+	
	Cell internalization[d]				+		+	+		+		+	
	Efficacy[e]	+	+	+	+	+	+	+	+	+		+	+
animal studies	Target localization[f]	+	+	*	-		-		+	-		+	
	Target specificity[g]		+	*	+	+		+	+	+		+	
	Cell internalization[d]				+		+						
	Efficacy[h]	+	+	+	+	+	+	+	+	+		+	+
clinical studies	Target localization[i]									+			+
	Target specificity												
	Cell internalization[d]									+			
	Efficacy	++			++		++	++	++	++			++

Table 2. Superior effect of actively-targeted nanomedicines versus passively-targeted nanomedicines in (pre)clinical studies. Scoring was based on studies reported in references between brackets. Positive scores (denoted by a + symbol) were granted if a superior effect mediated by the targeting ligand was observed. Negative scores (denoted by a – symbol) were granted when no superior effect mediated by the targeting ligand was observed. All scores (except clinical scores) were based on studies performed with the actively-targeted nanocarrier (ATNM) and passively-targeted nanocarrier (PTNM) as control. Open squares indicate that no PTNM was used as a control, the study was not performed or no data was accessible or available. Granted scores were based on the actively-targeted platform which may differ from the final clinical formulation. * These studies have not been reported for SGT-94 but have been performed with SGT-53 that exploits the same particulate nanocarrier.

‡ Since no actively-targeted nanomedicines have yet been evaluated in large phase III studies, scoring represents reported signs of efficacy in phase I and II trials. [a] Association to target-expressing cells; [b] Inhibition of cell association to target-expressing cells by addition of free targeting ligand or target substrate; [c] No cell association to cells that do not express target; [d] Target cell internalization of nanomedicine or therapeutic agent; [e] Induction of tumor cell death, inhibition of tumor cell proliferation or immune cell response (vaccines); [f] Nanomedicine accumulation in target tissue; [g] No accumulation or effect of nanomedicine in target-negative model or no accumulation or effect in target tissue of nanomedicine decorated with control targeting ligands ; [h] Inhibition/regression of tumor growth or induction of protective immune response; [i] Accumulation in target tissue.

different minicell formulations including $^{EGFR}minicells_{DOX}$, EGFR-targeted minicells loaded with PAC ($^{EGFR}minicells_{PAC}$) and HER2-targeted minicells loaded with DOX ($^{HER2}minicells_{DOX}$) demonstrated strong anti-tumor activity compared to passively-targeted control formulations [98]. For comparison, 100-fold higher doses of Doxil® (100 μg) were needed to achieve similar anti-tumor effects of $^{EGFR}minicells_{DOX}$ (1 μg) in mice bearing breast cancer xenografts [98]. The anti-cancer effect of DOX-loaded minicells was further demonstrated by tumor regression in two dogs with advanced T cell non-Hodgkin's lymphoma, and safety of minicells was demonstrated by multiple consecutive iv-injections in three healthy pigs [98]. Most interestingly, drug-resistance of colon cancer cells could be reversed with sequential treatment of EGFR-targeted minicells loaded with shRNA specific for the multi-drug resistance P glycoprotein MDR1 ($^{EGFR}minicells_{shMDR1}$) followed by targeted minicells loaded with chemotherapeutics. Furthermore, the sequential combination treatment effectively reversed multidrug resistance in colon, breast and uterine xenograft models *in vivo* [99]. Intermediate results of a phase I safety and tolerability study were recently presented [100]. Multiple doses of intravenously administered $^{EGFR}minicells_{PAC}$ were generally well tolerated in patients with advanced solid tumors and phase II studies are planned [100].

2.4 Retroviral vectors

The unraveling of the retroviral life cycle basic principles led to the introduction of replication-incompetent retroviruses in the 1980s [101]. Non-replicating retroviral vectors are able to efficiently integrate their genetic payload in the DNA of the target cell, making them attractive PNC for gene therapy.

2.4.1 Rexin-G

Rexin-G is murine leukemia virus-based nanomedicine for the treatment of osteosarcoma, soft tissue sarcoma and pancreatic cancer developed by Epeius Biotechnologies. The main issue with retroviral vectors has been the lack of tissue specificity [102]. However, Rexin-G is the first retrovector targeted to tumors and

associated neovasculature via a high-affinity collagen-binding motif derived from von Willebrand factor. Rexin-G elicits anti-tumor effects by interfering with cell cycle control with a mutant cyclin G1 gene [103]. In human tumor xenografts, Rexin-G markedly inhibited tumor growth and increased survival compared to non-targeted controls [104]. Results from early phase I/II clinical trials in the Philippines for the treatment of metastatic pancreatic cancer and other solid tumors showed that Rexin-G was well tolerated, did not induce organ damage and that there were signs of antitumor activity [105-106]. In phase I/II clinical trials in the U.S.A., for the treatment of advanced or metastatic pancreatic cancer, Rexin-G was well tolerated in phase I studies but there was no evidence of an anti-tumor response [107]. In phase II of these clinical trials which involved higher doses if Rexin-G, no dose-limiting toxicity was found. At none of the doses tested, organ-related toxicity, signs of an antibody response, off-target transfection or presence of replication-competent retrovirus were observed. A correlation between Rexin-G dosage and overall survival was established [108]. Similar results were found in phase I/II and phase II trials for the treatment of sarcoma and osteosarcoma [109]. Based on these results Rexin-G gained orphan drug status for treatment of soft tissue sarcoma, osteosarcoma and pancreatic cancer in the U.S.A. [105]. Of note, during clinical trials Rexin-G treatment was associated with improvement of physiological conditions (liver function, ascites, blood chemistry, wound healing) presumably due to the targeting of exposed collagen by Rexin-G [110].

3. Discussion

To date, 12 ATNM based on PNC have progressed into clinical trials. Out of these, 11 are currently under active evaluation while the development of MCC-465 appears to have been discontinued. Limited access to (pre)clinical data for SEL-068 prevents detailed discussion of this product.

With the exception of the anti-nicotine vaccine SEL-068, all of the described ATNM have been developed for the treatment of solid malignant neoplasms. As cancer remains the leading cause of death in the world today, the medical need to design more effective and safer anti-cancer drugs is evident. The anti-tumor effect of PTNM, largely mediated by the EPR effect, may be further enhanced by the addition of targeting ligands to increase target cell specificity and internalization (reviewed elsewhere [10-12]).

The encapsulated *therapeutic agent* in 6 anti-cancer nanomedicines is an established chemotherapeutic compound such as doxorubicin (MM-302, anti-EGFR ILS-DOX, MCC-465), oxaliplatin (MBP-426), docetaxel (BIND-014) or paclitaxel (Erbitux®EDVs$_{PAC}$). These compounds have been previously approved by the FDA

either as free drug or formulated as PTNM, thus lowering the development risk and reducing regulatory issues for the new actively-targeted formulations in development. Four ATNM contain plasmid DNA or siRNA (SGT-53, SGT-94, CALAA-01, Rexin-G). These molecules are unable to pass cell membranes and are dependent on ligand-induced receptor-mediated internalization for therapeutic activity. The two vaccine formulations actively-targeted to antigen-presenting cells (APC) contain antigen and adjuvants to stimulate the immune system to produce cytotoxic T-cells (Lipovaxin-MM) or neutralizing antibodies (SEL-068).

Of the 12 discussed ATNM, the exploited *particulate nanocarrier* (PNC) of 7 formulations are lipid-based, 3 are based on polymeric nanoparticles, 1 on a retroviral vector and 1 on a bacterial vector. The application of established lipid-based PNC is likely due to the clinical experience gained with these systems as PTNM, and to reduce development risks and regulatory issues associated with novel nanocarrier systems. For example, MM-302 and anti-EGFR ILs-DOX consist of a similar formulation as Doxil® but targeting ligands are introduced by post-insertion of micelles bearing targeting ligands for active targeting [44-45, 59]. The rapid development of ATNM based on polymers is noteworthy. Such systems are characterized by the production of self-assembling polymeric nanoparticles and high-throughput strategies giving advantages in terms of large-scale manufacturing and batch-to-batch variation. CALAA-01 is formulated prior to systemic administration by self-assembly of the (actively-targeted) polymeric components and siRNA [83]. BIND-014 and SEL-068, based on the Accurins™ technology, were developed by the design of pre-functionalized triblock co-polymers to create a library of self-assembling targeted polymeric nanoparticles allowing efficient tailoring of physicochemical characteristics [74-75]. Genetic engineering has led to the development of the replication incompetent retroviral vector Rexin-G, which is generated in human producer cells to generate a targeted biocompatible ATNM with a size of approximately 100 nm [110]. Interestingly, bacterially-derived minicells employed for the generation of Erbitux®EDVsPAC are characterized by a larger size (400 nm) compared to other PNC [97]. The size of synthetic nanocarriers is generally designed to remain below 200 nm to avoid rapid uptake by the MPS. Nevertheless, nanomedicines with sizes up to 400 nm have been shown to exploit the EPR effect [111].

Regarding the *targeting ligand* utilized for the discussed ATNM, 4 nanomedicines target the transferrin receptor (TfR). Specific tumor markers such as EGFR, HER2 and PSMA are targeted by 4 nanomedicines (the exact target receptor of MCC-465 is not known). In contrast, a tumor stromal target is exploited by one ATNM. Both vaccine formulations target APC. The transferrin receptor (TfR) is

a well-established target for cancer treatment by virtue of its overexpression on a range of tumors [112]. Attachment of transferrin to PNC for active targeting is exploited by MBP-426 and CALAA-01. The targeted lipoplex formulations SGT-53 and SGT-94 also target the TfR but make use of antibody fragments instead of transferrin [33]. Antibody fragments are smaller than transferrin and recombinant expression allows efficient large scale production and high quality control reducing batch-to-batch variation. When compared to full monoclonal antibodies, the use of antibody fragments for active targeting is preferred because they lack the Fc part of the antibody, preventing rapid recognition by cells of the immune system and subsequent clearance of the ATNM. In the case of Erbitux®EDVs$_{PAC}$ minicells, the Fc region is present, but complement-mediated toxicity is inhibited as protein A/G blocks the Fc part of the conjugated monoclonal antibodies [97]. Interestingly, while most ATNM are directed to a single surface receptor overexpressed on tumor cells, Rexin-G is equipped with more promiscuous high-affinity collagen-binding motifs as targeting ligands, resulting in efficient drug delivery to tumor cells, stroma cells, neovasculature and sites of metastasis without apparent significant toxicity towards healthy tissues [113]. This indicates that proteins overexpressed on tumor cells can be used to discriminate between tumor and healthy cells, but it may be beneficial for robust anti-cancer effects to target the tumor stroma rather than solely tumor cells. The 2 vaccine products show that ATNM can also be directed to antigen presenting cells for the generation of actively-targeted vaccines. Prolonged circulation time allows the nanomedicine to reach target sites and activate cells of the immune system. Besides general vaccine applications, the vaccine strategy can be applied to design effective anti-cancer nanomedicines that are not hampered by limitations of direct tumor cell targeting [114].

It is generally believed that PTNM and ATNM have comparable pharmacokinetic parameters, biodistribution and tumor targeting profiles. Studies of only 7 ATNM reported on *in vivo* localization studies which compared the actively-targeted formulation to the corresponding passively-targeted one (Table 2). Of those 7, 4 reported increased target localization compared to PTNM *in vivo*, while the other 3 studies demonstrated comparable target localization values for ATNM and PTNM. For MM-302, anti-EGFR ILs-DOX and CALAA-01, it was demonstrated that in murine xenograft models overall tumor accumulation was similar for ATNM and PTNM. However, in studies performed with MBP-462, SGT-53, BIND-014 and Erbitux®EDVs$_{PAC}$, a higher degree of tumor localization of the ATNM relative to the PTNM was observed. In the case of 5 ATNM, literature has reported on improved *in vitro* cellular internalization versus PTNM. The publications on MM-302 and anti-EGFR ILs-DOX reported results for *in vivo* cell internalization versus PTNM,

and both showed improvement over PTNM. Studies performed with CALAA-01 even reported on target cell internalization in phase I clinical studies. In light of these results it is possible that, while passively and actively-targeted formulations are both dependent on extravasation from the circulation into the tumor, ATNM are retained longer in the tumor than their passively-targeted counterparts due to increased cellular internalization or other targeting ligand-mediated interactions within the target. However, the number of ATNM tested for *in vivo* target cell internalization is too limited to provide conclusive evidence. Therefore, in tumors where the EPR effect is present, the use of targeting ligands may only be useful to increase cellular internalization or in cases where the targeting ligand itself has intrinsic anti-tumor effects.

Regarding efficacy, all ATNM included in this overview have shown increased efficacy *in vitro* and *in vivo* compared to their passively-targeted counterparts (with the exception of SEL-068). How improved efficacy is related to the presence of a targeting ligand can not yet be concluded due to a lack of information provided in the related literature, and the fact that clinical studies are not designed to compare ATNM and PTNM. In some cases, signs of efficacy in phase I and/or II trials were observed, although these studies did not include PTNM controls. While *in vitro* and *in vivo* model systems do not provide definite proof of efficacy in humans and no data beyond phase I and II trials have been reported as of yet, these results are encouraging for the concept of ATNM.
In the majority of the cases, there is insufficient literature that has reported on cellular and animal studies in which the ATNM have been compared to PTNM regarding the parameters in Table 2. The only exception is MM-302, which reported superior results to PTNM in all of these parameters except target localization in animal studies. This indicates that the improved efficacy of MM-302 might be due to improved cellular internalization but since several other ATNM reported improved target localization in animal studies, this does not necessarily hold true for all ATNM.

Since, phase I clinical trials for most of the ATNM reported in this overview are still ongoing, not all results have been published as of yet. Treatment with ATNM seemed to be well tolerated in patients in the studies that have been published so far. The toxicity of ATNM seems comparable to that of PTNM. For example, the maximum tolerated doses of MM-302 (50 mg/m^2) [53], anti-EGFR ILs-DOX (50 mg/m^2) [59] and MCC-465 (45.5 mg/m^2) [64] are comparable to that of Doxil® (50 mg/m^2). To our knowledge, there have been no cases in which functionalizing a nanomedicine with targeting ligands significantly increased toxicity compared to

the passively-targeted formulation. However, an actively-targeted HPMA copolymer bearing DOX and galactosamine (known as PK2) developed to target liver cancer cells had a significantly lower MTD than its passively-targeted counterpart (known as PK1) [115]. Later studies demonstrated that PK2 is less soluble in water and has a significantly altered structure, leading to a more 'open' coil structure [116]. A structural change in polymer assembly/folding was hypothesized to be the underlying reason for the increased toxicity of PK2 and indicates that direct conjugation of targeting ligands to polymer backbones may have unforeseen consequences. Nevertheless, such a toxicity increasing effect was only observed with the macromolecular PK2 and not with the PNC described in this review.

4. Future directions

ATNM may prove beneficial in increasing drug exposure due to increased target cell uptake and target tissue retention compared to PTNM. Additionally, there are several applications where the use of ATNM may have advantages over PTNM.

(1) Active targeting approaches are crucial for molecules that need to localize intracellularly for therapeutic activity but are not capable of crossing cellular membranes, such as nucleic acids. As a consequence, the development of systemically administered gene (regulating) therapy is evolving concurrently with the development of efficient actively-targeted PNC [117]. The therapeutic potential of RNA interference is illustrated by CALAA-01, which decreased target protein expression in a patient's tumor in a phase I trial [92]. The feasibility of therapeutic DNA is demonstrated by Rexin-G, which has shown promising anti-tumor activity in patients including inhibition of metastatic lesions, angiogenesis and intractable or resistant tumors [110].

(2) One common mechanism underlying multidrug resistance of tumors is the overexpression of drug-efflux pumps, which actively expel anti-cancer drugs. ATNM may be able to circumvent multi drug resistance (MDR) by virtue of another cellular fate after receptor-mediated endocytosis rather than passive diffusion over cell membranes of free drug released by PTNM [118]. For example, anti-EGFR ILs-DOX showed significantly enhanced antitumor activity in a MDR breast cancer xenograft tumor model compared to free DOX and PLD [57].

(3) Active targeting approaches can also be exploited to generate nanomedicines that exploit two therapeutic strategies simultaneously in order to achieve additive or synergistic anti-tumor effects. For example, DOX-loaded polymeric micelles decorated with intrinsically active anti-EGFR nanobodies significantly reduced tumor growth and prolonged survival of tumor-bearing mice when compared to DOX-loaded micelles without attached targeting ligands [119].

(4) An alternative approach to the targeted delivery of anti-cancer drugs to tumor cells

is targeting of the tumor blood supply. The endothelial cells of the tumor vasculature are readily accessible to targeted nanomedicines circulating in the bloodstream and more genetically stable than tumor cells limiting the occurrence of drug resistance phenomena. Delivery of DOX by ATNM targeting αvβ3 integrins overexpressed on tumor neovasculature reduced tumor growth of DOX-insensitive tumors while PLD did not [120]. In line with these results, it was shown that DOX-loaded ATNM targeting αvβ3 integrins suppressed metastasis [121].
(5) As discussed above, in addition to the development of ATNM for cancer treatment, active targeting approaches can be exploited for the generation of effective vaccines as demonstrated by the clinical evaluation of Lipovaxin-MM and SEL-068.

The clinical applicability of ATNM is ultimately determined by the balance between clinical benefits versus safety and cost-effectiveness of the production process. Current knowledge of nanotechnology, tumor biology and interactions of nanomedicines in the human body is (too) limited. To determine the feasibility of clinically relevant ATNM, further preclinical studies focused on relation between physicochemical properties (nanocarrier type, size and surface characteristics) in combination with targeting ligand properties (type and size) and biodistribution, safety and efficacy are encouraged.
The efficacy and safety of ATNM has been shown in animals, but the evidence for the added value of target ligand-coupling to nanomedicines in humans remains to be established. Progress of the ATNM described in this review through clinical phases will reveal in the upcoming years if ATNM will represent safe and efficacious drugs in the future.

Acknowledgements

R. van der Meel is supported by the Utrecht University Focus and Massa program Nanobullets: The next generation in drug targeting.

References

1. European Medical Research Counsils, European Science Foundation Forward Look on Nanomedicine 2005, http:www.esf.org/publications/forward-looks.html, Retrieved 05-03-2013.
2. Drexler, K.E., Peterson, C., Pergamit, G., Unbounding the Future: The Nanotechnology Revolution William Morrow/Quill Books, New York, 1991.
3. Duncan, R., Gaspar, R., Nanomedicine(s) under the microscope, Mol Pharm, 8 (2011) 2101-2141.
4. Allen, T.M., Cullis, P.R., Liposomal drug delivery systems: From concept to clinical applications, Adv Drug Deliv Rev, 65 (2013) 36-48.
5. Kamaly, N., Xiao, Z., Valencia, P.M., Radovic-Moreno, A.F., Farokhzad, O.C., Targeted polymeric therapeutic nanoparticles: design, development and clinical translation, Chem Soc Rev, 41 (2012) 2971-3010.

6. Huh, A.J., Kwon, Y.J., "Nanoantibiotics": a new paradigm for treating infectious diseases using nanomaterials in the antibiotics resistant era, J Control Release, 156 (2011) 128-145.
7. Lobatto, M.E., Fuster, V., Fayad, Z.A., Mulder, W.J., Perspectives and opportunities for nanomedicine in the management of atherosclerosis, Nat Rev Drug Discov, 10 (2011) 835-852.
8. Srikanth, M., Kessler, J.A., Nanotechnology-novel therapeutics for CNS disorders, Nat Rev Neurol, 8 (2012) 307-318.
9. Crielaard, B.J., Lammers, T., Schiffelers, R.M., Storm, G., Drug targeting systems for inflammatory disease: one for all, all for one, J Control Release, 161 (2012) 225-234.
10. Davis, M.E., Chen, Z.G., Shin, D.M., Nanoparticle therapeutics: an emerging treatment modality for cancer, Nat Rev Drug Discov, 7 (2008) 771-782.
11. Jain, R.K., Stylianopoulos, T., Delivering nanomedicine to solid tumors, Nat Rev Clin Oncol, 7 (2010) 653-664.
12. Peer, D., Karp, J.M., Hong, S., Farokhzad, O.C., Margalit, R., Langer, R., Nanocarriers as an emerging platform for cancer therapy, Nat Nanotechnol, 2 (2007) 751-760.
13. Svenson, S., Clinical translation of nanomedicines, Curr Opin Solid St M, 16 (2012) 287-294.
14. Hoffman, A.S., The origins and evolution of "controlled" drug delivery systems, J Control Release, 132 (2008) 153-163.
15. Petros, R.A., DeSimone, J.M., Strategies in the design of nanoparticles for therapeutic applications, Nat Rev Drug Discov, 9 (2010) 615-627.
16. Etheridge, M.L., Campbell, S.A., Erdman, A.G., Haynes, C.L., Wolf, S.M., McCullough, J., The big picture on nanomedicine: the state of investigational and approved nanomedicine products, Nanomedicine, 9 (2013) 1-14.
17. Cheng, Z., Al Zaki, A., Hui, J.Z., Muzykantov, V.R., Tsourkas, A., Multifunctional nanoparticles: cost versus benefit of adding targeting and imaging capabilities, Science, 338 (2012) 903-910.
18. Casi, G., Neri, D., Antibody-drug conjugates: basic concepts, examples and future perspectives, J Control Release, 161 (2012) 422-428.
19. Adair, J.R., Howard, P.W., Hartley, J.A., Williams, D.G., Chester, K.A., Antibody-drug conjugates - a perfect synergy, Expert Opin Biol Ther, 12 (2012) 1191-1206.
20. Ganta, S., Devalapally, H., Shahiwala, A., Amiji, M., A review of stimuli-responsive nanocarriers for drug and gene delivery, J Control Release, 126 (2008) 187-204.
21. Bangham, A.D., Standish, M.M., Watkins, J.C., Diffusion of univalent ions across the lamellae of swollen phospholipids, J Mol Biol, 13 (1965) 238-252.
22. Barenholz, Y., Doxil® - the first FDA-approved nano-drug: lessons learned, J Control Release, 160 (2012) 117-134.
23. Mebiopharm Co. Ltd., A Phase Ib/II Study of MBP-426 in Patients With Second Line Gastric, Gastro Esophageal, or Esophageal Adenocarcinoma, In: ClinicalTrials.gov [Internet], Bethesda (MD): National Library of Medicine (US), Retrieved 05-03-2013, Available from http://www.clinicaltrials.gov/ct2/show/NCT00964080, NLM Identifier: NCT00964080.
24. Graham, M.A., Lockwood, G.F., Greenslade, D., Brienza, S., Bayssas, M., Gamelin, E., Clinical pharmacokinetics of oxaliplatin: a critical review, Clin Cancer Res, 6 (2000) 1205-1218.
25. Ishida, O., Maruyama, K., Tanahashi, H., Iwatsuru, M., Sasaki, K., Eriguchi, M., Yanagie, H., Liposomes bearing polyethyleneglycol-coupled transferrin with intracellular targeting property to the solid tumors in vivo, Pharm Res, 18 (2001) 1042-1048.
26. Suzuki, R., Takizawa, T., Kuwata, Y., Mutoh, M., Ishiguro, N., Utoguchi, N., Shinohara, A., Eriguchi, M., Yanagie, H., Maruyama, K., Effective anti-tumor activity of oxaliplatin encapsulated in transferrin-PEG-liposome, Int J Pharm, 346 (2008) 143-150.
27. Izbicka, E., Diaz, A., Campos, D., Wick, M., Takimoto, C., Nagasawa, M., Hashimoto, C., Evaluation of antitumor activity and biomarkers for MBP-426 in human pancreatic cancer

xenograft models in vivo, AACR Meeting Abstracts, 2007 (2007) 5586-.
28. Mebiopharm Co. Ltd., A Phase I, Open Label Study of MBP-426 Given by Intravenous Infusion in Patients With Advanced or Metastatic Solid Tumors, In: ClinicalTrials.gov [Internet], Bethesda (MD): National Library of Medicine (US), Retrieved 05-03-2013, Available from http://www.clinicaltrials.gov/ct2/show/NCT00355888, NLM Identifier: NCT00355888.
29. Sankhala, K.K., Mita, A.C., Adinin, R., Wood, L., Beeram, M., Bullock, S., Yamagata, N., Matsuno, K., Fujisawa, T., Phan, A., A phase I pharmacokinetic (PK) study of MBP-426, a novel liposome encapsulated oxaliplatin, ASCO Meeting Abstracts, 27 (2009) 2535.
30. Senzer, N.N., Matsuno, K., Yamagata, N., Fujisawa, T., Wasserman, E., Sutherland, W., Sharma, S., Phan, A., Abstract C36: MBP-426, a novel liposome-encapsulated oxaliplatin, in combination with 5-FU/leucovorin (LV): Phase I results of a Phase I/II study in gastro-esophageal adenocarcinoma, with pharmacokinetics, Molecular Cancer Therapeutics, 8 (2009) C36.
31. Xu, L., Tang, W.H., Huang, C.C., Alexander, W., Xiang, L.M., Pirollo, K.F., Rait, A., Chang, E.H., Systemic p53 gene therapy of cancer with immunolipoplexes targeted by anti-transferrin receptor scFv, Mol Med, 7 (2001) 723-734.
32. Xu, L., Pirollo, K.F., Chang, E.H., Transferrin-liposome-mediated p53 sensitization of squamous cell carcinoma of the head and neck to radiation in vitro, Hum Gene Ther, 8 (1997) 467-475.
33. Xu, L., Huang, C.C., Huang, W., Tang, W.H., Rait, A., Yin, Y.Z., Cruz, I., Xiang, L.M., Pirollo, K.F., Chang, E.H., Systemic tumor-targeted gene delivery by anti-transferrin receptor scFv-immunoliposomes, Mol Cancer Ther, 1 (2002) 337-346.
34. Yu, W., Pirollo, K.F., Rait, A., Yu, B., Xiang, L.M., Huang, W.Q., Zhou, Q., Ertem, G., Chang, E.H., A sterically stabilized immunolipoplex for systemic administration of a therapeutic gene, Gene Ther, 11 (2004) 1434-1440.
35. Synergene Therapeutics Inc., A Phase I Open-Label Safety and Pharmacokinetic Study of Escalating Doses of SGT-53 for Infusion in Subjects With Advanced Solid Tumors, In: ClinicalTrials.gov [Internet], Bethesda (MD): National Library of Medicine (US), Retrieved 05-03-2013, Available from http://www.clinicaltrials.gov/ct2/show/NCT00470613, NLM Identifier: NCT00470613.
36. Pirollo, K.F., Rait, A., Zhou, Q., Zhang, X.Q., Zhou, J., Kim, C.S., Benedict, W.F., Chang, E.H., Tumor-targeting nanocomplex delivery of novel tumor suppressor RB94 chemosensitizes bladder carcinoma cells in vitro and in vivo, Clin Cancer Res, 14 (2008) 2190-2198.
37. Xu, H.J., Zhou, Y., Seigne, J., Perng, G.S., Mixon, M., Zhang, C., Li, J., Benedict, W.F., Hu, S.X., Enhanced tumor suppressor gene therapy via replication-deficient adenovirus vectors expressing an N-terminal truncated retinoblastoma protein, Cancer Res, 56 (1996) 2245-2249.
38. Zhang, X., Multani, A.S., Zhou, J.H., Shay, J.W., McConkey, D., Dong, L., Kim, C.S., Rosser, C.J., Pathak, S., Benedict, W.F., Adenoviral-mediated retinoblastoma 94 produces rapid telomere erosion, chromosomal crisis, and caspase-dependent apoptosis in bladder cancer and immortalized human urothelial cells but not in normal urothelial cells, Cancer Res, 63 (2003) 760-765.
39. Xu, H.J., Xu, K., Zhou, Y., Li, J., Benedict, W.F., Hu, S.X., Enhanced tumor cell growth suppression by an N-terminal truncated retinoblastoma protein, Proc Natl Acad Sci U S A, 91 (1994) 9837-9841.
40. Synergene Therapeutics Inc., A Phase I Study of Systemic Gene Therapy With SGT-94 in Patients With Solid Tumors, In: ClinicalTrials.gov [Internet], Bethesda (MD): National Library of Medicine (US), Retrieved 05-03-2013, Available from http://www.clinicaltrials.gov/ct2/show/NCT01517464, NLM Identifier: NCT01517464.
41. Merrimack Pharmaceuticals Inc., A Phase 1, Multi-Center, Open-Label, Dose-Escalation,

Safety, and Pharmacokinetic Clinical Study of Intravenously Administered MM-302 in Patients With Advanced Breast Cancer, In: ClinicalTrials.gov [Internet], Bethesda (MD): National Library of Medicine (US), Retrieved 05-03-2013, Available from http://www.clinicaltrials.gov/ct2/show/NCT01304797, NLM Identifier: NCT01304797.

42. Park, J.W., Benz, C.C., Martin, F.J., Future directions of liposome- and immunoliposome-based cancer therapeutics, Semin Oncol, 31 (2004) 196-205.
43. Park, J.W., Kirpotin, D.B., Hong, K., Shalaby, R., Shao, Y., Nielsen, U.B., Marks, J.D., Papahadjopoulos, D., Benz, C.C., Tumor targeting using anti-her2 immunoliposomes, J Control Release, 74 (2001) 95-113.
44. Nellis, D.F., Ekstrom, D.L., Kirpotin, D.B., Zhu, J., Andersson, R., Broadt, T.L., Ouellette, T.F., Perkins, S.C., Roach, J.M., Drummond, D.C., Hong, K., Marks, J.D., Park, J.W., Giardina, S.L., Preclinical manufacture of an anti-HER2 scFv-PEG-DSPE, liposome-inserting conjugate. 1. Gram-scale production and purification, Biotechnol Prog, 21 (2005) 205-220.
45. Nellis, D.F., Giardina, S.L., Janini, G.M., Shenoy, S.R., Marks, J.D., Tsai, R., Drummond, D.C., Hong, K., Park, J.W., Ouellette, T.F., Perkins, S.C., Kirpotin, D.B., Preclinical manufacture of anti-HER2 liposome-inserting, scFv-PEG-lipid conjugate. 2. Conjugate micelle identity, purity, stability, and potency analysis, Biotechnol Prog, 21 (2005) 221-232.
46. Park, J.W., Hong, K., Carter, P., Asgari, H., Guo, L.Y., Keller, G.A., Wirth, C., Shalaby, R., Kotts, C., Wood, W.I., et al., Development of anti-p185HER2 immunoliposomes for cancer therapy, Proc Natl Acad Sci U S A, 92 (1995) 1327-1331.
47. Kirpotin, D., Park, J.W., Hong, K., Zalipsky, S., Li, W.L., Carter, P., Benz, C.C., Papahadjopoulos, D., Sterically stabilized anti-HER2 immunoliposomes: design and targeting to human breast cancer cells in vitro, Biochemistry, 36 (1997) 66-75.
48. Kirpotin, D.B., Drummond, D.C., Shao, Y., Shalaby, M.R., Hong, K., Nielsen, U.B., Marks, J.D., Benz, C.C., Park, J.W., Antibody targeting of long-circulating lipidic nanoparticles does not increase tumor localization but does increase internalization in animal models, Cancer Res, 66 (2006) 6732-6740.
49. Park, J.W., Hong, K., Kirpotin, D.B., Colbern, G., Shalaby, R., Baselga, J., Shao, Y., Nielsen, U.B., Marks, J.D., Moore, D., Papahadjopoulos, D., Benz, C.C., Anti-HER2 immunoliposomes: enhanced efficacy attributable to targeted delivery, Clin Cancer Res, 8 (2002) 1172-1181.
50. Geretti, E., Reynolds, J., Hendriks, B., Eckelhofer, I., Espelin, C., Gaddy, D., Klinz, S., Lee, H., Leonard, S., Olivier, K., Agresta, S., Niyikiza, C., Nielsen, U., Wickham, T., Abstract C90: HER2-targeted liposomal doxorubicin MM-302 has a favorable cardiosafety profile in preclinical models, Molecular Cancer Therapeutics, 10 (2011) C90.
51. Klinz, S., Eckelhofer, I., Gaddy, D., Geretti, E., Hendriks, B., Lee, H., Leonard, S., Reynolds, J., Wickham, T., Abstract 3637: MM-302, a HER2-targeted liposomal doxorubicin, shows binding/uptake and efficacy in HER2 2+ cells and xenograft models, Cancer Research, 71 (2011) 3637.
52. Wickham, T., Reynolds, J., Drummond, D., Kirpotin, D., Lahdenranta, J., Leonard, S., Geretti, E., Lee, H., Klinz, S., Hendriks, B., Olivier, K., Eckelhofer, I., Park, J., Benz, C., Moyo, V., Niyikiza, C., Nielsen, U., Abstract P3-14-09: Preclinical Safety and Activity of MM-302, a HER2-Targeted Liposomal Doxorubicin Designed To Have an Improved Safety and Efficacy Profile over Approved Anthracyclines, Cancer Research, 70 (2011) P3-14-09.
53. Wickham, T., Futch, K., A Phase I Study of MM-302, a HER2-targeted Liposomal Doxorubicin, in Patients with Advanced, HER2- Positive Breast Cancer, Cancer Research, 72 (2012) P5-18-09.
54. Noble, C.O., Kirpotin, D.B., Hayes, M.E., Mamot, C., Hong, K., Park, J.W., Benz, C.C., Marks, J.D., Drummond, D.C., Development of ligand-targeted liposomes for cancer therapy, Expert Opin Ther Targets, 8 (2004) 335-353.
55. Mamot, C., Drummond, D.C., Greiser, U., Hong, K., Kirpotin, D.B., Marks, J.D., Park,

J.W., Epidermal growth factor receptor (EGFR)-targeted immunoliposomes mediate specific and efficient drug delivery to EGFR- and EGFRvIII-overexpressing tumor cells, Cancer Res, 63 (2003) 3154-3161.

56. Mamot, C., Drummond, D.C., Noble, C.O., Kallab, V., Guo, Z., Hong, K., Kirpotin, D.B., Park, J.W., Epidermal growth factor receptor-targeted immunoliposomes significantly enhance the efficacy of multiple anticancer drugs in vivo, Cancer Res, 65 (2005) 11631-11638.
57. Mamot, C., Ritschard, R., Wicki, A., Kung, W., Schuller, J., Herrmann, R., Rochlitz, C., Immunoliposomal delivery of doxorubicin can overcome multidrug resistance mechanisms in EGFR-overexpressing tumor cells, J Drug Target, 20 (2012) 422-432.
58. University Hospital Basel Switserland, A Phase I Study of Doxorubicin-loaded Anti-EGFR Immunoliposomes in Patients With Advanced Solid Tumors, In: ClinicalTrials.gov [Internet], Bethesda (MD): National Library of Medicine (US), Retrieved 05-03-2013, Available from http://www.clinicaltrials.gov/ct2/show/NCT01702129/, NLM Identifier: NCT01702129.
59. Mamot, C., Ritschard, R., Wicki, A., Stehle, G., Dieterle, T., Bubendorf, L., Hilker, C., Deuster, S., Herrmann, R., Rochlitz, C., Tolerability, safety, pharmacokinetics, and efficacy of doxorubicin-loaded anti-EGFR immunoliposomes in advanced solid tumours: a phase 1 dose-escalation study, Lancet Oncol, 13 (2012) 1234-1241.
60. Hosokawa, S., Tagawa, T., Niki, H., Hirakawa, Y., Nohga, K., Nagaike, K., Efficacy of immunoliposomes on cancer models in a cell-surface-antigen-density-dependent manner, Br J Cancer, 89 (2003) 1545-1551.
61. Hosokawa, S., Tagawa, T., Niki, H., Hirakawa, Y., Ito, N., Nohga, K., Nagaike, K., Establishment and evaluation of cancer-specific human monoclonal antibody GAH for targeting chemotherapy using immunoliposomes, Hybrid Hybridomics, 23 (2004) 109-120.
62. Hamaguchi, T., Matsumura, Y., Nakanishi, Y., Muro, K., Yamada, Y., Shimada, Y., Shirao, K., Niki, H., Hosokawa, S., Tagawa, T., Kakizoe, T., Antitumor effect of MCC-465, pegylated liposomal doxorubicin tagged with newly developed monoclonal antibody GAH, in colorectal cancer xenografts, Cancer Sci, 95 (2004) 608-613.
63. Shimada, K., Kasamatsu, T., Hasegawa, T., Kanai, Y., Niki, H., Tagawa, T., Matsumura, Y., The cytotoxicity and intracellular distributions of MCC-465, pegylated liposomal doxorubicin tagged with newly developed monoclonal antibody GAH, in ovarian cancer cell lines, AACR Meeting Abstracts, 2005 (2005) 334-a-.
64. Matsumura, Y., Gotoh, M., Muro, K., Yamada, Y., Shirao, K., Shimada, Y., Okuwa, M., Matsumoto, S., Miyata, Y., Ohkura, H., Chin, K., Baba, S., Yamao, T., Kannami, A., Takamatsu, Y., Ito, K., Takahashi, K., Phase I and pharmacokinetic study of MCC-465, a doxorubicin (DXR) encapsulated in PEG immunoliposome, in patients with metastatic stomach cancer, Ann Oncol, 15 (2004) 517-525.
65. Altin, J.G., Parish, C.R., Liposomal vaccines--targeting the delivery of antigen, Methods, 40 (2006) 39-52.
66. Altin, J., Atmosukarto, I., R. M. De Wildt, Parish, C., Price, J., Composition for targeting dendritic cells, US 2011/0212168 A1, 19-10-2009 (filing date).
67. van Broekhoven, C.L., Parish, C.R., Demangel, C., Britton, W.J., Altin, J.G., Targeting dendritic cells with antigen-containing liposomes: a highly effective procedure for induction of antitumor immunity and for tumor immunotherapy, Cancer Res, 64 (2004) 4357-4365.
68. Lipotek Pty. Ltd., A Phase I Open-label Study of the Safety and Immunogenicity of Escalating Doses of Lipovaxin-MM, a Novel Melanoma Immunotherapeutic, in Patients With Metastatic Melanoma, In: ClinicalTrials.gov [Internet], Bethesda (MD): National Library of Medicine (US), Retrieved 05-03-2013, Available from http://www.clinicaltrials.gov/ct2/show/NCT01052142, NLM Identifier: NCT01052142.
69. Ringsdorf, H., Structure and properties of pharmacologically active polymers, Journal of Polymer Science: Polymer Symposia, 51 (1975) 135-153.
70. Langer, R., Folkman, J., Polymers for the sustained release of proteins and other

macromolecules, Nature, 263 (1976) 797-800.
71. Hrkach, J., Von Hoff, D., Mukkaram Ali, M., Andrianova, E., Auer, J., Campbell, T., De Witt, D., Figa, M., Figueiredo, M., Horhota, A., Low, S., McDonnell, K., Peeke, E., Retnarajan, B., Sabnis, A., Schnipper, E., Song, J.J., Song, Y.H., Summa, J., Tompsett, D., Troiano, G., Van Geen Hoven, T., Wright, J., LoRusso, P., Kantoff, P.W., Bander, N.H., Sweeney, C., Farokhzad, O.C., Langer, R., Zale, S., Preclinical development and clinical translation of a PSMA-targeted docetaxel nanoparticle with a differentiated pharmacological profile, Sci Transl Med, 4 (2012) 128ra139.
72. Maresca, K.P., Hillier, S.M., Femia, F.J., Keith, D., Barone, C., Joyal, J.L., Zimmerman, C.N., Kozikowski, A.P., Barrett, J.A., Eckelman, W.C., Babich, J.W., A series of halogenated heterodimeric inhibitors of prostate specific membrane antigen (PSMA) as radiolabeled probes for targeting prostate cancer, J Med Chem, 52 (2009) 347-357.
73. Chang, S.S., O'Keefe, D.S., Bacich, D.J., Reuter, V.E., Heston, W.D., Gaudin, P.B., Prostate-specific membrane antigen is produced in tumor-associated neovasculature, Clin Cancer Res, 5 (1999) 2674-2681.
74. Gu, F., Zhang, L., Teply, B.A., Mann, N., Wang, A., Radovic-Moreno, A.F., Langer, R., Farokhzad, O.C., Precise engineering of targeted nanoparticles by using self-assembled biointegrated block copolymers, Proc Natl Acad Sci U S A, 105 (2008) 2586-2591.
75. Shi, J., Xiao, Z., Kamaly, N., Farokhzad, O.C., Self-assembled targeted nanoparticles: evolution of technologies and bench to bedside translation, Acc Chem Res, 44 (2011) 1123-1134.
76. Lupold, S.E., Hicke, B.J., Lin, Y., Coffey, D.S., Identification and characterization of nuclease-stabilized RNA molecules that bind human prostate cancer cells via the prostate-specific membrane antigen, Cancer Res, 62 (2002) 4029-4033.
77. Farokhzad, O.C., Jon, S., Khademhosseini, A., Tran, T.N., Lavan, D.A., Langer, R., Nanoparticle-aptamer bioconjugates: a new approach for targeting prostate cancer cells, Cancer Res, 64 (2004) 7668-7672.
78. Cheng, J., Teply, B.A., Sherifi, I., Sung, J., Luther, G., Gu, F.X., Levy-Nissenbaum, E., Radovic-Moreno, A.F., Langer, R., Farokhzad, O.C., Formulation of functionalized PLGA-PEG nanoparticles for in vivo targeted drug delivery, Biomaterials, 28 (2007) 869-876.
79. Farokhzad, O.C., Cheng, J., Teply, B.A., Sherifi, I., Jon, S., Kantoff, P.W., Richie, J.P., Langer, R., Targeted nanoparticle-aptamer bioconjugates for cancer chemotherapy in vivo, Proc Natl Acad Sci U S A, 103 (2006) 6315-6320.
80. BIND Biosciences, A Phase 1 Open Label, Safety, Pharmacokinetic and Pharmacodynamic Dose Escalation Study of BIND-014 (Docetaxel Nanoparticles for Injectable Suspension), Given by Intravenous Infusion to Patients With Advanced or Metastatic Cancer, In: ClinicalTrials.gov [Internet], Bethesda (MD): National Library of Medicine (US), Retrieved 05-03-2013, Available from http://www.clinicaltrials.gov/ct2/show/NCT01300533, NLM Identifier: NCT01300533.
81. BIND Biosciences, A Phase 2 Study to Determine the Safety and Efficacy of BIND-014 (Docetaxel Nanoparticles for Injectable Suspension), Administered to Patients With Metastatic Castration-Resistant Prostate Cancer, In: ClinicalTrials.gov [Internet], Bethesda (MD): National Library of Medicine (US), Retrieved 25-03-2013, Available from http://clinicaltrials.gov/ct2/show/NCT01812746, NLM Identifier: NCT01812746.
82. BIND Biosciences, A Phase 2 Study to Determine the Safety and Efficacy of BIND-014 (Docetaxel Nanoparticles for Injectable Suspension) as Second-line Therapy to Patients With Non-Small Cell Lung Cancer, In: ClinicalTrials.gov [Internet], Bethesda (MD): National Library of Medicine (US), Retrieved 05-03-2013, Available from http://www.clinicaltrials.gov/ct2/show/NCT01792479, NLM Identifier: NCT01792479.
83. Davis, M.E., The first targeted delivery of siRNA in humans via a self-assembling, cyclodextrin polymer-based nanoparticle: from concept to clinic, Mol Pharm, 6 (2009) 659-668.
84. Heidel, J.D., Liu, J.Y., Yen, Y., Zhou, B., Heale, B.S., Rossi, J.J., Bartlett, D.W., Davis, M.E.,

Potent siRNA inhibitors of ribonucleotide reductase subunit RRM2 reduce cell proliferation in vitro and in vivo, Clin Cancer Res, 13 (2007) 2207-2215.

85. Cerqueira, N.M., Pereira, S., Fernandes, P.A., Ramos, M.J., Overview of ribonucleotide reductase inhibitors: an appealing target in anti-tumour therapy, Curr Med Chem, 12 (2005) 1283-1294.
86. Bartlett, D.W., Davis, M.E., Physicochemical and biological characterization of targeted, nucleic acid-containing nanoparticles, Bioconjug Chem, 18 (2007) 456-468.
87. Bartlett, D.W., Su, H., Hildebrandt, I.J., Weber, W.A., Davis, M.E., Impact of tumor-specific targeting on the biodistribution and efficacy of siRNA nanoparticles measured by multimodality in vivo imaging, Proc Natl Acad Sci U S A, 104 (2007) 15549-15554.
88. Hu-Lieskovan, S., Heidel, J.D., Bartlett, D.W., Davis, M.E., Triche, T.J., Sequence-specific knockdown of EWS-FLI1 by targeted, nonviral delivery of small interfering RNA inhibits tumor growth in a murine model of metastatic Ewing's sarcoma, Cancer Res, 65 (2005) 8984-8992.
89. Rahman, M.A., Amin, A.R., Wang, X., Zuckerman, J.E., Choi, C.H., Zhou, B., Wang, D., Nannapaneni, S., Koenig, L., Chen, Z., Chen, Z.G., Yen, Y., Davis, M.E., Shin, D.M., Systemic delivery of siRNA nanoparticles targeting RRM2 suppresses head and neck tumor growth, J Control Release, 159 (2012) 384-392.
90. Heidel, J.D., Yu, Z., Liu, J.Y., Rele, S.M., Liang, Y., Zeidan, R.K., Kornbrust, D.J., Davis, M.E., Administration in non-human primates of escalating intravenous doses of targeted nanoparticles containing ribonucleotide reductase subunit M2 siRNA, Proc Natl Acad Sci U S A, 104 (2007) 5715-5721.
91. Calando Pharmaceuticals, A Phase I, Dose-Escalating Study of the Safety of Intravenous CALAA-01 in Adults With Solid Tumors Refractory to Standard-of-Care Therapies, In: ClinicalTrials.gov [Internet], Bethesda (MD): National Library of Medicine (US), Retrieved 05-03-2013, Available from http://www.clinicaltrials.gov/ct2/show/NCT00689065, NLM Identifier: NCT00689065.
92. Davis, M.E., Zuckerman, J.E., Choi, C.H., Seligson, D., Tolcher, A., Alabi, C.A., Yen, Y., Heidel, J.D., Ribas, A., Evidence of RNAi in humans from systemically administered siRNA via targeted nanoparticles, Nature, 464 (2010) 1067-1070.
93. Goniewicz, M.L., Delijewski, M., Nicotine vaccines to treat tobacco dependence, Hum Vaccin Immunother, 9 (2013) 13-25.
94. Kishimoto, K., Altreuter, D., Johnston, L., Keller, P., Pittet, L., SEL-068 A fully synthetic nanoparticle vaccine for smoking cessation and relapse prevention, in: Society for Research on Nicotine and Tobacco 18th Annual Meeting, Houston, Texas, 2012.
95. Pittet, L., Altreuter, D., Ilyinskii, P., Fraser, C., Gao, Y., Baldwin, S., Keegan, M., Johnston, L., Kishimoto, T., Development and preclinical evaluation of SEL-068, a novel targeted Synthetic Vaccine Particle (tSVP™) for smoking cessation and relapse prevention that generates high titers of antibodies against nicotine, The Journal of Immunology, 188 (2012) 75.11.
96. Selecta Biosciences Inc., A Phase 1 Randomized, Double-Blind, Placebo-Controlled Study to Assess the Safety and Pharmacodynamics of Increasing Subcutaneous Doses of SEL-068 in Healthy Non-Smoker and Smoker Adults, In: ClinicalTrials.gov [Internet], Bethesda (MD): National Library of Medicine (US), Retrieved 05-03-2013, Available from http://www.clinicaltrials.gov/ct2/show/NCT01478893, NLM Identifier: NCT01478893.
97. MacDiarmid, J.A., Brahmbhatt, H., Minicells: versatile vectors for targeted drug or si/shRNA cancer therapy, Curr Opin Biotechnol, 22 (2011) 909-916.
98. MacDiarmid, J.A., Mugridge, N.B., Weiss, J.C., Phillips, L., Burn, A.L., Paulin, R.P., Haasdyk, J.E., Dickson, K.A., Brahmbhatt, V.N., Pattison, S.T., James, A.C., Al Bakri, G., Straw, R.C., Stillman, B., Graham, R.M., Brahmbhatt, H., Bacterially derived 400 nm particles for encapsulation and cancer cell targeting of chemotherapeutics, Cancer Cell, 11 (2007) 431-445.

99. MacDiarmid, J.A., Amaro-Mugridge, N.B., Madrid-Weiss, J., Sedliarou, I., Wetzel, S., Kochar, K., Brahmbhatt, V.N., Phillips, L., Pattison, S.T., Petti, C., Stillman, B., Graham, R.M., Brahmbhatt, H., Sequential treatment of drug-resistant tumors with targeted minicells containing siRNA or a cytotoxic drug, Nat Biotechnol, 27 (2009) 643-651.
100. Solomon, B., Desai, J., Scott, A., Rosenthal, M., McArthur, G., Rischin, D., Segelov, E., MacDiarmid, J., Brambhatt, H., 585 First-in-man, Multicenter, Phase I Trial Evaluating the Safety of First-in-class Therapeutic, EGFR-targeted, Paclitaxel-Packaged Minicells, European journal of cancer (Oxford, England : 1990), 48 (2012) 179.
101. Mann, R., Mulligan, R.C., Baltimore, D., Construction of a retrovirus packaging mutant and its use to produce helper-free defective retrovirus, Cell, 33 (1983) 153-159.
102. Hall, F.L., Liu, L., Zhu, N.L., Stapfer, M., Anderson, W.F., Beart, R.W., Gordon, E.M., Molecular engineering of matrix-targeted retroviral vectors incorporating a surveillance function inherent in von Willebrand factor, Hum Gene Ther, 11 (2000) 983-993.
103. Gordon, E.M., Hall, F.L., Rexin-G, a targeted genetic medicine for cancer, Expert Opin Biol Ther, 10 (2010) 819-832.
104. Gordon, E.M., Chen, Z.H., Liu, L., Whitley, M., Wei, D., Groshen, S., Hinton, D.R., Anderson, W.F., Beart, R.W., Jr., Hall, F.L., Systemic administration of a matrix-targeted retroviral vector is efficacious for cancer gene therapy in mice, Hum Gene Ther, 12 (2001) 193-204.
105. Gordon, E.M., Lopez, F.F., Cornelio, G.H., Lorenzo, C.C., 3rd, Levy, J.P., Reed, R.A., Liu, L., Bruckner, H.W., Hall, F.L., Pathotropic nanoparticles for cancer gene therapy Rexin-G IV: three-year clinical experience, Int J Oncol, 29 (2006) 1053-1064.
106. Gordon, E.M., Cornelio, G.H., Lorenzo, C.C., 3rd, Levy, J.P., Reed, R.A., Liu, L., Hall, F.L., First clinical experience using a 'pathotropic' injectable retroviral vector (Rexin-G) as intervention for stage IV pancreatic cancer, Int J Oncol, 24 (2004) 177-185.
107. Galanis, E., Carlson, S.K., Foster, N.R., Lowe, V., Quevedo, F., McWilliams, R.R., Grothey, A., Jatoi, A., Alberts, S.R., Rubin, J., Phase I trial of a pathotropic retroviral vector expressing a cytocidal cyclin G1 construct (Rexin-G) in patients with advanced pancreatic cancer, Mol Ther, 16 (2008) 979-984.
108. Chawla, S.P., Chua, V.S., Fernandez, L., Quon, D., Blackwelder, W.C., Gordon, E.M., Hall, F.L., Advanced phase I/II studies of targeted gene delivery in vivo: intravenous Rexin-G for gemcitabine-resistant metastatic pancreatic cancer, Mol Ther, 18 (2010) 435-441.
109. Chawla, S.P., Chua, V.S., Fernandez, L., Quon, D., Saralou, A., Blackwelder, W.C., Hall, F.L., Gordon, E.M., Phase I/II and phase II studies of targeted gene delivery in vivo: intravenous Rexin-G for chemotherapy-resistant sarcoma and osteosarcoma, Mol Ther, 17 (2009) 1651-1657.
110. Gordon, E.M., Hall, F.L., The 'timely' development of Rexin-G: first targeted injectable gene vector (review), Int J Oncol, 35 (2009) 229-238.
111. Bae, Y.H., Park, K., Targeted drug delivery to tumors: myths, reality and possibility, J Control Release, 153 (2011) 198-205.
112. Daniels, T.R., Bernabeu, E., Rodriguez, J.A., Patel, S., Kozman, M., Chiappetta, D.A., Holler, E., Ljubimova, J.Y., Helguera, G., Penichet, M.L., The transferrin receptor and the targeted delivery of therapeutic agents against cancer, Biochim Biophys Acta, 1820 (2012) 291-317.
113. Gordon, E.M., Hall, F.L., Noteworthy clinical case studies in cancer gene therapy: tumor-targeted Rexin-G advances as an efficacious anti-cancer agent, Int J Oncol, 36 (2010) 1341-1353.
114. Lammers, T., Kiessling, F., Hennink, W.E., Storm, G., Drug targeting to tumors: principles, pitfalls and (pre-) clinical progress, J Control Release, 161 (2012) 175-187.
115. Seymour, L.W., Ferry, D.R., Anderson, D., Hesslewood, S., Julyan, P.J., Poyner, R., Doran, J., Young, A.M., Burtles, S., Kerr, D.J., Hepatic drug targeting: phase I evaluation of polymer-bound doxorubicin, J Clin Oncol, 20 (2002) 1668-1676.

116. Paul, A., Vicent, M.J., Duncan, R., Using small-angle neutron scattering to study the solution conformation of N-(2-hydroxypropyl)methacrylamide copolymer-doxorubicin conjugates, Biomacromolecules, 8 (2007) 1573-1579.
117. Pecot, C.V., Calin, G.A., Coleman, R.L., Lopez-Berestein, G., Sood, A.K., RNA interference in the clinic: challenges and future directions, Nat Rev Cancer, 11 (2011) 59-67.
118. Gao, Z., Zhang, L., Sun, Y., Nanotechnology applied to overcome tumor drug resistance, J Control Release, 162 (2012) 45-55.
119. Talelli, M., Oliveira, S., Rijcken, C.J., Pieters, E.H., Etrych, T., Ulbrich, K., van Nostrum, R.C., Storm, G., Hennink, W.E., Lammers, T., Intrinsically active nanobody-modified polymeric micelles for tumor-targeted combination therapy, Biomaterials, 34 (2013) 1255-1260.
120. Schiffelers, R.M., Koning, G.A., ten Hagen, T.L., Fens, M.H., Schraa, A.J., Janssen, A.P., Kok, R.J., Molema, G., Storm, G., Anti-tumor efficacy of tumor vasculature-targeted liposomal doxorubicin, J Control Release, 91 (2003) 115-122.
121. Murphy, E.A., Majeti, B.K., Barnes, L.A., Makale, M., Weis, S.M., Lutu-Fuga, K., Wrasidlo, W., Cheresh, D.A., Nanoparticle-mediated drug delivery to tumor vasculature suppresses metastasis, Proc Natl Acad Sci U S A, 105 (2008) 9343-9348.
122. Abuchowski, A., McCoy, J.R., Palczuk, N.C., van Es, T., Davis, F.F., Effect of covalent attachment of polyethylene glycol on immunogenicity and circulating life of bovine liver catalase, J Biol Chem, 252 (1977) 3582-3586.
123. Knop, K., Hoogenboom, R., Fischer, D., Schubert, U.S., Poly(ethylene glycol) in drug delivery: pros and cons as well as potential alternatives, Angew Chem Int Ed Engl, 49 (2010) 6288-6308.
124. Gref, R., Minamitake, Y., Peracchia, M.T., Trubetskoy, V., Torchilin, V., Langer, R., Biodegradable long-circulating polymeric nanospheres, Science, 263 (1994) 1600-1603.
125. Klibanov, A.L., Maruyama, K., Torchilin, V.P., Huang, L., Amphipathic polyethyleneglycols effectively prolong the circulation time of liposomes, FEBS Lett, 268 (1990) 235-237.
126. Blume, G., Cevc, G., Liposomes for the sustained drug release in vivo, Biochim Biophys Acta, 1029 (1990) 91-97.
127. Romberg, B., Hennink, W.E., Storm, G., Sheddable coatings for long-circulating nanoparticles, Pharm Res, 25 (2008) 55-71.
128. Moghimi, S.M., Andersen, A.J., Hashemi, S.H., Lettiero, B., Ahmadvand, D., Hunter, A.C., Andresen, T.L., Hamad, I., Szebeni, J., Complement activation cascade triggered by PEG-PL engineered nanomedicines and carbon nanotubes: the challenges ahead, J Control Release, 146 (2010) 175-181.
129. Dams, E.T., Laverman, P., Oyen, W.J., Storm, G., Scherphof, G.L., van Der Meer, J.W., Corstens, F.H., Boerman, O.C., Accelerated blood clearance and altered biodistribution of repeated injections of sterically stabilized liposomes, J Pharmacol Exp Ther, 292 (2000) 1071-1079.
130. Laverman, P., Carstens, M.G., Boerman, O.C., Dams, E.T., Oyen, W.J., van Rooijen, N., Corstens, F.H., Storm, G., Factors affecting the accelerated blood clearance of polyethylene glycol-liposomes upon repeated injection, J Pharmacol Exp Ther, 298 (2001) 607-612.
131. Matsumura, Y., Maeda, H., A new concept for macromolecular therapeutics in cancer chemotherapy: mechanism of tumoritropic accumulation of proteins and the antitumor agent smancs, Cancer Res, 46 (1986) 6387-6392.
132. Maeda, H., Nakamura, H., Fang, J., The EPR effect for macromolecular drug delivery to solid tumors: Improvement of tumor uptake, lowering of systemic toxicity, and distinct tumor imaging in vivo, Adv Drug Deliv Rev, 65 (2013) 71-79.
133. Kwon, I.K., Lee, S.C., Han, B., Park, K., Analysis on the current status of targeted drug delivery to tumors, J Control Release, (2012).
134. Bellocq, N.C., Pun, S.H., Jensen, G.S., Davis, M.E., Transferrin-containing, cyclodextrin polymer-based particles for tumor-targeted gene delivery, Bioconjug Chem, 14 (2003) 1122-

1132.
135. Gordon, E.M., Liu, P.X., Chen, Z.H., Liu, L., Whitley, M.D., Gee, C., Groshen, S., Hinton, D.R., Beart, R.W., Hall, F.L., Inhibition of metastatic tumor growth in nude mice by portal vein infusions of matrix-targeted retroviral vectors bearing a cytocidal cyclin G1 construct, Cancer Res, 60 (2000) 3343-3347.

Chapter 3
Tumor-targeted Nanobullets: Anti-EGFR nanobody-liposomes loaded with anti-IGF-1R kinase inhibitor for cancer treatment

Roy van der Meel[a], Sabrina Oliveira[b,c], Işil Altintaş[a], Rob Haselberg[d], Joris van der Veeken[a], Rob C. Roovers[b], Paul M.P. van Bergen en Henegouwen[b], Gert Storm[a], Wim E. Hennink[a], Raymond M. Schiffelers[a,e], Robbert J. Kok[a]

[a] Department of Pharmaceutics, Utrecht Institute for Pharmaceutical Sciences (UIPS), Faculty of Science, Utrecht University, Universiteitsweg 99, 3584 CG Utrecht, The Netherlands

[b] Division Cell Biology, Department of Biology, Faculty of Science, Utrecht University, Padualaan 8, 3584 CH Utrecht, The Netherlands

[c] Department of Pathology, University Medical Center Utrecht, Utrecht, The Netherlands

[d] Biomolecular Analysis, Faculty of Science, Utrecht University, Universiteitsweg 99, 3584 CG Utrecht, The Netherlands

[e] Department of Clinical Chemistry and Hematology, University Medical Center Utrecht, Utrecht, The Netherlands

Journal of Controlled Release, 159 (2): 281-289 (2012)

Abstract

The epidermal growth factor receptor (EGFR) is a validated target for anti-cancer therapy and several EGFR inhibitors are used in the clinic. Over the years, an increasing number of studies have reported on the cross-talk between EGFR and other receptors that can contribute to accelerated cancer development or even acquisition of resistance to anti-EGFR therapies. Combined targeting of EGFR and insulin-like growth factor 1 receptor (IGF-1R) is a rational strategy to potentiate anticancer treatment and possibly retard resistance development. In the present study, we have pursued this by encapsulating the kinase inhibitor AG538 in anti-EGFR nanobody (Nb)-liposomes. The thus developed dual-active Nb-liposomes associated with EGFR-(over)expressing cells in an EGFR-specific manner and blocked both EGFR and IGF-1R activation, due to presence of the EGFR-blocking Nb EGa1 and the anti-IGF-1R kinase inhibitor AG538 respectively. AG538-loaded Nb-liposomes induced a strong inhibition of tumor cell proliferation even upon short-term exposure followed by a drug-free wash-out period. Therefore, AG538-loaded Nb-liposomes are a promising anti-cancer formulation due to efficient intracellular delivery of AG538 in combination with antagonistic and downregulating properties of the EGa1 Nb-liposomes.

Graphical abstract

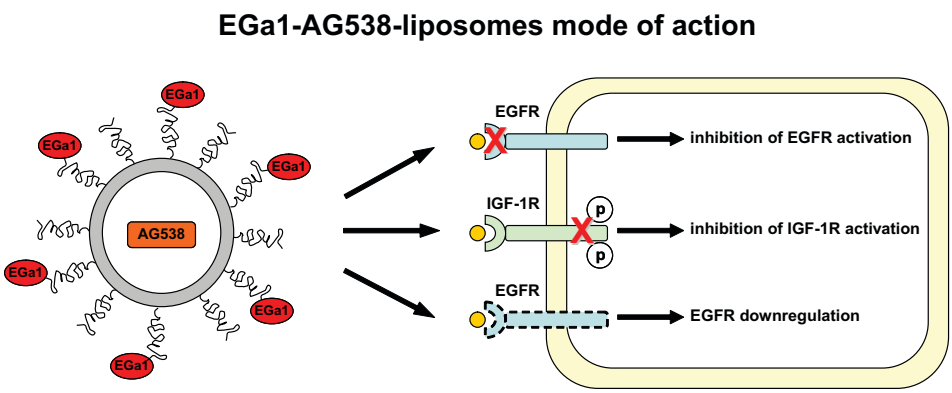

1. Introduction

The epidermal growth factor receptor (EGFR) can contribute to tumorigenesis and metastasis and is a well established target for anti-cancer therapy [1-2]. Overexpression of EGFR occurs in a number of epithelial tumors such as head and neck squamous-cell carcinoma (HNSCC), non-small-cell lung cancer, colorectal cancer and pancreatic cancer [1-2]. EGFR targeted therapeutics that have been approved by the FDA include the tyrosine kinase inhibitors (TKIs) erlotinib and gefitinib and the monoclonal antibodies (mAbs) cetuximab and panitumumab [2-3]. Despite good initial clinical response, many tumors eventually develop acquired resistance to EGFR-targeted therapies [4]. One of the underlying mechanisms of acquired tumor resistance is crosstalk between EGFR and insulin-like growth factor-1 receptor (IGF-1R) signaling [4-5]. Interaction of EGFR and IGF-1R signaling pathways can occur directly by heterodimerization of the receptors, or indirectly via common downstream signaling molecules [5]. Similar to EGFR, IGF-1R can stimulate tumor progression and development by activating signaling cascades regulating processes such as cell proliferation, apoptosis and survival [6]. Upregulated expression of IGF-1R has been described in a variety of human cancers and several IGF-1R inhibitors are currently undergoing clinical trials [7]. Combinations of EGFR/IGF-1R inhibitors have been utilized to demonstrate enhanced inhibition of tumor cell proliferation when compared to mono-targeted therapies, underlining the importance of crosstalk between these signaling networks in tumor progression and resistance [5]. We have previously reported on anti-EGFR Nb-liposomes that are able to inhibit ligand binding to EGFR and to induce its downregulation [8]. Anti-EGFR Nbs or VHHs are small antigen-binding fragments derived from heavy chain-only antibodies which occur naturally in the blood of *camelidae* [9]. Anti-EGFR Nb-liposomes demonstrated increased tumor cell proliferation inhibition compared to free Nb in vitro and downregulation of EGFR in vivo [8]. In the present study, we employed these anti-EGFR Nb-liposomes for the development of a targeted dual-active nanomedicine that simultaneously inhibits both EGFR and IGF-1R. To accomplish this, AG538, a potent inhibitor of IGF-1R kinase [10], was encapsulated in anti-EGFR Nb-liposomes by remote loading. We assessed the efficacy of AG538-loaded Nb-liposomes on EGFR-(over)expressing UM-SCC-14C tumor cells in vitro by investigating the capability of the liposomal system to deliver its cargo within the targeted tumor cells and their effects on the targeted pathways as well as tumor cell proliferation. AG538-loaded Nb-liposomes showed strongly enhanced inhibition of tumor cell proliferation after short-term exposure to tumor cells, demonstrating the beneficial effects of anti-EGFR/IGF-1R combination therapy.

2. Material and methods

2.1 Nanobodies

Nb EGa1 is an antagonist of EGFR and has been described by Hofman *et al.* [11]. The Nb R2 directed against the azo-dye reactive red 6 (RR6) [12] was used as a negative control Nb for this study. The Nb EGc9 binds to domain I of EGFR, and does not compete with the substrate for the receptor (Heukers *et al.*, *manuscript in preparation*). Induction of protein expression and purification of Nbs from the periplasmic space of *E. coli* BL21-CodonPlus(DE3)-RIL cells (Agilent Technologies, Inc., Santa Clara, CA, USA) was performed as previously described [13] with minor adjustments. Briefly, pET28a was modified to contain a pelB leader sequence, a multiple cloning site for Nb insertion, a cMyc-derived epitope tag and hexahistidine tag for detection and purification of Nb respectively and two stop codons. The vector was a kind gift from Dr. R. Klooster (dept. of Human Genetics, LUMC, Leiden, the Netherlands). Nb-encoding cDNAs were inserted in this vector using the Sfi1 and BstEII restriction sites flanking the cDNA. The produced Nbs were purified on an ÄKTApurifier 10 (GE Healthcare Europe GmbH, Munich, Germany) using a HisTrap™ Column (GE Healthcare) according to the manufacturer's protocol. Nbs were eluted with an imidazole gradient (10-500 mM, pH 8) and the collected fractions were dialyzed overnight to PBS pH 7.4 and stored at 4 °C.

2.2 Preparation of liposomes

Dioleoyltrimethylammoniumpropane, DOTAP (Avanti Polar Lipids, Birmingham, AL, USA), dioleoylphosphatidylethanolamine, DOPE (Lipoid, Ludwigshafen, Germany), and maleimide-polyethyleneglycol 2000 distearoylphosphatidylethanolamine, mal-PEG-DSPE (Avanti Polar Lipids) were dissolved in chloroform:methanol (1:1, v/v) in a round-bottom flask in a molar ratio of 1.43:1.29:0.28, respectively. L-α-Phosphatidylethanolamine-N-(lissamine rhodamine B sulfonyl), Rho-PE (Avanti Polar Lipids), was added at 0.2 mol % for fluorescent labeling. Liposomes were formed by rehydration of the lipid film with 300 mM calcium acetate solution pH 7, to a final concentration of 30 mM total lipid (TL). Liposome size was reduced by multiple extrusion steps using a Lipex™ Extruder (Northern Lipids, Burnaby, BC, Canada) through polycarbonate membranes (Nuclepore, Pleasanton, CA, USA) with a final pore size of 100 nm.

2.3 Remote loading of liposomes with AG538

Remote loading of liposomes with AG538 was performed using a calcium acetate gradient [14]. In short, the external liposomal medium (300 mM calcium acetate buffer pH 7) was replaced by 10 mM Hepes/135 mM NaCl buffer pH 7.4 (HBS)

using PD-10 desalting columns (GE Healthcare). The anti-IGF-1R kinase inhibitor AG538 (Calbiochem, San Diego, CA, USA) was dissolved in dimethylsulfoxide to a final concentration of 10 mM. The molar ratio of kinase inhibitor to TL used was 40 nmol/μmol (Supp. Table 1). Liposomes were incubated with AG538 for 45 min at room temperature (RT) and used without purification for Nb coupling as described in Section 2.4 and subsequently purified by Vivaspin centrifugation. Control AG538-liposomes were directly purified or stored overnight at 4 °C before Vivaspin purification (see next section).

2.4 Nanobody coupling to liposomes

Coupling of SATA-modified Nbs to the surface of liposomes was performed as described previously [8]. The molar ratio of Nb to mal-PEG-DSPE used was 8.6 nmol/μmol. After overnight coupling at 4 °C, non-coupled Nb was removed by washing/filtration with HBS and Vivaspin centrifugal concentrators (Sartorius) with a molecular weight membrane cut-off of 100 kDa. In detail, liposomes and an equal volume of HBS were transferred to Vivaspin centrifugal concentrators and centrifuged for 45 min at 4000 G after which the passed volume was replenished with fresh HBS. This was considered one washing/filtration step. This step was repeated once more to ensure that all of the free AG538 and Nb had been removed. To confirm completion of the purification procedure, we have monitored by HPLC whether the final ultrafiltrate of the Vivaspin flowthrough was devoid of free AG538.

2.5 Nanobody capillary electrophoresis-mass spectrometry

Capillary electrophoresis (CE) experiments were carried out on a P/ACE MDQ™ CE instrument (Beckman Coulter, Brea, CA, USA). The separation voltage was -30 kV and the capillary temperature was 20 °C. Fused-silica capillaries (total length, 100 cm; inner diameter, 30 μm, outer diameter, 150 μm) were obtained from Beckman Coulter and were equipped with a porous tip (length, 3-4 cm) to allow sheathless CE-mass spectrometry (MS) interfacing [15-16]. The capillaries were coated with polyethylenimine (PEI) and conditioned by flushing the capillary at 50 psi with air (10 min), methanol (20 min), deionized water (5 min) and background electrolyte (BGE; 10 min). The BGE was 100 mM acetic acid (pH 3.1) containing 5% (v/v) isopropanol (Merck, Darmstadt, Germany). Nb was hydrodynamically injected for 10 s at 5 psi (equal to 1% of the capillary volume). MS detection was performed using a micrOTOF orthogonal-accelerated time-of-flight (TOF) mass spectrometer (Bruker Daltonics, Bremen, Germany). Transfer parameters were optimized by direct infusion of an electrospray ionization (ESI) tuning mix (Agilent Technologies, Waldbronn, Germany). The capillary with the high sensitivity porous sprayer tip was placed in a grounded stainless-steel needle positioned in the ESI source of the

mass spectrometer as described previously [15-16]. The needle was filled with BGE (static conductive liquid) to establish electrical contact with the porous tip. The dry gas temperature and flow were 180°C and 1.0 L min^{-1}, respectively. Electrospray in positive ionization mode was achieved using an ESI voltage of -2.3 kV. CE-MS data were analyzed using Bruker Daltonics DataAnalysis software. For the determination of peak areas, extracted-ion electropherograms (EIEs) were constructed for the respective protein species from their most abundant m/z signal ([M+12H]12+). Protein charge assignment and molecular weight determinations were performed using the 'charge deconvolution' utility of the DataAnalysis software.

2.6 Characterization of liposomes

The phosphate content of the liposome dispersion was determined with a phosphate assay according to Rouser *et al.* [17]. The mean particle size distribution of the liposomes and the polydispersity index were determined by dynamic light scattering using a Malvern CGS-3 multiangle goniometer (Malvern Instruments Ltd., Worcestershire, UK) with a JDS Uniphase 22 mW He–Ne laser operating at 632 nm, an optical fiber-based detector and a digital LV/LSE-5003 correlator. Autocorrelation functions were analyzed by the cumulants method (fitting a single exponential to the correlation function to obtain the mean size and the polydispersity index, PDI) and the CONTIN routine (fitting a multiple exponential to the correlation function to obtain the distribution of particle sizes). All measurements were performed at a 90° angle. The zeta-potential (ζ potential) of the liposomes was determined by laser Doppler electrophoresis using a Zetasizer Nano-Z (Malvern Instruments Ltd.). Liposomes were dissolved in 5 mM Hepes buffer pH 7.4 prior to measurements. AG538 content of the liposomes was determined by high-performance liquid chromatography (HPLC). Vivaspin flow through fractions obtained after liposome purification (Section 2.4) and samples of free AG538 with known concentration were applied to a Waters Acquity HPLC system (Waters Corporation, Milford, MA, USA) using a Sunfire C18 column, at a flow rate of 1 mL/min. Gradient mobile phase was changed during 15 min from 100% solvent A (acetonitrile:H2O:tri fluoroacetic acid 5:95:0.1 w/w/w) to 100% solvent B (acetonitrile:trifluoroacetic acid 100:0.1 w/w), and operated additionally for 7 min on 100% solvent B. UV detection was performed at 380 nm. Nb coupling to liposomes was determined by Western Blotting. Samples were subjected to SDS-PAGE using 4-12% gradient NuPAGE Novex Bis-Tris mini-gels (Invitrogen, Breda, The Netherlands). Proteins were electro-transferred to a nitrocellulose membrane using the iBlot® Dry Blotting system (Invitrogen). Membranes were blocked for 1 h with 5% BSA in Tris-buffered saline containing 0.1% Tween-20 (TBS-T). Membranes were subsequently incubated overnight at 4 °C with rabbit polyclonal anti-VHH serum diluted 1:5000 in 5%

BSA in TBS-T. After washing with TBS-T, membranes were incubated for 1 h at RT with goat anti-rabbit peroxidase-conjugated secondary antibody (Thermo Fischer Scientific, Rockford, IL, USA) diluted 1:1000 in 5% BSA in TBS-T. Proteins were visualized and detected using SuperSignal West Femto Chemiluminescent Substrate (Thermo Fischer Scientific) and a Gel Doc Imaging system equipped with a XRS camera and Quantity One analysis software (Bio-Rad, Hercules, CA, USA).

2.7 Cell line and culture conditions

The human HNSCC cell line UM-SCC-14C (abbreviated as 14C, developed by Dr. T.E. Carey, Ann Arbor, MI, USA) and NIH 3T3 clone 2.2 murine fibroblasts (abbreviated as 3T3 2.2, selected for low endogenous EGFR expression [18]) were cultured in Dulbecco's Modified Eagle's medium (DMEM, PAA, Pasching, Austria) containing 3.7 g/L sodium bicarbonate, 4.5 g/L L-glucose, 2 mM L-glutamine and supplemented with 5% (v/v) foetal bovine serum, penicillin (100 IU/mL), streptomycin (100 µg/mL), and amphotericin B (0.25 µg/mL) at 37 °C in a humidified atmosphere containing 5% CO_2. Tests for mycoplasma infection were regularly performed and cells were consistently found to be mycoplasma-free.

2.8 Competition assay

14C cells were seeded at 15,000 cells/well in 96-well plates (NUNC AS, Roskilde, Denmark). One day after, cells were washed two times with serum free medium and incubated for 1.5 h at 4 °C with 10 nM near-infrared fluorescent (NIRF) IRDye® 800CW EGF Optical Probe (LI-COR Biosciences, Lincoln, NE, USA) and Nb or Nb-coupled liposomes diluted in serum free medium at a final concentration of 0.1 nM-1.0 µM. Cells were washed once with serum free medium and subsequently incubated with DRAQ5™ (Biostatus Limited, Leicestershire, UK) diluted in PBS for 5 min at 4 °C. Cells were washed two times with serum free medium before measurements were performed with an Odyssey® Infrared Imaging System (LI-COR Biosciences) equipped with a solid-state diode laser at 685 nm and at 785 nm. The NIRF-EGF intensity was measured by the 800 nm channel while the DRAQ5 fluorescence intensity was measured by the 700 nm channel for normalization of cell number. Ratios of fluorescence intensities (800/700 nm) were plotted versus the concentrations of the Nbs or Nb-liposomes.

2.9 Flow cytometry

14C or 3T3 2.2 cells were seeded at 50,000 cells/well in 96-well plates (Becton & Dickinson, Mountain View, CA, USA). Cells were incubated in 5% BSA in PBS in the dark at 4 °C for 1 h with rhodamine-labeled liposomes loaded with AG538 (AG538-RhoL), rhodamine-labeled R2-coupled liposomes loaded with AG538

(R2-AG538-RhoL) and rhodamine-labeled EGa1-coupled liposomes loaded with AG538 (EGa1-AG538-RhoL) at a final concentration of 7.8 μM – 1.0 mM TL. Thereafter, cells were washed three times with 0.3% BSA in PBS and fixed with 10% formalin. The mean rhodamine fluorescence intensity was determined with a BD FACSCanto II (Becton & Dickinson). Generally, 10,000 events were acquired per sample, and samples were prepared in triplicates. Data were analyzed with BD FACSDiva™ software (Becton & Dickinson).

2.10 Confocal microscopy

14C or 3T3 2.2 cells were seeded at 8000 cells/well in 16-well chamber slides (Thermo Fischer Scientific). After 24 h, the cells were incubated with rhodamine-labeled liposomes at 0.5 mM TL for either 1 h at 4 °C or 4 h at 37 °C. Next, the cells were washed with PBS and fixed with 4% paraformaldehyde (Fluka, Zwijndrecht, The Netherlands) in PBS. Subsequently, the cells were washed with PBS and incubated with DAPI diluted in PBS for 5 min at RT for nuclear staining. After washing, slides were mounted on glass cover slides, using FluorSave (Calbiochem, San Diego, CA, USA). Cells were analyzed on a Zeiss Axiovert 200 M LSM 5 Pascal confocal laser-scanning microscope (Carl Zeiss MicroImaging GmbH, Jena, Germany) equipped with three lasers: 405 nm diode, 458-488-514 nm argon and 543 nm HeNe.

2.11 Western Blotting

14C or 3T3 2.2 cells were seeded at 100,000 cells/well in 6-well plates. The following day, medium was replaced with either serum free medium (in the case of the phosphoEGFR Western Blot) or serum free medium containing liposomes (in the case of phosphoIGF-1R Western Blot) with a final concentration of 2 mM TL for 4 h at 37 °C. Then, cells were washed with PBS and activated with serum free medium containing 25 ng/mL epidermal growth factor (EGF) and liposomes with a final concentration of 2 mM TL or serum free medium containing 30 ng/mL insulin like growth factor-1 (IGF-1) for 10 min at 37 °C. In case of the EGFR downregulation experiment, overnight seeded cells were incubated for 4 h at 37 °C with liposomes diluted in complete medium to a final concentration of 1 mM TL. After 4 h, the cells were washed with PBS and lysed (see below) or incubated in liposome-free medium for another 20 h, 44 h or 68 h at 37 °C before washing with PBS and lysis. Cells were lysed in radioimmunoprecipitation assay (RIPA) buffer containing protease inhibitors and EDTA for 30 min on ice. Samples were centrifuged for 15 min at 14,000 g and the obtained supernatant was collected. The total protein content was determined using the Micro BCA Assay (Pierce Biotechnology, Rockford, IL, USA). Proteins were size-separated by SDS-PAGE using 4-12% gradient NuPAGE Novex Bis-Tris mini-gels (Invitrogen). Proteins were electro-transferred to a nitrocellulose

membrane using the iBlot® Dry Blotting system (Invitrogen). Membranes were blocked with 5% BSA in TBS-T for 1 h. Membranes were stained overnight at 4 °C with either a rabbit polyclonal antibody against phosphorylated tyrosine residue 1068 of EGFR (Cell Signaling Technology, Inc., Danvers, MA, USA), a rabbit monoclonal antibody against EGFR (Cell Signaling Technology, Inc.), a rabbit monoclonal antibody against phosphorylated tyrosine residue 1135 of IGF-1R β (Cell Signaling Technology, Inc.), a rabbit monoclonal antibody against IGF-1R β (Cell Signaling Technology, Inc.) or a rabbit polyclonal antibody against β-actin (Cell Signaling Technology, Inc.) diluted 1:1000 in 5% BSA in TBS-T. After washing with TBS-T, the membranes were incubated for 1 h at RT with goat anti-rabbit peroxidase-conjugated secondary antibody (Thermo Fischer Scientific) diluted 1:1000 in 5% BSA in TBS-T. Proteins were visualized and detected using SuperSignal West Femto Chemiluminescent Substrate (Thermo Fischer Scientific) and a Gel Doc Imaging system equipped with a XRS camera and Quantity One analysis software (Bio-Rad).

2.12 Cell proliferation assays

Assays were performed to determine the effects of liposome treatment on total cell number and the number of dividing cells. Both assays were performed as a 48 h continuous exposure and a short-term exposure pulse chase assay (4 h pulse followed by 44 h chase). For both assays, 4000 cells/well were seeded into 96-well plates. After 24 h, medium was replaced by fresh medium and a liposome dispersion diluted in HBS was added in final concentrations of 7.8 μM – 2.0 mM TL in sextuplicate. Free AG538 diluted in HBS was added in final concentrations of 0.6 – 80 μM. For the short term exposure assay, the medium was refreshed 4 h after incubation with liposomes. To determine the total cell number, cellular proteins were precipitated by the addition of trichloroacetic acid (TCA) to 4% after 2 days of growth. Cells were washed with water, dried at RT and stained with 0,4% sulforhodamine B (SRB) in 1% acetic acid for 30 min. Excess dye was washed away with 1% acetic acid and cells were dried at RT. Bound dye was extracted with unbuffered 10 mM Tris for 15 minutes and OD values were measured at 510 nm with a Bio-Rad Novapath Microplate Reader (Bio-Rad Laboratories, Veenendaal, The Netherlands). To determine the number of dividing cells, BrdU reagent was added to the cells after 2 days of growth. One day later, the ELISA BrdU-colorimetric immunoassay (Roche Applied Science, Penzberg, Germany) was performed, according to the manufacturer's protocol. After stopping the colorimetric reaction with H_2SO_4, the OD values were measured at 450 nm with the reference wavelength set to 655 nm using a Bio-Rad Novapath Microplate Reader (Bio-Rad Laboratories).

3. Results and discussion

3.1 Preparation and characterization of AG538-loaded nanobody-liposomes

We have recently described EGa1 Nb-liposomes for the inhibition of EGFR positive tumor cells [8]. Although very effective in downregulating EGFR in vitro and in vivo, these empty EGa1 Nb-liposomes only showed a minor effect on tumor growth in vivo [8]. Based on the recognized crosstalk between EGFR and other growth factor receptors [5], we therefore encapsulated an inhibitor of IGF-1R, i.e. AG538, in the interior compartment of the liposomes, forming a targeted dual-active nanomedicine for inhibition of two growth factor signaling cascades involved in tumor cell proliferation. PEGylated liposomes were prepared as described previously [8] by lipid film rehydration in a 300 mM calcium acetate buffer pH 7 and extrusion. After exchange of the external buffer to HBS, AG538 was encapsulated in the liposomes by remote loading based on the calcium acetate trans-membrane gradient [14]. HPLC analysis on non-encapsulated AG538 revealed an average encapsulation efficiency of >90% (Table 1). AG538-loaded liposomes were subsequently equipped

Name	Mean size (nm)	PDI	Mean zeta potential (mV)	AG538 encapsulation efficiency (%)
EGa1-L	134 ± 5	0.08 ± 0.04	17 ± 9	n/a*
AG538-L	130 ± 5	0.08 ± 0.03	19 ± 11	> 90%
EGa1-AG538-L	140 ± 7	0.13 ± 0.04	18 ± 10	> 90%

Table 1. Liposome characteristics. *n/a = not applicable

with EGa1 Nb via maleimidyl groups present on the distal end of PEG chains on the liposomes. For this purpose, EGa1 was first modified with an 8-fold excess of the thioacetyl linker SATA, thus allowing the attachment of multiple PEG-anchor groups per Nb. The number of introduced SATA groups in the Nb was determined by CE-TOF-MS showing a cluster of nine peaks for the SATA-modified EGa1 (Fig. 1A). Deconvolution of the mass spectra obtained in the apices of the respective peaks revealed the masses of the parent EGa1 (peak 9) and of EGa1 modified to varying degrees (peaks 1-8, respectively) (Fig. 1B). The increase in masses corresponded to the calculated increase in mass resulting from introduction of SATA groups (116 Da) (Fig. 1B). EGa1 carrying 3-6 SATA modifications accounted for more than 85% of the relative peak area (Fig. 1B). Next, several liposome formulations were prepared: empty EGa1-coupled liposomes (EGa1-L), non-targeted liposomes loaded with AG538 (AG538-L) and EGa1-coupled liposomes loaded with AG538 (EGa1-

AG538-L). On average, the produced liposomes possessed a mean size of about 130 nm and a mean zeta-potential of 18 mV (Table 1).

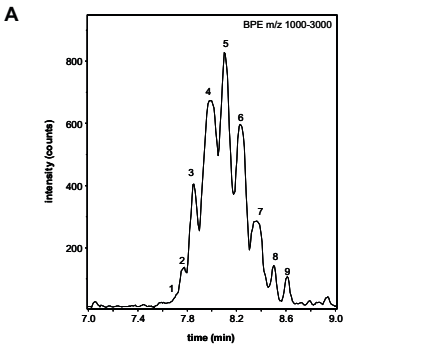

Number of SATA modifications/ nanobody	Peak no.	Theoretical M_w (Da)	Measured M_w (Da)	Relative peak area (%)
non-modified	9	18300	18300.8	0.7
1 SATA	8	18416	18416.8	1.6
2 SATA	7	18532	18532.6	5.7
3 SATA	6	18648	18649.8	15
4 SATA	5	18764	18765.9	25
5 SATA	4	18880	18881.5	33
6 SATA	3	18996	18997.4	13
7 SATA	2	19112	19114.8	3.6
8 SATA	1	19228	19230.6	1.9

86%

Figure 1. Characterization of EGa1 nanobody and its coupling to liposomes. **A**. Base-peak electropherogram (m/z 1000-3000) obtained during the CE-TOF-MS analysis of SATA-modified EGa1. **B**. Assignment of peaks, theoretical and measured deconvoluted molecular masses (Mw) and relative peak area detected during CE-TOF-MS of SATA-modified EGa1. **C**. EGa1, SATA-EGa1, empty control liposomes (L), AG538-loaded liposomes (AG538-L), nanobody (Nb)-liposomes (EGa1-L) and AG538-loaded Nb-liposomes (EGa1-AG538-L) were size separated by SDS-PAGE and Nb coupling to liposomes was determined by Western blotting. **D**. EGFR-(over)expressing 14C cells were simultaneously incubated with 10 nM of near-infrared fluorescently-labeled EGF (NIRF-EGF) and either control Nb that does not compete with EGF for receptor binding (EGc9), anti-EGFR Nb (EGa1), SATA-modified EGa1 (SATA-EGa1) or EGa1-AG538-L for 1.5 h at 4 °C. The NIRF-EGF signal was plotted vs. the free or liposomal Nb concentration. Data are presented as mean ± SEM of one representative experiment performed in triplicate.

To confirm that EGa1 was successfully conjugated to the liposomes, Western Blotting was performed (Fig. 1C). Both unmodified EGa1 and SATA-modified EGa1 (SATA-EGa1) migrated as a band of approximately 18 kDa, corresponding to the molecular weight of one molecule of EGa1 (18.3 kDa). Empty non-targeted control liposomes (L) and AG538-L did not display any bands while both EGa1-L and EGa1-AG538-L displayed bands between 20 and 30 kDa. Visible bands in Figure 1C corresponded to the molecular weight of EGa1 coupled to one, two or

three maleimide-PEG-DSPE anchors (2.9 kDa per unit). When the brightness of the photo was increased, an additional band was observed corresponding to the molecular weight of EGa1 coupled to four maleimide-PEG-DSPE anchors, as well as a band corresponding to the molecular weight of unmodified EGa1, indicating a small fraction of uncoupled EGa1 (data not shown). These results are in line with our previous findings [8]. The number of maleimide-PEG-DSPE anchors that were ultimately coupled (1-4) to EGa1 was lower than the available SATA-modifications (3-6) introduced in the majority of the Nb, indicating that not all available SATA-groups were accessible for coupling, possibly by steric hindrance or due to shielding of the Nb surface by the attached PEG chains. Given that EGa1 is an antagonist of EGFR [11], competition assays with EGF can be performed to determine whether SATA-modification of EGa1 or its coupling to liposomes had compromised its binding capacity to EGFR. For this, binding assays on EGFR-(over)expressing 14C cells in the presence of EGF labeled with a near-infrared fluorescent (NIRF)-EGF were performed (Fig. 1D). As expected, EGa1, SATA-EGa1 and EGa1-AG538-L displayed similar competition with NIRF-EGF for binding to 14C cells indicating that neither SATA-modification nor coupling to liposomes prohibited the interaction of EGa1 with the targeted receptor. In addition, the control Nb EGc9 was not able to compete with NIRF-EGF, not even when there was a 100-fold molar excess present, which is in agreement with other studies (Heukers *et al., manuscript in preparation*).

3.2 Anti-EGFR nanobody-liposomes bind specifically to EGFR-(over) expressing cells

The ability of EGa1 to recognize EGFR-(over)expressing cells was then demonstrated with cell association studies. For this purpose, rhodamine-labeled liposomes were prepared, as well as fluorescently labeled negative control liposomes equipped with the anti-RR6 Nb R2 [12]. Characteristics of the rhodamine-labeled liposomes

Figure 2. Cell association and uptake of AG538-loaded nanobody-liposomes. **A**. EGFR-(over)expressing 14C cells were incubated for 1 h at 4 °C with rhodamine-labeled liposomes (RhoL) loaded with AG538 (AG538-RhoL), R2 nanobody-coupled liposomes loaded with AG538 (R2-AG538-RhoL) as a control formulation or EGa1-coupled liposomes loaded with AG538 (EGa1-AG538-RhoL). The mean fluorescence intensity was determined by flow cytometry. Data are presented as mean ± SEM of one representative experiment performed in duplicate. **B**. EGFR-/- 3T3 2.2 cells were incubated for 1h at 4 °C with AG538-RhoL, R2-AG538-RhoL and EGa1-AG538-RhoL and mean fluorescence intensity values were determined by flow cytometry. Data are presented as mean ± SEM of one representative experiment performed in duplicate. **C**. Confocal microscopy images of 14C cells (blue staining represents cell nuclei) incubated for 1 h at 4 °C with RhoL (red staining represents liposomes). **D**. Confocal microscopy images of 3T3 2.2 cells incubated for 1 h at 4 °C with RhoL. **E**. Confocal microscopy images of 14C cells incubated for 4 h at 37 °C with RhoL. F. Confocal microscopy images of 3T3 2.2 cells incubated for 4 h at 37 °C with RhoL.

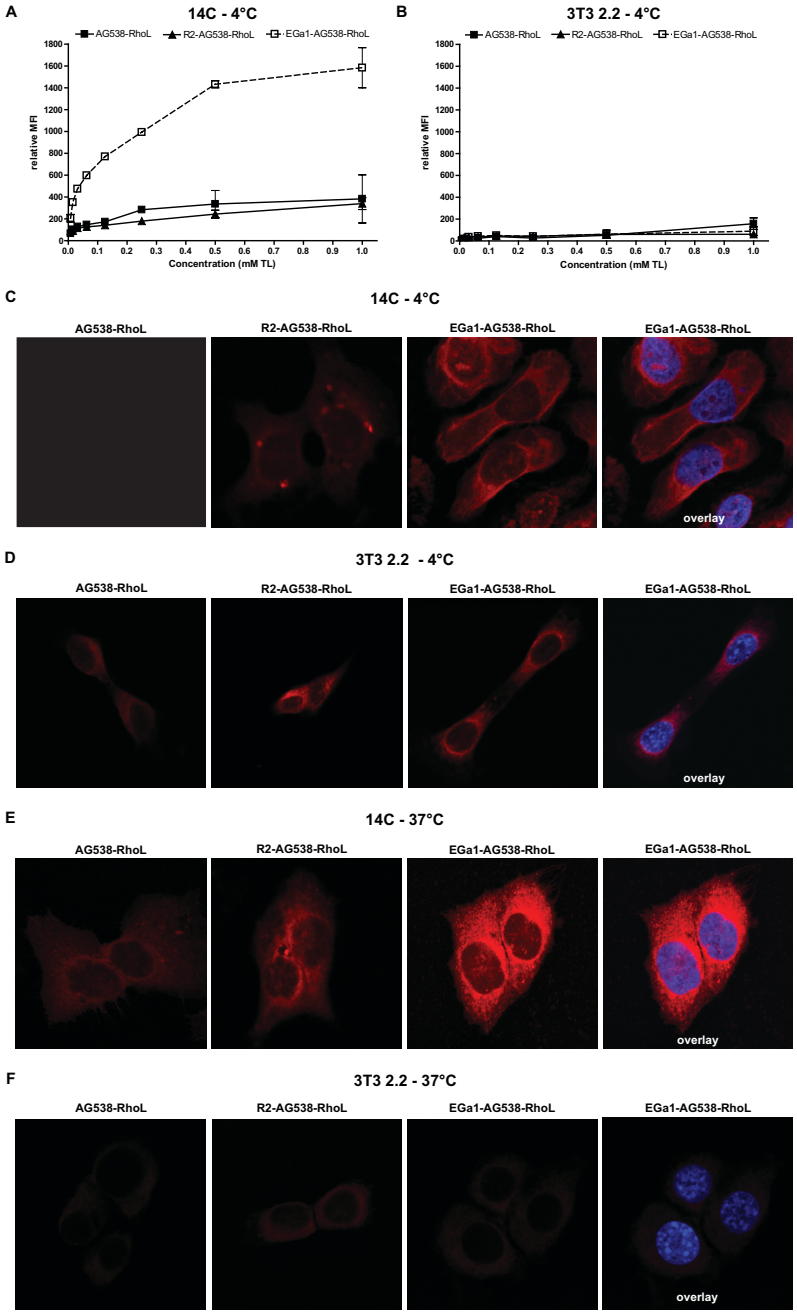

(RhoL) such as size and zeta-potential were similar to unlabeled liposomes (Supp. Table 1). 14C cells or 3T3 2.2 cells as a non-EGFR expressing control were incubated with liposomes for 1 h at 4 °C (to inhibit cell uptake processes) after which cell association was determined by flow cytometry. EGa1-AG538-RhoL associated with 14C cells in a dose-dependent manner whereas AG538-RhoL or R2-AG538-RhoL

did not (Fig. 2A).
Indeed, EGa1-AG538-RhoL at a concentration of 0.3 mM TL and at higher concentrations generally displayed mean fluorescence intensity values four times higher than control formulations (Fig. 2A). These results are in agreement with our previous findings with empty EGa1-liposomes, indicating that encapsulation of AG538 did not compromise the interaction of the EGa1-liposomes with the cells. Incubation of 3T3 2.2 cells with all types of RhoL demonstrated only low levels of cell association, demonstrating that non-specific cellular interactions are low for the developed liposomal platform (Fig. 2B). Expression levels of EGFR in the used cell types were confirmed by Western blotting (Supp. Fig. 1). Interaction of the liposomes with 14C and 3T3 2.2 cells was also visualized by means of confocal microscopy, confirming the above described data when RhoL were incubated with 14C cells (Fig. 2C) or 3T3 2.2 cells (Fig. 2D) for 1 h at 4 °C. Only EGa1 equipped liposomes showed association with the intended target cell type but not to the cells devoid of EGFR. When cells were incubated for 4 h at 37 °C, thus allowing internalization of EGa1-AG538-RhoL, a distinct dotted pattern of the rhodamine fluorescence could be observed, suggesting uptake of EGa1-AG538-L via receptor mediated endocytosis (Fig. 2E). Incubation of 3T3 2.2 cells for 4 h at 37 °C did not result in uptake of any of the formulations which is in agreement with cell association results at 4 °C (Fig. 2F). The observed high degree of cell association and uptake of EGa1-liposomes by EGFR-expressing 14C cells is probably due to a combination of the high affinity and specificity of EGa1 for EGFR and the coupling of multiple EGa1 to one liposome (Fig. 1C). It is highly likely that this multivalent system interacts with multiple EGFR simultaneously, resulting in clustering of EGFR followed by swift internalization and lysosomal degradation of the receptor (Heukers *et al., manuscript in preparation*) [8, 19].

3.3 Nanobody-liposomes prevent activation of EGFR

EGa1 present on the liposomes serves as a targeting ligand to specifically target EGFR-(over)expressing cells and to enhance the uptake of AG538-loaded liposomes by clustering of EGFR (Heukers *et al., manuscript in preparation*). In addition, EGa1 can antagonize binding of EGF to EGFR, thereby blocking activation of the receptor and subsequent downstream signaling. To determine whether EGa1-AG538-L were indeed able to block EGFR activation, the phosphorylation EGFR was detected by Western Blotting (Fig. 3). 14C cells were serum-starved for 4 h at 37 °C followed by 10 min incubation with EGF and liposomes. Figure 3 demonstrates that tyrosine residue (Tyr) 1068 was strongly phosphorylated in presence of EGF, while cells that were incubated with EGF and EGa1-L or EGa1-AG538-L did not display Tyr1068 phosphorylation. No change in total levels of EGFR was detected in this assay setup,

demonstrating that the observed inhibition in tyrosine phosphorylation was due to the antagonistic blockade of EGF-EGFR interaction by EGa1-liposomes. These results are consistent with our previous study, showing that loading of AG538 did not compromise the antagonistic action of the EGa1-liposomes.

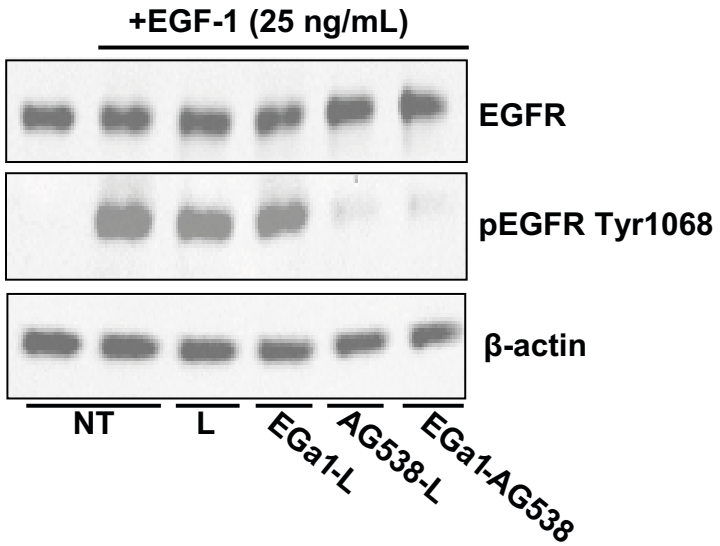

Figure 3. EGa1 nanobody-liposomes block activation of EGFR. 14C cells were serum starved for 4 h followed by simultaneous incubation with EGF and either empty control liposomes (L), kinase inhibitor-loaded liposomes (AG538-L), anti-EGFR nanobody (Nb)-liposomes (EGa1-L) or anti-EGFR Nb-liposomes loaded with kinase inhibitor (EGa1-AG538-L). Cell lysates were collected and subjected to SDS-PAGE. Levels of total EGFR, phosphorylated EGFR (pEGFR Tyr1068) and β-actin (loading control) were detected by Western Blotting.

3.4 AG538-loaded nanobody-liposomes block IGF-1R activation

The ability of EGa1-AG538-L to block IGF-1R activation was investigated by detecting the phosphorylation of Tyr1135 of IGF-1R by means of Western Blotting (Fig. 4). 14C cells were incubated with liposomes in serum free medium for 4 h at 37 °C followed by 10 min incubation with IGF-1 in serum free medium. Unlike blockade of EGFR by EGa1 on the liposomes which can occur extracellularly, internalization of EGa1-AG538-L and processing of the liposomes are necessary for AG538 to execute its function. The liposomal structure needs to destabilize and AG538 has to dissociate from its counterion calcium, and finally AG538 needs to escape from the endosome or lysosome and reach the cytosol to associate with IGF-1R. Figure 4 demonstrates that phosphorylation of Tyr1135 in IGF-1R occurred when 14C cells were activated with IGF-1. Non-targeted AG538-L appeared to have no effect on Tyr1135 phosphorylation. Importantly, cells that were incubated with EGa1-AG538-L had an almost completely blocked IGF-1R Tyr1135 phosphorylation

while levels of total IGF-1R were not affected. These results demonstrated the cellular uptake of EGa1-AG538-L and intracellular release of AG538 within 4 h. The results depicted in Figure 3 and 4 taken together demonstrate that EGa1-AG538-L were able to block the activation of both EGFR and that of IGF-1R.

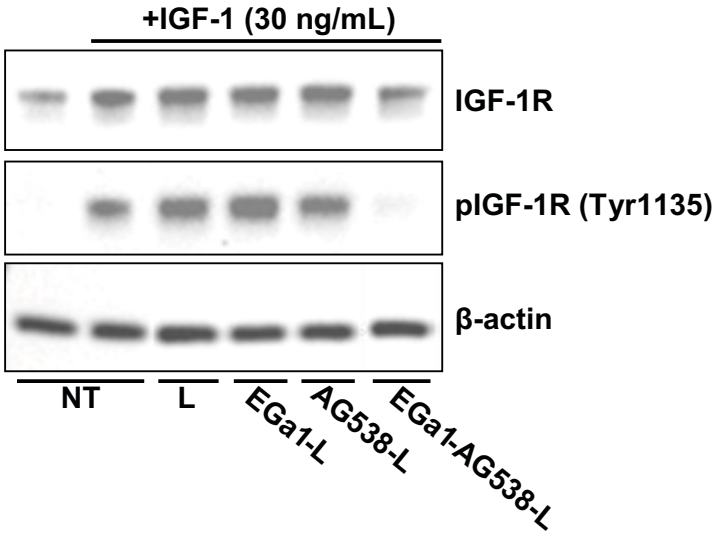

Figure 4. EGa1 nanobody-liposomes loaded with AG538 block activation of IGF-1R. 14C cells were simultaneously serum starved and incubated with either empty control liposomes (L), kinase inhibitor-loaded liposomes (AG538-L), anti-EGFR nanobody (Nb)-liposomes (EGa1-L) or anti-EGFR Nb-liposomes loaded with kinase inhibitor (EGa1-AG538-L) for 4 h followed by 10 min activation with IGF-1. Cell lysates were collected and subjected to SDS-PAGE. Levels of total IGF-1R, phosphorylated IGF-1R (pIGF-1R Tyr1135) and β-actin (loading control) were detected by Western blotting.

3.5 Nanobody-liposomes induce EGFR downregulation

In addition to antagonistic blockade of EGFR-phosphorylation, multivalent EGa1-liposomes have been shown to reduce total EGFR levels by enhanced sequestration and degradation if the receptor [8]. Figure 5 shows that EGa1-AG538-L strongly reduced EGFR expression, as determined by Western Blotting. 14C cells were exposed to liposomes for 4 h after which the medium was replaced by drug-free medium. As shown in the upper panels (Fig. 5A), EGFR downregulation was most pronounced at 44 h and 68 following the initial incubation with EGa1-equipped liposomes, while empty control liposomes or AG538-L did not reduce EGFR expression. Remarkably, EGa1-AG538-L induced stronger EGFR downregulation when compared to EGa1-L which was most pronounced after three days, i.e. at the 4 + 68 h timepoint (Fig. 5B). This results suggests that blocking IGF-1R activation via AG538 will effectuate cellular responses that contribute to overall downregulation

of the EGFR pathway

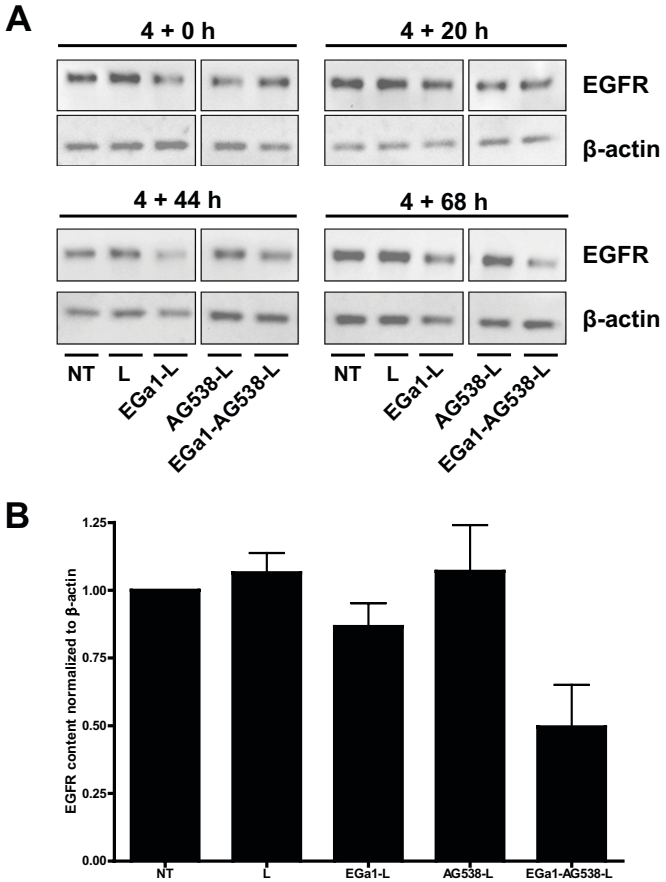

Figure 5. EGa1-AG538-L induce EGFR downregulation. **A**. 14C cells were exposed for 4 h to control liposomes (L), anti-EGFR nanobody (Nb)-liposomes (EGa1-L), kinase inhibitor-loaded liposomes (AG538-L) or anti-EGFR Nb-liposomes loaded with kinase inhibitor (EGa1-AG538-L) after which the medium was replaced and cells were left to proliferate for 68 h. Cells lysates were taken after 0 h, 20 h, 44 h and 68 h after incubation and subjected to SDS-PAGE. Levels of total EGFR and β-actin (loading control) were detected by Western blotting. **B**. Ratio's of the intensity of EGFR bands normalized to β-actin bands (non-treated set to 100%) after 4 h incubation with the indicated liposomal formulation followed by incubation in drug-free medium for 68 h. Data are presented as mean ± SEM of two independent experiments.

3.6 AG538-loaded nanobody-liposomes induce strongly enhanced inhibition of tumor cell proliferation

To compare the efficacy of EGa1-AG538-L and empty EGa1-L on the growth of 14C cells, effects of liposome treatment on the total cell number and cell division

were determined by SRB assay and BrdU ELISA, respectively. These experiments were conducted upon continuous exposure to the liposomes for 48 h and after

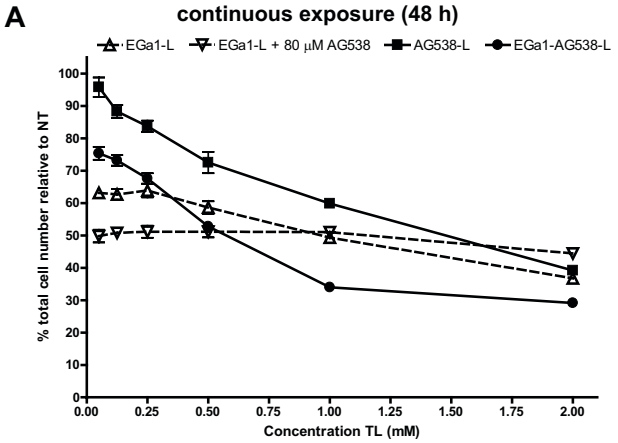

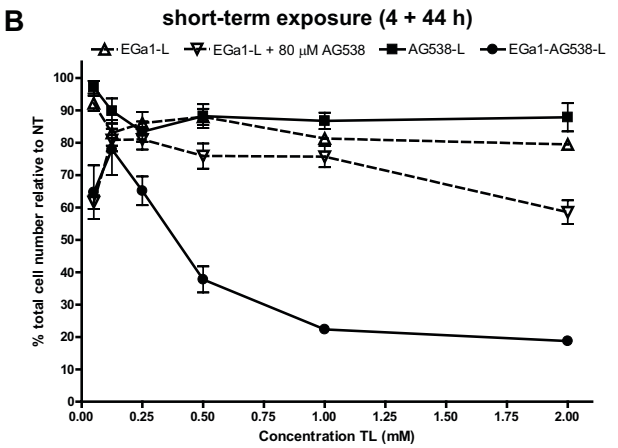

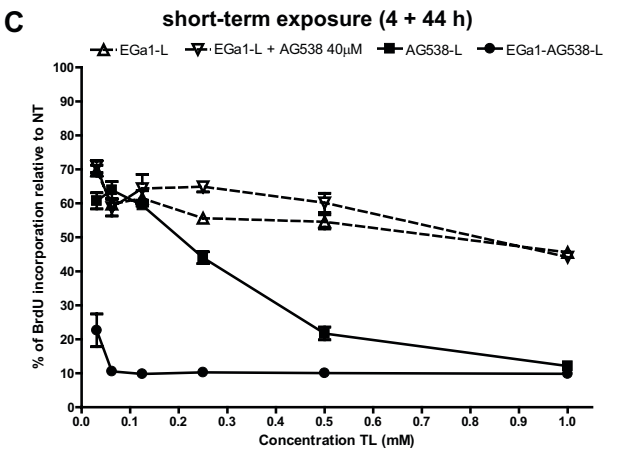

Figure 5. AG538-loaded EGa1 nanobody-liposomes inhibit tumor cell proliferation. A. 14C cells were exposed for 48 h to nanobody (Nb)-liposomes (EGa1-L), Nb-liposomes in the presence of free kinase inhibitor (EGa1-L + 80 μM AG538), kinase inhibitor-loaded liposomes (AG538-L) and kinase inhibitor-loaded Nb-liposomes (EGa1-AG538-L). Total cell number was determined by sulforhodamine B (SRB) assay. Data are presented as mean ± SEM of one representative experiment performed in sextuplicate. B. 14C cells were exposed for 4 h to EGa1-L, EGa1-L + 80 μM AG538, AG538-L and EGa1-AG538-L after which the medium was replaced and cells were allowed to proliferate for 44 h. Total cell number was determined by SRB assay. Data are presented as mean ± SEM of one representative experiment performed in sextuplicate. C. 14C cells were exposed for 4 h to EGa1-L, EGa1-L + 40 μM AG538, AG538-L and EGa1-AG538-L after which the medium was replaced and cells were allowed to proliferate for 44 h. After 48 h the medium was replaced with medium containing BrdU and cells were left to proliferate overnight, after which BrdU incorporation was determined by ELISA. Data are presented as mean ± SEM of one representative experiment performed in sextuplicate.

short-term exposure for 4 h followed by a 44 h treatment-free period. Such latter experimental conditions mimic in vivo drug exposure, in which drug peak levels are alternated with drug-free periods.

Free AG538 showed partial inhibition of tumor cell proliferation in a dose-dependent way, reaching ~60% inhibition of total cell numbers (Supp. Fig. 2A) and ~40% inhibition of proliferation (Supp. Fig 2B) at a concentration of 40 μM upon continuous exposure. These effects were however lost when the compound was tested in the short-term exposure assay, due to redistribution of the small molecule drug from the cells into the drug-free medium. Empty EGa1-L and EGa1-AG538-L showed efficacy upon continuous exposure, reducing cell numbers by ~70% at a concentration of 2 mM TL (Fig. 6A). The effects of EGa1-L are in accordance with results of our previous study [8]. In contrast, upon short-term exposure, EGa1-L reduced cell numbers by only ~20% at similar concentrations while the combination with a high dose of free AG538 only increased the efficacy of EGa1-L to ~40% reduction of total cell numbers (Fig. 6B). EGa1-AG538-L, on the other hand, showed a strong inhibition of total cell number, reducing total cell numbers by 70% in continuous exposure assays (Fig. 6A) and 80% in short-term exposure assays (Fig. 6B). Lastly, AG538-L without Nb ligands were inactive in the short-term assay and only showed activity after continuous exposure, which can be explained by some residual aspecific uptake of the liposomes upon continuous incubation (Fig. 6A-B). Effects on 14C cell division were studied by quantification of BrdU incorporation (Fig. 6C). EGa1-AG538-L effectively reduced the number of proliferating cells by ~90% even in the short-term assay (Fig. 6C). Interestingly, AG538-L demonstrated similar efficacy at high concentrations, but both formulations showed largely different IC_{50} values (21.7 μM TL versus 210 μM TL for EGa1-AG538-L and AG538-L, corresponding to a 10-fold difference in potency). EGa1-L and EGa1-L plus free

AG538 (40 μM) reduced the number of proliferating cells by just ~50% (Fig. 6C). These results highlight the added value of Nb-liposomes for the intracellular delivery of AG538 into tumor cells. Although AG538-L (at high concentrations) is able to inhibit the number of dividing cells by delivery of AG538, only EGa1-AG538-L is able to significantly reduce the total number of cells after short-term exposure. The rapid cell uptake and robust effect of EGa1-AG538-L that already takes place within a short incubation period results in efficient delivery of AG538 and in combination with EGFR antagonism and downregulation, a long-lasting inhibitory effect on 14C tumor cell proliferation is observed. We also investigated the efficacy of EGa1-AG538-L on a different EGFR-positive cell line, i.e. MDA-MB-468 human breast cancer cells. In the short-term exposure assay, EGa1-AG538-L reduced total cell numbers by ~75% where control formulations barely reduced cell numbers (Supp. Fig. 3A), indicating that the developed nanomedicine might be effective in inhibiting proliferation of a range of tumor cell types which are dependent on EGFR/IGF-1R signaling. Of note, free AG538 partially reduced total cell numbers in a dose-dependent way upon continuous exposure but did not so upon short-term exposure (Supp. Fig. 3B).

A number of studies have demonstrated enhanced efficacy of simultaneous inhibition of EGFR/IGF-1R as compared to mono-targeted growth factor receptor inhibiting therapies, generally by combining existing anti-EGFR and anti-IGFR therapeutics such as TKIs and mAbs. For example, combination treatment of colon adenoma bearing mice with the anti-EGFR KI gefitinib and the anti-IGF-1R KI AZ12253801 was more effective than either treatment alone [20]. Dual treatment of mice bearing cutaneous squamous-cell carcinoma xenografts with a combination of the anti-EGFR mAb cetuximab and the anti-IGF-1R mAb A12 resulted in a significant reduction in tumor volume compared to mono-treatment [21]. The now developed EGa1-AG538-L nanomedicine possesses several advantages when compared to classical combination therapies. Liposomal encapsulation of AG538 might reduce side-effects when compared to the free drug given systemically by avoiding non-targeted tissues. Due to long circulation and leaky vasculature of tumors, long-circulating liposomes accumulate to a higher extent in tumors when compared to free drug because of the enhanced permeability and retention effect [22]. Moreover, the presence of EGa1 on the liposomes ensures cell-specific and rapid uptake into the targeted cells. Finally, the intracellularly deposited liposomes provide a depot of AG538, which was capable of maintaining active intracellular drug levels even when extracellular drug was washed away. It is now apparent that targeting of multiple kinase pathways is required for achieving effective anti-cancer therapy and to reduce the risk of therapy-induced tumor resistance. In this study, simultaneous targeting of EGFR/IGF-1R was shown to be much more effective when compared to targeting of

a single pathway. The multivalent Nb liposomal system loaded with kinase inhibitor utilized in this study is easily adjustable and very well suited for cancer treatment by targeting different combinations of (over)expressed receptors on tumors such as EGFR/HER-2 and EGFR/vascular endothelial growth factor.
In conclusion, AG538-loaded anti-EGFR Nb-liposomes are able to block EGFR and IGF-1R activation, cause EGFR downregulation and induce a strong inhibition of tumor cell proliferation in short-term exposure assays. This targeted nanomedicine is a promising anti-cancer therapy for tumors that are dependent on (over)expression of EGFR and IGF-1R and their in vivo applicability is currently under investigation.

Acknowledgements

R. van der Meel and I. Altintaş are supported by the Utrecht University Focus and Massa program Nanobullets: The next generation in drug targeting. S. Oliveira is supported by the Center for Translational Molecular Medicine (MAMMOTH project). R.C. Roovers is supported by STW grant 10074.

References

1. Oliveira, S., van Bergen en Henegouwen, P.M., Storm, G., Schiffelers, R.M., Molecular biology of epidermal growth factor receptor inhibition for cancer therapy, Expert Opin Biol Ther, 6 (2006) 605-617.
2. Ciardiello, F., Tortora, G., EGFR antagonists in cancer treatment, N Engl J Med, 358 (2008) 1160-1174.
3. Harandi, A., Zaidi, A.S., Stocker, A.M., Laber, D.A., Clinical Efficacy and Toxicity of Anti-EGFR Therapy in Common Cancers, J Oncol, 2009 (2009) 567486.
4. Wheeler, D.L., Dunn, E.F., Harari, P.M., Understanding resistance to EGFR inhibitors-impact on future treatment strategies, Nat Rev Clin Oncol, 7 (2010) 493-507.
5. van der Veeken, J., Oliveira, S., Schiffelers, R.M., Storm, G., van Bergen En Henegouwen, P.M., Roovers, R.C., Crosstalk between epidermal growth factor receptor- and insulin-like growth factor-1 receptor signaling: implications for cancer therapy, Curr Cancer Drug Targets, 9 (2009) 748-760.
6. Pollak, M., Insulin and insulin-like growth factor signalling in neoplasia, Nat Rev Cancer, 8 (2008) 915-928.
7. Gualberto, A., Pollak, M., Emerging role of insulin-like growth factor receptor inhibitors in oncology: early clinical trial results and future directions, Oncogene, 28 (2009) 3009-3021.
8. Oliveira, S., Schiffelers, R.M., van der Veeken, J., van der Meel, R., Vongpromek, R., van Bergen En Henegouwen, P.M., Storm, G., Roovers, R.C., Downregulation of EGFR by a novel multivalent nanobody-liposome platform, J Control Release, 145 (2010) 165-175.
9. Hamers-Casterman, C., Atarhouch, T., Muyldermans, S., Robinson, G., Hamers, C., Songa, E.B., Bendahman, N., Hamers, R., Naturally occurring antibodies devoid of light chains, Nature, 363 (1993) 446-448.
10. Blum, G., Gazit, A., Levitzki, A., Substrate competitive inhibitors of IGF-1 receptor kinase, Biochemistry, 39 (2000) 15705-15712.
11. Hofman, E.G., Ruonala, M.O., Bader, A.N., van den Heuvel, D., Voortman, J., Roovers, R.C., Verkleij, A.J., Gerritsen, H.C., van Bergen En Henegouwen, P.M., EGF induces coalescence of different lipid rafts, J Cell Sci, 121 (2008) 2519-2528.
12. Spinelli, S., Frenken, L.G., Hermans, P., Verrips, T., Brown, K., Tegoni, M., Cambillau,

C., Camelid heavy-chain variable domains provide efficient combining sites to haptens, Biochemistry, 39 (2000) 1217-1222.
13. Roovers, R.C., Henderikx, P., Helfrich, W., van der Linden, E., Reurs, A., de Bruine, A.P., Arends, J.W., de Leij, L., Hoogenboom, H.R., High-affinity recombinant phage antibodies to the pan-carcinoma marker epithelial glycoprotein-2 for tumour targeting, Br J Cancer, 78 (1998) 1407-1416.
14. Zucker, D., Marcus, D., Barenholz, Y., Goldblum, A., Liposome drugs' loading efficiency: a working model based on loading conditions and drug's physicochemical properties, J Control Release, 139 (2009) 73-80.
15. Haselberg, R., Harmsen, S., Dolman, M.E., de Jong, G.J., Kok, R.J., Somsen, G.W., Characterization of drug-lysozyme conjugates by sheathless capillary electrophoresis-time-of-flight mass spectrometry, Anal Chim Acta, 698 (2011) 77-83.
16. Haselberg, R., Ratnayake, C.K., de Jong, G.J., Somsen, G.W., Performance of a sheathless porous tip sprayer for capillary electrophoresis-electrospray ionization-mass spectrometry of intact proteins, J Chromatogr A, 1217 (2010) 7605-7611.
17. Rouser, G., Fkeischer, S., Yamamoto, A., Two dimensional then layer chromatographic separation of polar lipids and determination of phospholipids by phosphorus analysis of spots, Lipids, 5 (1970) 494-496.
18. Honegger, A.M., Dull, T.J., Felder, S., Van Obberghen, E., Bellot, F., Szapary, D., Schmidt, A., Ullrich, A., Schlessinger, J., Point mutation at the ATP binding site of EGF receptor abolishes protein-tyrosine kinase activity and alters cellular routing, Cell, 51 (1987) 199-209.
19. Friedman, L.M., Rinon, A., Schechter, B., Lyass, L., Lavi, S., Bacus, S.S., Sela, M., Yarden, Y., Synergistic down-regulation of receptor tyrosine kinases by combinations of mAbs: implications for cancer immunotherapy, Proc Natl Acad Sci U S A, 102 (2005) 1915-1920.
20. Shaw, P.H., Maughan, T.S., Clarke, A.R., Dual inhibition of epidermal growth factor and insulin-like 1 growth factor receptors reduce intestinal adenoma burden in the Apc(min/+) mouse, Br J Cancer, 105 (2011) 649-657.
21. Galer, C.E., Corey, C.L., Wang, Z., Younes, M.N., Gomez-Rivera, F., Jasser, S.A., Ludwig, D.L., El-Naggar, A.K., Weber, R.S., Myers, J.N., Dual inhibition of epidermal growth factor receptor and insulin-like growth factor receptor I: reduction of angiogenesis and tumor growth in cutaneous squamous cell carcinoma, Head Neck, 33 (2011) 189-198.
22. Fang, J., Nakamura, H., Maeda, H., The EPR effect: Unique features of tumor blood vessels for drug delivery, factors involved, and limitations and augmentation of the effect, Adv Drug Deliv Rev, 63 (2011) 136-151.

Supplementary material

Name	Molar ratio AG538 / TL (nmol/µmol)	Mean size (nm)	PDI	Mean zeta potential (mV)	AG538 encapsulation efficiency (%)
AG538-L	10	119	0.08	18	> 90%
AG538-L	20	124	0.06	19	> 90%
AG538-RhoL	40	133	0.05	14	> 90%
R2-AG538-RhoL	40	133	0.07	17	> 90%
EGa1-AG538-RhoL	40	141	0.11	17	> 90%
R2-AG538-L	40	130	0.03	15	> 90%

Supplementary Table 1. Liposome characteristics. Data are presented as mean values of one representative batch of liposomes

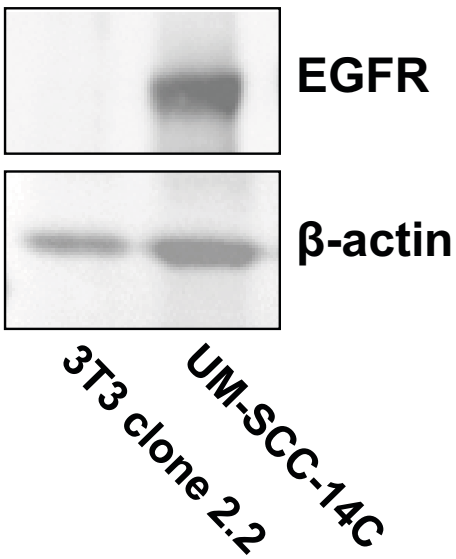

Supplementary Figure 1. 14C and 3T3 2.2 expression EGFR. Cell lysates of NIH 3T3 clone 2.2 and UM-SCC-14C cells were collected and subjected to SDS-PAGE. Levels of total EGFR and β-actin (loading control) were detected by Western Blotting.

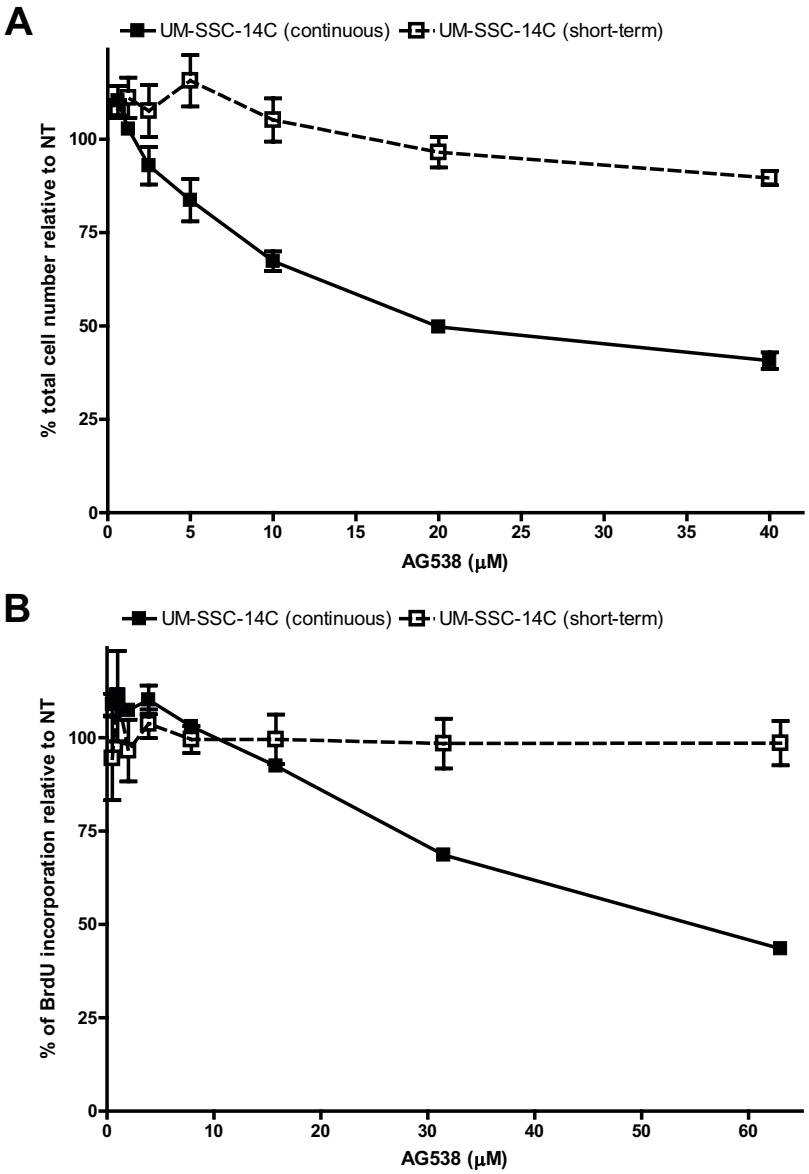

Supplementary Figure 2. AG538 inhibits 14C tumor cell proliferation. **A**. UM-SCC-14C (14C) cells were exposed to AG538 either continuously for 48 h or for 4 h after which the medium was replaced and cells were allowed to proliferate for 44 h. Total cell number was determined by sulforhodamine B (SRB) assay. Data are presented as mean ± SEM of one representative experiment performed in sextuplicate. **B**. 14C cells were exposed to AG538 either continuously for 48 h or for 4 h after which the medium was replaced and cells were allowed to proliferate for 44 h. After 48 h the medium was replaced with medium containing BrdU and cells were left to proliferate overnight, after which BrdU incorporation was determined by ELISA. Data are presented as mean ± SEM of one representative experiment performed in sextuplicate.

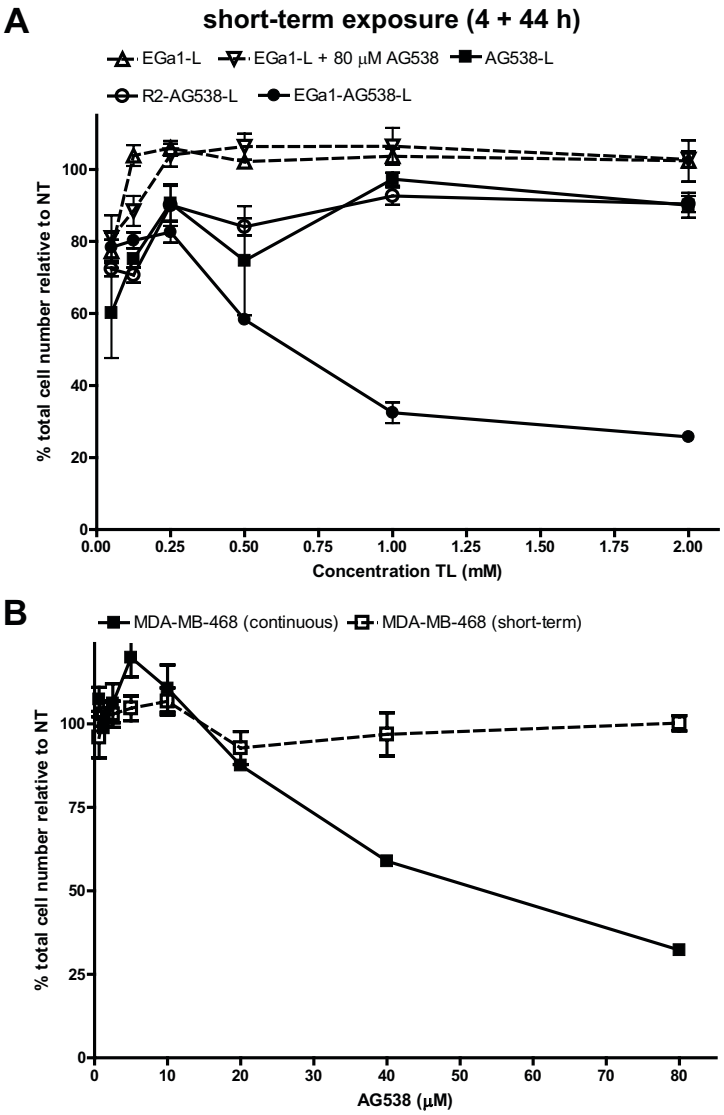

Supplementary Figure 3. Free and liposomal AG538 inhibit MDA-MB-468 tumor cell proliferation. **A**. MDA-MB-468 cells were exposed to nanobody (Nb)-liposomes (EGa1-L), Nb-liposomes in the presence of free kinase inhibitor (EGa1-L + 80 μM AG538), kinase inhibitor-loaded liposomes (AG538-L), R2 Nb-coupled liposomes loaded with kinase inhibitor (R2-AG538-L) and kinase inhibitor-loaded Nb-liposomes (EGa1-AG538-L) for 4 h after which the medium was replaced and cells were allowed to proliferate for 44 h. Total cell number was determined by sulforhodamine B (SRB) assay. Data are presented as mean ± SEM of one representative experiment performed in sextuplicate. **B**. MDA-MB-468 cells were exposed to AG538 either continuously for 48 h or for 4 h after which the medium was replaced and cells were allowed to proliferate for 44 h. Total cell number was determined by SRB assay. Data are presented as mean ± SEM of one representative experiment performed in sextuplicate.

Chapter 4
Inhibition of cell survival pathways *in vitro* by targeted anti-EGFR/IGF-1R Nanobullets predicts anti-tumor efficacy

Roy van der Meel[a], Sabrina Oliveira[b,c], Işil Altintaş[a], Raimond Heukers[b], Ebel H.E. Pieters[a], Paul M.P. van Bergen en Henegouwen[b], Gert Storm[a,d], Wim E. Hennink[a], Robbert J. Kok[a], Raymond M. Schiffelers[a,e]

[a] Department of Pharmaceutics, Utrecht Institute for Pharmaceutical Sciences (UIPS), Faculty of Science, Utrecht University, Universiteitsweg 99, 3584 CG Utrecht, The Netherlands

[b] Division Cell Biology, Department of Biology, Faculty of Science, Utrecht University, Padualaan 8, 3584 CH Utrecht, The Netherlands

[c] Department of Pathology, University Medical Center Utrecht, Utrecht, The Netherlands

[d] Department of Targeted Therapeutics, MIRA Institute for Biomedical Technology and Technical Medicine, University of Twente, Enschede, The Netherlands

[e] Department of Clinical Chemistry and Hematology, University Medical Center Utrecht, Utrecht, The Netherlands

Submitted for publication

Abstract

The clinical efficacy of epidermal growth factor receptor (EGFR)-targeted inhibitors is limited due to resistance mechanisms of the tumor such as activation of compensatory pathways. Crosstalk between EGFR and insulin-like growth factor 1 (IGF-1R) signaling has been frequently described to be involved in tumor proliferation and resistance. One of the attractive features of nanomedicines is the possibility to co-deliver agents that inhibit different molecular targets in one nanocarrier system, thereby strengthening the anti-tumor effects of the individual agents. Additionally, exposure to healthy tissues and related unwanted side-effects can be reduced. To this end, we have recently developed anti-EGFR nanobody (Nb)-liposomes loaded with the anti-IGF-1R kinase inhibitor AG538, which showed promising anti-proliferative effects *in vitro*. In the present study, we have further evaluated the potential of this dual-active nanomedicine *in vitro* and for the first time *in vivo*. As intended, the nanomedicine inhibited EGFR and IGF-1R signaling and subsequent activation of downstream cell proliferation and survival pathways. The degree of inhibition induced by the nanomedicine on a molecular level correlated with cytotoxicity in tumor cell proliferation assays. In addition, response to nanomedicine treatment in tumor xenograft models corresponded in a similar way. Combination therapy with kinase inhibitor-loaded Nb-liposomes is therefore an appealing strategy for inhibiting the proliferation of tumors that are highly dependent on EGFR and IGF-1R signaling.

Graphical abstract

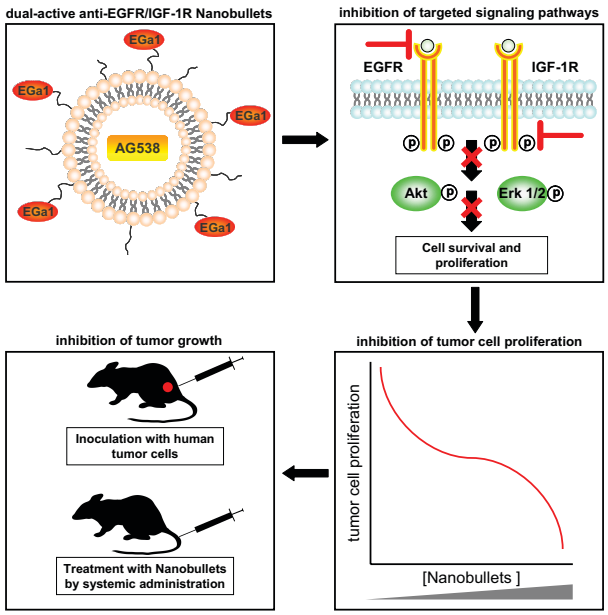

1. Introduction

The fundamental role of epidermal growth factor receptor (EGFR) signaling in proliferation of various cancer types has resulted in the development and approval of several EGFR inhibitors in the last decade, such as monoclonal antibodies (mAb) and tyrosine kinase inhibitors (TKI) [1]. The potency of EGFR signaling inhibition has been recently outlined by two meta-analyses of clinical trials involving patients suffering from non-small-cell lung cancer (NSCLC) carrying EGFR-mutations. In both analyses it was concluded that these patients benefit more from anti-EGFR TKI treatment (gefitinib, erlotinib) than from standard chemotherapy [2-3]. At the same time, it is clear that in spite of initial responses to EGFR-directed therapy, patients eventually progress due to resistance mechanisms including secondary EGFR mutations and activation of compensatory signaling pathways [4].

For certain tumors, insulin-like growth factor 1 receptor (IGF-1R) signaling is considered to be as crucial as EGFR signaling, and potent IGF-1R inhibitors have been developed in recent years. Although initial results seemed promising, phase III trials have, however, not demonstrated clinical benefits of IGF-1R inhibitors, suggesting that targeting only the IGF-1R signaling pathway is not sufficient for robust anti-cancer effects [5-6].

EGFR and IGF-1R are both receptor tyrosine kinases with considerate homology in their structure and have crosstalk in their functions in downstream targets. As a result, inhibition of EGFR or IGF-1R separately, does not protect against eventual tumor regrowth. Several studies have reported increased IGF-1R activation as a consequence of EGFR inhibition, thus counteracting the benefit of EGFR inhibitors. Synergistic anti-tumor effects of combined inhibition of EGFR and IGF-1R have been reported, as well as the revoking of resistance to EGFR-targeted therapy by inhibition of IGF-1R [7-13]. These studies point towards crosstalk mechanisms between EGFR and IGF-1R and provide a rationale for combined inhibition of both signaling networks.

To enhance the potency of combined EGFR/IGF-1R inhibition and to reduce unwanted side effects of IGF-1R inhibitors, we have developed a targeted dual-active nanomedicine [14]. The nanomedicine consists of anti-EGFR nanobody (Nb)-liposomes (so called "Nanobullets") loaded with the anti-IGFR kinase inhibitor AG538 [15]. Nanobodies, or VHHs, are small antigen binding fragments derived from the variable domain of the *camelidae* heavy chain antibodies [16]. Grafting of anti-EGFR Nbs to the surface of liposomes was first described by Oliveira *et al.*[17]. In that study, it was demonstrated that anti-EGFR Nbs could be exploited for targeting of $EGFR^+$ tumor cells and additionally, inhibited tumor cell proliferation *in vitro* due to intrinsic antagonistic and downregulating properties of the anti-EGFR Nb [17]. Although promising *in vitro*, these anti-EGFR Nb-liposomes

were almost ineffective *in vivo*. Thereafter, anti-EGFR Nb-liposomes were loaded with AG538 to render them more effective. These Nanobullets strongly inhibited tumor cell proliferation after short-term exposure *in vitro* [15].
In the current study, we have explored the potential of anti-EGFR/IGF-1R nanobullets for *in vivo* studies. First, we assessed the efficacy of the nanobullets by their ability to inhibit the targeted signaling pathways and the inhibition of tumor cell growth in a panel of tumor cell lines. Next, nanobullet efficacy *in vivo* was evaluated in two tumor xenograft models in mice.

2. Material and methods

2.1 Nanobodies

EGa1 is an antagonistic anti-EGFR Nb and has been described by Hofman *et al.*[18] EGc9 is an anti-EGFR Nb that does not compete with EGF for the receptor (Heukers *et al.*, *manuscript submitted*). Production of EGa1 was performed as described previously [19] with minor adjustments. Briefly, *E. coli* BL21-CodonPlus(DE3)-RIL cells (Agilent Technologies, Inc., Santa Clara, CA, USA) were transformed with pET28-Nb [15]. Bacterial growth conditions and induction of protein expression have been described in detail by Altintas *et al.*[20]. The produced EGa1 Nb was purified on an ÄKTApurifier 10 (GE Healthcare Europe GmbH, Munich, Germany) using a HisTrap™ Column (GE Healthcare) according to the manufacturer's protocol. Nb was eluted with an imidazole gradient (10–500 mM, pH 8.0) and the collected fractions were dialyzed overnight to PBS pH 7.4 and stored at -20 °C. This procedure resulted in a yield of 10 mg EGa1 per liter of bacterial culture [20].

2.2 Preparation of liposomes

Dipalmitoylphosphatidylcholine (abbreviated as DPPC, a generous gift from Lipoid GmbH, Ludwigshafen, Germany), cholesterol (Sigma-Aldrich Chemie B.V., Zwijndrecht, The Netherlands) and maleimide-polyethylene glycol 2000 distearoylphosphatidylethanolamine (abbreviated as mal-PEG-DSPE, Avanti Polar Lipids, Birmingham, AL, USA) were dissolved in chloroform:methanol (1:1, v:v) in a round-bottom flask in a molar ratio of 1.36:1.36:0.28, respectively. A lipid film was prepared by rotary evaporation (Büchi Labortechnik AG, Flawil, Switzerland) followed by drying under a stream of nitrogen. Liposomes were formed by rehydration of the lipid film with 300 mM calcium acetate solution pH 7, to a final concentration of 50 mM total lipid (TL) for *in vitro* assays and 100 mM TL for *in vivo* studies. Liposome size was reduced by multiple extrusion steps using a Lipex™ Extruder (Northern Lipids, Burnaby, BC, Canada) through polycarbonate membranes (Nuclepore, Pleasanton, CA, USA) with a final pore size of 100 nm.

2.3 Remote loading of liposomes with AG538

Remote loading of liposomes with AG538 was performed using a calcium acetate gradient. The external liposomal medium (300 mM calcium acetate buffer pH 7.0) was replaced by 10 mM Hepes/135 mM NaCl buffer pH 7.4 (HBS) using PD-10 desalting columns (GE Healthcare Europe GmbH, Munich, Germany). The anti-IGF-1R kinase inhibitor AG538 (Calbiochem, San Diego, CA, USA) was dissolved in dimethylsulfoxide to a final concentration of 25 mM. The molar ratio of kinase inhibitor to TL used was 40 nmol/μmol and later optimized to 80 nmol/μmol. Liposomes were incubated with AG538 for 45 min at room temperature (RT) and used without further purification for Nb coupling. Control AG538-liposomes devoid of Nb were stored overnight at 4 °C before purification (see next section).

2.4 Nanobody coupling to liposomes

Nbs were modified by reaction with N-succinimidyl-S-acetylthioacetate (abbreviated as SATA, Pierce Biotechnology, Rockford,IL, USA) in a 1:8 (Nb:SATA) molar ratio followed by deacetylation to generate a thioacetylated protein which is reactive towards maleimide groups on the distal end of PEG chains present on the liposomes, as described before [17]. The standard molar ratio of Nb to TL used was 0.8 nmol/μmol corresponding to a molar ratio of Nb to mal-PEG-DSPE of 8.6 nmol/μmol. This ratio was estimated to result in approximately 40 Nbs per liposome. After overnight coupling at 4 °C, non-coupled Nbs were removed by washing/filtration steps with HBS and Vivaspin centrifugal concentrators (Sartorius Stedim Biotech S.A., Aubagne, France) with a molecular weight membrane cut-off of 100 kDa. In the case of formulations for *in vivo* studies, liposomes were dialyzed for 48 h against HBS 4 °C followed by a concentration step with a 100 kDa cut-off Vivaspin centrifugal concentrators (Sartorius Stedim Biotech S.A).

2.5 Near-infrared fluorescent labeling of liposomes

Micelles were prepared by mixing 4 μmol of PEG (2000)-DSPE-NH_2 and 4 μmol of PEG (2000)-DSPE in 1 mL 0.1 M sodium bicarbonate solution pH 8.3. This mixture was heated at 60 °C for 10 min. Hereafter, 250 μL of the micelles were incubated with 0.5 mg of near-infrared fluorescent (NIRF) IRDye® 800CW NHS ester (LI-COR Biosciences, Lincoln, NE, USA) for 10 min at 60 °C followed by 60 min at RT while continuously stirred to facilitate covalent conjugation. NIRF-labeled micelles (50 μL) were added to 1 mL of preformed liposomes (Section 2.2) and heated for 5 min at 60 °C followed by 10 min at RT while continuously stirred. This cycle was repeated three times. NIRF-labeled liposomes were purified by Vivaspin centrifugal concentrators (Sartorius Stedim Biotech S.A.) as described in the previous

section.

2.6 Characterization of liposomes

The mean particle size distribution and the polydispersity index of the liposomes were determined by dynamic light scattering using a Malvern CGS-3 multiangle goniometer (Malvern Instruments Ltd., Worcestershire, UK) with a JDS Uniphase 22 mWHe–Ne laser operating at 632 nm, an optical fiber-based detector and a digital LV/LSE-5003 correlator. Autocorrelation functions were analyzed by the cumulants method (fitting a single exponential to the correlation function to obtain the mean size and the polydispersity index, PDI) and the CONTIN routine (fitting a multiple exponential to the correlation function to obtain the distribution of particle sizes). All measurements were performed at a 90 ° angle. The zeta-potential (ζ potential) of the liposomes was determined by laser Doppler electrophoresis using a Zetasizer Nano-Z (Malvern Instruments Ltd.). Liposomes were dissolved in 10 mM HEPES buffer pH 7.4 prior to measurements. The concentration of the liposomes (mM TL) was calculated after determination of the liposomal phosphate content according to Rouser [21]. Coupling of Nbs to liposomes was determined by Western blotting. Samples were subjected to SDS-PAGE using 4–12% gradient NuPAGE Novex Bis-Tris mini-gels (Life Technologies Europe B.V., Bleijswijk, The Netherlands). Proteins were electro-transferred onto a nitrocellulose membrane using the I-Blot Dry Blotting system (Life Technologies Europe B.V.). Membranes were blocked for 1 h with 5% BSA in Tris-buffered saline containing 0.1% Tween-20 (TBS-T) and incubated overnight at 4 °C with rabbit polyclonal anti-VHH serum diluted 1:5000 in 5% BSA in TBS-T. After washing with TBS-T, membranes were incubated for 1 h at RT with goat anti-rabbit peroxidase-conjugated secondary antibody (Cell Signaling Technology, Inc., Danvers, MA, USA) diluted 1:3000 in 5% BSA in TBS-T. Proteins were visualized and detected using SuperSignal West Femto Chemiluminescent Substrate (Thermo Fischer Scientific, Inc., Rockford, IL, USA) and a Gel Doc Imaging system equipped with a XRS camera and Quantity One analysis software (Bio-Rad, Hercules, CA, USA).

2.7 Cell lines and culture conditions

The human head and neck squamous cell carcinoma (HNSCC) cell line UM-SCC-14C (abbreviated as 14C, developed by Dr. T.E. Carey, Ann Arbor, MI, USA [22]) and the human epidermoid carcinoma cell line A431 were cultured in Dulbecco's Modified Eagle's Medium (abbreviated as DMEM, PAA Laboratories GmbH, Pasching, Austria) containing 3.7 g/L sodium bicarbonate, 4.5 g/L L-glucose, 2 mM L-glutamine and supplemented with 5% and 7.5% (v/v) fetal bovine serum (FBS) respectively. The human breast adenocarcinoma cell line MDA-MB-468 (MB-468)

was cultured in DMEM/F12 medium (Life Technologies Europe B.V.) containing 1.2 g/L sodium bicarbonate, 3.6 g/L HEPES, 3.2 g/L D-glucose, 2.5 mM L-glutamine and supplemented with 9% FBS. Human alveolar basal epithelial adenocarcinoma A549 cells (ATCC, Manassas, VA, USA) were cultured in HAM's F12 medium (PAA Laboratories) containing 1.2 g/L sodium bicarbonate, 1.8 g/L D-glucose, 1 mM L-alanyl-L-glutamine and supplemented with 10% FBS. Cell culture media for all cell lines were supplemented with Antibiotic-Antimycotic solution (PAA Laboratories) to contain a final concentration of 100 IU/mL penicillin, 100 µg/mL streptomycin and 0.25 µg/mL amphotericin B. All cell lines were kept in culture at 37 °C in a humidified atmosphere containing 5% CO_2. Tests for mycoplasma infection were carried out regularly with a MycoAlert™ Mycoplasma Detection Kit (Lonza Benelux BV, Breda, The Netherlands) and were consistently found to be free of mycoplasma.

2.8 Competition assay

MB-468 cells were seeded at 10.000 cells/well in 96-well plates (NUNC A/S, Roskilde, Denmark). Two days after, cells were washed twice with serum free medium and incubated for 1.5 h at 4 °C with 10 nM of the NIRF IRDye® 800CW EGF Optical Probe (NIRF-EGF, LI-COR Biosciences) and Nb or Nb-liposomes diluted in serum free medium at a final concentration of 0.01 nM - 1.00 µM. Cells were washed twice with serum free medium and incubated with 5 µM DRAQ5™ (Cell Signaling Technology, Inc.) diluted in PBS for 5 min at 4 °C. Cells were washed two times with serum free medium before measurements were performed with an Odyssey® Infrared Imaging System (LI-COR Biosciences) equipped with a solid-state diode laser at 685 nm and at 785 nm. The NIRF-EGF fluorescence intensity was measured by the 800 nm channel while the DRAQ5 fluorescence intensity was measured by the 700 nm channel for normalization of cell number. Ratios of fluorescence intensities (800/700 nm) were plotted versus the concentrations of the Nbs or Nb-liposomes.

2.9 Cell association

MB-468 cells were seeded at 10.000 cells/well in 96-well plates (NUNC A/S). Two days after, cells were exposed to NIRF-labeled liposomes (Section 2.5) diluted in complete culture medium to a final concentration of 15.6 µM – 2.0 mM in the dark at 4 °C. Cells were washed three times with 0.3% bovine serum albumin (BSA) in PBS and fixed with 10% formalin. The NIRF-signal of the IRDye® 800CW was measured by the 800 nm channel of the Odyssey® Infrared Imaging System (LI-COR Biosciences). Fluorescence intensities were plotted versus the concentrations of the liposomes.

2.10 Western Blotting

A431, A549 and 14C cells were seeded at 150.000 cells/well in 6-well plates one day before exposure to liposomes. MB-468 cells were seeded at 200.000 cells/well in 6-well plates two days prior to treatment. At the day of the experiment, culture medium was replaced by serum free medium containing liposomes with a final concentration of 2 mM TL for 4 h at 37 °C. Cells were then washed with PBS and activated with serum free medium containing 50 ng/mL epidermal growth factor (EGF) and insulin-like growth factor-1 receptor (IGF-1, Biovision, Inc., Milpitas, CA, USA) for 10 min at 37 °C. After washing with cold PBS, cells were lysed in radioimmunoprecipitation assay (RIPA) buffer (Teknova, Inc., Hollister, CA, USA) supplemented with HALT™ protease and phosphatase inhibitor cocktail (Thermo Fischer Scientific, Inc.) for 30 min on ice. Lysates were centrifuged at 4 °C for 15 min at 14.000 rpm and the obtained supernatant was stored at -20 °C. Protein content of the lysates was determined by Micro BCA assay (Thermo Fischer Scientific, Inc.). Lysates were subjected SDS-PAGE using 4–12% gradient NuPAGE Novex Bis-Tris mini-gels (Life Technologies Europe B.V.). Proteins were electrotransferred onto a nitrocellulose membrane using the iBlot® Dry Blotting system (Life Technologies Europe B.V.) Membranes were blocked with 5% BSA in TBS-T for 1 h. Membranes were stained overnight at 4 °C with one of the following primary antibodies (Cell Signaling Technology, Inc.): XP® rabbit monoclonal antibody (mAb) against phosphorylated tyrosine residue (Tyr) 1068 of EGFR, XP® rabbit mAb against EGFR, XP® rabbit mAb against phosphorylated Tyr1135 of IGF-1R, XP® rabbit mAb against IGF-1R, XP® rabbit mAb against phosphorylated threonine residues (Thr) and Tyr of p44/p42 MAP kinase (Erk1/Erk2), rabbit mAb against p44/p42 MAP kinase (Erk1/Erk2), XP® rabbit mAb against phosphorylated serine residue (Ser) 473 of Akt, rabbit mAb against Akt or a rabbit polyclonal antibody against β-actin diluted 1:1000 or 1:2000 (according to the manufacturer's protocol) in 5% BSA in TBS-T. After washing with TBS-T, membranes were incubated for 1 h at RT with goat anti-rabbit peroxidase-conjugated secondary antibody (Cell Signaling Technology, Inc.) diluted 1:3000 in 5% BSA in TBS-T. Proteins were visualized and detected using SuperSignal West Femto Chemiluminescent Substrate (Thermo Fischer Scientific, Inc.) and a Gel Doc Imaging system equipped with a XRS camera and Quantity One analysis software (Bio-Rad).

2.11 Cell proliferation assays

The sulforhodamine B (SRB) assay was performed to determine the effect of liposome treatment on total cell numbers [23]. A431, A549 and 14C cells were seeded at 4000 cells/well in 96-well plates one day before treatment. MB-468 cells were seeded at 8000 cells/well in 96-well plates two days prior to treatment. On the day of the

experiment, culture medium was replaced by medium containing liposomes in final concentrations of 15.6 μM – 2.0 mM TL in sextuplicate. Free AG538 diluted in medium was added in final concentrations of 1.25 – 160 μM. After two days, cells were fixed by the addition of trichloroacetic acid (TCA) to a final concentration of 10%. Cells were washed with water, dried at RT and stained with 0.4% SRB in 1% acetic acid for 30 min. Excess dye was washed away with 1% acetic acid and cells were dried at RT. Bound dye was extracted with unbuffered 10 mM Tris for 30 min and OD values were measured at 490 - 550 nm with a SPECTROstar^{Nano} absorbance microplate reader (BMG LABTECH, Ortenberg, Germany). The BrdU assay (Roche Diagnostics GmbH, Mannheim, Germany) was performed to determine the effect of liposome treatment on the number of proliferating cells. Experimental setup and liposomal treatments were identical to SRB assays. After two days of growth, medium was replaced by medium containing BrdU. The following day, the colorimetric BrdU assay was performed according to the manufacturer's protocol. After stopping the colorimetric reaction with H_2SO_4, the OD values were measured at 450 nm with the reference wavelength set to 655 nm using a SPECTROstar^{Nano} absorbance microplate reader (BMG LABTECH).

2.12 Efficacy study in a 14C model

Male athymic NU/NU nude mice weighing 20 - 25 g were obtained from Charles River (Maastricht, The Netherlands). Mice were housed under standard conditions and had access to water and food *ad libitum*. 14C cells were cultured as described in Section 2.7. A subcutaneous xenograft tumor model was induced by inoculating 1 x 10^6 cells (dispersed in 100 μL cold PBS) in the right flank of each mouse. Tumors were measured every second day using a digital caliper. The tumor volume V (in mm^3) was calculated using the formula $V = \pi/6 \times L \times S^2$ where L is the largest and S is the smallest superficial diameter. When tumors reached a volume of ~100 mm^3, mice were included in the study. Treatment consisted of saline (n=11), Nb-liposomes (n=9, EGa1-AG538-L) or cationic Nb-liposomes (n=10, cationic EGa1-AG538-L [15]). Mice received 100-150 μL intravenous (i.v.) injections in the tail vein once every two days for a total of 10 injections. Each injected liposomal dose corresponded with 60 μg EGa1 and 49 μg AG538. Tumor volume and body weight were monitored every second day. When tumors reached the humane endpoint (i.e. 1500 mm^3), mice were sacrificed by cervical dislocation. The experiments were carried out according to national regulations and after approval by local animal experiments ethical committee. Statistical analysis was performed using GraphPad Prism 4.00 (GraphPad Software, Inc., La Jolla, CA, USA) using 2-way ANOVA analysis with Bonferroni post-test. A p-value<0.05 was considered to indicate significant differences.

2.13 Efficacy study in a MB-468 xenograft model

Female athymic NU/NU nude mice weighing 20 - 25 g were obtained from Charles River. Mice were housed under standard conditions and had access to water and food *ad libitum*. MB-468 cells were cultured as described in Section 2.7. A subcutaneous xenograft tumor model was induced by inoculating 5 x 10^6 cells (dispersed in 100 µL cold PBS) in the right flank of each mouse. Tumors were measured every second day using a digital caliper and calculated as described in the previous section. When tumors reached a volume of 50 - 100 mm^3, mice were included in the study. Treatment consisted of saline (n=7), Nb-liposomes (EGa1-L, n=6), AG538-loaded liposomes (AG538-L n=6), a combination of EGa1-L and AG538-L (n=6) and Nb-liposomes loaded with AG538 (EGa1-AG538-L, n=7). The mice received 100 - 200 µL i.v. injections in the tail vein three times per week for a total of 10 injections. Each injected liposomal dose corresponded with 45 µg EGa1 and 70 µg AG538. Tumor volumes and body weight were monitored three times per week. When tumors reached the humane endpoint (i.e. 1500 mm^3), the mice were sacrificed by cervical dislocation. The experiments were carried out according to national regulations and after approval by local animal experiments ethical committee.

3. Results and discussion

3.1 Preparation and characterization of nanobody-liposomes

We have recently reported on the anti-proliferative effects of dual-active anti-EGFR Nb-liposomes loaded with an anti-IGF-1R kinase inhibitor *in vitro* [15]. In the present study, we further evaluated the anti-tumor efficacy of the Nb-liposomes or nanobullets on a panel of tumor cell lines and subsequently in xenograft models. We therefore developed a stable PEGylated formulation based on DPPC and cholesterol appropriate for *in vivo* applications. These slightly anionic PEGylated liposomes were produced following the same method as described previously [15]. The external liposomal medium was replaced by HBS to establish a trans-membrane gradient for the remote loading of the anti-IGF-1R kinase inhibitor AG538 [24]. The prepared liposomal formulations were then modified with anti-EGFR Nb EGa1 via conjugation to maleimide groups attached to PEG chains present on the surface of the liposomes, as previously described [15, 17]. To accomplish this, EGa1 was first modified with the N-hydroxysuccinimide (NHS) ester of S-acetylthioacetic acid (SATA) to introduce sulfhydryl groups available for forming thioether bonds with maleimide groups. We have shown before that the modification of EGa1 with an 8-fold molar excess of SATA leads to the introduction of 3-6 sulfhydryl groups, resulting in the conjugation of multiple PEG chains per Nb on the same liposome [15]. Four formulations were prepared for *in vitro* studies: empty control liposomes

(L), empty EGa1-coupled liposomes (EGa1-L), non-targeted liposomes loaded with AG538 (AG538-L) and EGa1-coupled liposomes loaded with AG538 (EGa1-AG538-L). The average size of the liposomes was 0.12 µm and the low polydispersity index (PDI<0.1) indicated uniform preparations. A negative mean zeta potential of ~ -23 mV was observed for all formulations (Table 1).

Name	Mean size (µm)	PDI	Mean zeta potential (mV)
L	0.12 ± 0.03	0.05 ± 0.02	-23.8 ± 6.4
EGa1-L	0.12 ± 0.03	0.07 ± 0.03	-21.6 ± 5.6
AG538-L	0.12 ± 0.03	0.08 ± 0.03	-24.8 ± 5.1
EGa1-AG538-L	0.12 ± 0.03	0.10 ± 0.05	-23.2 ± 2.6

Table 1. Liposome characteristics. Data are presented as average ± SD of three separately prepared batches of liposomes

The coupling of EGa1 to the liposomes was demonstrated with Western blotting (Fig. 1A) using anti-VHH serum to detect the Nb. EGa1 was detected around 18 kDa corresponding to its calculated molecular weight (18.3 kDa). EGa1-L and EGa1-AG538-L showed a similar EGa1 migration pattern displaying several positively stained bands between 18 and 35 kDa, indicating the conjugation of 1-3 molecules of mal-PEG-DSPE (2.9 kDa) per Nb. These results are in agreement with earlier studies [15, 17].

To determine whether the SATA-modification of the Nb or the coupling to the PEG-liposomes had interfered with the antagonistic and binding capacities of EGa1, competition assays in the presence of NIRF-labeled EGF (NIRF-EGF) on EGFR-(over)expressing ($EGFR^+$) human breast cancer MB-468 cells were performed (Fig. 1B). Unlabeled EGF was used as a positive control for competition with NIRF-EGF. EGa1, SATA-modified EGa1 (SATA-EGa1) and EGa1-L all competed with NIRF-EGF for binding to MB-468 cells in a comparable fashion indicating that neither introduction of sulfhydryl groups nor conjugation to PEG-chains on the liposomes had compromised the interaction of EGa1 with EGFR. The Nb EGc9 was used as a negative control and did not display any competition with NIRF-EGF.

3.2 Nanobody-liposomes bind to EGFR-(over)expressing tumor cells

NIRF-labeled liposomes with or without EGa1 were prepared to determine the ability of EGa1-L to associate with $EGFR^+$ MB-468 cells. NIRF-liposomes displayed similar size and zeta-potential characteristics as unlabeled liposomes (Supp. Table 1). MB-468 cells were incubated with liposomes for 1 h at 4 °C after which the liposomal NIRF signal was measured with an Odyssey® imaging system (Figure 2A). NIRF-EGa1-L associated with MB-468 cells 3 to 4-fold higher than untargeted

NIRF-L. In previous studies, cationic EGa1-L induced similar differences in EGFR+ 14C cell association compared to untargeted formulations [15, 17].

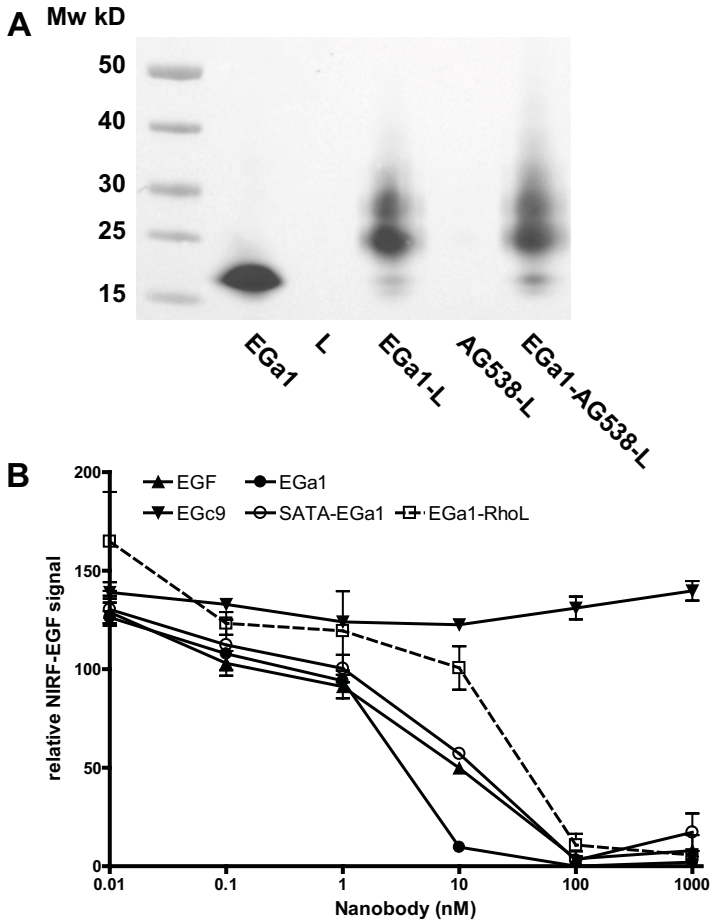

Figure 1. Characterization of EGa1 coupling to liposomes. **A**. EGa1, empty control liposomes (L), nanobody (Nb)-liposomes (EGa1-L), AG538-loaded liposomes (AG538-L) and Nb-liposomes loaded with AG538 (EGa1-AG538-L) were subjected to SDS-PAGE and Nb coupling was determined by Western Blotting. **B**. EGFR+ MDA-MB-468 cells were concurrently incubated with 10 nM of near-infrared fluorescently (NIRF) labeled-EGF and increasing concentrations of negative control Nb EGc9, unlabeled EGF as a positive control, EGa1, SATA-EGa1 or EGa1-L for 1.5 h at 4 °C. The NIRF-EGF signal was plotted versus the free or liposomal Nb concentration. Data are presented as mean ± SEM of one representative experiment performed in triplicate.

3.3 Nanobullets inhibit activation of molecular signaling pathways in tumor cells

To determine whether EGa1-AG538-L could effectively inhibit activation of molecular signaling pathways, a panel of different tumor cell lines including UM-SCC-14C

(14C, HNSSC), A431 (epidermoid carcinoma), A549 (lung carcinoma) MDA-MB-468 (MB-468, breast carcinoma) was exposed to the nanobullets.

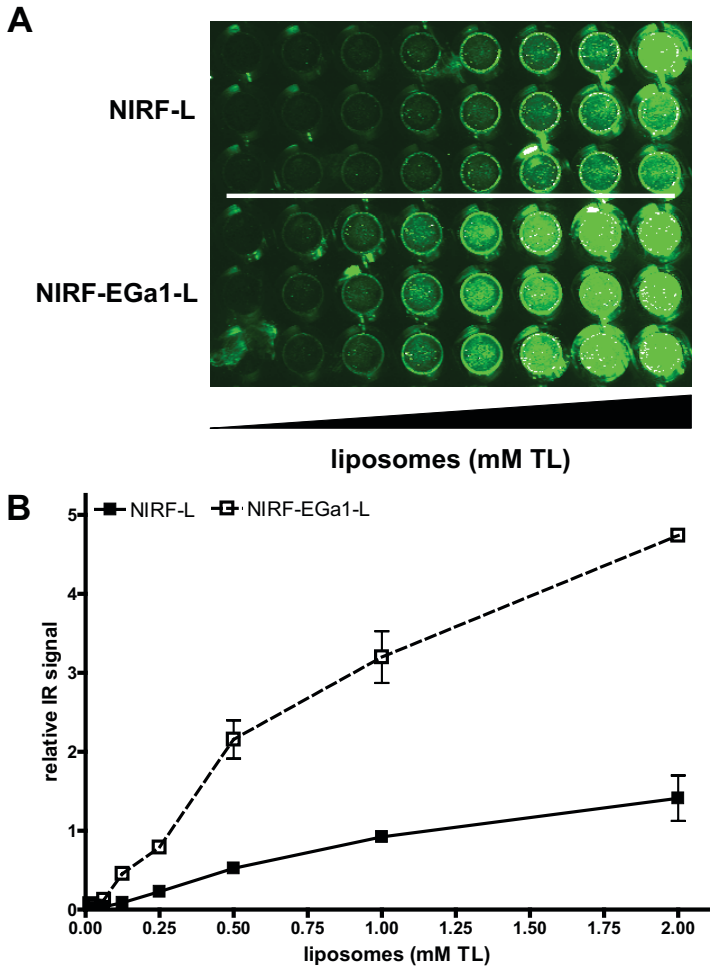

Figure 2. Cell association of nanobody-liposomes. **A**. EGFR+ MB-468 cells were incubated for 1 h at 4 °C with near-infrared fluorescently (NIRF)-labeled liposomes (NIRF-L) and NIRF-labeled nanobody-liposomes (NIRF-EGa1-L). The liposomal NIRF signal was measured with an Odyssey® imaging system. **B**. NIRF intensities are plotted versus the liposomal concentration. Data are presented as mean ± SEM of one representative experiment performed in triplicate.

Of note, the selected tumor cell lines express different levels of EGFR and IGF-1R (Supp. Fig. 1). The cells were serum starved and simultaneously exposed to liposomes for 4 h followed by 10 min activation with EGF and IGF-1 after which cell lysates were collected. Protein levels of activated and total EGFR and IGF-1R as well as the activation of their downstream effector proteins Akt and Erk 1/2 (p44/42 MAPK)

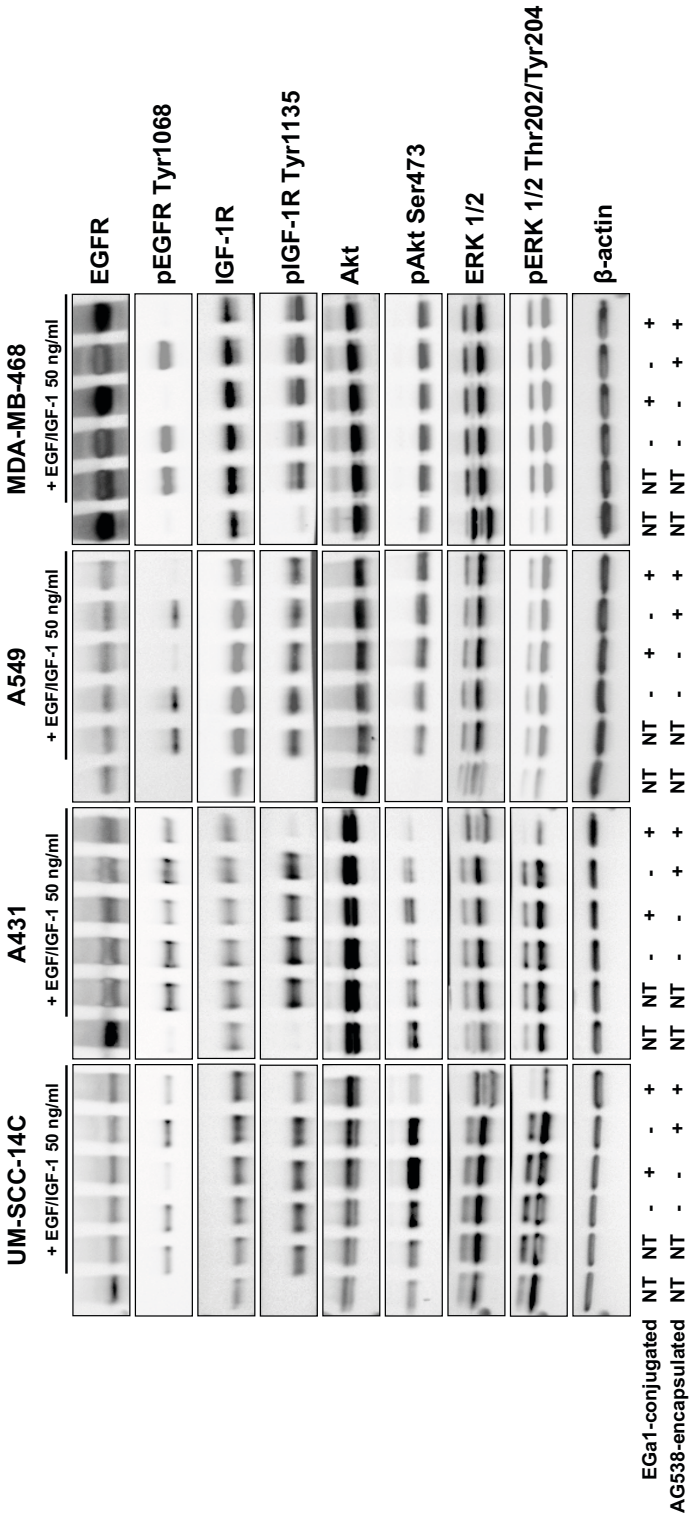
UM-SCC-14C
A431
A549
MDA-MB-468
+ EGF/IGF-1 50 ng/ml
EGFR
pEGFR Tyr1068
IGF-1R
pIGF-1R Tyr1135
Akt
pAkt Ser473
ERK 1/2
pERK 1/2 Thr202/Tyr204
β-actin
EGa1-conjugated NT NT - + - + NT NT - + - + NT NT - + - + NT NT - + - +
AG538-encapsulated NT NT - - + + NT NT - - + + NT NT - - + + NT NT - - + +

Figure 3. Nanobullets inhibit activation of targeted tumor cell signal transduction pathways. UM-SCC-14C (14C), A431, A549 and MDA-MB-468 cells were simultaneously serum starved and exposed to empty control liposomes, nanobody-liposomes (EGa1-conjugated) liposomes loaded with AG538 (AG538-encapsulated) or both for 4 h followed by 10 min activation with EGF and IGF-1. Cell lysates were collected and subjected to SDS-PAGE. Levels of total EGFR, phosphorylated EGFR (pEGFR Tyr1068), total IGF-1R, phosphorylated IGF-1R (pIGF-1R Tyr1135), total Akt, phosphorylated Akt (Akt Ser473), total Erk 1/2, phosphorylated Erk 1/2 (pERK 1/2 Thr202/Tyr204) and β-actin as a loading control were detected by Western Blotting.

[25] were detected by phospho-Western blotting (Fig. 3). Upon stimulating cells with EGF and IGF-1, all tumor cell lines displayed a strong phosphorylation of EGFR Tyr1068, a major site of autophosphorylation which occurs after binding of EGF to its receptor [26]. In all four cell lines both EGa1-L and EGa1-AG538-L inhibited or completely blocked activation of EGFR demonstrating the robust antagonistic effect of EGa1. Inhibition of IGF-1R signaling by the kinase inhibitor AG538 has to occur intracellularly, which requires efficient uptake of AG538-containing liposomes and subsequent cytoplasmic release of AG538. Activation of all tumor cell lines with EGF and IGF-1 induced robust phosphorylation of IGF-1R Tyr1135, which is autophosphorylated upon ligand binding to the receptor [26]. Only EGa1-AG538-L were able to inhibit IGF-1R phosphorylation in 14C and A431 cells, demonstrating that this formulation is capable of efficient cytosolic delivery of AG538 in these cell lines, while liposomes without anti-EGFR Nb failed to deliver AG538 intracellularly. In contrast, in A549 and MB-468 cells, no inhibitory effects were observed for EGa1-AG538-L. As A549 cells express lower amounts of EGFR than 14C, A431 and MB-468 cells (Supp. Fig. 1), it is possible that uptake of the Nb-targeted liposomes is insufficient in this cell line to deliver AG538 intracellularly, hence resulting in inadequate inhibition of IGF-1R phosphorylation. With respect to MB-468 cells, which express EGFR levels comparable to 14C cells (Supp. Fig. 1), such an explanation appears not to be valid. A different intracellular routing of the liposomes, differences in cellular breakdown or the involvement of other signaling cascades not affected by AG538 may be responsible for the lack of drug-related effects in MB-468 cells.

We also evaluated the effects of anti-EGFR/IGF-1R nanobullets on the signaling mediators Akt and Erk 1/2, i.e. downstream of EGFR and IGF-1R. EGa1-AG538-L inhibited phosphorylation of Akt and Erk 1/2 (Fig. 3) in 14C and A431 cells but again, similar as for IGF-1R phosphorylation, not in A549 and MB-468 cells. These results show that suppression of both EGFR and IGF-1R signaling is necessary for efficient inhibition of important downstream cell proliferation and survival pathways, which only occurred in 14C and A431 cells. Mono-targeted inhibition of EGFR activation by EGa1-L devoid of AG538 did not result in inhibition of Akt

and Erk 1/2 in 14C and A431 cells, and even seemed to increase phosphorylation of Akt. As such, these results illustrate that despite efficient EGFR inhibition such monotherapy with only an EGFR inhibitor can be bypassed by other signaling cascades, such as IGF-1R signaling.

3.4 Nanobullets inhibit proliferation in responsive tumor cell lines

We investigated the antiproliferative effect of the anti-EGFR/IGF1-R nanobullets on the above listed panel of tumor cell lines, via determination of total cell numbers by the sulforhodamine B (SRB) assay [23] after continuous exposure for 48 h to the liposomal formulations or reference compounds.

Free AG538 induced dose-dependent effects after continuous 48 h exposure in all four cell lines, ranging from ~80% reduction of total A549 and MB-468 cell numbers to ~75% reduction of 14C cells and ~70% reduction of A431 cells (Supp. Fig. 2).

In 14C cells (Fig. 4A), empty EGa1-L demonstrated modest efficacy and decreased total cell numbers by ~40%. This effect was increased by combining EGa1-L with a high dose of free AG538 (80 μM) resulting in ~80% reduction of total cell number at the highest concentration of EGa1-L (2 mM TL). Non-targeted AG538-L showed comparable efficacy and also reduced total cell numbers by ~80% at a concentration of 2 mM TL, corresponding to 160 μM AG538. EGa1-AG538-L was much more efficacious as it achieved comparable inhibition already at 0.25 mM TL, corresponding to 20 μM AG538. These results underline the efficient delivery of AG538 by Nb-liposomes and correlate with the inhibition of the targeted molecular pathways demonstrated in Figure 3. The anti-proliferative effects on 14C cells of EGa1-AG538-L after continuous exposure (Fig. 4A) and short-term exposure (Supp.Fig. 3) show comparable results to our previous studies with cationic EGa1-AG538-L, with slight differences likely to be caused by the electrostatic interactions between the positively charged liposomes and negatively charged cell membranes [15].

A431 cells responded in a similar way as 14C cells to 48 h continuous treatment with EGa1-AG538-L formulations, reducing total cell numbers by 95% at 2 mM TL (Fig. 4B). However, 14C cell treatment with EGa1-AG538-L showed a slightly higher efficacy (IC_{50} value 0.13 mM TL) when compared to A431 treatment (IC_{50} value 0.31 mM TL). A431 treatment with EGa1-L resulted in ~20% reduction in total cell numbers at a concentration of 2 mM TL, which and was increased to ~40% in the presence of 80 μM AG538. Importantly, non-targeted AG538-L modestly decreased total cell numbers.

EGa1-AG538-L treatment resulted in similar but only partial anti-proliferative effects in A549 cells (Fig. 4C, 45% reduction in total cell number) and MB-468 cells (Fig. 4D, 50% reduction in total cell number) even at the highest concentration, with

no clear differences in anti-proliferative effect between targeted and non-targeted formulations. Studies in which the cellular proliferation was determined by another assay, i.e. by BrdU assay, produced similar datasets (Supp. Fig. 4). In previously performed assays with cationic EGa1-AG538-liposomes on MB-468 cells, we did observe a reduction of total cell number while untargeted control formulations only

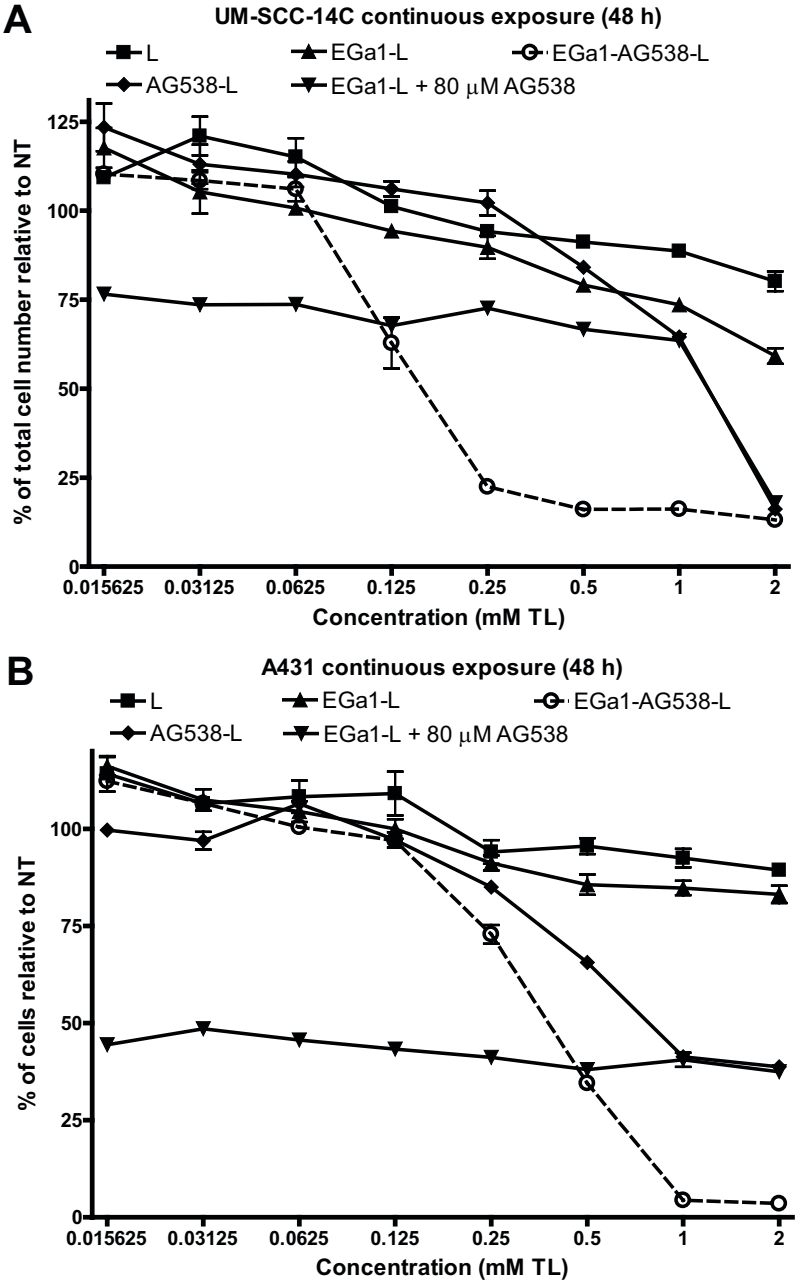

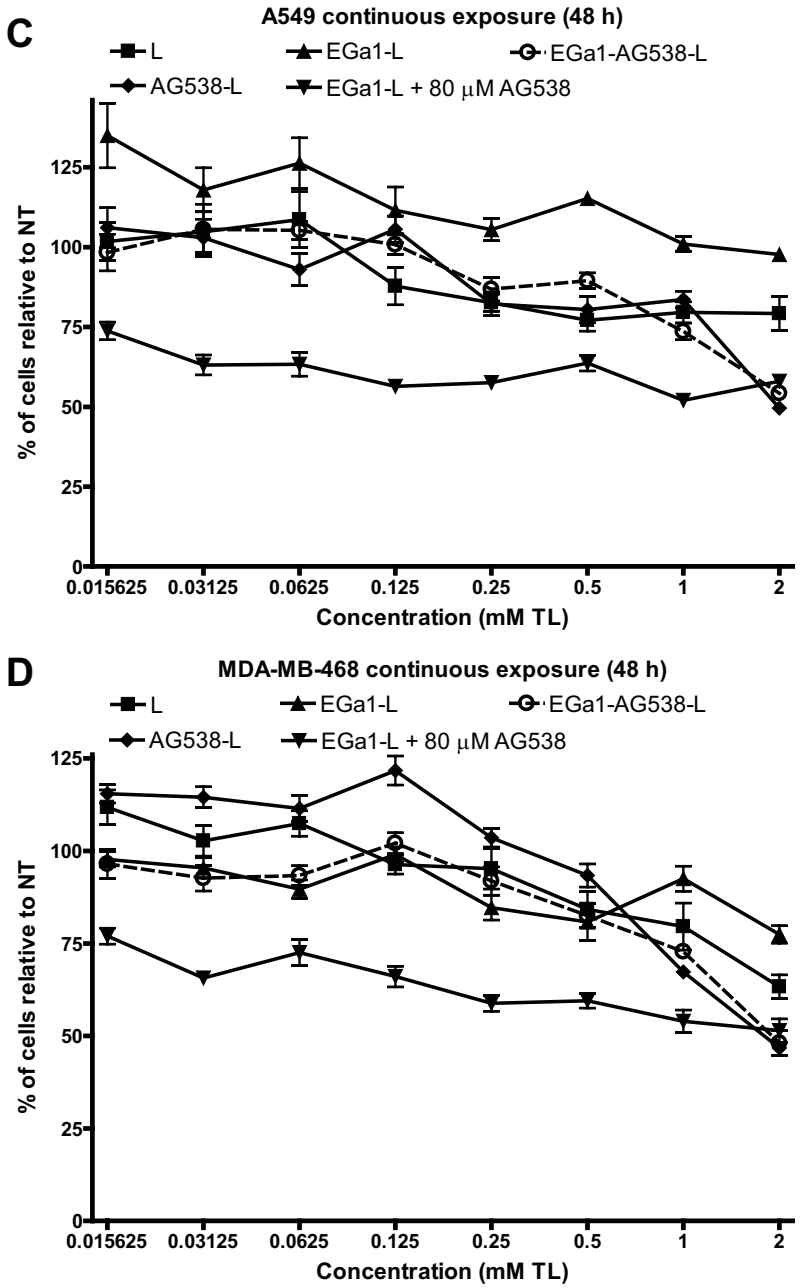

Figure 4. Nanobullets induce tumor cell toxicity. UM-SCC-14C (**A**), A431 (**B**), A549 (**C**) and MDA-MB-468 cells (**D**) were exposed for 48 h to empty control liposomes (L), nanobody (Nb)-liposomes (EGa1-L), Nb-liposomes in the presence of free kinase inhibitor (EGa1-L + 80 μM AG538) or Nb-liposomes loaded with AG538 (EGa1-AG538-L). Molar ratio of kinase inhibitor to total lipid was 80 nmol/μmol. Total cell number was determined by sulforhodamine B (SRB) assay. Data are presented as mean ± SEM of one representative experiment performed in sextuplicate.

had a modest effect [15]. It is possible that cationic liposomes are able to more effectively deliver AG538 in the cytosol due to their less stable liposomal bilayer and/or due to charge interactions of the positively charged liposomes and the negatively charged (organelle) membranes of the cell. The relative potency of anti-EGFR/IGF-1R nanobullets in the tested cell lines correlates well between cellular proliferation and activity of the studied signaling pathways. These results underline that targeted inhibition of a single growth factor pathway is not sufficient to effectively inhibit tumor cell proliferation as alternative molecular pathways and resulting crosstalk-induced activation of downstream effectors can bypass the loss of this growth factor. The limited responses of both A549 and MB-468 cells *in vitro* might have been influenced by crosstalk between EGFR and other growth factor signaling pathways such as hepatocyte growth factor receptor (HGFR or c-MET) [27]. Additionally, A549 cells have a mutated K-RAS gene [28], and MB-468 have amplificated EGFR and loss of the PTEN tumor suppressor protein [29], which can lead to activation of the Akt pathway and may impair treatment with EGFR inhibitors.

3.5 Anti-tumor efficacy of nanobullets

The observed correlation between the inhibition of crucial cellular signaling activation and tumor cell proliferation encouraged the evaluation of the nanobullet anti-tumor efficacy *in vivo*. To this aim, xenograft models were established by implanting cell lines which showed either a strong (14C) or medium (MB-468) *in vitro* response pattern. In the fast-growing 14C xenograft model, EGa1-AG538-L (Supp. Table 2) significantly inhibited tumor growth compared to saline control (p-value < 0.01) corresponding to the strong 14C cell responsiveness *in vitro* (Fig. 5A). Of note, a cationic EGa1-AG538-L (Supp. Table 2) formulation did not significantly inhibit 14C tumor growth, likely due to electrostatic interactions with serum proteins which can influence circulation time and subsequent tumor accumulation via the EPR effect [30]. Although previous studies have reported the use of 14C xenograft models [17, 31-34], isolation and cross-sectioning of tumors after completion of the study revealed that especially large tumors were fluid filled rather than a solid mass (Supp. Fig. 5), possibly influencing tumor volume calculations based on external caliper measurements. It appears that subcutaneous implantation of 14C cells in mice results in the growth of cystic tumors (Prof. Dr. R. Brakenhoff, VU University Medical Center, Amsterdam, The Netherlands, *personal communication*).

In the slow-growing MB-468 xenograft model, representing a medium response pattern *in vitro* to nanobullet treatment, EGa1-AG538-L (Supp. Table 3) did not significantly inhibit tumor growth compared to control formulations (Supp. Table 3) or saline (Fig. 5B). The observed effects *in vivo* are in good agreement with the above discussed results *in vitro*, where EGa1-AG538-L exposure to MB-468 cells did not

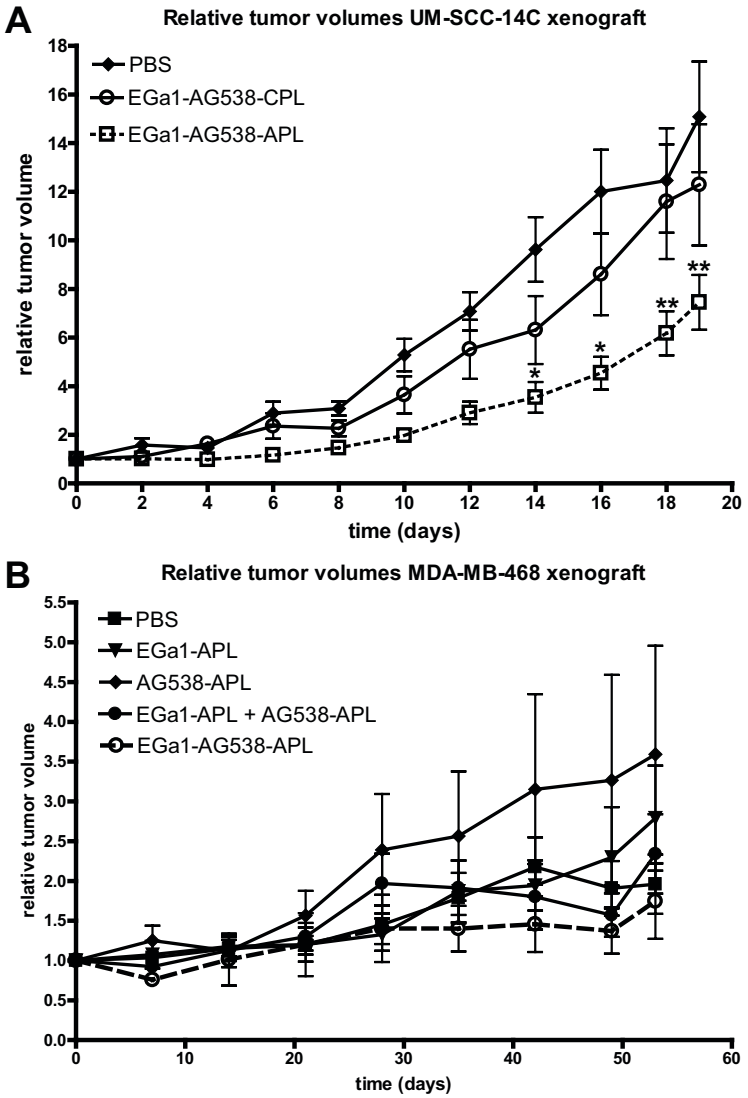

Figure 5. Anti-tumor efficacy of nanobullets. **A**. Relative tumor growth of UM-SCC-14C xenografts in mice. Treatment consisted of intravenous (i.v.) injections of saline, nanobody (Nb)-liposomes loaded with AG538 (EGa1-AG538-L) or cationic Nb-liposomes loaded with AG538 (cationic EGa1-AG538-L) at a concentration 41 mM TL resulting in 60 μg EGa1 and 49 μg AG538 per injection; every second day for a total of 10 injections. Data are presented as mean ± SEM. Data analyzed by 2-way ANOVA with Bonferroni post-test. * p-value < 0.01 EGa1-AG538-L versus PBS. ** p-value < 0.01 EGa1-AG538-L vs. PBS and p-value < 0.05 EGa1-AG538-L versus cationic EGa1-AG538-L. **B**. Relative tumor growth of MDA-MB-468 xenografts in mice. Treatment consisted of i.v. injections of Nb-liposomes (EGa1-L), AG538-loaded liposomes (AG538-L), a combination of EGa1-L and AG538-L and Nb-liposomes loaded with AG538 (EGa1-AG538-L) at a concentration of 31 mM TL resulting in 45 μg EGa1 and 70 μg AG538 per injection, every second day for a total of 10 injections. Data are presented as mean ± SEM.

result in efficient inhibition of cell proliferation and survival pathway activation (Fig. 3), and only modestly inhibited cell proliferation (Fig. 4D).

The correlating *in vitro* and *in vivo* response patterns observed in our studies underline that establishing the expression level of the targeted tumor marker is not sufficient to predict tumor response of molecular targeted therapies. 14C and MB-468 have comparable EGFR expression levels but tumor growth inhibition was only observed in the 14C xenograft model. By determining the mutational status of the targeted protein and vital downstream signaling mediators involved in tumor cell proliferation and survival, patient selection and treatment eligibility are improved ultimately resulting in enhanced clinical benefits of molecular targeted therapies.

EGFR-targeted anti-cancer therapeutics that block proliferation and survival pathways in tumor cells are now in widespread clinical use because of their specificity and favorable toxicity profile compared to standard anti-cancer therapies [1]. Nonetheless, responses to molecular targeted treatment are eventually followed by disease progression due to intrinsic and acquired resistance mechanisms of the tumor [4].

It is evident that despite increased specificity, inhibition of a single signal transduction pathway by molecular targeted drugs is not sufficient to achieve long-lasting therapeutic effects. Indeed, numerous studies have reported on additive or synergistic anti-tumor effects or overcoming of resistance to targeted therapeutics by simultaneous inhibition of EGFR and IGF-1R signaling pathways [7-13]. In agreement, we have demonstrated that concurrent targeting of EGFR and IGF-1R in the investigated tumor models is essential for efficient inhibition of cell proliferation and survival pathways and resulting anti-tumor effects. As such, these Nb-functionalized nanomedicines appear to be versatile systems that can be readily tailored for effective anti-cancer therapy by virtue of intrinsically active Nbs that serve as targeting ligands, in combination with the encapsulation of a therapeutic agent in a long-circulating drug delivery system. The versatility is underlined by the development of Nbs directed at important cellular targets involved in tumorigenesis such as HER2 [35] and vascular endothelial growth factor receptor-2 [36]. Also other drug delivery systems including albumin nanoparticles [20], polymeric micelles [33] and gold nanoparticles [37] have been equipped with Nbs.

The currently developed Nb-modified nanomedicine platform may offer advantages over combination strategies with conventional inhibitors. Prolonged circulation time and the EPR effect contribute to higher tumor accumulation of liposomal drug and reduced side effects when compared to free drug administered systemically [30]. The EGa1 Nb increases cell specific uptake and induces rapid internalization but has additional antagonistic and receptor downregulating properties. In addition, co-delivery of two therapeutic agents in one delivery system equalizes the circulation

time and biodistribution of both therapeutics thereby promoting optimal conditions for additive or synergistic therapeutic effects.

In conclusion, categorizing the response of cell lines after combined inhibition of EGFR and IGF-1R signaling by Nanobullets *in vitro*, produced two distinct response patterns: medium or strong inhibition of pathways and tumor cell growth. When cell lines from either category were implanted *in vivo*, the antitumor efficacy of anti-EGFR/IGF-1R nanobullets correlated well with the response pattern *in vitro*, underlining the importance of pre-screening target protein expression and mutational status of patient tumor biopsies to determine eligibility for molecular targeted therapies and subsequently improve clinical efficacy.

Acknowledgements

R. van der Meel, I. Altintaş and R. Heukers are supported by the Utrecht University Focus and Massa program Nanobullets: The next generation in drug targeting. The authors would like to thank L. van Bloois for assisting with the preparation of NIRF-labeled liposomes and W.W. Kassing-Van der Ven for assisting with the animal studies.

References

1. Yarden, Y., Pines, G., The ERBB network: at last, cancer therapy meets systems biology, Nat Rev Cancer, 12 (2012) 553-563.
2. Petrelli, F., Borgonovo, K., Cabiddu, M., Barni, S., Efficacy of EGFR tyrosine kinase inhibitors in patients with EGFR-mutated non-small-cell lung cancer: a meta-analysis of 13 randomized trials, Clin Lung Cancer, 13 (2012) 107-114.
3. Gao, G., Ren, S., Li, A., Xu, J., Xu, Q., Su, C., Guo, J., Deng, Q., Zhou, C., Epidermal growth factor receptor-tyrosine kinase inhibitor therapy is effective as first-line treatment of advanced non-small-cell lung cancer with mutated EGFR: A meta-analysis from six phase III randomized controlled trials, Int J Cancer, 131 (2012) E822-829.
4. Wheeler, D.L., Dunn, E.F., Harari, P.M., Understanding resistance to EGFR inhibitors-impact on future treatment strategies, Nat Rev Clin Oncol, 7 (2010) 493-507.
5. Yee, D., Insulin-like growth factor receptor inhibitors: baby or the bathwater?, J Natl Cancer Inst, 104 (2012) 975-981.
6. Pollak, M., The insulin and insulin-like growth factor receptor family in neoplasia: an update, Nat Rev Cancer, 12 (2012) 159-169.
7. Morgillo, F., Kim, W.Y., Kim, E.S., Ciardiello, F., Hong, W.K., Lee, H.Y., Implication of the insulin-like growth factor-IR pathway in the resistance of non-small cell lung cancer cells to treatment with gefitinib, Clin Cancer Res, 13 (2007) 2795-2803.
8. Guix, M., Faber, A.C., Wang, S.E., Olivares, M.G., Song, Y., Qu, S., Rinehart, C., Seidel, B., Yee, D., Arteaga, C.L., Engelman, J.A., Acquired resistance to EGFR tyrosine kinase inhibitors in cancer cells is mediated by loss of IGF-binding proteins, J Clin Invest, 118 (2008) 2609-2619.
9. Buck, E., Eyzaguirre, A., Rosenfeld-Franklin, M., Thomson, S., Mulvihill, M., Barr, S., Brown, E., O'Connor, M., Yao, Y., Pachter, J., Miglarese, M., Epstein, D., Iwata, K.K., Haley, J.D., Gibson, N.W., Ji, Q.S., Feedback mechanisms promote cooperativity for small molecule inhibitors of epidermal and insulin-like growth factor receptors, Cancer Res, 68 (2008) 8322-8332.

10. Galer, C.E., Corey, C.L., Wang, Z., Younes, M.N., Gomez-Rivera, F., Jasser, S.A., Ludwig, D.L., El-Naggar, A.K., Weber, R.S., Myers, J.N., Dual inhibition of epidermal growth factor receptor and insulin-like growth factor receptor I: reduction of angiogenesis and tumor growth in cutaneous squamous cell carcinoma, Head Neck, 33 (2011) 189-198.
11. Dong, J., Sereno, A., Aivazian, D., Langley, E., Miller, B.R., Snyder, W.B., Chan, E., Cantele, M., Morena, R., Joseph, I.B., Boccia, A., Virata, C., Gamez, J., Yco, G., Favis, M., Wu, X., Graff, C.P., Wang, Q., Rohde, E., Rennard, R., Berquist, L., Huang, F., Zhang, Y., Gao, S.X., Ho, S.N., Demarest, S.J., Reff, M.E., Hariharan, K., Glaser, S.M., A stable IgG-like bispecific antibody targeting the epidermal growth factor receptor and the type I insulin-like growth factor receptor demonstrates superior anti-tumor activity, MAbs, 3 (2011) 273-288.
12. Shaw, P.H., Maughan, T.S., Clarke, A.R., Dual inhibition of epidermal growth factor and insulin-like 1 growth factor receptors reduce intestinal adenoma burden in the Apc(min/+) mouse, Br J Cancer, 105 (2011) 649-657.
13. Cortot, A.B., Repellin, C.E., Shimamura, T., Capelletti, M., Zejnullahu, K., Ercan, D., Christensen, J.G., Wong, K.K., Gray, N.S., Janne, P.A., Resistance to irreversible EGF receptor tyrosine kinase inhibitors through a multistep mechanism involving the IGF1R pathway, Cancer Res, 73 (2013) 834-843.
14. Duncan, R., Gaspar, R., Nanomedicine(s) under the microscope, Mol Pharm, 8 (2011) 2101-2141.
15. van der Meel, R., Oliveira, S., Altintas, I., Haselberg, R., van der Veeken, J., Roovers, R.C., van Bergen en Henegouwen, P.M., Storm, G., Hennink, W.E., Schiffelers, R.M., Kok, R.J., Tumor-targeted Nanobullets: Anti-EGFR nanobody-liposomes loaded with anti-IGF-1R kinase inhibitor for cancer treatment, J Control Release, 159 (2012) 281-289.
16. Hamers-Casterman, C., Atarhouch, T., Muyldermans, S., Robinson, G., Hamers, C., Songa, E.B., Bendahman, N., Hamers, R., Naturally occurring antibodies devoid of light chains, Nature, 363 (1993) 446-448.
17. Oliveira, S., Schiffelers, R.M., van der Veeken, J., van der Meel, R., Vongpromek, R., van Bergen En Henegouwen, P.M., Storm, G., Roovers, R.C., Downregulation of EGFR by a novel multivalent nanobody-liposome platform, J Control Release, 145 (2010) 165-175.
18. Hofman, E.G., Ruonala, M.O., Bader, A.N., van den Heuvel, D., Voortman, J., Roovers, R.C., Verkleij, A.J., Gerritsen, H.C., van Bergen En Henegouwen, P.M., EGF induces coalescence of different lipid rafts, J Cell Sci, 121 (2008) 2519-2528.
19. Roovers, R.C., Henderikx, P., Helfrich, W., van der Linden, E., Reurs, A., de Bruine, A.P., Arends, J.W., de Leij, L., Hoogenboom, H.R., High-affinity recombinant phage antibodies to the pan-carcinoma marker epithelial glycoprotein-2 for tumour targeting, Br J Cancer, 78 (1998) 1407-1416.
20. Altintas, I., Heukers, R., van der Meel, R., Lacombe, M., Amidi, M., van Bergen En Henegouwen, P.M., Hennink, W.E., Schiffelers, R.M., Kok, R.J., Nanobody-albumin nanoparticles (NANAPs) for the delivery of a multikinase inhibitor 17864 to EGFR overexpressing tumor cells, J Control Release, 165 (2013) 110-118.
21. Rouser, G., Fkeischer, S., Yamamoto, A., Two dimensional then layer chromatographic separation of polar lipids and determination of phospholipids by phosphorus analysis of spots, Lipids, 5 (1970) 494-496.
22. Brenner, J.C., Graham, M.P., Kumar, B., Saunders, L.M., Kupfer, R., Lyons, R.H., Bradford, C.R., Carey, T.E., Genotyping of 73 UM-SCC head and neck squamous cell carcinoma cell lines, Head Neck, 32 (2010) 417-426.
23. Vichai, V., Kirtikara, K., Sulforhodamine B colorimetric assay for cytotoxicity screening, Nat Protoc, 1 (2006) 1112-1116.
24. Zucker, D., Marcus, D., Barenholz, Y., Goldblum, A., Liposome drugs' loading efficiency: a working model based on loading conditions and drug's physicochemical properties, J Control Release, 139 (2009) 73-80.
25. McCubrey, J.A., Steelman, L.S., Chappell, W.H., Abrams, S.L., Wong, E.W., Chang, F.,

Lehmann, B., Terrian, D.M., Milella, M., Tafuri, A., Stivala, F., Libra, M., Basecke, J., Evangelisti, C., Martelli, A.M., Franklin, R.A., Roles of the Raf/MEK/ERK pathway in cell growth, malignant transformation and drug resistance, Biochim Biophys Acta, 1773 (2007) 1263-1284.

26. van der Veeken, J., Oliveira, S., Schiffelers, R.M., Storm, G., van Bergen En Henegouwen, P.M., Roovers, R.C., Crosstalk between epidermal growth factor receptor- and insulin-like growth factor-1 receptor signaling: implications for cancer therapy, Curr Cancer Drug Targets, 9 (2009) 748-760.
27. Zhang, Y.W., Staal, B., Essenburg, C., Su, Y., Kang, L., West, R., Kaufman, D., Dekoning, T., Eagleson, B., Buchanan, S.G., Vande Woude, G.F., MET kinase inhibitor SGX523 synergizes with epidermal growth factor receptor inhibitor erlotinib in a hepatocyte growth factor-dependent fashion to suppress carcinoma growth, Cancer Res, 70 (2010) 6880-6890.
28. Choi, E.J., Ryu, Y.K., Kim, S.Y., Wu, H.G., Kim, J.S., Kim, I.H., Kim, I.A., Targeting epidermal growth factor receptor-associated signaling pathways in non-small cell lung cancer cells: implication in radiation response, Mol Cancer Res, 8 (2010) 1027-1036.
29. She, Q.B., Solit, D.B., Ye, Q., O'Reilly, K.E., Lobo, J., Rosen, N., The BAD protein integrates survival signaling by EGFR/MAPK and PI3K/Akt kinase pathways in PTEN-deficient tumor cells, Cancer Cell, 8 (2005) 287-297.
30. Fang, J., Nakamura, H., Maeda, H., The EPR effect: Unique features of tumor blood vessels for drug delivery, factors involved, and limitations and augmentation of the effect, Adv Drug Deliv Rev, 63 (2011) 136-151.
31. van Dongen, G.A., Braakhuis, B.J., Leyva, A., Hendriks, H.R., Kipp, B.B., Bagnay, M., Snow, G.B., Anti-tumor and differentiation-inducing activity of N,N-dimethylformamide (DMF) in head-and-neck cancer xenografts, Int J Cancer, 43 (1989) 285-292.
32. Ruiz van Haperen, V.W., Veerman, G., Boven, E., Noordhuis, P., Vermorken, J.B., Peters, G.J., Schedule dependence of sensitivity to 2',2'-difluorodeoxycytidine (Gemcitabine) in relation to accumulation and retention of its triphosphate in solid tumour cell lines and solid tumours, Biochem Pharmacol, 48 (1994) 1327-1339.
33. Talelli, M., Oliveira, S., Rijcken, C.J., Pieters, E.H., Etrych, T., Ulbrich, K., van Nostrum, R.C., Storm, G., Hennink, W.E., Lammers, T., Intrinsically active nanobody-modified polymeric micelles for tumor-targeted combination therapy, Biomaterials, 34 (2013) 1255-1260.
34. Coimbra, M., Isacchi, B., van Bloois, L., Torano, J.S., Ket, A., Wu, X., Broere, F., Metselaar, J.M., Rijcken, C.J., Storm, G., Bilia, R., Schiffelers, R.M., Improving solubility and chemical stability of natural compounds for medicinal use by incorporation into liposomes, Int J Pharm, 416 (2011) 433-442.
35. Vaneycken, I., Devoogdt, N., Van Gassen, N., Vincke, C., Xavier, C., Wernery, U., Muyldermans, S., Lahoutte, T., Caveliers, V., Preclinical screening of anti-HER2 nanobodies for molecular imaging of breast cancer, FASEB J, 25 (2011) 2433-2446.
36. Behdani, M., Zeinali, S., Khanahmad, H., Karimipour, M., Asadzadeh, N., Azadmanesh, K., Khabiri, A., Schoonooghe, S., Habibi Anbouhi, M., Hassanzadeh-Ghassabeh, G., Muyldermans, S., Generation and characterization of a functional Nanobody against the vascular endothelial growth factor receptor-2; angiogenesis cell receptor, Mol Immunol, 50 (2012) 35-41.
37. Van de Broek, B., Devoogdt, N., D'Hollander, A., Gijs, H.L., Jans, K., Lagae, L., Muyldermans, S., Maes, G., Borghs, G., Specific cell targeting with nanobody conjugated branched gold nanoparticles for photothermal therapy, ACS Nano, 5 (2011) 4319-4328.

Supplementary material

Name	Mean size (μm)	PDI	Mean zeta potential (mV)
NIRF-L	0.13	0.08	-23.8
NIRF-EGa1-L	0.13	0.06	-17

Supplementary Table 1. Near-infrared fluorescently-labeled liposome characteristics. Data are presented as the values of one prepared batch of liposomes.

Name	Mean size (μm)	PDI	Mean zeta potential (mV)
EGa1-AG538-L	0.12 ± 0.03	0.15 ± 0.04	-18.0 ± 1.7
Cationic EGa1-AG538-L	0.13 ± 0.01	0.25 ± 0.03	7.3 ± 1.5

Supplementary Table 2. Liposomes utilized for UM-SCC-14C tumor xenograft study. Molar ratio of kinase inhibitor to total lipid was 40 nmol/μmol. Data are presented as average ± SD of three separately prepared batches of liposomes

Name	Mean size (μm)	PDI	Mean zeta potential (mV)
EGa1-L	0.12 ± 0.03	0.10 ± 0.07	-21.2 ± 9.6
AG538-L	0.11 ± 0.03	0.06 ± 0.03	-24.4 ± 8.2
EGa1-AG538-L	0.11 ± 0.03	0.08 ± 0.03	-24.1 ± 6.4

Supplementary Table 3. Liposomes utilized for MDA-MB-468 tumor xenograft study. Molar ratio of kinase inhibitor to total lipid was 80 nmol/μmol. Data are presented as average ± SD of two separately prepared batches of liposomes.

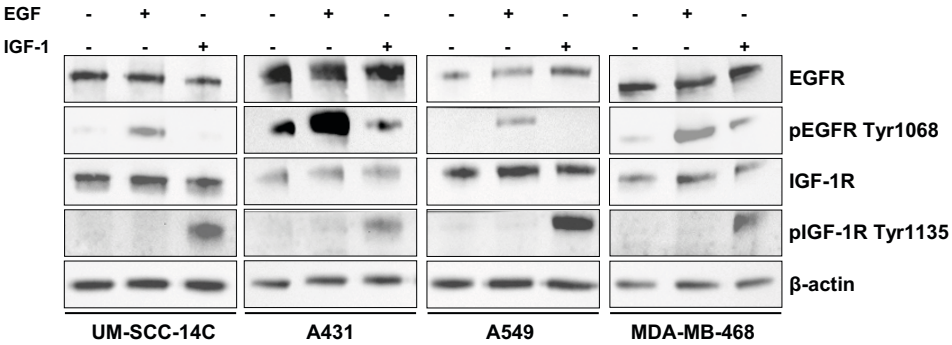

Supplementary Figure 1. EGFR and IGF-1R expression levels in tumor cells. UM-SCC-14C, A431, A549 and MDA-MB-468 cells were starved for 4 h followed by 10 min activation with 25 ng/mL EGF/IGF-1. Cell lysates were collected and subjected to SDS-PAGE. Levels of total EGFR, phosphorylated EGFR (pEGFR Tyr1068), total IGF-1R, phosphorylated IGF-1R (pIGF-1R Tyr1135) and β-actin as a loading control were detected by Western Blotting.

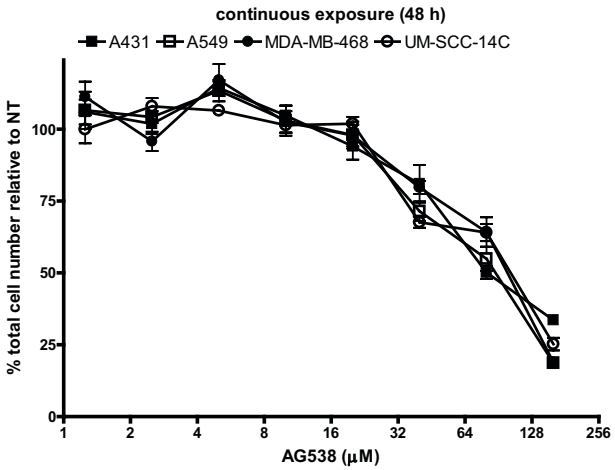

Supplementary Figure 2. AG538-induced cytotoxicity. A431, A549, MDA-MB-468 and UM-SCC-14C cells were exposed to AG538 continuously for 48 h. Total cell number was determined by sulforhodamine B (SRB) assay. Data are presented as mean ± SEM of one representative experiment performed in sextuplicate.

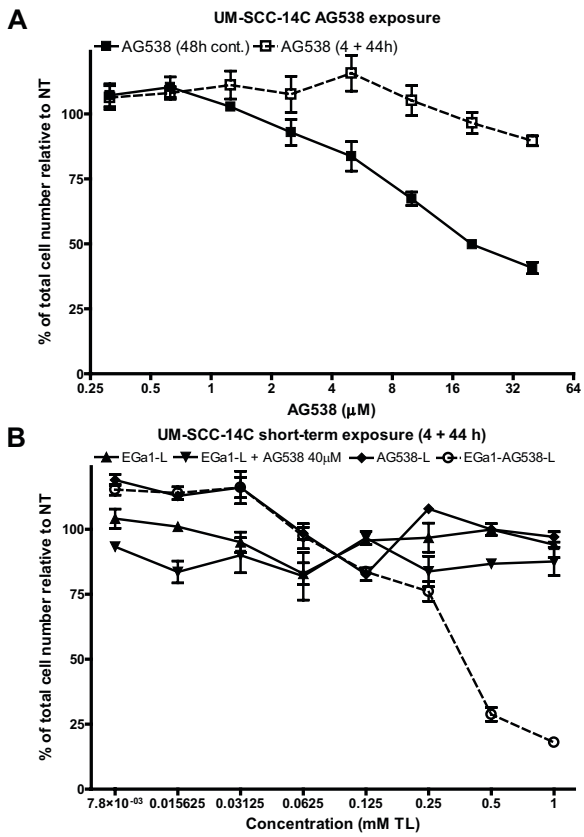

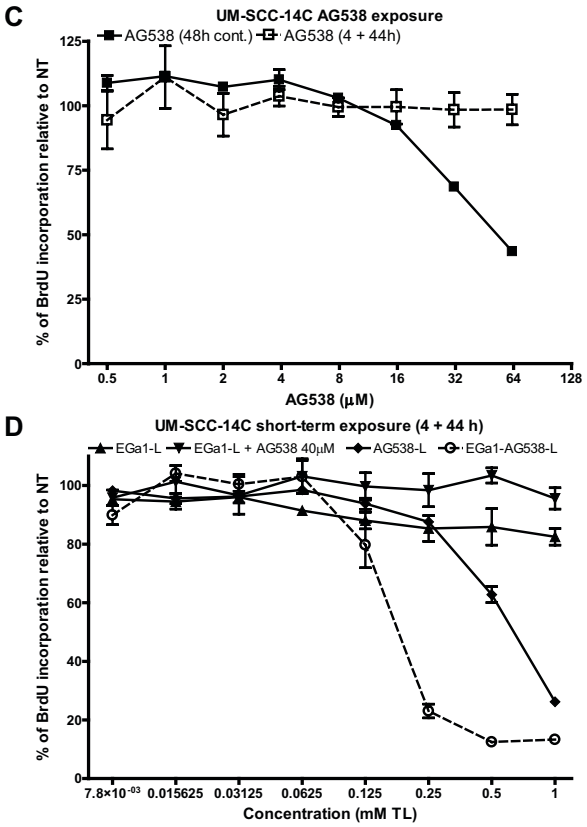

Supplementary Figure 3. UM-SCC-14C cytotoxicity and proliferation after short-term exposure to liposomes. Cells were exposed to AG538 continuously for 48 h, or for 4 h followed by refreshing of the medium and 44 h proliferation. Total cell number was determined sulforhodamine B (SRB) assay (**A**) and number of proliferating cells by BrdU assay (**C**). Cells were exposed to nanobody (Nb)-liposomes (EGa1-L), Nb-liposomes in the presence of free kinase inhibitor (EGa1-L + 40 µM AG538), AG538-loaded liposomes (AG538-L) or Nb-liposomes loaded with AG538 (EGa1-AG538-L) for 4 h followed by refreshing of the medium and 44 h proliferation. Molar ratio of kinase inhibitor to total lipid was 40 nmol/µmol. Total cell number was determined by SRB assay (**B**) and number of proliferating cells by BrdU assay (**D**). Data are presented as mean ± SEM of one representative experiment performed in triplicate.

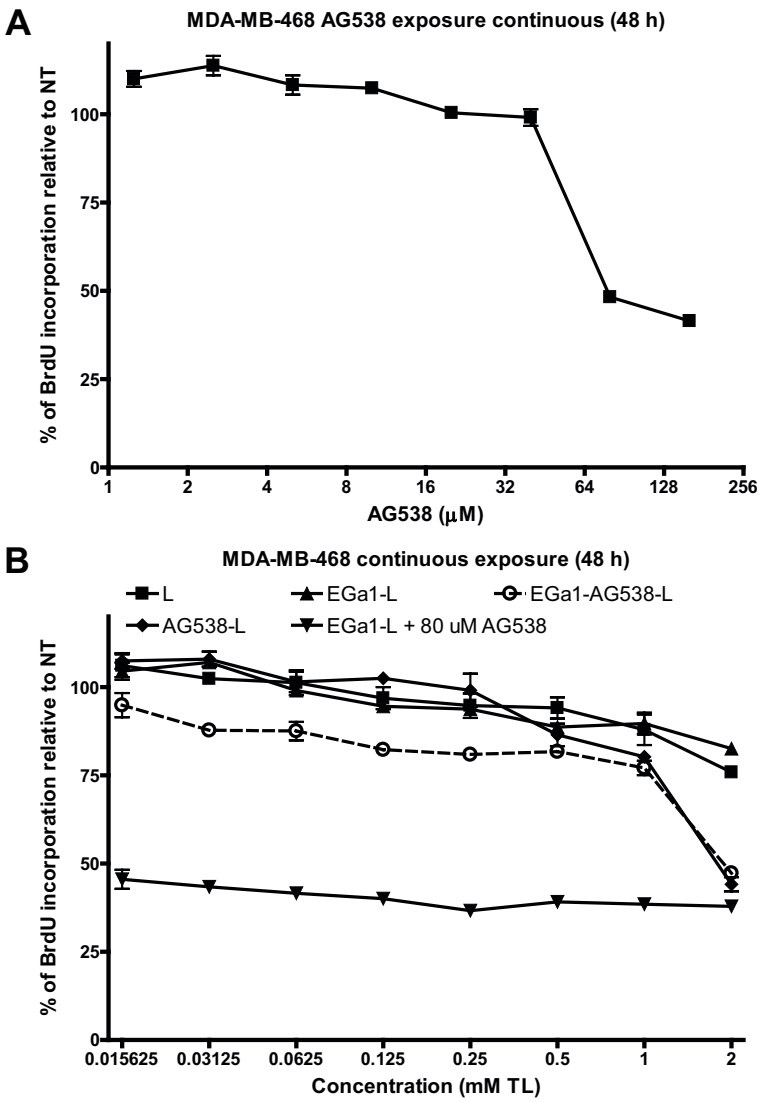

Supplementary Figure 4. MDA-MB-468 proliferation after continuous exposure to liposomes. Cells were exposed to AG538 (**A**); empty control liposomes, nanobody (Nb)-liposomes (EGa1-L), Nb-liposomes in the presence of free kinase inhibitor (EGa1-L + 80 μM AG538), AG538-loaded liposomes (AG538-L) or Nb-liposomes loaded with AG538 (EGa1-AG538-L) (**B**) continuously for 48 h. Molar ratio of kinase inhibitor to total lipid was 80 nmol/μmol. Number of proliferating cells was determined by BrdU assay. Data are presented as mean ± SEM of one representative experiment performed in sextuplicate.

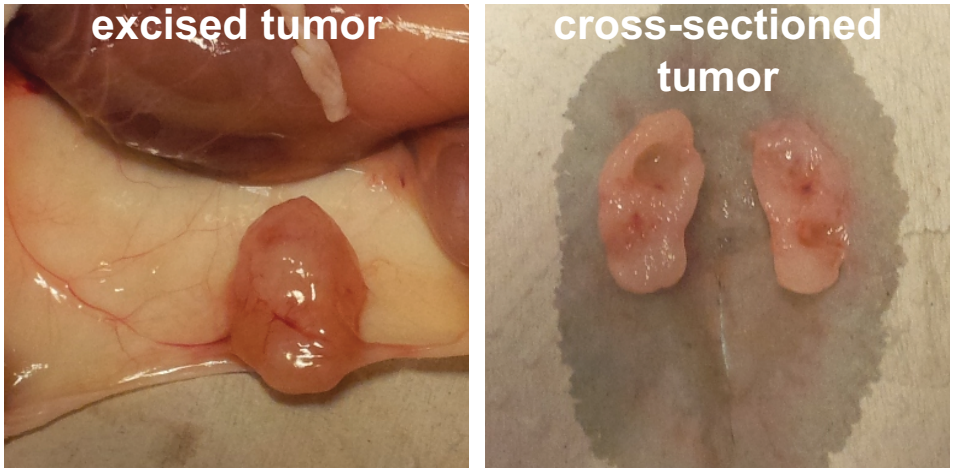

Supplementary Figure 5. Large UM-SCC-14C fluid filled xenograft tumor. Mice were sacrificed upon completion of the efficacy study and UM-SCC-14C xenograft tumors were isolated. Tumors were cross-sectioned for further processing. Representative image of a large fluid filled tumor.

Chapter 5
The VEGF/Rho signaling pathway: A promising target for anti-angiogenic/anti-invasion therapy

Roy van der Meel[a], Marc H. Symons[b], Robert Kudernatsch[c], Robbert J. Kok[a], Raymond M. Schiffelers[a,d], Gert Storm[a,e], William M. Gallagher[f] and Annette T. Byrne[g]

[a] Department of Pharmaceutics, Utrecht Institute for Pharmaceutical Sciences (UIPS), Faculty of Science, Utrecht University, Universiteitsweg 99, 3584 CG Utrecht, The Netherlands

[b] Center for Oncology and Cell Biology, The Feinstein Institute for Medical Research at North Shore-LIJ, 350 Community Drive, Manhasset, NY 11030, USA

[c] Institute of Medicial Immunology, Charité Universitätsmedizin Berlin, Campus Mitte, 10117 Berlin, Germany

[d] Department of Clinical Chemistry and Hematology, University Medical Center Utrecht, Utrecht, The Netherlands

[e] Department of Targeted Therapeutics, MIRA Institute for Biomedical Technology and Technical Medicine, University of Twente, Enschede, The Netherlands

[f] UCD School of Biomolecular and Biomedical Science, UCD Conway Institute, University College Dublin, Belfield, Dublin 4, Ireland

[g] Department of Physiology and Medical Physics, Royal College of Surgeons in Ireland, Reservoir House, Sandyford Industrial Estate, Ballymoss Road, Dublin 18, Ireland

Drug Discovery Today, 16 (5-6): 219-228 (2011)

Abstract

It has become increasingly apparent that current anti-angiogenic therapy elicits modest effects in clinical settings. In addition, it remains challenging to treat cancer metastasis through anti-angiogenic regimes. Rho GTPases are essential for vascular endothelial growth factor (VEGF)-mediated angiogenesis and are involved in tumor cell invasion. This review discusses novel therapeutic strategies that interfere with Rho GTPase signaling and further explores this network as a target for anti-cancer therapy through interference with tumor angiogenesis and invasion. Recent findings describe the development of innovative Rho GTPase inhibitors. Positive clinical effects of Rho GTPase targeting in combination with conventional anti-cancer therapy is of increasing interest.

1. Introduction

The hypothesis introduced by the late Professor Judah Folkman that chronic angiogenesis is necessary to support the growth of many tumor types is now firmly established [1]. Several anti-angiogenic agents are now approved including monoclonal antibodies and small molecule inhibitors [2].

Tumor angiogenesis is controlled by a balance in pro- and anti-angiogenic factors. During tumor growth the balance is shifted and favours pro-angiogenic factors, also referred to as the angiogenic switch [3]. Following the adaptation of an angiogenic phenotype, tumors produce and excrete pro-angiogenic factors, which activate the endothelial cells (ECs) of nearby blood vessels such as basic fibroblast growth factor (bFGF), epidermal growth factor (EGF), platelet-derived growth factor (PDGF) and angiopoietins. Vascular endothelial growth factor (VEGF) is arguably the most important angiogenic factor implicated in both physiological and pathological angiogenesis. Different factors can increase VEGF expression in the tumor such as inflammatory cytokines, growth factors and hypoxia [4]. VEGF signals through binding of several receptor tyrosine kinases (RTKs) including VEGF receptor (VEGFR)-1, -2 and -3. Upon binding of VEGF, these receptors hetero- or homodimerize initiating downstream signaling. VEGF-A is the major mediator of tumor angiogenesis. There are several spliced variants of VEGF-A which can be produced simultaneously. The most predominant forms are VEGF-A_{121} and VEGF-A_{165}. These isoforms signal mainly through VEGFR-2, the receptor that regulates tumor angiogenesis. Binding of VEGF-A to VEGFR-2 results in autophosphorylation of the receptor, and the phosphorylated tyrosine residues function as a docking site for various signal transduction proteins that eventually activate cellular processes involved in angiogenesis [5]. One of the signaling cascades activated by VEGF is the Rho GTPase pathway. Rho GTPases are small proteins that function as molecular switches. They are a sub-family of the Ras superfamily of small GTPases and control cellular processes such as vesicle trafficking, cytoskeleton regulation, cell polarity, microtubule dynamics, membrane transport and transcription factor activity [6]. The Rho-family of small GTPases consists of >20 members and can be divided into typical and atypical Rho GTPases. Typical Rho GTPases, which include Cdc42 and the Rac and Rho subfamily members, cycle between an inactive state in which guanine diphosphate (GDP) is bound to the signaling protein, and an active state when guanine triphosphate (GTP) replaces GDP. In the active state Rho GTPases can bind downstream effector proteins, and transduce signals from various membrane receptors for cytokines, growth factors, adhesion molecules and G-protein coupled receptors (Fig. 1).

As for many other anti-cancer agents, initial sensitivity of the tumor towards anti-angiogenic agents gives way to the development of resistance [7-8]. In addition,

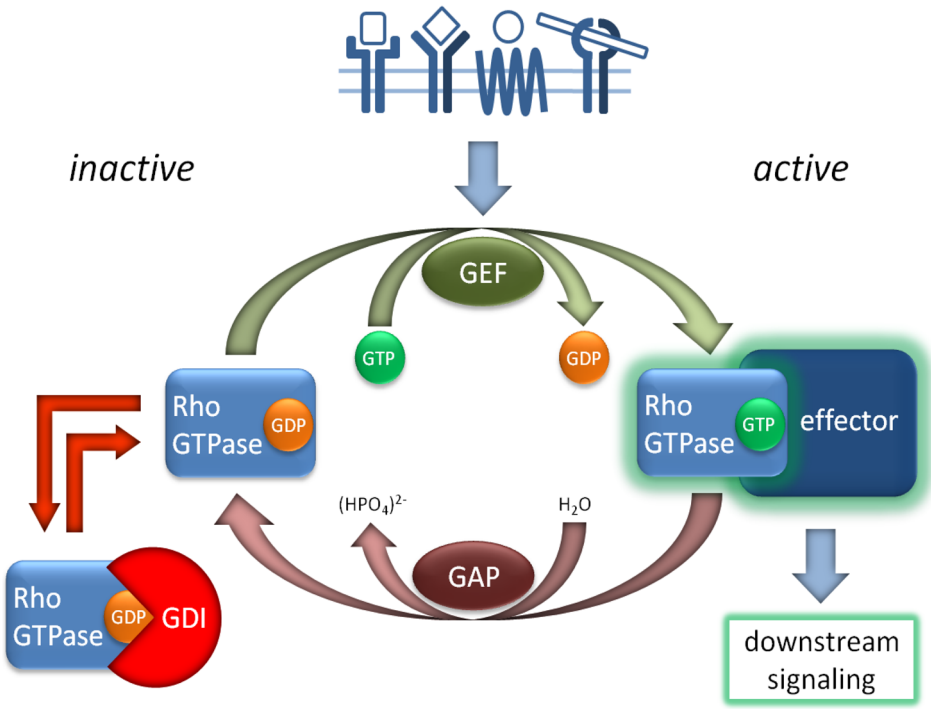

Figure 1. Regulation of Rho GTPases. The spatio-temporal regulation of typical Rho GTPases is controlled by >150 regulatory proteins, divided in three classes: guanine nucleotide exchange factors (GEFs), GTPase-activating proteins (GAPs) and guanine nucleotide dissociation inhibitors (GDIs) [6]. Activation of typical Rho proteins is controlled by GEFs, which catalyze the exchange of guanine diposphate (GDP) for guanine triphosphate (GTP). To date, >80 GEFs have been described and are divided in two distinct families. The diffuse B-cell lymphoma-related (Dbl) family of GEFs possess a Dbl homology (DH) catalytic domain which executes GEF activity and a pleckstrin homology (PH) domain for auto-inhibition [11]. The dedicator of cytokinesis (DOCK) related or CDM and Zizimin homology (CZH) family of proteins contain DOCK homology region (DHR) 1 and 2 catalytic domains which are responsible for GEF activity. The action of DOCKs appears to be restricted to Cdc42 and Rac subfamily members, in contrast to Dbl GEFs [12].GAPs inactivate typical Rho GTPases by enhancing their ability to hydrolyze bound GTP to GDP. Like GEFs, RhoGAPs outnumber the Rho GTPases they regulate and ~70 RhoGAPS have been identified [13].GDIs function by clamping Rho GTPases in the GDP-bound state by preventing access to GEFs. GDIs can also prevent signaling by Rho GTPases by retaining them in the cytosol. GDIs can bind the C-terminal prenyl group of Rho GTPases, which is needed for association with cell membranes where activation and subsequent downstream signaling can take place. Phosphorylation can lead to dissociation of GDIs from Rho GTPases allowing translocation to the cell membrane. To date, three human GDI proteins have been described [14]. Over 70 downstream effectors of Rho proteins have been identified, with a wide variety of functions including tyrosine kinases, serine/threonine kinases, lipases, lipid kinases, phosphatase subunits and scaffolding proteins. Rho GTPases associate with multiple effector proteins, and some effector proteins can interact with multiple Rho GTPases. [15].

anti-angiogenic therapy may paradoxically select for more invasive and metastatic tumor types [9-10]. Combinatorial strategies that target proteins involved in angiogenesis and invasion mechanisms in both tumor and endothelial cells could improve therapeutic outcome and provide a useful approach towards enduring and effective anti-cancer responses. This review will outline that Rho GTPases are an attractive target for such an improved anti-cancer therapy.

2. Rho GTPases in angiogenesis

Following the discovery of Rho GTPases, studies were performed with dominant negative (dn) or constitutively active (ca) Rho proteins to gain insight into their cellular functions. In addition, bacterial toxins, RNA interference (RNAi) and knockout approaches have been used to investigate the effect of Rho GTPase inhibition *in vitro* and *in vivo*. While some results in knockout mice correlate with dn approaches *in vitro*, others produce conflicting results. A considerable drawback of dn mutants is that they non-specifically block the action of guanine exchange factors (GEFs) that act on multiple GTPases [16]. In addition, adaptive compensation by upregulation of related Rho GTPases or isoforms after loss of a certain Rho GTPase could also be a factor that masks phenotypes in knockout mice [17]. Global knockout of Rac1 or Cdc42 in mice results in embryonic lethality, indicating that these Rho GTPases are essential for development. In contrast, global knockout of other Rho proteins (including Rac2, Rac3, RhoB, RhoC, RhoG and RhoH) does not result in severe developmental defects. Conditional knockout mice models have also been utilized to study the effects of organ or cell specific deletion of Rho proteins [6, 17].

A growing body of evidence indicates a critical role for Rho GTPases (and their regulatory and effector proteins) in ECs during all processes involved in angiogenesis such as vascular permeability, extra cellular matrix (ECM) degradation, cellular migration, proliferation and lumen formation [18]. Moreover, several studies have shown that these processes are mediated by VEGF-induced activation of Rho GTPases through VEGFR-2 (Fig. 2) [5, 19].

2.1 Vascular permeability

Paracellular vascular permeability is controlled by adherens and tight junctions between ECs. Rho GTPases are involved in the regulation of actin cytoskeleton and microtubule dynamics and thus can interfere with these cellular junctions. In the case of angiogenesis, VEGF secreted by tumors activates Rho GTPases in ECs and destabilizes endothelial barrier integrity, primarily by disruption of adherens junctions [20].

VEGF treatment induced an increase in reactive oxygen species (ROS) production and vascular permeability in human pulmonary microvessel ECs (HPMECs).

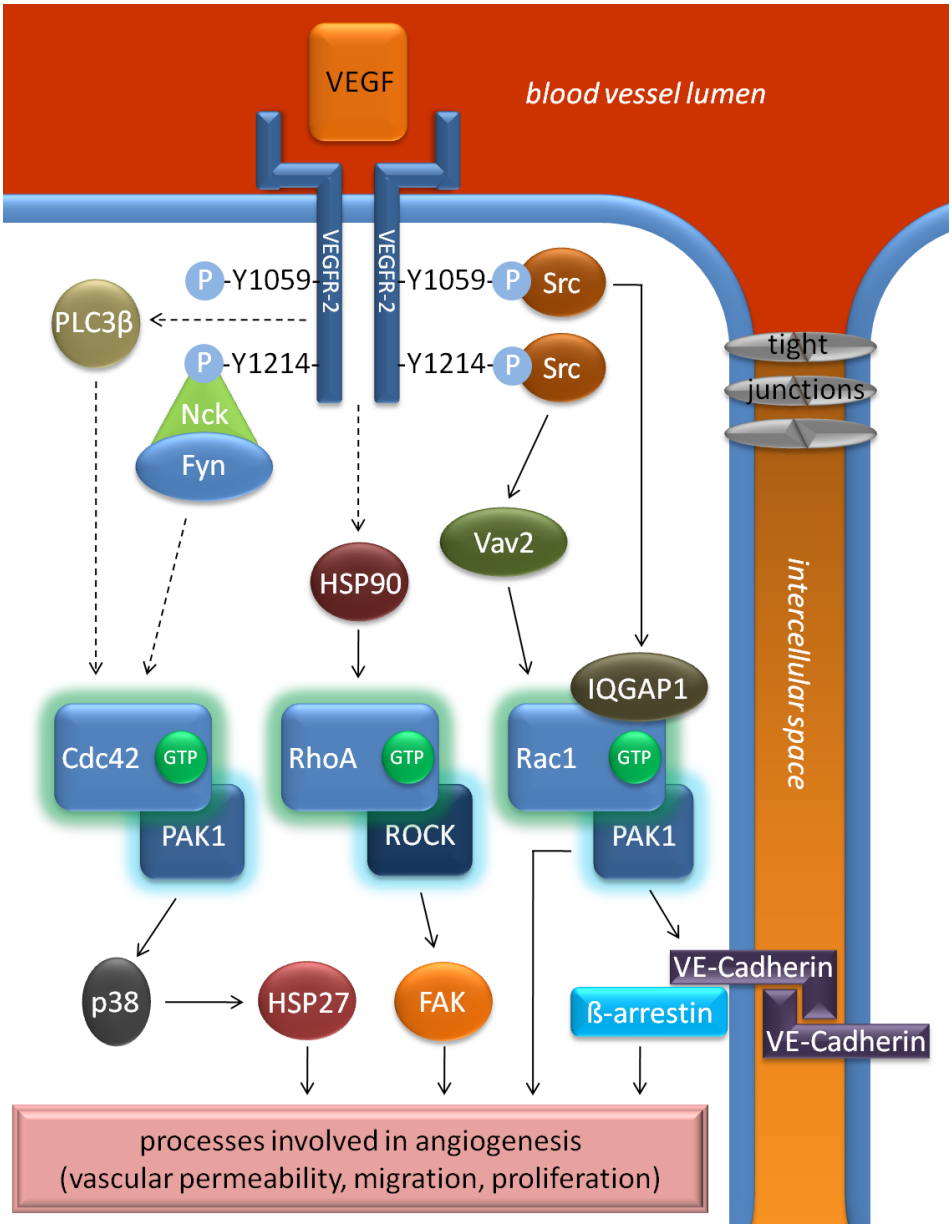

Figure 2. VEGF mediated VEGFR-2 activation of Rho GTPases. VEGF-driven VEGFR-2 activation induces recruitment of proteins to the phosphorylated tyrosine residues such as c-Src [23]. Rho GTPase-dependent cellular processes activated in this way include Vav2-mediated migration and vascular permeability [24-25] and IQ motif containing GTPase activating protein (IQGAP)-1-induced migration, proliferation and vascular permeability [26-28]. Other signaling pathways involved in VEGF-mediated cellular processes include RhoA dependent activation of focal adhesion kinase (FAK) [29-30] and activation of Cdc42 in a phospolipase β3 (PLCβ3)- [31] or Nck/Fyn-dependent manner [29-30]. Solid arrows display direct interactions and dashed arrows display indirect interactions.

Knockdown of Rac1 prevented VEGF-induced ROS production, adherens junction protein phosphorylation and vascular permeability [21].
A recent study has shown that treatment of bovine retinal ECs (BRECs) with VEGF increases cell permeability, an effect that could be reduced by simultaneous treatment with the Rho-associated coiled-coil-forming kinase (ROCK) inhibitor Y-27632, indicating a role for RhoA-mediated signaling [22].

2.2 Degradation of the basement membrane

Basement membrane degradation by matrix metalloproteinases (MMPs) allows ECs to migrate and invade into the ECM.
One study describes antagonistic roles for RhoA and Cdc42 in regulating MMP-2 activation by increasing Cdc42 activity and decreasing RhoA activity [32]. More recently, it has been demonstrated that Rho/ROCK signaling was not required for VEGF-mediated MMP-1 and MMP-9 expression as treatment of BRECs with Y-27632 did not suppress VEGF-stimulated MMP expression [22]. Human microvascular ECs (HMECs) expressing a ca form of RhoA displayed greater invasive ability when compared to control cells likely caused by the induction of MMP-9 expression in the RhoA overexpressing cells. Addition of tissue inhibitor of metalloproteinases (TIMP)-1, a natural MMP inhibitor, reduced the invasion of RhoA expressing cells [33].

2.3 Migration

During EC migration, activation of Rho GTPases is required to regulate the actin cytoskeleton resulting in a forward force at the front of the cell, while simultaneously adhesion forces at the rear of the cell are disrupted. Cdc42 controls the formation of filopodia, which are important for cell-cell contact and sensing the environment. Cdc42 also controls directional migration. Rac1 is responsible for the formation of lamellopodial membrane protrusions at the front of the cell, and RhoA regulates the formation of stress fibres in the rear of the cell and the cell body. These stress fibres mediate cell contractility and thereby allowing forward movement [6, 34].
Although the role of RhoA in EC migration has been debated, treatment of HMECs with Y-27632 blocked VEGF-mediated migration [35]. Recently, it was reported that VEGF-mediated BRECs wound closure could be blocked by the ROCK inhibitor Y-27632 [22]. Deletion of Rac1 in primary ECs derived from mice by the Cre/Flox approach inhibited VEGF-stimulated cell migration [36]. Knockout mice based studies and morpholino approaches in zebrafish identified the Rho GEF Syx (PLEKHG5) as essential for angiogenesis [37]. Knockdown of Syx in rat ECs reduced basal and VEGF-induced migration and tube formation but no effect of Syx inhibition on EC invasion was shown, indicating that Syx does not play a role

in EC invasion [37]. RNA levels of Cdc42GAP, a GTPase activating protein (GAP), were reduced in tubule forming HMECs [38]. HMECs transfected to overexpress Cdc42GAP had reduced tubule-forming capacity compared to control cells while small interfering RNA (siRNA)-mediated knockdown of Cdc42GAP increased tube formation [38]. Similar effects were demonstrated in EC migration, indicating that the effect on tube formation was predominantly due to reduced cell migration [38].

2.4 Proliferation

Local cellular proliferation is required for the formation of vascular branches. Rho GTPases are required for the G1/S transition phase in cell cycle progression [39]. RNAi mediated inhibition of RhoA and RhoC in HMECs decreased cell proliferation by 80% [40]. However, Y-27632 treatment did not interfere with VEGF-stimulated BREC proliferation, indicating that Rho signaling is not required [22].

2.5 Lumen formation

The final step in the angiogenesis process consists of lumen formation and stabilization of the newly formed vessel. Studies performed in zebrafish and in mice suggest that ECs can form lumens by two distinct mechanisms termed cell-hollowing and cord-hollowing [41]. Cell-hollowing involves intracellular vacuole formation and fusion of these vacuoles to form lumens. Kamei *et al.* showed that lumen formation in the intersomitic vessels of zebrafish is mediated by formation and fusion of pinocytic intracellular vacuoles which co-localize with Cdc42 [42]. Although, traditionally, the cell-hollowing mechanism has been regarded as the method by which ECs form lumens, recent evidence derived from studies in zebrafish and mice has shown that lumen formation occurs through the cord-hollowing mechanism [43]. Strilic *et al.* demonstrated that VEGF-mediated ROCK activation results in EC shape changes that ultimately lead to extracellular lumen formation [43].

The role of RhoA/ROCK I/II in angiogenesis signaling is controversial and studies investigating the effects of pharmacological inhibition of RhoA/ROCK report conflicting results. Kroll *et al.* have utilized the oxygen-induced retinopathy mouse model to demonstrate effects of ROCK I/II inhibition by H-1152P [44]. In this assay, inhibition of ROCK increased neovascularisation. Treatment with the VEGF receptor antagonist PTK787/ZK222584 (vatalanib) inhibited neovascularisation, and a combination of H-1152P and vatalanib did not reverse the effect of vatalanib treatment alone, suggesting that ROCK I/II act downstream of VEGF. Interestingly, in the presence of H-1152P and VEGF, human umbilical vein ECs (HUVECs) failed to induce stress fibres. Stress fibres are involved in cell contractility which is required for migration. In the same assay, siRNA-mediated knockdown of ROCK I/II enhanced sprouting angiogenesis and could be inhibited by treatment with

vatalanib. The results of the experiments taken together suggest that ROCK I/II act as negative regulators of VEGF-mediated angiogenesis [44].

In another study, Bryan *et al.* provide results suggesting that blocking Rho inhibits VEGF-stimulated angiogenesis [22]. Murine retinal explants showed VEGF-induced sprouting in a collagen gel, which could be inhibited by ROCK I/II inhibitor Y-27632. BRECs plated between collagen layers formed vessels after VEGF treatment. Interestingly, a combination of VEGF and Y-27632 enhanced cord formation when compared to VEGF alone, but the formed network appeared morphologically distinguishable, indicating immature vessel formation. Furthermore, in a Matrigel™ tube formation assay with ROCK I/II siRNA-transfected mouse pancreatic ECs, it was shown that ROCK II largely mediates VEGF-driven angiogenesis. This effect was confirmed *in vivo* showing lower vascular density in lungs from heterozygote knockout ROCK1 and ROCK2 mice than wild type (wt) mice [22].

In contrast to studies claiming an essential role for Rac1 in angiogenesis, D'Amico *et al.* recently showed that Rac1 depletion in the tumor endothelium of adult wt mice had no effect on tumor growth, tumor angiogenesis and VEGF-mediated angiogenesis [45]. However, in β3-integrin-null mice these processes were dependent on Rac1 expression. Furthermore, Rac1 depletion inhibited VEGF-mediated tube formation and cell migration in 2D scratch wound healing assays in wt and β3-null ECs. Interestingly, knockdown of Rac1 in wt ECs had no effect on VEGF-induced cell migration in 3D Boyden chamber assays but did so in β3-null ECs. This correlates with normal tumor angiogenesis found in wt mice with Rac1 depleted ECs [45]. The αvβ3 integrin, a receptor for both fibronectin and vitronectin expressed on vascular ECs is involved in angiogenesis; and αvβ3-induced activation of Rac1 has been suggested by previous studies [19]. D'Amico *et al.* suggest that increased levels of active Rac1 might compensate for β3-integrin loss because β3-integrin expression rescue in β3-null ECs resulted in active Rac1 levels comparable to wt ECs. The authors conclude that Rac1 might be an attractive target for anti-angiogenesis therapy in tumors that display low levels of β3-integrin in the vasculature, or in combination with anti-β3-integrin therapy [45].

In contrast to the results obtained by D'Amico *et al.* with a Tie1-driven endothelium specific knockout of Rac1 [45], conditional knockout of Rac1 in a Tie2-driven model results in embryonic lethality due to severe defects in the development of major blood vessels [36]. There are several possible explanations for the variation in outcome between the different models. Deletion of Rac1 in the Tie2/Cre-driven model is from early embryogenesis, while the Tie1-driven model used by D'Amico and colleagues induced Rac1 deletion mostly in adult tumor or endothelial cells [45]. Moreover, Cre activity in the Tie2 model also induces Rac1 depletion in hematopoietic cells while it is likely that the lentiviral Tie1/Cre-lox regulated model

does not affect these cells [36, 45].

3. Rho GTPases in tumor invasion

In addition to the requirement for Rho GTPase signaling in ECs mediating angiogenesis, numerous studies have highlighted Rho GTPase involvement in tumorigenesis *in vitro*, more recently, in knock-out mouse models *in vivo* and most importantly in patients [46]. Interestingly, in contrast to RAS proteins, no mutations of Rho GTPases causing ca forms of the protein in tumor cells have been reported. However, overexpression and reduced expression have been frequently documented. Furthermore, mutations in Rho GTPase regulatory proteins that might eliminate or hyperactivate Rho GTPase signaling have also been reported [46].

Of particular interest is Rho GTPase control of tumor cell movement, as migration properties of tumor cells form the basis of tumor cell invasion into the surrounding tissue and subsequent metastasis. Tumor cell migration occurs in two different ways: amoeboid and mesenchymal movements. Amoeboid migration is characterized by rounded cell morphology, the active formation of blebbing protrusions and high cortical tension. In mesenchymal migration cells have an elongated morphology and move through cellular protrusions that attach and drive the cell forward which requires local extracellular proteolysis of the ECM. There seems little difference in the rate of invasion of both these types, as the amoeboid type of migration allows cells to squeeze through the matrix [47].

Sanz-Moreno *et al.* have shown that Rho proteins are not only required for tumor cell migration but even control if tumor cells migrate in an amoeboid or mesenchymal manner. A systematic siRNA screen of all known human GEFs and GAPs in melanoma cells was performed to identify Rho GTPase regulators of the mode of tumor cell invasion. A mechanism was proposed in which mesenchymal migration is dependent on Rac, whereas amoeboid movement is RhoA-dependent. The GEF dedicator of cytokinesis (DOCK)-3 acts together with the adaptor protein neural precursor cell expressed, developmentally down-regulated 9 (NEDD9) to activate Rac. Rac induces mesenchymal migration through Wiskott-Aldrich syndrome protein (WAVE)-2, which simultaneously suppresses amoeboid movement through negative regulation of myosin light chain (MLC)-2 phosphorylation and subsequent inhibition of actomyosin contractility. RhoA/ROCK signaling promotes amoeboid migration and simultaneously activates the Rac GAP ARHGAP22 leading to suppression of mesenchymal tumor cell movement [48]. Furthermore, the same group has demonstrated that Cdc42 is activated by DOCK10 resulting in amoeboid movement. Assays performed with cells expressing a dn form or knocked down Cdc42 revealed that Cdc42 is also required for mesenchymal migration, indicating that there are specific Cdc42 activating pathways involved in both types of tumor

cell motility [49].

The involvement of Rho proteins in mechanisms regulating invasive and metastasizing cancer types has been extensively documented. For example, studies performed with RhoC knockout mice and mice that develop mammary carcinomas and lung metastases demonstrated that loss of RhoC decreased the metastatic potential of tumor cells *in vivo* and reduced migration and invasion of these cells *in vitro* [50]. The role of Rac1 in tumor invasion has been shown in two types of brain tumors: glioma and medulloblastoma. Rac1 transfected cells demonstrated reduced tumor cell migration and invasion [16]. A similar approach was utilized to study the invasive behavior of medulloblastoma cells [51]. Importantly, immunohistochemical (IHC) analysis demonstrated overexpression of Rac1 in both glioblastoma and medulloblastoma tissue versus non-neoplastic brain, and marked plasma membrane staining of Rac1 indicated hyperactivation of this GTPase in these tumors [51-52]. Besides Rho GTPases, GEFs and GAPs have also been shown to be deregulated in tumor invasion and metastasis. Melanoma cells stably transfected to express a constitutively active GTPase-deficient mutant of the G-protein Gα13 displayed reduced chemokine-induced invasion compared to cells expressing the wt protein. Additionally, cells expressing mutant Gα13 displayed higher p190RhoGAP chemokine-mediated phosphorylation when compared with wt-expressing cells. Knockdown of p190RhoGAP reversed the reduced invasion of the mutant-expressing cells and recovered RhoA activation, indicating that p190RhoGAP activation reduces RhoA mediated invasion of melanoma cells [53]. The GEFs Ect2, triple functional domain protein (Trio) or Vav3 are overexpressed in glioblastoma when compared to low-grade glioma or normal brain tissue. Silencing of the GEFs in SNB19 and U-87 glioma cell lines inhibited migration *in vitro* and invasion in an *ex vivo* rat brain slice model [52]. The involvement of Rho proteins in tumor invasion and metastasis is confirmed by frequently reported correlation between Rho protein expression and clinical outcome [46]. For example, levels of RhoC expression are elevated in head and neck squamous cell carcinoma cell lines, and IHC analysis on a tissue microarray demonstrated the correlation of RhoC expression *in vivo* with advanced clinical stage and lymph node metastasis [46, 54]. Analysis of matched tumor, non-tumor and metastatic lymph node tissue from patients with urothelial carcinoma of the upper urinary tract revealed that levels of active GTP-bound Rac1 and p21-activated kinase (PAK)-1 protein expression were increased in tumor tissue and metastatic tissue when compared with non-tumor tissue. Furthermore, high levels of Rac1 activity and PAK1 expression correlated to muscle invasion, lymphovascular invasion and lymph node metastasis [55-56].

4. Targeting Rho GTPases

Currently, several strategies targeting Rho GTPases are explored including specific Rho protein inhibitors, RNAi and lipid modification inhibitors (Fig. 3).

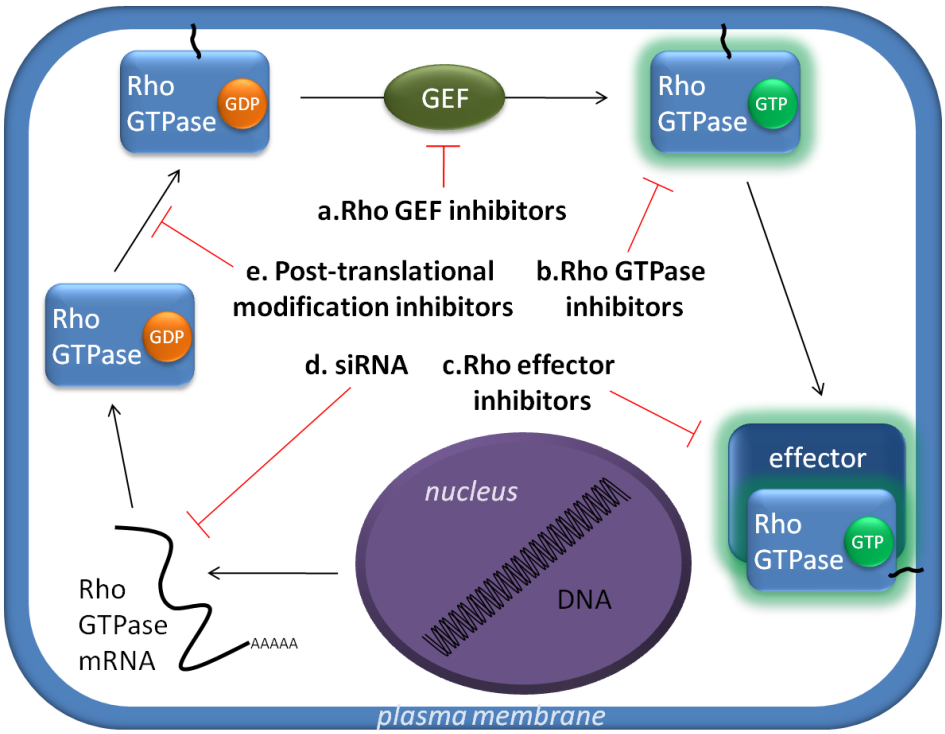

Figure 3. Strategies to interfere with the Rho signaling pathway. Several strategies are exploited to target proteins of the Rho signaling network. **A.** Specific inhibition of Rho GEFs blocks activation of Rho GTPases. **B.** Rho GTPase activation can be inhibited by prevention of GEF or GTP binding. **C.** Activation of downstream Rho effector proteins such as serine/threonine kinases activation is prevented with ATP competitive or non-ATP competitive kinase inhibitors. **D.** RNAi is a highly specific strategy utilized to prevent Rho protein translation. **E.** Inhibition of post-translational modifications is a broadly acting strategy to interfere with the Rho signaling network.

4.1 Small molecule inhibitors

The emerging role of Rho GTPases, regulatory and effector proteins in angiogenesis has led to an increasing interest in the development of specific small molecule inhibitors. The large number of cellular functions that are known to be controlled by RhoA, Rac1 and Cdc42 strongly suggests that systemic inhibition of these GTPases would lead to significant toxicity, implying that targeting GEFs and/or GTPase effectors may be better therapeutic opportunities at present [57]. Indeed, most therapeutic molecules are kinase inhibitors which compete with ATP and block kinase activity of Rho GTPase effector proteins such as ROCK and PAK.

Other inhibitors are aimed at blocking Rho GTPase activation by preventing binding of GTP or GEFs. Specific inhibitors are required to further dissect Rho GTPase pathways in preclinical settings and can be useful clinically to improve anti-angiogenic and anti-tumor therapy. Established and novel small-molecule inhibitors targeting Rho GTPase signaling pathways in angiogenesis are highlighted (Table 1).

The most commonly used pharmacological inhibitors to interfere with angiogenesis by targeting Rho signaling are the ROCK inhibitors Y-27632, Y-32885 (Wf-536), HA1077 (Fasudil) and H-1152P.

Fasudil has been approved in Japan since 1995 for the treatment of cerebral vasospasm and is currently under clinical investigation for beneficial effects in cardiovascular patients [58]. A growing number of studies now describe its effects on tumor growth and angiogenesis. Fasudil has been shown to inhibit VEGF-stimulated HUVEC migration, viability and tube formation. Furthermore, fasudil reduced VEGF-mediated vessel formation in a directed *in vivo* angiogenesis assay [59]. Treatment of breast cancer and fibrosarcoma cells with 50 μmol/L fasudil and its metabolite fasudil-OH inhibited cell migration with 26% and 50% respectively. Fasudil and fasudil-OH inhibited anchorage-dependent growth of breast cancer cells. Additionally, fasudil treatment significantly reduced the amount of tumors in a rat peritoneal tumor model and a murine experimental lung metastasis xenograft model when compared with control treatment groups. Interestingly, in an orthotopic xenograft mouse model fasudil treatment did not reduce tumor size. However, the number of tumor-bearing animals in the treatment group was considerably lower when compared with the control group [60].

In a recent study (as mentioned above) by Bryan *et al.* [22], inhibitory effects of Y-27632 on *in vitro* and *ex vivo* angiogenesis have been demonstrated [22]. The effects of Wf-536 on angiogenesis *in vitro* and tumor growth *in vivo* in combination with the MMP inhibitor Marimastat have also been investigated. Wf-536 inhibited sphingosine-1-phosphate (S1P)-induced HUVEC vacuole formation, one of the earliest events in angiogenesis. Wf-536 interrupted S1P-mediated HUVEC tube formation in Matrigel™ assays and the inhibiting effect could be increased by combination treatment. Similar effects of combination treatments on sprout formation were obtained in rabbit thoracic aortic explants embedded in collagen gels supplemented with VEGF and hepatocyte growth factor (HGF). In addition, Wf-536, the MMP inhibitor marimastat or combination treatment of both agents inhibited S1P- and EGF-mediated HUVEC migration. Finally, combination treatment inhibited tumor growth when compared to control treatment in mice bearing human prostate cancer xenografts. Moreover, the combination treatment

plus paclitaxel (Taxol®) was significantly more effective than paclitaxel alone in the same tumor model [61]. H-1152P, a dimethylated analogue of fasudil, is the most potent ROCK inhibitor available. H1152P inhibits ROCK activity in an ATP-competitive manner with a Ki value of 1.6 nM. By comparison, fasudil and Y-27632 have Ki values of 0.33 μM and 0.14 μM, respectively [62]. Interestingly, H1152P treatment enhanced VEGF-induced in-gel sprouting angiogenesis and increased preretinal vessel formation in the oxygen-induced retinopathy (OIR) model in a study by Kroll *et al.* discussed earlier [44].

The selective small-molecule Rac1 inhibitor NSC23766 fits in a surface groove essential for GEF binding and has been shown to prevent activation by GEFs Trio and T-cell lymphoma invasion and metastasis (Tiam) [63]. Treatment of prostate cancer cells with NSC23766 in a dose dependent manner inhibited cell proliferation and anchorage-independent cell growth. Furthermore, the invasion of tumor cells treated with 25 μM NSC23766 was inhibited by 85% [63]. Inhibition of Rac1 by NSC23766 (again in a dose dependent manner) reduced both basal HUVEC proliferation as well as proliferation induced by VEGF, HGF or a combination of the two [64].

Development of several novel Rho protein inhibitors have been reported which might be useful in targeting Rho proteins in tumor invasion and angiogenesis.

Evelyn *et al.* have shown the small-molecule inhibitor CCG-1423 to have anti-proliferative effects on various cancer cells and anti-invasion effects in prostate cancer cells [65].

PAK4, a downstream effector protein of Rac1 and Cdc42, is involved in EC lumen formation, and knockdown of PAK4 inhibited tube formation and invasion of HUVECs in 3D collagen gel matrices [66]. More recently, a small molecule inhibitor of PAK4 was identified by structure-based design and high throughput screening. PF3758309 showed inhibiting effects on a broad selection of tumor cell lines in anchorage-independent and -dependent proliferation assays. Furthermore, PE3758309 inhibited tumor growth in a panel of human xenograft tumor models [67].

The novel Rac inhibitor EHT1864 interferes with the guanine nucleotide exchange process. In assays performed in mouse fibroblasts, EHT1864 inhibited Rac downstream signaling and cell growth transformation [68].

The PAK1 inhibitor IPA-3 was identified in a high throughput screen which utilized ATP hydrolysis as an indication of PAK1 activation. PAK1 is autoinhibited by formation of inactive homodimers where an autoregulatory region of one monomer binds the catalytic domain of its partner. Upon activation of PAK1 by Rac or Cdc42, monomer dissociation and displacement of the autoinhibitory domain occurs, followed by autophosphorylation to stabilize the active monomer. IPA-3

targets this autoregulatory mechanism, and possibly altering the conformation of PAK1, making it catalytically inactive [69]. A similar mechanism of action has been demonstrated for the neural-WASP (N-WASP) inhibitor wiskostatin. N-WASP is can be activated by Cdc42 in the same way as PAK1. Wiskostatin interacts with the regulatory GTPase-binding domain of N-WASP, thereby promoting this domain to fold into the autoinhibitory confirmation and blocking N-WASP to function normally [70]. Targeting autoregulatory domains of kinases may provide more specific inhibition than ATP-competitive approaches, reducing the risk of off-target effects and toxicity [71].Utilizing a high throughput bead-based flow cytometric fluorescent GTP-binding assay for screening compounds that target GTP binding to Rho GTPases, MLS000532223 was identified. MLS000532223 is a general inhibitor of Rho GTPases that prevents binding of GTP in a dose dependent manner. It was shown that MLS000532223 inhibited EGF-stimulated Rac1 activation and EGF stimulated-stress fibre formation in mouse embryonic fibroblasts. In addition, MLS00053223 inhibited IgE-induced cell morphology changes in rat mast cells [72].

Class	Target	Mode of action	Ref.
Rho GEF inhibitor			
ITX3	Trio	Inhibition of N-terminal GEF domain activity	[59]
Rho GTPase inhibitor			
NSC23766	Rac	Competitive inhibitor of GEF activation	[50]
EHT 1864	Rac	Blocking Rac downstream signaling by guanine nucleotide displacement	[54]
MLS000532223	Rho GTPases	Prevention of GTP binding	[58]
Rho effector inhibitor			
Y-27632	ROCK	Kinase inhibitor	[17,48]
Y-32885 (Wf-536)	ROCK	Kinase inhibitor	[47]
Fasudil (HA-1077)	ROCK	Kinase inhibitor	[45,48]
H-1152P	ROCK	Kinase inhibitor	[30,48]
PF-3758309	PAK4	Kinase inhibitor	[53]
IPA-3	PAK1	Non-ATP competitive inhibitor	[55]
Wiskostatin	N-WASP	Non-ATP competitive inhibitor	[58]

Table 1. Small-molecule inhibitors targeting Rho GTPase signaling.

In a yeast based system, the chemical ITX3 was identified which inhibits the activity of the N-terminal GEF domain of Trio, which acts on Rac1 and RhoG. ITX3 blocked Trio N-terminal domain (TrioN)-mediated cell structures in a dose dependent manner in rat fibroblasts, nerve growth factor (NGF)-induced nerve outgrowth in rat phaeochromocytoma cells and myotube formation in mouse myoblasts [73].

4.2 RNAi

RNAi is now used extensively *in vitro* as an efficient tool to inhibit Rho proteins specifically. One study has shown that siRNA mediated knockdown of the Vav2 GEF in ECs prevents VEGF-induced Rac1 activation and subsequent cell migration [24].

Pille *et al.* [40] have reported on the anti-angiogenic effects of RhoA siRNA treatments *in vitro* and *in vivo*. Human ECs were transiently transfected with siRNA against RhoA or RhoC utilizing the commercially available cationic lipid carrier Cytofectin™. Transfected ECs showed decreased proliferation and bFGF-stimulated tube formation was perturbed when compared with control cells. Intratumoral injection of siRNA in Cytofectin™ in mice bearing breast tumor xenografts resulted in inhibition of tumor growth and angiogenesis indices based on IHC staining with platelet-endothelial cell adhesion molecule (PECAM)-1 that was lower in tumors derived from mice treated with RhoA siRNA [40]. In a follow-up study, RhoA siRNA was encapsulated in chitosan-coated polyisohexylcyanoacrylate particles and injected intravenously in the same mouse model. Tumor growth was inhibited with this treatment and IHC staining revealed fewer ECs present in treated (versus untreated) tumors [74].

4.3 Post-translational modification inhibitors

Rho GTPases contain a CAAX motif at their C-terminus (C = cysteine, A = any aliphatic amino acid, X = any amino acid). The CAAX sequence undergoes post-translational prenylation (farnesylation or geranylgeranylation) targeting the proteins to the endoplasmatic reticulum (ER). At the ER, the AAX section is removed by RAS converting enzyme (RCE)-1 and the carboxyl group of the cysteine is methylated by isoprenylcysteine carboxymethyltransferase (ICMT). Rho guanine nucleotide dissociation factors (GDIs) bind to the prenylation moiety and guide Rho GTPases to membranes. Prenylation of Rho GTPases can be targeted by mevalonate pathway inhibitors such as statins or bisphosphonates; prenylation inhibitors such as farnesyltransferase inhibitors; or post-prenylation inhibitors including RCE1 and ICMT inhibitors [75].

Statins are widely used in the clinic as cholesterol-reducing agents and considered safe. Many studies demonstrate anti-angiogenic effects of statins, for

example simvastatin. In mouse corneal pocket assays fibroblast growth factor (FGF)-2-induced vascularization could be suppressed by simvastatin. In chick chorioallantoic membrane (CAM) assays, VEGF-mediated angiogenesis was inhibited by simvasatin in a dose dependent manner, which was also seen in an FGF-2/VEGF-stimulated tube formation of human dermal microvascular ECs (HDMECs) on a 3D collagen matrix. This effect could be reversed by transfecting the cells with a dominant-activating mutant of RhoA, suggesting that the anti-angiogenic effects of simvastatin are mediated by an effect on RhoA. Finally, simvastatin treatment of HDMECs decreased RhoA membrane localization. Geranylgeranyl pyrophosphate reversed the effects of simvastatin on tube formation and RhoA membrane localization, indicating that the effect is mediated via geranylgeranylation of RhoA [76]. However, several studies have shown conflicting pro-angiogenic effects of statin treatment [77]. The most likely hypothesis describes a biphasic effect of statins on angiogenesis where pro-angiogenic effects are observed at low concentrations, and anti-angiogenic effects at high concentrations. As well as dosage, other factors such as cancer type or statin type could be of influence. The biphasic mechanism has been shown by Katsumoto *et al.* in FGF-2 induced neovascularization in CAM assays [78].

Migration and invasive properties of several melanoma cell lines could be dose dependently inhibited by treatment with the statins lovastatin, mevastatin and simvastatin [79]. Bisphosphonates interfere with prenylation of Rho GTPases by inhibiting enzymes in the mevalonate pathway which are required for the production of farnesyl pyrophosphate and geranylgeranyl pyrophosphate [75]. Treatment of HUVECs with alendronate inhibited VEGF-mediated EC migration, tube formation and suppressed Rho activation. These effects could be restored by simultaneous treatment with geranylgeraniol, which is metabolized to geranylgeranyl pyrophosphate, indicating that the effects are caused by inhibition of Rho geranylgeranylation. Finally, alendronate treatment of mice bearing ovarian carcinoma xenografts inhibited intra-tumor angiogenesis with 75% when compared to non-treated mice [80]. Treatment of ECs derived from multiple myeloma patients (MMECs) with the bisphosphonate zoledronic acid inhibited cell proliferation, VEGF-mediated cell migration and tube formation. Furthermore, zoledronic acid inhibited *in vivo* angiogenesis in CAM assays when compared to sponges loaded with MMEC conditioned medium [81].

Despite strong anti-angiogenic effects of post-translational modification inhibitors *in vitro*, results from clinical trials of these drugs as monotherapy only displayed modest effects, possibly due to the lack of specificity and requirement of high doses leading to toxicities. However, combinations with conventional anti-cancer therapies might improve therapeutic outcome [75]. Moreover, the vast clinical experience

with statins is beneficial for designing clinical trials and treatments that target Rho GTPases to interfere with tumor growth and angiogenesis [82].

5. Discussion

Rho proteins are rational targets to interfere with both EC angiogenesis and invasion/metastasis of tumor cells. Indeed, it was suggested that tumor growth inhibition in studies performed with RhoA siRNA or Vav2/3 deficient mice might be due to combined effects on angiogenesis and tumor cells [74, 83]. Besides the direct effect in ECs, targeting Rho proteins might indirectly contribute to the overall anti-angiogenic effect by inhibiting the production and subsequent secretion of pro-angiogenic factors produced by tumor cells, such as VEGF, that are produced by tumor cells [84]. At present, strategies exploring combinations of conventional anti-cancer therapies and targeting of Rho proteins are of particular interest. For example, potential beneficial effects of NSC23766 treatment of trastuzumab-resistant cancer cells [85]. Although conflicting outcomes have been reported previously, recent clinical trial data have suggested beneficial effects of statin or bisphosphonate treatment combined with conventional anti-cancer therapy [86-87]. There is still much to unravel about the mechanisms that are involved in the activation, regulation and downstream signaling of Rho GTPases. For this purpose, it is important to develop specific inhibitors of proteins involved in this pathway. It is now evident that Rho proteins are essential for both tumor angiogenesis and invasion; and targeting of this signaling network is a promising strategy to improve current anti-tumor therapy. An interesting challenge remains in determining which (combinations of) Rho proteins are the most promising druggable targets and how significant the beneficial effects of targeting this signaling network in combination with conventional anti-cancer therapies, will be.

Conflict of interest statement

The authors declare no conflicts in interest.

Acknowledgements

Funding is acknowledged from Science Foundation Ireland in the context of the Molecular Therapeutics for Cancer Ireland, Strategic Research Cluster. We further acknowledge funding received from the EU Marie Curie Industry Academia Pathways & Partnership program in the context of the 'AngioTox'initiative .

References

1. Folkman, J., Tumor angiogenesis: therapeutic implications, N Engl J Med, 285 (1971) 1182-1186.
2. Kerbel, R.S., Tumor angiogenesis, N Engl J Med, 358 (2008) 2039-2049.

3. Bergers, G., Benjamin, L.E., Tumorigenesis and the angiogenic switch, Nat Rev Cancer, 3 (2003) 401-410.
4. Ferrara, N., Vascular endothelial growth factor: basic science and clinical progress, Endocr Rev, 25 (2004) 581-611.
5. Olsson, A.K., Dimberg, A., Kreuger, J., Claesson-Welsh, L., VEGF receptor signalling - in control of vascular function, Nat Rev Mol Cell Biol, 7 (2006) 359-371.
6. Heasman, S.J., Ridley, A.J., Mammalian Rho GTPases: new insights into their functions from in vivo studies, Nat Rev Mol Cell Biol, 9 (2008) 690-701.
7. Bergers, G., Hanahan, D., Modes of resistance to anti-angiogenic therapy, Nat Rev Cancer, 8 (2008) 592-603.
8. Saltz, L.B., Clarke, S., Diaz-Rubio, E., Scheithauer, W., Figer, A., Wong, R., Koski, S., Lichinitser, M., Yang, T.S., Rivera, F., Couture, F., Sirzen, F., Cassidy, J., Bevacizumab in combination with oxaliplatin-based chemotherapy as first-line therapy in metastatic colorectal cancer: a randomized phase III study, J Clin Oncol, 26 (2008) 2013-2019.
9. Ebos, J.M., Lee, C.R., Cruz-Munoz, W., Bjarnason, G.A., Christensen, J.G., Kerbel, R.S., Accelerated metastasis after short-term treatment with a potent inhibitor of tumor angiogenesis, Cancer Cell, 15 (2009) 232-239.
10. Paez-Ribes, M., Allen, E., Hudock, J., Takeda, T., Okuyama, H., Vinals, F., Inoue, M., Bergers, G., Hanahan, D., Casanovas, O., Antiangiogenic therapy elicits malignant progression of tumors to increased local invasion and distant metastasis, Cancer Cell, 15 (2009) 220-231.
11. Rossman, K.L., Der, C.J., Sondek, J., GEF means go: turning on RHO GTPases with guanine nucleotide-exchange factors, Nat Rev Mol Cell Biol, 6 (2005) 167-180.
12. Cote, J.F., Vuori, K., GEF what? Dock180 and related proteins help Rac to polarize cells in new ways, Trends Cell Biol, 17 (2007) 383-393.
13. Tcherkezian, J., Lamarche-Vane, N., Current knowledge of the large RhoGAP family of proteins, Biol Cell, 99 (2007) 67-86.
14. DerMardirossian, C., Bokoch, G.M., GDIs: central regulatory molecules in Rho GTPase activation, Trends Cell Biol, 15 (2005) 356-363.
15. Bustelo, X.R., Sauzeau, V., Berenjeno, I.M., GTP-binding proteins of the Rho/Rac family: regulation, effectors and functions in vivo, Bioessays, 29 (2007) 356-370.
16. Chan, A.Y., Coniglio, S.J., Chuang, Y.Y., Michaelson, D., Knaus, U.G., Philips, M.R., Symons, M., Roles of the Rac1 and Rac3 GTPases in human tumor cell invasion, Oncogene, 24 (2005) 7821-7829.
17. Wang, L., Zheng, Y., Cell type-specific functions of Rho GTPases revealed by gene targeting in mice, Trends Cell Biol, 17 (2007) 58-64.
18. Bryan, B.A., D'Amore, P.A., What tangled webs they weave: Rho-GTPase control of angiogenesis, Cell Mol Life Sci, 64 (2007) 2053-2065.
19. Lamalice, L., Le Boeuf, F., Huot, J., Endothelial cell migration during angiogenesis, Circ Res, 100 (2007) 782-794.
20. Beckers, C.M., van Hinsbergh, V.W., van Nieuw Amerongen, G.P., Driving Rho GTPase activity in endothelial cells regulates barrier integrity, Thromb Haemost, 103 (2010) 40-55.
21. Monaghan-Benson, E., Burridge, K., The regulation of vascular endothelial growth factor-induced microvascular permeability requires Rac and reactive oxygen species, J Biol Chem, 284 (2009) 25602-25611.
22. Bryan, B.A., Dennstedt, E., Mitchell, D.C., Walshe, T.E., Noma, K., Loureiro, R., Saint-Geniez, M., Campaigniac, J.P., Liao, J.K., D'Amore, P.A., RhoA/ROCK signaling is essential for multiple aspects of VEGF-mediated angiogenesis, Faseb J, 24 (2010) 3186-3195.
23. Meyer, R.D., Dayanir, V., Majnoun, F., Rahimi, N., The presence of a single tyrosine residue at the carboxyl domain of vascular endothelial growth factor receptor-2/FLK-1 regulates its autophosphorylation and activation of signaling molecules, J Biol Chem, 277 (2002) 27081-27087.
24. Garrett, T.A., Van Buul, J.D., Burridge, K., VEGF-induced Rac1 activation in endothelial

cells is regulated by the guanine nucleotide exchange factor Vav2, Exp Cell Res, 313 (2007) 3285-3297.
25. Gavard, J., Gutkind, J.S., VEGF controls endothelial-cell permeability by promoting the beta-arrestin-dependent endocytosis of VE-cadherin, Nat Cell Biol, 8 (2006) 1223-1234.
26. Meyer, R.D., Sacks, D.B., Rahimi, N., IQGAP1-dependent signaling pathway regulates endothelial cell proliferation and angiogenesis, PLoS One, 3 (2008) e3848.
27. Yamaoka-Tojo, M., Ushio-Fukai, M., Hilenski, L., Dikalov, S.I., Chen, Y.E., Tojo, T., Fukai, T., Fujimoto, M., Patrushev, N.A., Wang, N., Kontos, C.D., Bloom, G.S., Alexander, R.W., IQGAP1, a novel vascular endothelial growth factor receptor binding protein, is involved in reactive oxygen species--dependent endothelial migration and proliferation, Circ Res, 95 (2004) 276-283.
28. Yamaoka-Tojo, M., Tojo, T., Kim, H.W., Hilenski, L., Patrushev, N.A., Zhang, L., Fukai, T., Ushio-Fukai, M., IQGAP1 mediates VE-cadherin-based cell-cell contacts and VEGF signaling at adherence junctions linked to angiogenesis, Arterioscler Thromb Vasc Biol, 26 (2006) 1991-1997.
29. Lamalice, L., Houle, F., Jourdan, G., Huot, J., Phosphorylation of tyrosine 1214 on VEGFR2 is required for VEGF-induced activation of Cdc42 upstream of SAPK2/p38, Oncogene, 23 (2004) 434-445.
30. Lamalice, L., Houle, F., Huot, J., Phosphorylation of Tyr1214 within VEGFR-2 triggers the recruitment of Nck and activation of Fyn leading to SAPK2/p38 activation and endothelial cell migration in response to VEGF, J Biol Chem, 281 (2006) 34009-34020.
31. Bhattacharya, R., Kwon, J., Li, X., Wang, E., Patra, S., Bida, J.P., Bajzer, Z., Claesson-Welsh, L., Mukhopadhyay, D., Distinct role of PLCbeta3 in VEGF-mediated directional migration and vascular sprouting, J Cell Sci, 122 (2009) 1025-1034.
32. Ispanovic, E., Serio, D., Haas, T.L., Cdc42 and RhoA have opposing roles in regulating membrane type 1-matrix metalloproteinase localization and matrix metalloproteinase-2 activation, Am J Physiol Cell Physiol, 295 (2008) C600-610.
33. Abecassis, I., Olofsson, B., Schmid, M., Zalcman, G., Karniguian, A., RhoA induces MMP-9 expression at CD44 lamellipodial focal complexes and promotes HMEC-1 cell invasion, Exp Cell Res, 291 (2003) 363-376.
34. Raftopoulou, M., Hall, A., Cell migration: Rho GTPases lead the way, Dev Biol, 265 (2004) 23-32.
35. van Nieuw Amerongen, G.P., Koolwijk, P., Versteilen, A., van Hinsbergh, V.W., Involvement of RhoA/Rho kinase signaling in VEGF-induced endothelial cell migration and angiogenesis in vitro, Arterioscler Thromb Vasc Biol, 23 (2003) 211-217.
36. Tan, W., Palmby, T.R., Gavard, J., Amornphimoltham, P., Zheng, Y., Gutkind, J.S., An essential role for Rac1 in endothelial cell function and vascular development, Faseb J, 22 (2008) 1829-1838.
37. Garnaas, M.K., Moodie, K.L., Liu, M.L., Samant, G.V., Li, K., Marx, R., Baraban, J.M., Horowitz, A., Ramchandran, R., Syx, a RhoA guanine exchange factor, is essential for angiogenesis in Vivo, Circ Res, 103 (2008) 710-716.
38. Engelse, M.A., Laurens, N., Verloop, R.E., Koolwijk, P., van Hinsbergh, V.W., Differential gene expression analysis of tubule forming and non-tubule forming endothelial cells: CDC42GAP as a counter-regulator in tubule formation, Angiogenesis, 11 (2008) 153-167.
39. Hirano, K., Hirano, M., Nishimura, J., Kanaide, H., A critical period requiring Rho proteins for cell cycle progression uncovered by reversible protein transduction in endothelial cells, FEBS Lett, 570 (2004) 149-154.
40. Pille, J.Y., Denoyelle, C., Varet, J., Bertrand, J.R., Soria, J., Opolon, P., Lu, H., Pritchard, L.L., Vannier, J.P., Malvy, C., Soria, C., Li, H., Anti-RhoA and anti-RhoC siRNAs inhibit the proliferation and invasiveness of MDA-MB-231 breast cancer cells in vitro and in vivo, Mol Ther, 11 (2005) 267-274.
41. Iruela-Arispe, M.L., Davis, G.E., Cellular and molecular mechanisms of vascular lumen

formation, Dev Cell, 16 (2009) 222-231.
42. Kamei, M., Saunders, W.B., Bayless, K.J., Dye, L., Davis, G.E., Weinstein, B.M., Endothelial tubes assemble from intracellular vacuoles in vivo, Nature, 442 (2006) 453-456.
43. Strilic, B., Kucera, T., Eglinger, J., Hughes, M.R., McNagny, K.M., Tsukita, S., Dejana, E., Ferrara, N., Lammert, E., The molecular basis of vascular lumen formation in the developing mouse aorta, Dev Cell, 17 (2009) 505-515.
44. Kroll, J., Epting, D., Kern, K., Dietz, C.T., Feng, Y., Hammes, H.P., Wieland, T., Augustin, H.G., Inhibition of Rho-dependent kinases ROCK I/II activates VEGF-driven retinal neovascularization and sprouting angiogenesis, Am J Physiol Heart Circ Physiol, 296 (2009) H893-899.
45. D'Amico, G., Robinson, S.D., Germain, M., Reynolds, L.E., Thomas, G.J., Elia, G., Saunders, G., Fruttiger, M., Tybulewicz, V., Mavria, G., Hodivala-Dilke, K.M., Endothelial-Rac1 is not required for tumor angiogenesis unless alphavbeta3-integrin is absent, PLoS One, 5 (2010) e9766.
46. Karlsson, R., Pedersen, E.D., Wang, Z., Brakebusch, C., Rho GTPase function in tumorigenesis, Biochim Biophys Acta, 1796 (2009) 91-98.
47. Friedl, P., Wolf, K., Plasticity of cell migration: a multiscale tuning model, J Cell Biol, 188 11-19.
48. Sanz-Moreno, V., Gadea, G., Ahn, J., Paterson, H., Marra, P., Pinner, S., Sahai, E., Marshall, C.J., Rac activation and inactivation control plasticity of tumor cell movement, Cell, 135 (2008) 510-523.
49. Gadea, G., Sanz-Moreno, V., Self, A., Godi, A., Marshall, C.J., DOCK10-mediated Cdc42 activation is necessary for amoeboid invasion of melanoma cells, Curr Biol, 18 (2008) 1456-1465.
50. Hakem, A., Sanchez-Sweatman, O., You-Ten, A., Duncan, G., Wakeham, A., Khokha, R., Mak, T.W., RhoC is dispensable for embryogenesis and tumor initiation but essential for metastasis, Genes Dev, 19 (2005) 1974-1979.
51. Zavarella, S., Nakada, M., Belverud, S., Coniglio, S.J., Chan, A., Mittler, M.A., Schneider, S.J., Symons, M., Role of Rac1-regulated signaling in medulloblastoma invasion. Laboratory investigation, J Neurosurg Pediatr, 4 (2009) 97-104.
52. Salhia, B., Tran, N.L., Chan, A., Wolf, A., Nakada, M., Rutka, F., Ennis, M., McDonough, W.S., Berens, M.E., Symons, M., Rutka, J.T., The guanine nucleotide exchange factors trio, Ect2, and Vav3 mediate the invasive behavior of glioblastoma, Am J Pathol, 173 (2008) 1828-1838.
53. Bartolome, R.A., Wright, N., Molina-Ortiz, I., Sanchez-Luque, F.J., Teixido, J., Activated G(alpha)13 impairs cell invasiveness through p190RhoGAP-mediated inhibition of RhoA activity, Cancer Res, 68 (2008) 8221-8230.
54. Kleer, C.G., Teknos, T.N., Islam, M., Marcus, B., Lee, J.S., Pan, Q., Merajver, S.D., RhoC GTPase expression as a potential marker of lymph node metastasis in squamous cell carcinomas of the head and neck, Clin Cancer Res, 12 (2006) 4485-4490.
55. Kamai, T., Shirataki, H., Nakanishi, K., Furuya, N., Kambara, T., Abe, H., Oyama, T., Yoshida, K., Increased Rac1 activity and Pak1 overexpression are associated with lymphovascular invasion and lymph node metastasis of upper urinary tract cancer, BMC Cancer, 10 164.
56. Molli, P.R., Li, D.Q., Murray, B.W., Rayala, S.K., Kumar, R., PAK signaling in oncogenesis, Oncogene, 28 (2009) 2545-2555.
57. Van Aelst, L., D'Souza-Schorey, C., Rho GTPases and signaling networks, Genes Dev, 11 (1997) 2295-2322.
58. Dong, M., Yan, B.P., Liao, J.K., Lam, Y.Y., Yip, G.W., Yu, C.M., Rho-kinase inhibition: a novel therapeutic target for the treatment of cardiovascular diseases, Drug Discov Today, 15 (2010) 622-629.
59. Yin, L., Morishige, K., Takahashi, T., Hashimoto, K., Ogata, S., Tsutsumi, S., Takata, K.,

Ohta, T., Kawagoe, J., Takahashi, K., Kurachi, H., Fasudil inhibits vascular endothelial growth factor-induced angiogenesis in vitro and in vivo, Mol Cancer Ther, 6 (2007) 1517-1525.

60. Ying, H., Biroc, S.L., Li, W.W., Alicke, B., Xuan, J.A., Pagila, R., Ohashi, Y., Okada, T., Kamata, Y., Dinter, H., The Rho kinase inhibitor fasudil inhibits tumor progression in human and rat tumor models, Mol Cancer Ther, 5 (2006) 2158-2164.
61. Somlyo, A.V., Phelps, C., Dipierro, C., Eto, M., Read, P., Barrett, M., Gibson, J.J., Burnitz, M.C., Myers, C., Somlyo, A.P., Rho kinase and matrix metalloproteinase inhibitors cooperate to inhibit angiogenesis and growth of human prostate cancer xenotransplants, Faseb J, 17 (2003) 223-234.
62. Sasaki, Y., Suzuki, M., Hidaka, H., The novel and specific Rho-kinase inhibitor (S)-(+)-2-methyl-1-[(4-methyl-5-isoquinoline)sulfonyl]-homopiperazine as a probing molecule for Rho-kinase-involved pathway, Pharmacol Ther, 93 (2002) 225-232.
63. Gao, Y., Dickerson, J.B., Guo, F., Zheng, J., Zheng, Y., Rational design and characterization of a Rac GTPase-specific small molecule inhibitor, Proc Natl Acad Sci U S A, 101 (2004) 7618-7623.
64. Sulpice, E., Ding, S., Muscatelli-Groux, B., Berge, M., Han, Z.C., Plouet, J., Tobelem, G., Merkulova-Rainon, T., Cross-talk between the VEGF-A and HGF signalling pathways in endothelial cells, Biol Cell, (2009).
65. Evelyn, C.R., Wade, S.M., Wang, Q., Wu, M., Iniguez-Lluhi, J.A., Merajver, S.D., Neubig, R.R., CCG-1423: a small-molecule inhibitor of RhoA transcriptional signaling, Mol Cancer Ther, 6 (2007) 2249-2260.
66. Koh, W., Mahan, R.D., Davis, G.E., Cdc42- and Rac1-mediated endothelial lumen formation requires Pak2, Pak4 and Par3, and PKC-dependent signaling, J Cell Sci, 121 (2008) 989-1001.
67. Murray, B.W., Guo, C., Piraino, J., Westwick, J.K., Zhang, C., Lamerdin, J., Dagostino, E., Knighton, D., Loi, C.M., Zager, M., Kraynov, E., Popoff, I., Christensen, J.G., Martinez, R., Kephart, S.E., Marakovits, J., Karlicek, S., Bergqvist, S., Smeal, T., Small-molecule p21-activated kinase inhibitor PF-3758309 is a potent inhibitor of oncogenic signaling and tumor growth, Proc Natl Acad Sci U S A, 107 (2010) 9446-9451.
68. Shutes, A., Onesto, C., Picard, V., Leblond, B., Schweighoffer, F., Der, C.J., Specificity and mechanism of action of EHT 1864, a novel small molecule inhibitor of Rac family small GTPases, J Biol Chem, 282 (2007) 35666-35678.
69. Deacon, S.W., Beeser, A., Fukui, J.A., Rennefahrt, U.E., Myers, C., Chernoff, J., Peterson, J.R., An isoform-selective, small-molecule inhibitor targets the autoregulatory mechanism of p21-activated kinase, Chem Biol, 15 (2008) 322-331.
70. Peterson, J.R., Bickford, L.C., Morgan, D., Kim, A.S., Ouerfelli, O., Kirschner, M.W., Rosen, M.K., Chemical inhibition of N-WASP by stabilization of a native autoinhibited conformation, Nat Struct Mol Biol, 11 (2004) 747-755.
71. Zhang, J., Yang, P.L., Gray, N.S., Targeting cancer with small molecule kinase inhibitors, Nat Rev Cancer, 9 (2009) 28-39.
72. Surviladze, Z., Waller, A., Wu, Y., Romero, E., Edwards, B.S., Wandinger-Ness, A., Sklar, L.A., Identification of a small GTPase inhibitor using a high-throughput flow cytometry bead-based multiplex assay, J Biomol Screen, 15 (2010) 10-20.
73. Bouquier, N., Vignal, E., Charrasse, S., Weill, M., Schmidt, S., Leonetti, J.P., Blangy, A., Fort, P., A cell active chemical GEF inhibitor selectively targets the Trio/RhoG/Rac1 signaling pathway, Chem Biol, 16 (2009) 657-666.
74. Pille, J.Y., Li, H., Blot, E., Bertrand, J.R., Pritchard, L.L., Opolon, P., Maksimenko, A., Lu, H., Vannier, J.P., Soria, J., Malvy, C., Soria, C., Intravenous delivery of anti-RhoA small interfering RNA loaded in nanoparticles of chitosan in mice: safety and efficacy in xenografted aggressive breast cancer, Hum Gene Ther, 17 (2006) 1019-1026.
75. Konstantinopoulos, P.A., Karamouzis, M.V., Papavassiliou, A.G., Post-translational

modifications and regulation of the RAS superfamily of GTPases as anticancer targets, Nat Rev Drug Discov, 6 (2007) 541-555.

76. Park, H.J., Kong, D., Iruela-Arispe, L., Begley, U., Tang, D., Galper, J.B., 3-hydroxy-3-methylglutaryl coenzyme A reductase inhibitors interfere with angiogenesis by inhibiting the geranylgeranylation of RhoA, Circ Res, 91 (2002) 143-150.
77. Kureishi, Y., Luo, Z., Shiojima, I., Bialik, A., Fulton, D., Lefer, D.J., Sessa, W.C., Walsh, K., The HMG-CoA reductase inhibitor simvastatin activates the protein kinase Akt and promotes angiogenesis in normocholesterolemic animals, Nat Med, 6 (2000) 1004-1010.
78. Katsumoto, M., Shingu, T., Kuwashima, R., Nakata, A., Nomura, S., Chayama, K., Biphasic effect of HMG-CoA reductase inhibitor, pitavastatin, on vascular endothelial cells and angiogenesis, Circ J, 69 (2005) 1547-1555.
79. Glynn, S.A., O'Sullivan, D., Eustace, A.J., Clynes, M., O'Donovan, N., The 3-hydroxy-3-methylglutaryl-coenzyme A reductase inhibitors, simvastatin, lovastatin and mevastatin inhibit proliferation and invasion of melanoma cells, BMC Cancer, 8 (2008) 9.
80. Hashimoto, K., Morishige, K., Sawada, K., Tahara, M., Shimizu, S., Ogata, S., Sakata, M., Tasaka, K., Kimura, T., Alendronate suppresses tumor angiogenesis by inhibiting Rho activation of endothelial cells, Biochem Biophys Res Commun, 354 (2007) 478-484.
81. Scavelli, C., Di Pietro, G., Cirulli, T., Coluccia, M., Boccarelli, A., Giannini, T., Mangialardi, G., Bertieri, R., Coluccia, A.M., Ribatti, D., Dammacco, F., Vacca, A., Zoledronic acid affects over-angiogenic phenotype of endothelial cells in patients with multiple myeloma, Mol Cancer Ther, 6 (2007) 3256-3262.
82. Wang, C.Y., Liu, P.Y., Liao, J.K., Pleiotropic effects of statin therapy: molecular mechanisms and clinical results, Trends Mol Med, 14 (2008) 37-44.
83. Brantley-Sieders, D.M., Zhuang, G., Vaught, D., Freeman, T., Hwang, Y., Hicks, D., Chen, J., Host deficiency in Vav2/3 guanine nucleotide exchange factors impairs tumor growth, survival, and angiogenesis in vivo, Mol Cancer Res, 7 (2009) 615-623.
84. Xue, Y., Bi, F., Zhang, X., Zhang, S., Pan, Y., Liu, N., Shi, Y., Yao, X., Zheng, Y., Fan, D., Role of Rac1 and Cdc42 in hypoxia induced p53 and von Hippel-Lindau suppression and HIF1alpha activation, Int J Cancer, 118 (2006) 2965-2972.
85. Dokmanovic, M., Hirsch, D.S., Shen, Y., Wu, W.J., Rac1 contributes to trastuzumab resistance of breast cancer cells: Rac1 as a potential therapeutic target for the treatment of trastuzumab-resistant breast cancer, Mol Cancer Ther, 8 (2009) 1557-1569.
86. Gutt, R., Tonlaar, N., Kunnavakkam, R., Karrison, T., Weichselbaum, R.R., Liauw, S.L., Statin use and risk of prostate cancer recurrence in men treated with radiation therapy, J Clin Oncol, 28 (2010) 2653-2659.
87. Gnant, M., Mlineritsch, B., Schippinger, W., Luschin-Ebengreuth, G., Postlberger, S., Menzel, C., Jakesz, R., Seifert, M., Hubalek, M., Bjelic-Radisic, V., Samonigg, H., Tausch, C., Eidtmann, H., Steger, G., Kwasny, W., Dubsky, P., Fridrik, M., Fitzal, F., Stierer, M., Rucklinger, E., Greil, R., Marth, C., Endocrine therapy plus zoledronic acid in premenopausal breast cancer, N Engl J Med, 360 (2009) 679-691.

Chapter 6
Examining the role of Rac1 in tumor angiogenesis and growth: A clinically relevant RNAi-mediated approach

Roy van der Meel[a*], P. Vader[a*], Marc H. Symons[b], Marcel H.A.M Fens[a], Ebel Pieters[a], Karlijn J. Wilschut[a], Gert Storm[a,c], Monica Jarzabek[d], William M. Gallagher[e], Raymond M. Schiffelers[a,f] and Annette T. Byrne[d]

[a] Department of Pharmaceutics, Utrecht Institute for Pharmaceutical Sciences (UIPS), Faculty of Science, Utrecht University, Universiteitsweg 99, 3584 CG Utrecht, The Netherlands

[b] Center for Oncology and Cell Biology, The Feinstein Institute for Medical Research at North Shore-LIJ, 350 Community Drive, Manhasset, NY 11030, USA

[c] Department of Targeted Therapeutics, MIRA Institute for Biomedical Technology and Technical Medicine, University of Twente, Enschede, The Netherlands

[d] Department of Physiology and Medical Physics, Royal College of Surgeons in Ireland, Reservoir House, Sandyford Industrial Estate, Ballymoss Road, Dublin 18, Ireland

[e] UCD School of Biomolecular and Biomedical Science, UCD Conway Institute, University College Dublin, Belfield, Dublin 4, Ireland

[f] Department of Clinical Chemistry and Hematology, University Medical Center Utrecht, Utrecht, The Netherlands

[*] These authors contributed equally to this work

Angiogenesis, 14 (4): 457-466 (2011)

Abstract

Angiogenesis, the sprouting of new blood vessels from the pre-existing vasculature, is a well established approach in anti-cancer therapy. It is thought that the Rho GTPase Rac1 is required during vascular endothelial growth factor (VEGF)-mediated angiogenesis. In the present study, we have used a clinically relevant RNA interference approach to silence Rac1 expression. HUVECs were transiently transfected with non-specific control siRNA (siNS) or Rac1 siRNA (siRac1) using electroporation or Lipofectamine 2000. Functional assays with transfected endothelial cells were performed to determine the effect of Rac1 knockdown on angiogenesis *in vitro*. Silencing of Rac1 inhibited VEGF-mediated tube formation, cell migration, invasion and proliferation. In addition, treatment with Rac1 siRNA inhibited angiogenesis in an *in vivo* Matrigel plug assay. Intratumoral injections of siRac1 almost completely inhibited the growth of grafted Neuro2A tumors and reduced tumor angiogenesis. Together, these data indicate that Rac1 is an important regulator of VEGF-mediated angiogenesis. Knockdown of Rac1 may represent an attractive approach to inhibit tumor angiogenesis and growth.

1. Introduction

During angiogenesis, new blood vessels sprout from the pre-existing vasculature. Physiological angiogenesis is important in embryonic development and postnatally, this process plays a role in wound healing and repair, during the female reproductive cycle and placentation during pregnancy. Aberrant angiogenesis can lead to vascular overgrowth which occurs in age related macular degeneration, psoriasis, rheumatoid arthritis and cancer [1]. Angiogenesis is necessary for tumors to grow beyond 1-2 mm^3 in size and is controlled by a balance in pro- and anti-angiogenic factors. However, a tumor can acquire an angiogenic phenotype, also referred to as the angiogenic switch, when this balance is shifted in favor of pro-angiogenic factors [2]. In response to these factors, endothelial cells are activated, resulting in invasion of the extracellular matrix, migration to the site of recruitment, proliferation and vessel formation and stabilization [3]. Arguably, the most critical pro-angiogenic factor is vascular endothelial growth factor (VEGF-A). VEGF stimulates endothelial cells following binding to integral membrane tyrosine receptor kinases VEGFR-1 and VEGFR-2, which results in activation of multiple intracellular effectors, including the Rho family of small GTPases.

Rho GTPases are small molecule members of the Ras superfamily of small GTPases which function as molecular switches in the cell. These proteins broadly play a role in an array of cellular processes such as cell polarity, transcription factor activity, membrane transport, cytoskeleton regulation and vesicle trafficking [4]. Rho GTPases cycle between a guanine diphosphate (GDP) bound, inactive state, and a guanine triphosphate (GTP) bound active state. In the active state, Rho GTPases can bind effector proteins and transduce downstream signals from various receptors. It is likely that Rho GTPases play an important role in critical aspects of the angiogenesis process, and therefore represent an attractive target for cancer therapy [5-6]. The most studied Rho GTPases include Rac1, Cdc42 and RhoA, of which Rac1 appears to be the major GTPase responsible for VEGF mediated angiogenesis [7]. Rac1 is ubiquitously expressed. It is required at the leading edge of the cell to regulate actin polymerization and to induce membrane ruffling and formation of lamellopodia [4, 8]. Rac1 also plays a key role in EC lumen and tubule formation [9-10]. Furthermore, endothelial specific excision of Rac1 leads to defective development of vessels and embryonic lethality, supporting an essential role in vascular development [11]. The involvement of Rac1 in tumorigenesis is indicated by several reports demonstrating overexpression or increased activation of Rac1 or its effectors in a variety of cancers [12-14].

In the current study, we have employed RNA interference to selectively silence Rac1 expression. RNA interference is a novel approach in which delivery of small interfering RNAs (siRNAs) into the cytoplasm of target cells induces sequence-specific gene

silencing [15] and offers great potential as a therapeutic strategy. We have explored the effects of Rac1 knockdown on VEGF induced angiogenesis and tumor growth *in vitro* and *in vivo*. Our data implicate Rac1 in the tumor angiogenesis process and as such, Rac1 may represent a potential target for anti-cancer therapy.

2. Material and methods

2.1 Cell culture

Human umbilical vein endothelial cells (HUVECs) (Lonza, Verviers, Belgium) were grown in endothelial cell growth medium-2 (EGM-2) (Lonza), consisting of endothelial basal medium-2 (EBM-2) supplemented with a SingleQuots kit (containing growth factors, 2% FBS and antibiotics). Cells were used between passages 3–7. Neuro2A (murine neuroblastoma) cells (ATCC CCL-131) were cultured in RPMI 1640 medium supplemented with 10% FCS and antibiotics (100 U/mL penicillin, 100 µg/mL streptomycin, 0.25 µg/mL amphotericin B).

2.2 siRNAs

siRNAs were purchased from Eurogentec (Maastricht, The Netherlands). Sequence of Rac1 siRNA against the human sequence was 5'-AAG-GAG-AUU-GGU-GCU-GUA-AAA-3' and 5'-UUU-UAC-AGC-ACC-AAU-CUC-CUU-3' and sequence of Rac1 siRNA against the murine sequence was 5'-GAC-GUG-UUC-UUA-AUU-UGC-UTT-3' and 5'-AGC-AAA-UUA-AGA-ACA-CGU-CTT-3'. As control sequences, a negative control siRNA (Eurogentec) (siNS) was used.

2.3 Transfection

1.0 x 10^5 HUVECs were resuspended in 500 µL EGM-2 containing 700 pmol of siRNA and transferred into 4 mm gap electroporation cuvettes from Harvard Apparatus (Holliston, MA). Cells were electroporated for 70 ms at 180 V, using an ECM 830 Electroporation system (Harvard Apparatus). After electroporation, cells were seeded in a 6-well plate and EGM-2 was added to a total volume of 2 mL per well. After 4 h, cells were washed 3 times with phosphate buffered saline (PBS) and fresh medium was added. Alternatively, 8.0 x 10^4 cells were seeded in 6-well plates and incubated for 24 h. Medium was replaced with serum-free medium and cells were transfected with 100 pmol siRNA per well using Lipofectamine 2000 (Invitrogen, UK). After 4 h, medium was replaced with EGM-2.

2.4 Western Blot analysis

Forty-eight hours following transfection, cells were lysed in radioimmunoprecipitation assay (RIPA) buffer containing protease inhibitors and EDTA for 30 min on ice.

Following removal of debris by centrifugation, lysates were subjected to SDS-PAGE and transferred onto membranes. Membranes were blocked in 5% milk in Tris-buffered saline containing 0.1% Tween-20 and incubated with primary monoclonal antibody against Rac1 (1:2000) (Clone 23A-8, Millipore, Lake Placid, N.Y.) followed by peroxidase-conjugated secondary antibody. Bands were visualized using SuperSignal West Femto Chemiluminescent Substrate (Pierce, Rockford, IL).

2.5 Tubule formation assay

Nintety-six-well plates were coated with 50 µL Matrigel™ (BD Biosciences, San Jose, CA). 48 h after transfection, HUVECs were seeded at 1.0 x 10^4 cells per well in Opti-Mem (Invitrogen), supplemented with 10 ng/mL recombinant human $VEGF_{165}$ (R&D Systems, Minneapolis, MN) and 0.1% gentamycin, or EGM-2. Cells were incubated for 4-5 h, after which wells were photographed at 40x magnification with a Nikon TE2000 microscope. Tubule formation was quantified by counting the number of branching points and measuring the total length of capillary tubes in at least three images using NIH ImageJ software.

2.6 Scratch wound assay

Forty-eight hours after transfection, HUVECs were seeded at 1.0 x 10^5 cells per well in 24-well plates in EGM-2 and allowed to grow to 100% confluency for 24 h. Cells were washed with PBS and serum-starved for 1 h with Opti-Mem supplemented with 0.1% gentamycin. A scratch was induced with a pipette tip, cells were washed 3 times with PBS and fresh Opti-Mem supplemented with 0.1% gentamycin and 10 ng/mL recombinant human $VEGF_{165}$ was added. Migration was checked after 24 h. Scratch wound size was analyzed using NIH ImageJ software.

2.7 Invasion assay

Forty-eight hours after transfection, 0.5 x 10^5 HUVECs in 0.5 mL Opti-Mem supplemented with 0.1% gentamycin were added to BD Biocoat Matrigel Invasion Chambers, pore-size 8 µm (BD Biosciences). Inserts were placed in 24 well plates containing 0.75 mL Opti-Mem supplemented with 0.1% gentamycin and 20 ng/mL recombinant human $VEGF_{165}$ as a chemoattractant and allowed to invade for 24 h. After 24 h, inserts were removed from well plates and medium was removed from the inserts which were then washed with PBS. Inserts were placed in 10% formalin for 10 minutes and left to dry. H&E staining was performed on cells on the bottom side of the inserts. Membranes were fixed on a glass microscope slide, scanned and cells present on the filter were counted.

2.8 Proliferation assays

Cell proliferation was measured using the sulforhodamine B (SRB) colorimetric assay [16]. 24 h after transfection, 4.0 x 10^3 cells per well were seeded in 96-well plates. At indicated time points, cells were fixed in 4% trichloroacetic acid for at least 1 h at 4 °C, washed and stained with 0.4% SRB in 1% acetic acid for 30 min followed by air drying. Finally, bound dye was solubilized in 200 µL 10 mM Tris for 15 minutes. OD values were read at 490 nm.

2.9 Matrigel plug assay

All animal experiments were performed according to Dutch national regulations and approved by the local animal experiments ethical committee. Six to eight-week old male A/J mice (Harlan) were injected subcutaneously with 400 µL High Concentration Matrigel (BD Biosciences) supplemented with either $VEGF_{165}$ (0.3 µg/mL) or Neuro2A cells (2 x 10^6 cells/mL). On day 1 and 4 after injection, mice were treated locally with 10 µg siRNA, followed by electroporation (200V/cm, 2x2 pulses at perpendicular angles, 100 mS) under anesthesia. On day 7, mice were sacrificed and plugs were removed. Plugs were photographed, homogenized in RIPA buffer on ice followed by removal of debris by centrifugation. Hemoglobin content was determined using the QuantiChrom™ Hemoglobin Assay Kit (BioAssay Systems, Hayward, CA) according to the manufacturer's instructions.

2.10 In vivo tumor model

Six to eight-week old male A/J mice (Harlan, The Netherlands) were subcutaneously injected with 100 µL Neuro2A cells (1 x 10^7 cells/mL). Tumor sizes were measured using digital calipers and calculated using the formula: Size = length x $width^2$ x 0.52. Mice with established tumors (approximately 100 mm^3) were treated intratumorally on day 0, 2, 4 and 6 with 10 µg of negative control or Rac1 siRNA followed by electroporation. On day 7, mice were sacrificed and tumors were excised. For determination of Rac1, CD31 or VEGFR-2 levels, tumors were homogenized in RIPA buffer on ice, allowed to stand for 30 min followed by removal of debris by centrifugation. Protein levels were determined by Western Blot analysis as described, using a polyclonal antibody against CD31 (1:500) (Clone M-20, Santa Cruz Biotechnology, Santa Cruz, CA) or a monoclonal antibody against VEGFR-2 (1:1000) (Clone 55B11, Cell Signaling Technology, Denvers, MA). For immunohistochemical staining, frozen sections were fixed in acetone, rehydrated and blocked in 5% normal goat serum. For detection of CD31, sections were incubated with primary polyclonal antibody against CD31 (1:500) followed by biotinylated secondary antibody and HRP-conjugated streptavidin complex. Sections were stained with 3-amino-9-ethylcarbazole (AEC). Microvessel density (MVD) was quantified by

counting the positively stained luminal structures in three representative images per animal. For Ki-67 detection, sections were incubated with primary polyclonal antibody against Ki-67 (1:300) (Ab66155, Abcam, Inc, Cambridge, MA) followed by poly-HRP goat anti-rabbit IgG (BrightVision, Immunologic, Duiven, The Netherlands). Sections were stained with 3,3'-diaminobenzidine (DAB). The number of Ki-67-positive cells was counted in two representative images per animal. In all staining procedures, endogenous peroxidase activity was blocked using 0.3% H_2O_2/PBS and sections were counterstained using hematoxylin.

2.11 Statistical analysis

To assess statistical significances, Student's t-tests were performed. For multiple comparisons, ANOVA with Bonferroni post-tests was used.

3. Results

3.1 Electroporation-mediated transfection of siRac1 silences Rac1 protein in HUVECs

HUVECs were transiently transfected using electroporation. To optimize the electrical parameters, cells were transferred into electroporation cuvettes and electroporated for 70 ms at a voltage of 160 and 180 V, using siRNA (450 and 700 pmol). After 2 days, silencing was determined using Western Blot analysis. Electroporation at a voltage of 180 V using 700 pmol siRNA resulted in effective knockdown of Rac1 protein. This effect was specific for siRac1, as electroporation at the same settings and siRNA dose using siNS did not induce silencing (Fig. 1). For further experiments, cells were treated using these optimized settings. Alternatively, where indicated, cells were transfected using Lipofectamine 2000, which also led to effective silencing of Rac1 protein (Supp. Fig. 1).

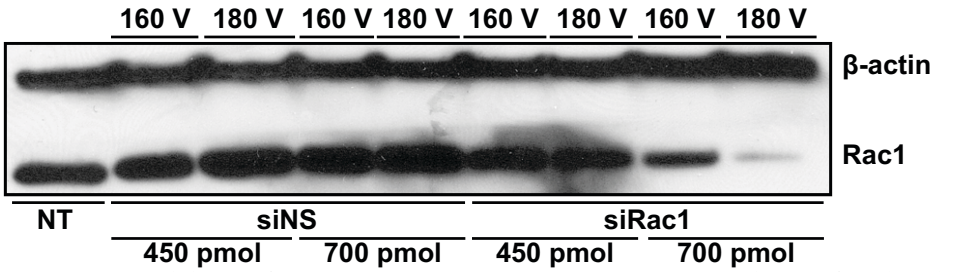

Figure 1. Knockdown of Rac1 in HUVECs. HUVECs were transiently transfected with siNS or siRac1 by electroporation. HUVECs were transfected with 450 or 700 pmol of siRNA per 1 * 10^5 cells using a single pulse of 160 or 180 V. Silencing of the Rac1 protein was determined by Western blotting.

Rac1 silencing inhibits VEGF-induced tubule formation of HUVECs

To examine the effect of Rac1 silencing on HUVEC tubule formation, transfected cells were seeded on Matrigel in serum-free medium containing VEGF. HUVECs transfected with control siRNA comprehensively formed tubular structures. In contrast, cells transfected with Rac1 siRNA formed considerably less tubular structures (Fig. 2A). Quantification of tubule formation by counting the total tube

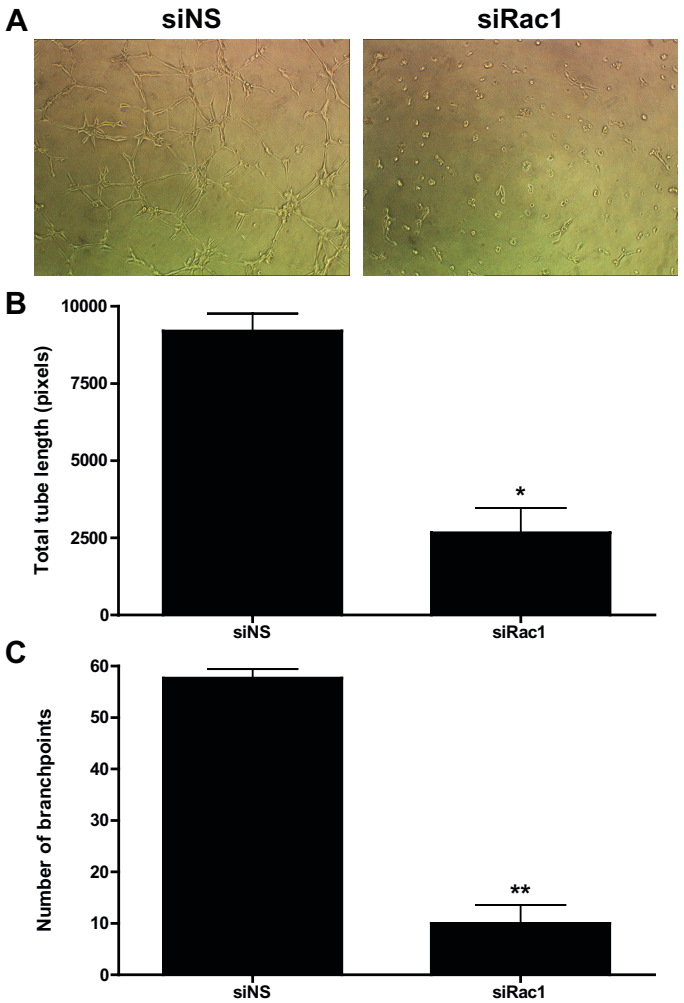

Figure 2. Rac1 silencing by siRNA reduces VEGF-induced tube formation of HUVECs on Matrigel. HUVECs transfected with siNS or siRac1 were seeded on Matrigel in Opti-Mem supplemented with 10 ng/mL recombinant human VEGF165 and incubated for 4-5 h. Tube formation was visualized by microscopy at 40x magnification (**A**) and quantified by measuring the total length of capillary tubes (**B**) and counting the number of branching points (**C**) per picture. Data are presented as mean ± SEM of three individual experiments. **p*-value < 0.01; ***p*-value < 0.001 versus siNS.

length and number of branching points per sample revealed that transfection with siRac1 inhibited total tube length by ±70% and reduced the number of branching points by ±80% compared to transfection with siNS (Fig. 2B, C). Similar results were observed with HUVECs transfected using Lipofectamine 2000 and seeded on Matrigel in complete medium (EGM-2) (Supp. Fig. 2).

3.2 Rac1 silencing inhibits VEGF-induced migration and invasion of HUVECs

Rac1 is well known for its role in endothelial cell migration [17]. To confirm that inhibition of Rac1 in HUVECs influences motility, a monolayer of transfected HUVECs was wounded and allowed to heal for 24 h. While VEGF induced repair of the wounded monolayer of HUVECs transfected with siNS, monolayer repair was reduced for HUVECs transfected with siRac1 (Fig. 3A). After 24 h, VEGF-induced wound closure was 5-fold lower for Rac1-depleted HUVECs compared to control (Fig. 3B).

To examine HUVEC invasiveness, transfected cells were allowed to invade through a Matrigel-coated filter in an invasion chamber, using VEGF as a chemoattractant in the lower chamber. The number of HUVECs that invaded through the Matrigel was almost two-fold lower for siRac1 transfected cells compared to siNS transfected cells (Figs. 3C, D).

3.3 Rac1 silencing inhibits proliferation of HUVECs

The effect of Rac1 silencing on HUVEC proliferation was assessed using the SRB assay. Cells were transfected using Lipofectamine 2000. Cell counts of control transfected cells rose by approximately 80% following one and 300% following three days after seeding. In contrast, only a 30% and 180% increase during these periods of time was seen for siRac1-transfected cells (Fig. 4).

3.4 Rac1 silencing inhibits VEGF-induced angiogenesis in vivo

To investigate the inhibitory effect of Rac1 silencing on angiogenesis *in vivo*, a Matrigel plug assay was performed. Mice, subcutaneously inoculated with Matrigel supplemented with VEGF, were treated locally with siNS or siRac1. After 7 days, plugs were removed and examined for vessel formation. While plugs treated with siNS appeared red, siRac1-treated plugs were light-yellow, indicating reduced blood vessel formation and thus red blood cells, inside plugs. Matrigel plugs without VEGF appeared white/yellow (Fig. 5A). Determination of hemoglobin concentrations in plugs showed a decrease in hemoglobin content of siRac1-treated plugs versus siNS-treated plugs by almost 50% (Fig. 5B). Comparable results were observed in an assay using Matrigel plugs containing Neuro2A cells, demonstrating the importance

of Rac1 in tumor angiogenesis (Supp. Fig. 3).

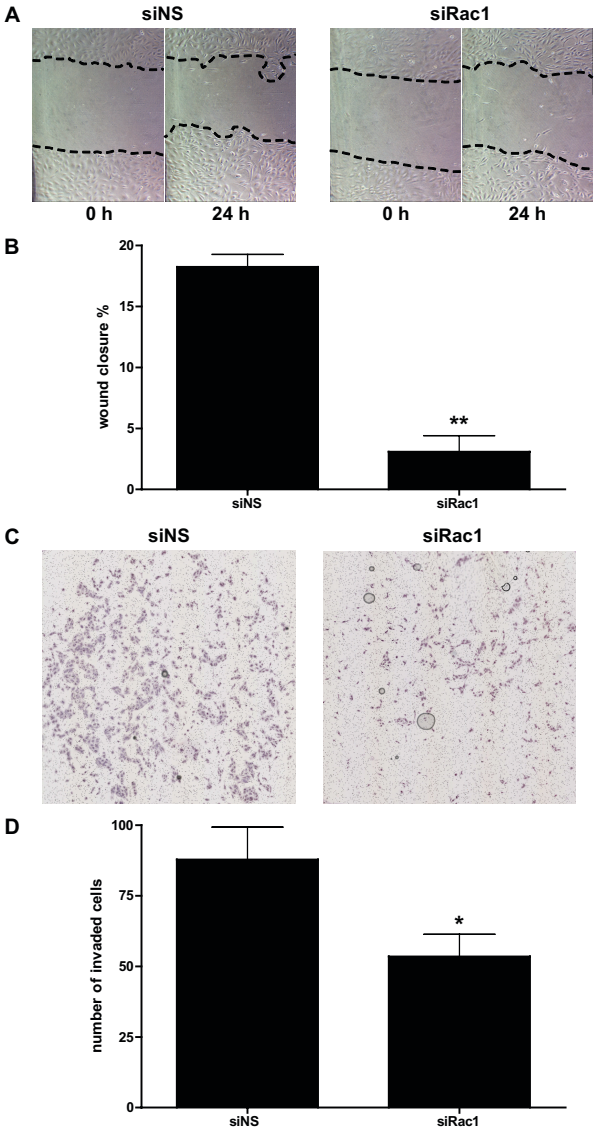

Figure 3. Rac1 silencing reduces VEGF-induced migration and invasion of HUVECs. HUVECs transfected with siNS or siRac1 were serum-starved, wounded and allowed to migrate in Opti-Mem supplemented with 10 ng/mL recombinant human $VEGF_{165}$. After 24 h, wound closure was visualized by microscopy at 40x magnification (**A**) and quantified using NIH ImageJ software (**B**). HUVECs transfected with siNS or siRac1 were added to BD Biocoat Matrigel Invasion Chambers in Opti-Mem, placed in 24 well plates containing 0.75 mL Opti-Mem supplemented with 20 ng/mL recombinant human VEGF165 and allowed to migrate for 24 h. Filters were photographed (**C**) and invasion was quantified by counting the amount of invaded cells on the filter (**D**). Data are presented as mean ± SEM and are representative of 2 individual experiments. *p-value < 0.05; **p-value < 0.001 versus siNS.

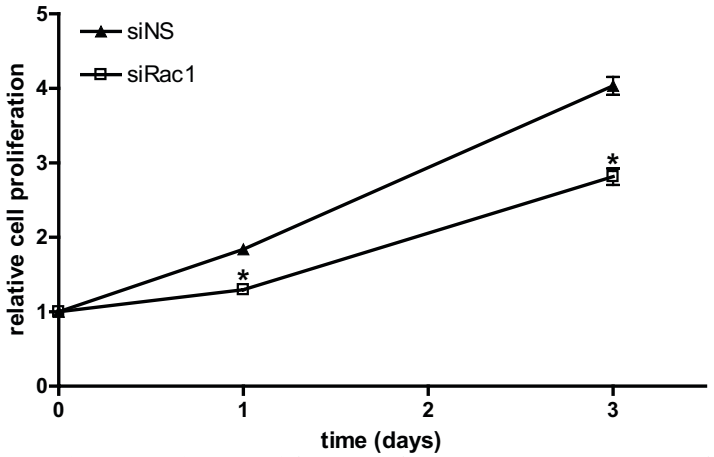

Figure 4. Rac1 silencing reduces proliferation of HUVECs. HUVECs transfected with siNS or siRac1 were seeded in 96-well plates. At indicated time points, cells were fixed and quantified using SRB assay. Data are presented as mean ± SEM and are representative of 3 individual experiments. *p-value < 0.05 versus siNS.

3.5 Rac1 silencing inhibits tumor growth and angiogenesis

The anti-tumoral and anti-angiogenic effects of Rac1 siRNA were investigated in subcutaneous Neuro2A neuroblastoma tumors. Established tumors (approximately 100 mm^3) were treated intratumorally every two days with 10 μg siRNA, followed by electroporation. As shown in Fig. 6A, treatment with siRac1 almost completely inhibited tumor growth, compared to treatment with control siRNA or no treatment. At day 7 following the first treatment, the average increase in size of tumors of siRac1-treated animals was 1.6-fold. In contrast, tumor sizes of untreated or siNS-treated animals increased eightfold or ninefold, respectively. Western blot analysis of Rac1-levels in tumors after sacrificing the animals on day 7 revealed efficient knockdown of Rac1 in tumors treated with siRac1 (Fig. 6B).

To determine the effect of siRac1 on tumor angiogenesis, vascularization in the tumors was evaluated on day 7. First, tumors were analyzed for expression of two endothelial cell markers, CD31 and vascular endothelial growth factor receptor 2 (VEGFR-2), by Western blotting. Expression of both markers was reduced in siRac1-treated tumors, indicating a reduction in vessel density compared to tumors excised from untreated or siNS-treated mice (Fig. 6C). CD31 expression was also determined by immunohistochemical analysis. Immunolabeling of tumor sections showed intense staining of untreated or siNS-treated tumors, while staining was less abundant in tumors treated with siRac1. Quantification of microvessel density by counting positively stained luminal structures revealed that siRac1 treatment significantly inhibited tumor angiogenesis, compared to siNS treatment. Furthermore, necrotic areas were observed in the centers of these tumors, which is also likely due to

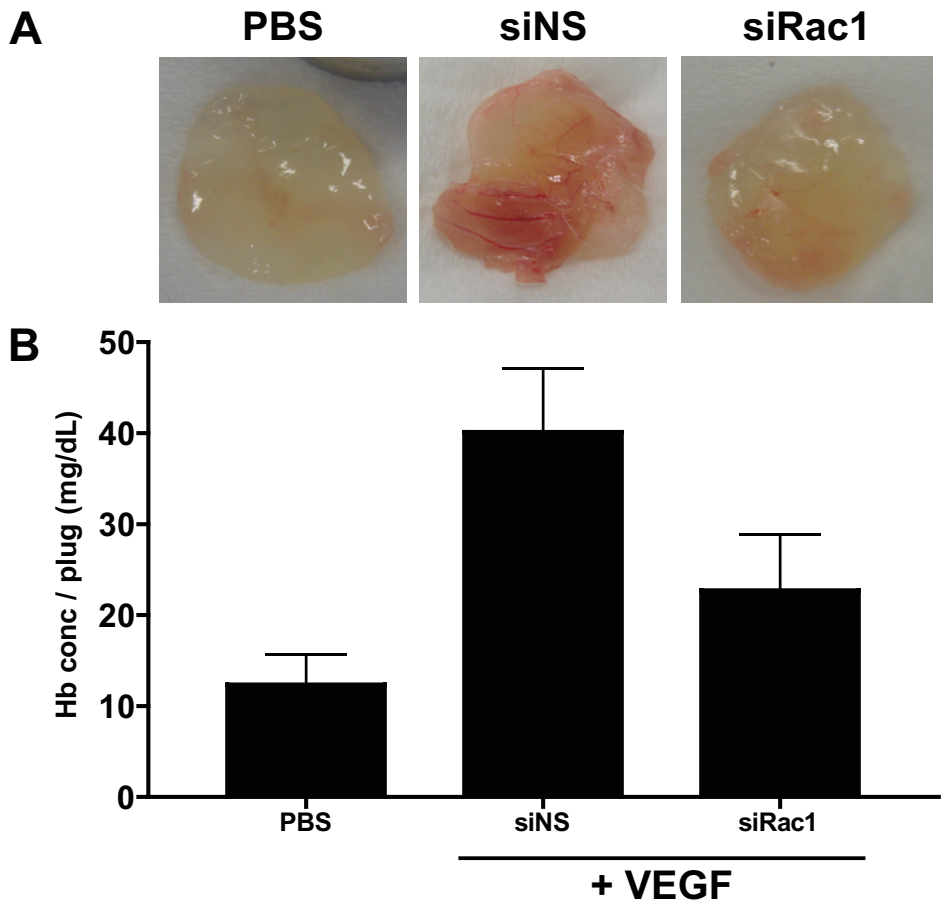

Figure 5. Rac1 silencing reduces VEGF-induced angiogenesis *in vivo*. Mice were injected subcutaneously with Matrigel supplemented with VEGF. On day 1 and 4 after injection, mice were treated locally with 10 µg siRNA. On day 7, mice were sacrificed and plugs were removed. New vessel formation was visualized by photography (**A**) and quantified by measuring the hemoglobin contents in Matrigel plugs (**B**). Data are presented as mean ± SEM. *p*-value = 0.0865 for siRac1-treated versus siNS-treated.

siRac1-mediated inhibition of angiogenesis [18] (Fig. 6D).

Besides effects in endothelial cells, knockdown of Rac1 in tumor cells might also contribute to the overall anti-angiogenic effect by inhibiting the hypoxia-induced production of VEGF by tumor cells [19]. Therefore, VEGF levels in the tumors were determined by Western blot analysis. As shown in Supp .Fig. 4, treatment with siRac1 did not alter VEGF expression in tumors compared to controls. This result suggests that the observed inhibition of angiogenesis originates from a direct effect of siRac1 on endothelial cells and not from an indirect effect caused by decreased VEGF secretion by tumor cells.

Furthermore, to exclude the possibility that the observed inhibition of tumor growth

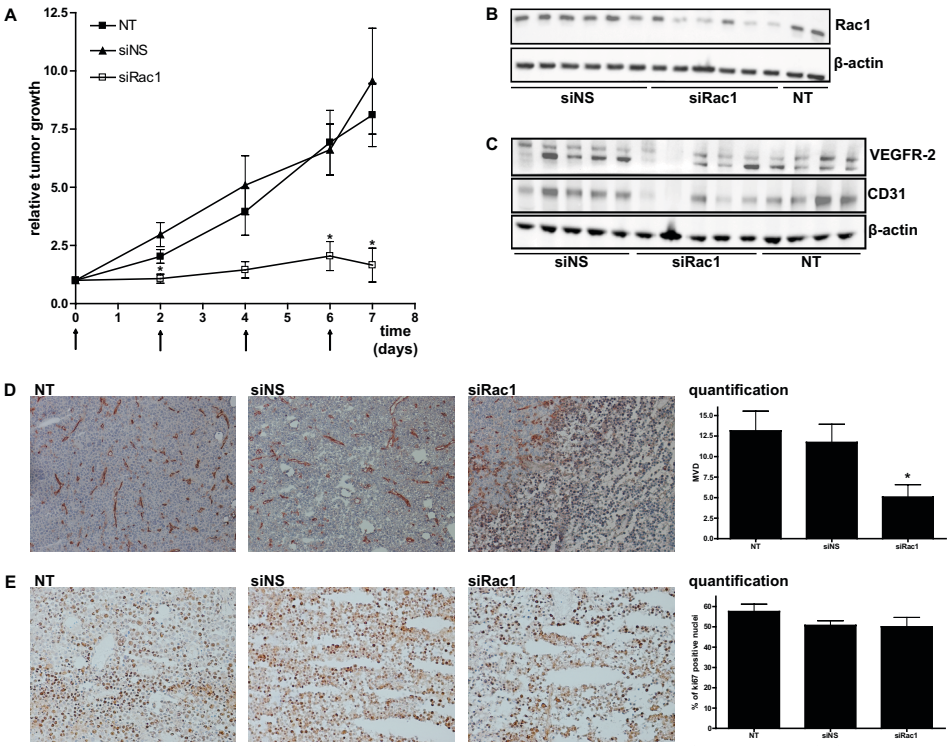

Figure 6. Local treatment of mice bearing Neuro2A tumors with siRac1 inhibits tumor growth and angiogenesis. Mice were inoculated subcutaneously with Neuro2A cells. After 7 days treatment was started. Mice were treated intratumorally on day 0, 2, 4 and 6 with 10 μg of siNS or siRac1 followed by electroporation. Tumor growth was measured for 7 days (**A**). On day 7, mice were sacrificed and tumors were excised. Knockdown of Rac1 in tumor lysates was confirmed by Western Blotting (**B**). Expression of the endothelial markers CD31 and VEGFR-2 in tumor lysates were determined by Western Blotting (**C**). Expression of CD31 (**D**) and proliferation marker Ki-67 (**E**) were determined by immunohistochemistry. Representative images are shown. Quantification of MVD was done by counting the positively stained luminal structures in three representative images per animal. The number of Ki-67-positive cells was counted in two representative images per animal. Data are presented as mean ± SEM. **p*-value < 0.05 versus siNS.

was caused by siRac1-induced inhibition of proliferation of the grafted Neuro2A cells, we determined if Rac1 silencing had an effect on proliferation of Neuro2A cells *in vitro* and *in vivo*. siRac1 transfection had no effect on *in vitro* cell proliferation as compared to controls (Supp. Fig. 5A, B). Moreover, staining of the proliferation marker Ki-67 in tumor sections showed no differences in expression between treatments, with moderate staining in the centre (Fig. 6E) and intense staining in the periphery of the tumors (Supp. Fig. 5C).

4. Discussion

Rac1 is a key member of the Rho family of GTPases and is involved in several cellular processes including endothelial cell migration, cell cycle control and lumen formation [5, 7]. As these processes are important for tumor angiogenesis, interference with Rac1 signaling may represent a novel approach to inhibit tumor neovascularization and subsequently tumor growth.

To inhibit signaling through Rac1, we implemented a clinically relevant siRNA approach to specifically knockdown expression of Rac1. Experimental delivery of siRNA into cells *in vitro* and *in vivo* was mediated using an established electroporation approach, which has been extensively used for delivery of plasmid DNA and siRNA into target cells or tissue, including tumors [20]. By means of electroporation, cellular plasma membranes are transiently destabilized by externally applied, localized and controlled electric fields, facilitating the entry of foreign molecules into cells and tissues. Several clinical trials are currently investigating electroporation as a drug delivery technology in humans, including several cases involving gene therapy via electroporation as applied in the oncology setting [21]. Following optimization of the electrical parameters for efficient transfection in HUVECs, effects of Rac1 knockdown on angiogenic properties of cells were investigated. siRac1-transfected HUVECs demonstrated reduced ability to form capillary-like tubules as well as showing reduced migration, invasion and proliferation phenotypes compared to cells transfected with siNS. Reduced VEGF-induced tube formation and migration after Rac1 depletion in endothelial cells is in line with other studies [9, 22-24]. Nevertheless, controversy exists regarding the role of Rac1 in endothelial cell invasion and proliferation. In agreement with our observations, silencing of Rac1 decreases HUVEC invasion through a fibronectin-coated Transwell filter [23]. In contrast, Rac1-depleted mouse lung endothelial cells have been shown to invade Matrigel-coated Transwells to the same degree as controls [22]. In the same study, no effect of Rac1 silencing on VEGF-induced proliferation was found. A possible explanation for this apparent discrepancy could be differences in cell type and growth conditions (e.g. serum concentration [25]). However, more studies are necessary to shed light on this issue.

To evaluate the effect of Rac1 knockdown on angiogenesis *in vivo*, a Matrigel plug assay was performed. Intratumoral injections of Rac1 siRNA resulted in decreased infiltration of endothelial cells in VEGF-containing plugs, indicating an important role of endothelial Rac1 in VEGF-induced angiogenesis. In our Neuro2A xenograft model, the inhibitory effect of siRac1 on tumor angiogenesis was also likely to be a result of its direct effect on endothelial cells. The importance of endothelial Rac1 for angiogenesis *in vivo* has been suggested by several other studies. For example, endothelial-specific Rac1 haploinsufficient mice display impaired eNOS activity and

angiogenesis in a hind limb ischemia model and aortic capillary sprouting assay [26]. In addition, transduction of endothelial cells with active L61Rac1 improves VEGF-mediated neovascularization and lumen formation *in vivo*, while transfection with dominant-negative N17Rac1 inhibited formation of vessels [27]. In contrast, D'Amico *et al.* [22] demonstrated that inducible deletion of Rac1 in wild-type endothelial cells does not affect tumor angiogenesis or VEGF-mediated angiogenesis in mice, unless β3-integrin is absent. The apparent difference in results between these studies may arise from differences in experimental model and setup.

Besides inhibiting angiogenesis, our data show that intratumoral injections of siRNA against Rac1 almost completely block the growth of established Neuro2A neuroblastoma tumors. Similar results using RNAi were apparent for a different Rho GTPase, RhoA, in xenografted MDA-MB-231 breast cancer tumors [18]. The authors suggest that the reduced tumor growth is the result of a combination of inhibition of proliferation of tumor cells and inhibition of angiogenesis. We did not find an effect of Rac1 silencing on proliferation of Neuro2A cells *in vitro* and *in vivo*, which makes it unlikely that reduced proliferation of grafted Neuro2A cells accounts for the observed reduction in tumor growth. However, we cannot exclude that, besides effects on angiogenesis pathways, inhibition of other Rac1-regulated processes in stromal cells may have contributed to the decrease in tumor growth.

Although several strategies to interfere with the process of angiogenesis have been therapeutically validated in both preclinical and clinical trials, recent studies have shown that anti-angiogenic therapy may paradoxically select for more invasive and metastatic tumor types [28-30]. Combinatorial strategies that target proteins involved in both angiogenesis and invasion mechanisms might overcome this adaptive-invasive resistance. As several studies have indicated a crucial role for Rac1 in tumor cell migration and invasion, interfering with Rac1 signaling in both tumor- and endothelial cells could improve therapeutic outcome and provide a useful approach towards enduring and effective anti-cancer responses [31].

While current therapeutic strategies to inhibit Rac1 function such as lipid modification [32] and other small molecule inhibitors lack specificity, RNA interference technology may provide a means to specifically and efficiently inhibit Rac1 expression. However, the use of siRNA in the clinic is still hampered by ineffective delivery into target cells or tissues. Nevertheless, Davis *et al.* [33] have recently demonstrated that RNA interference may be successfully employed in humans via systemically delivered siRNA, delivered using targeted nanoparticles, thus demonstrating that siRNA can be used as a gene-specific therapeutic.

As Rac1 is ubiquitously expressed throughout the body and controls a large number of cellular functions, interfering with Rac1 signaling could result in undesired side-effects [4, 34]. Strategies to target tumor-associated cells without affecting

normal cells may offer a larger therapeutic window. As a number of targeted delivery systems that specifically deliver siRNA to tumor sides are currently under preclinical and clinical development [33, 35-36], this approach may soon appear applicable.
In summary, we have shown that Rac1 is an important regulator of VEGF-induced angiogenesis in endothelial cells. Our data further suggest that inhibition of Rac1 using RNA interference is an effective tool for inhibiting angiogenesis and tumor growth. As Rac1 is also involved in tumor cell migration and invasion, siRNA-mediated Rac1 silencing in both tumor and tumor-associated endothelial cells using targeted delivery systems represents a promising therapeutic strategy.

Acknowledgements

Funding is acknowledged from Science Foundation Ireland in the context of the Molecular Therapeutics for Cancer Ireland, Strategic Research Cluster. We further acknowledge funding received from the EU Marie Curie Industry Academia Pathways & Partnership program in the context of the 'AngioTox' initiative.

References

1. Carmeliet, P., Angiogenesis in life, disease and medicine, Nature, 438 (2005) 932-936.
2. Bergers, G., Benjamin, L.E., Tumorigenesis and the angiogenic switch, Nat Rev Cancer, 3 (2003) 401-410.
3. Hanahan, D., Folkman, J., Patterns and emerging mechanisms of the angiogenic switch during tumorigenesis, Cell, 86 (1996) 353-364.
4. Jaffe, A.B., Hall, A., Rho GTPases: biochemistry and biology, Annu Rev Cell Dev Biol, 21 (2005) 247-269.
5. Bryan, B.A., D'Amore, P.A., What tangled webs they weave: Rho-GTPase control of angiogenesis, Cell Mol Life Sci, 64 (2007) 2053-2065.
6. Merajver, S.D., Usmani, S.Z., Multifaceted role of Rho proteins in angiogenesis, J Mammary Gland Biol Neoplasia, 10 (2005) 291-298.
7. Fryer, B.H., Field, J., Rho, Rac, Pak and angiogenesis: old roles and newly identified responsibilities in endothelial cells, Cancer Lett, 229 (2005) 13-23.
8. Heasman, S.J., Ridley, A.J., Mammalian Rho GTPases: new insights into their functions from in vivo studies, Nat Rev Mol Cell Biol, 9 (2008) 690-701.
9. Bayless, K.J., Davis, G.E., The Cdc42 and Rac1 GTPases are required for capillary lumen formation in three-dimensional extracellular matrices, J Cell Sci, 115 (2002) 1123-1136.
10. Koh, W., Mahan, R.D., Davis, G.E., Cdc42- and Rac1-mediated endothelial lumen formation requires Pak2, Pak4 and Par3, and PKC-dependent signaling, J Cell Sci, 121 (2008) 989-1001.
11. Tan, W., Palmby, T.R., Gavard, J., Amornphimoltham, P., Zheng, Y., Gutkind, J.S., An essential role for Rac1 in endothelial cell function and vascular development, Faseb J, 22 (2008) 1829-1838.
12. Fritz, G., Just, I., Kaina, B., Rho GTPases are over-expressed in human tumors, Int J Cancer, 81 (1999) 682-687.
13. Schnelzer, A., Prechtel, D., Knaus, U., Dehne, K., Gerhard, M., Graeff, H., Harbeck, N., Schmitt, M., Lengyel, E., Rac1 in human breast cancer: overexpression, mutation analysis, and characterization of a new isoform, Rac1b, Oncogene, 19 (2000) 3013-3020.
14. Aznar, S., Fernandez-Valeron, P., Espina, C., Lacal, J.C., Rho GTPases: potential candidates

for anticancer therapy, Cancer Lett, 206 (2004) 181-191.
15. Meister, G., Tuschl, T., Mechanisms of gene silencing by double-stranded RNA, Nature, 431 (2004) 343-349.
16. Skehan, P., Storeng, R., Scudiero, D., Monks, A., McMahon, J., Vistica, D., Warren, J.T., Bokesch, H., Kenney, S., Boyd, M.R., New colorimetric cytotoxicity assay for anticancer-drug screening, J Natl Cancer Inst, 82 (1990) 1107-1112.
17. Raftopoulou, M., Hall, A., Cell migration: Rho GTPases lead the way, Dev Biol, 265 (2004) 23-32.
18. Pille, J.Y., Li, H., Blot, E., Bertrand, J.R., Pritchard, L.L., Opolon, P., Maksimenko, A., Lu, H., Vannier, J.P., Soria, J., Malvy, C., Soria, C., Intravenous delivery of anti-RhoA small interfering RNA loaded in nanoparticles of chitosan in mice: safety and efficacy in xenografted aggressive breast cancer, Hum Gene Ther, 17 (2006) 1019-1026.
19. Xue, Y., Bi, F., Zhang, X., Zhang, S., Pan, Y., Liu, N., Shi, Y., Yao, X., Zheng, Y., Fan, D., Role of Rac1 and Cdc42 in hypoxia induced p53 and von Hippel-Lindau suppression and HIF1alpha activation, Int J Cancer, 118 (2006) 2965-2972.
20. Golzio, M., Mazzolini, L., Ledoux, A., Paganin, A., Izard, M., Hellaudais, L., Bieth, A., Pillaire, M.J., Cazaux, C., Hoffmann, J.S., Couderc, B., Teissie, J., In vivo gene silencing in solid tumors by targeted electrically mediated siRNA delivery, Gene Ther, 14 (2007) 752-759.
21. Bodles-Brakhop, A.M., Heller, R., Draghia-Akli, R., Electroporation for the delivery of DNA-based vaccines and immunotherapeutics: current clinical developments, Mol Ther, 17 (2009) 585-592.
22. D'Amico, G., Robinson, S.D., Germain, M., Reynolds, L.E., Thomas, G.J., Elia, G., Saunders, G., Fruttiger, M., Tybulewicz, V., Mavria, G., Hodivala-Dilke, K.M., Endothelial-Rac1 is not required for tumor angiogenesis unless alphavbeta3-integrin is absent, PLoS One, 5 (2010) e9766.
23. Garrett, T.A., Van Buul, J.D., Burridge, K., VEGF-induced Rac1 activation in endothelial cells is regulated by the guanine nucleotide exchange factor Vav2, Exp Cell Res, 313 (2007) 3285-3297.
24. Connolly, J.O., Simpson, N., Hewlett, L., Hall, A., Rac regulates endothelial morphogenesis and capillary assembly, Mol Biol Cell, 13 (2002) 2474-2485.
25. Chan, A.Y., Coniglio, S.J., Chuang, Y.Y., Michaelson, D., Knaus, U.G., Philips, M.R., Symons, M., Roles of the Rac1 and Rac3 GTPases in human tumor cell invasion, Oncogene, 24 (2005) 7821-7829.
26. Sawada, N., Salomone, S., Kim, H.H., Kwiatkowski, D.J., Liao, J.K., Regulation of endothelial nitric oxide synthase and postnatal angiogenesis by Rac1, Circ Res, 103 (2008) 360-368.
27. Hoang, M.V., Nagy, J.A., Senger, D.R., Active Rac1 improves pathologic VEGF neovessel architecture and reduces vascular leak: mechanistic similarities with angiopoietin-1, Blood, 117 (2011) 1751-1760.
28. Ebos, J.M., Lee, C.R., Cruz-Munoz, W., Bjarnason, G.A., Christensen, J.G., Kerbel, R.S., Accelerated metastasis after short-term treatment with a potent inhibitor of tumor angiogenesis, Cancer Cell, 15 (2009) 232-239.
29. Paez-Ribes, M., Allen, E., Hudock, J., Takeda, T., Okuyama, H., Vinals, F., Inoue, M., Bergers, G., Hanahan, D., Casanovas, O., Antiangiogenic therapy elicits malignant progression of tumors to increased local invasion and distant metastasis, Cancer Cell, 15 (2009) 220-231.
30. Keunen, O., Johansson, M., Oudin, A., Sanzey, M., Rahim, S.A., Fack, F., Thorsen, F., Taxt, T., Bartos, M., Jirik, R., Miletic, H., Wang, J., Stieber, D., Stuhr, L., Moen, I., Rygh, C.B., Bjerkvig, R., Niclou, S.P., Anti-VEGF treatment reduces blood supply and increases tumor cell invasion in glioblastoma, Proc Natl Acad Sci U S A, 108 (2011) 3749-3754.
31. van der Meel, R., Symons, M.H., Kudernatsch, R., Kok, R.J., Schiffelers, R.M., Storm, G., Gallagher, W.M., Byrne, A.T., The VEGF/Rho GTPase signalling pathway: A promising

target for anti-angiogenic/anti-invasion therapy, Drug Discov Today, 16 (2011) 219-228.
32. Konstantinopoulos, P.A., Karamouzis, M.V., Papavassiliou, A.G., Post-translational modifications and regulation of the RAS superfamily of GTPases as anticancer targets, Nat Rev Drug Discov, 6 (2007) 541-555.
33. Davis, M.E., Zuckerman, J.E., Choi, C.H., Seligson, D., Tolcher, A., Alabi, C.A., Yen, Y., Heidel, J.D., Ribas, A., Evidence of RNAi in humans from systemically administered siRNA via targeted nanoparticles, Nature, 464 (2010) 1067-1070.
34. Sun, D., Xu, D., Zhang, B., Rac signaling in tumorigenesis and as target for anticancer drug development, Drug Resist Updat, 9 (2006) 274-287.
35. Santel, A., Aleku, M., Roder, N., Mopert, K., Durieux, B., Janke, O., Keil, O., Endruschat, J., Dames, S., Lange, C., Eisermann, M., Loffler, K., Fechtner, M., Fisch, G., Vank, C., Schaeper, U., Giese, K., Kaufmann, J., Atu027 prevents pulmonary metastasis in experimental and spontaneous mouse metastasis models, Clin Cancer Res, 16 (2010) 5469-5480.
36. Han, H.D., Mangala, L.S., Lee, J.W., Shahzad, M.M., Kim, H.S., Shen, D., Nam, E.J., Mora, E.M., Stone, R.L., Lu, C., Lee, S.J., Roh, J.W., Nick, A.M., Lopez-Berestein, G., Sood, A.K., Targeted gene silencing using RGD-labeled chitosan nanoparticles, Clin Cancer Res, 16 (2010) 3910-3922.

Supplementary material

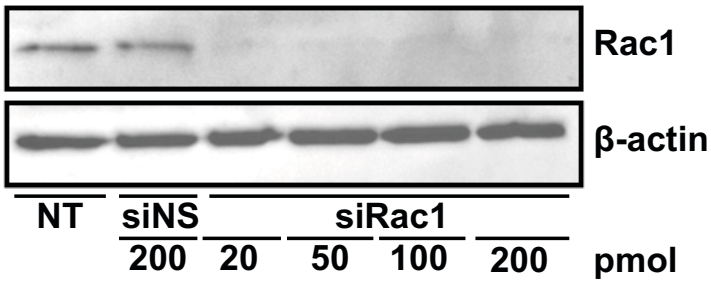

Supplementary Figure 1. Knockdown of Rac1 in HUVECs. HUVECs were transiently transfected with siNS or increasing concentrations of siRac1 complexed with Lipofectamine 2000. Silencing of the Rac1 gene was determined by Western blot analysis.

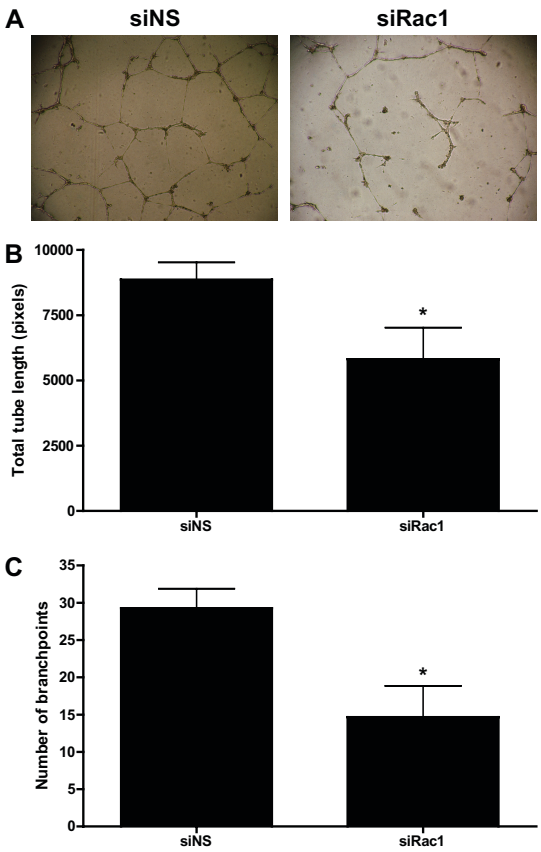

Supplementary Figure 2. Rac1 silencing by siRNA reduces tube formation of HUVECs on Matrigel. HUVECs transfected with siNS or siRac1 using Lipofectamine 2000 were seeded on Matrigel in EGM-2 and incubated for 4-5 h. Tube formation was visualized by microscopy at 40x magnification (**A**) and quantified by measuring the total length of capillary tubes (**B**) and counting the number of branching points (**C**) per picture. Data are presented as mean ± SEM of three individual experiments. **p*-value < 0.05 versus siNS.

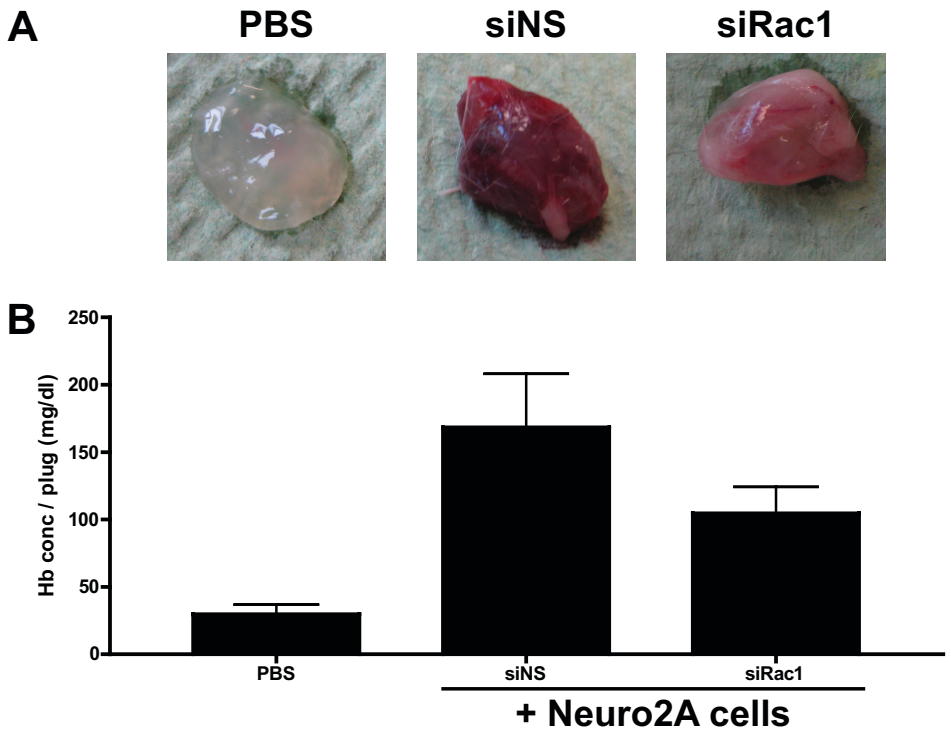

Supplementary Figure 3. Rac1 silencing reduces Neuro2A-induced angiogenesis *in vivo*. Mice were injected subcutaneously with Matrigel mixed with Neuro2A cells. On day 1 and 4 after injection, mice were treated locally with 10 µg siRNA. On day 7, mice were sacrificed and plugs were removed. New vessel formation was visualized by photography (**A**) and quantified by measuring the hemoglobin contents in Matrigel plugs (**B**). Data are presented as mean ± SEM. *p*-value = 0.1765 for siRac1-treated versus siNS-treated.

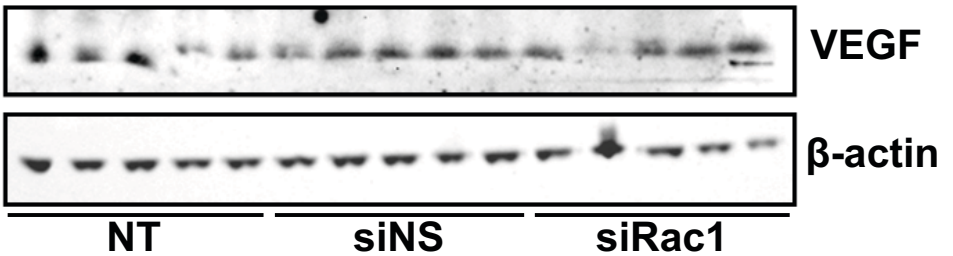

Supplementary Figure 4. Rac1 silencing does not increase VEGF production in tumors cells *in vivo*. Tumors were homogenized in RIPA buffer on ice, allowed to stand for 30 min followed by removal of debris by centrifugation. VEGF levels were determined by Western blot analysis as described, using a polyclonal antibody against VEGF (1:200) (sc-507, Santa Cruz Biotechnology, Santa Cruz, CA).

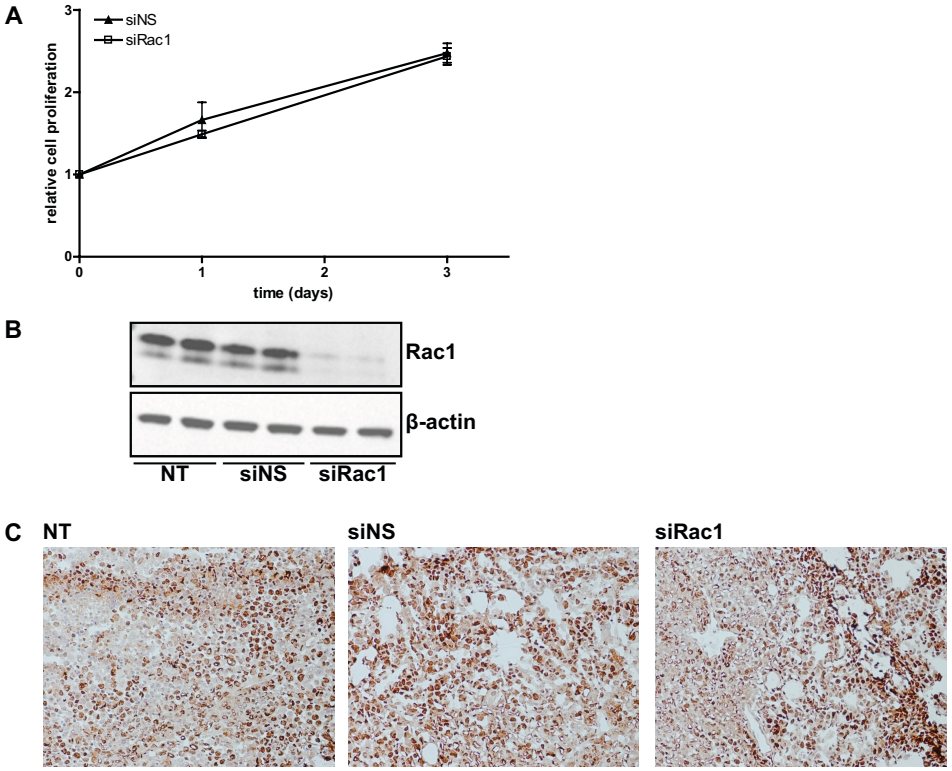

Supplementary Figure 5. Rac1 silencing has no effect on proliferation of Neuro2A cells *in vitro* and *in vivo*. Neuro2A cells transfected with siNS or siRac1 were seeded in 96-well plates. At indicated time points, cells were fixed and quantified using SRB assay. Data are presented as mean ± SEM and are representative of 3 individual experiments (**A**). Knockdown of Rac1 in Neuro2A cells was confirmed by Western blot analysis (**B**). Expression of proliferation marker Ki-67 in the periphery of tumors was determined by immunohistochemistry (**C**).

Chapter 7
Summarizing discussion

1. Actively-targeted anti-cancer nanomedicines

Almost 20 years ago the first anti-cancer nanomedicine Doxil® (Caelyx) was approved and has been used in the clinic since then. Encapsulation of the DNA-intercalating anthracycline doxorubicin (DOX) in long-circulating liposomes increased tumor accumulation of the drug resulting in at least equivalent or sometimes even increased efficacy compared to free doxorubicin observed in a number of cancers. More importantly, Doxil® demonstrated a major reduction in cardiotoxicity compared to treatment with free drug [1], showing the benefit of evasion of toxicity sensitive tissues. Since then, several nanomedicines for cancer treatment have been approved such as the polymeric micelle formulation of paclitaxel (Genexol-PM, approved in Korea) and albumin-bound paclitaxel (Abraxane). At present, a few dozen nanomedicines have been approved and it is estimated that approximately 250 nanomedicines are in (pre)clinical testing with the majority aimed at cancer treatment as indication [2-3]. All currently approved anti-cancer nanomedicines, with the exception of antibody-drug conjugates (ADC), can be considered as passively-targeted nanomedicines (PTNM). The fate of PTNM after systemic administration is determined by their physicochemical properties that dictate their interaction with proteins, cells and tissues. The properties of PTNM are such that they couple nanosize (generally around 100 nm) to a long circulatory half-life. These properties in combination with the pathophysiology of the tumor endothelium that contributes to the enhanced permeability and retention (EPR) effect, allows tumor accumulation of PTNM [4-5].

The conjugation of targeting ligands to generate actively-targeted nanomedicines (ATNM) is a strategy aimed at increasing target cell recognition and uptake into target cells, to ultimately increase efficacy. However, to this date, clinical translation of active targeting has been poor with several approved ADC but no ATNM that have progressed into the clinic. The reasons behind the limited bench to bedside translation of actively-targeted nanomedicines appear to fall in four categories [6]:

- Difficult rational design of actively-targeted therapeutic nanocarriers
- Unpredictable interactions and behavior in the circulation
- (Patho)physiological differences between preclinical models of cancer and human disease
- Scaling up and pharmaceutical good manufacturing practice (GMP)-grade production

In **Chapter 2**, an objective presentation is given of available data for target localization, safety and efficacy of twelve ATNM to evaluate the added benefits of conjugating targeting ligands to particulate nanomedicines.

Of the 12 analyzed ATNM based on particulate nanocarriers, 11 are under active evaluation while the development of MCC-465 seems to have been discontinued.

All of the 12 analyzed ATNM are in various stages of clinical evaluation for the treatment of solid malignant neoplasms with the exception of the anti-nicotine vaccine SEL-068.

The ATNM in this overview are defined by three components: *the particulate nanocarrier* (PNC), *targeting ligands* and *therapeutic agent*. The majority of the discussed ATNM are composed of established PNC and compounds to lower development risks and to avoid regulatory issues associated with novel nanocarrier systems or molecules.

The encapsulated *therapeutic agent* in 6 of the discussed anti-cancer ATNM is an established chemotherapeutic agent such as DOX (MM-302, anti-EGFR ILs DOX, MCC-465), oxaliplatin (MBP-426), docetaxel (BIND-014) or paclitaxel (Erbitux®EDVs$_{PAC}$). Four ATNM contain plasmid DNA or short interfering RNA (SGT-53, SGT-94, CALAA-01, Rexin-G) that needs to localize intracellularly to be therapeutically active. Two actively-targeted vaccine formulations (Lipovaxin-MM, SEL-068) contain antigen and adjuvants to stimulate the immune system.

The exploited *particulate nanocarrier* of 7 ATNM is lipid-based which is likely due to the clinical experience gained with these systems as PTNM. The rapid development of ATNM based on polymers is remarkable. Three ATNM are polymer-based (BIND-014, CALAA-01, SEL-068) and these systems are characterized by self-assembly into polymeric nanoparticles and/or the use of high-throughput approaches that may be beneficial in terms of development time and large-scale manufacturing. One ATNM is a replication incompetent retroviral vector (Rexin-G) that is generated in human producer cells. Interestingly, 1 ATNM is based on bacterially-derived minicells (Erbitux®EDVs$_{PAC}$) that are characterized by a larger size (400 nm) compared to other PNC.

Regarding the *targeting ligands* exploited for the discussed ATNM, 8 targeted anti-cancer nanomedicines are targeted to established specific markers often overexpressed on tumor cells such as the transferrin receptor, epidermal growth factor receptor (EGFR), HER2 or prostate specific membrane antigen (PSMA) while the exact target receptor of MCC-465 is not known. In contrast, Rexin-G is targeted to exposed collagen resulting in efficient drug delivery to tumor cells, stroma cells, tumor vasculature and sites of metastasis indicating that targeting the tumor stroma is a valuable strategy to achieve anti-cancer treatment with ATNM. The two vaccine products show that active-targeting in combination with long-circulating properties of the ATNM can be exploited to target antigen presenting cells. Next to general vaccine applications, this strategy can be applied to generate anti-cancer nanomedicines that are not restricted by the drawbacks of direct tumor cell targeting.

All of the discussed ATNM (with the exception of SEL-068) have shown increased efficacy *in vitro* and in animal studies compared to PTNM. However, it is too early

to relate improved efficacy of ATNM in humans to the presence of targeting ligands due to the fact that clinical studies are not designed to compare ATNM and PTNM. It seems that functionalizing a nanomedicine with targeting ligands does not significantly increase the toxicity when compared to PTNM. For example, the maximum tolerated doses of 3 of the discussed DOX-loaded ATNM were comparable to that of Doxil®.

It is widely believed that PTNM and ATNM have comparable pharmacokinetic parameters, biodistribution and tumor accumulation profiles. Studies of 7 discussed ATNM have reported on *in vivo* localization studies. Of those 7, 4 showed increased target localization compared to PTNM *in vivo*, while the other 3 ATNM showed comparable target accumulation compared to PTNM. It is possible that ATNM may increase drug exposure by virtue of increased target cell uptake and target tissue retention compared to PTNM but the number of ATNM tested *in vivo* is too low to provide conclusive evidence.

There are several other applications where the use of ATNM may be beneficial when compared to PTNM.

(1) Active targeting is vital for drugs that need to localize intracellularly for therapeutic activity but are unable or inefficient in crossing the cell membrane. This is exemplified by the therapeutic application of nucleic acids. Systemic administration of unprotected nucleic acids leads to rapid clearance and degradation. The therapeutic success of systemically administered gene (regulating) therapy is therefore dependent on the development of suitable nanocarriers. The therapeutic potential of RNA interference is demonstrated by CALAA-01, of which intermediate results from the currently ongoing phase I trial reported that target protein expression in a patient's tumor was decreased after treatment with the ATNM [7]. The application of therapeutic DNA is illustrated by Rexin-G, which has shown encouraging anti-tumor activity in patients including inhibition of angiogenesis and metastasis and has advanced to phase III trials [8].

(2) Increased expression of drug-efflux pumps in tumor cells that actively expel chemotherapeutics is a common mechanism in multi drug resistant (MDR) tumors. The efficacy of systemically administered chemotherapy (whether administered as free drug, or formulated as PTNM) that releases the drug in the vicinity of the tumor cells, can be severely decreased in MDR tumors. Anti-EGFR immunoliposomes loaded with DOX showed significant anti-tumor activity compared to free drug or PEGylated liposomal DOX (PLD) in a MDR breast cancer xenograft model by intracellular delivery of the chemotherapeutic effectively overcoming the drug efflux rate [9].

(3) Active-targeting can be applied to develop nanomedicines that exploit two therapeutic strategies simultaneously to achieve additive or synergistic anti-tumor

effects. For example, DOX-loaded polymeric micelles decorated with intrinsically active anti-EGFR nanobodies (Nb) significantly reduced tumor growth and increased survival of tumor-bearing mice when compared to DOX-loaded micelles devoid of targeting ligands [10].
(4) An alternative approach to the targeted delivery of anti-cancer drugs to tumor cells is targeting of tumor angiogenesis. The endothelial cells of the tumor vasculature are more exposed to targeted nanomedicines circulating in the blood and present better genetic stability limiting the development of drug resistance. Treatment with DOX-loaded liposomes targeting αvβ3 integrins overexpressed on tumor endothelium reduced tumor growth of DOX-resistant tumors while treatment with PLD did not [11]. The formation of neovasculature is indispensable for tumors to grow beyond microscopic size. In line with this, it was shown that DOX-loaded ATNM targeting αvβ3 integrins suppressed metastasis [12].
(5) In addition to the development of ATNM for cancer treatment, active targeting approaches can be applied for the development of effective vaccines demonstrated by the clinical evaluation of the anti-melanoma vaccine Lipovaxin-MM and the anti-nicotine vaccine SEL-068.

The balance between clinical benefits and cost-effectiveness of production will eventually determine the clinical applicability of ATNM. At present, the knowledge of nanomedicine interactions in the body is too limited. Studies that focus on the relation between the physicochemical properties of ATNM in relation to biodistribution, safety and efficacy are recommended. The efficacy and safety of ATNM in (pre)clinical animal models has been shown, but the added value of targeting ligands on nanomedicines in humans remains to be established.

2. Tumor-targeted Nanobullets for anti-cancer combination treatment

EGFR is a well established target for anti-cancer therapy which has translated in the approval of EGFR inhibitors including monoclonal antibodies (mAb) and kinase inhibitors (KI) [13]. EGFR-targeted therapy can be very effective and in many cases elicits fewer side-effects compared to conventional anti-cancer treatment. For example, patients with EGFR-mutated non-small-cell lung cancer (NSCLC) derive greater benefit from treatment with KI erlotinib and gefitinib than chemotherapy [14-15]. Nevertheless, disease eventually progresses due to secondary (EGFR) mutations, making the KI ineffective, or activation of bypass signaling pathways that do not require the activation of EGFR anymore [16]. One frequently reported compensatory pathway is the insulin-like growth factor 1 receptor (IGF-1R) signaling cascade [17]. Crosstalk between EGFR and IGF-1R signaling can circumvent mono-targeted therapies and activate proliferation and survival pathways in tumor cells

[18].

In **Chapter 3**, we have pursued a therapeutic strategy to simultaneously interfere with EGFR and IGF-1R signaling for enhanced inhibition of tumor cell proliferation. To this aim, we developed a dual-active targeted nanomedicine or Nanobullet which consisted of liposomes decorated with anti-EGFR Nbs EGa1 and the anti-IGF-1R KI AG538 as payload. The anti-EGFR Nb EGa1 is an antagonist of EGFR [19]. Empty EGa1-coupled liposomes induced robust EGFR sequestration and downregulation [20]. Modification of EGa1 to introduce reactive sulfhydryl groups and the subsequent conjugation to the distal end of PEG chains on the surface of the liposomes did not compromise the antigen association of EGa1. Anti-EGFR Nb-liposomes loaded with AG538 (EGa1-AG538-L) displayed a 4-fold increase in cell association and considerably more cell uptake in EGFR-positive ($EGFR^+$) UM-SCC-14C (14C) tumor cells compared to control formulations. In contrast, none of the formulations were taken up by EGFR-negative ($EGFR^-$) NIH 3T3 clone 2.2 mouse fibroblasts, indicating EGFR-specific interactions mediated by EGa1.

In addition to its function as a targeting ligand, EGa1 has intrinsic antagonistic properties that prevent activation of EGFR. EGa1-liposomes either empty or loaded with AG538, blocked substrate-induced activation of EGFR signaling in 14C cells determined by phoshpo-specific Western blotting (WB), showing that the antagonistic activity is preserved after coupling to the liposome surface.

While the blockade of EGFR by EGa1 occurs extracellularly, the AG538 site of action is intracellular. Phospho-specific WB of IGF-1R showed that EGa1-AG538-L efficiently blocked IGF-1R signaling in 14C cells after 4 h incubations indicating that the nanobullets are capable of blocking both EGFR and IGF-1R signaling. The nanobullets induced strongly enhanced and dose dependent cytotoxicity compared to control formulations as well as effective inhibition of cell proliferation.

Encouraged by these results, we further evaluated the nanobullets for *in vivo* applications in **Chapter 4.** We assessed efficacy by inhibition of targeted pathway activation, anti-proliferative effects *in vitro* and antitumor activity in xenograft models. To accomplish this, we developed a stable PEGylated nanobullet formulation based on DPPC and cholesterol for *in vivo* applications. Studies performed with $EGFR^+$ human MDA-MB-468 (MB-468) breast cancer cells demonstrated 3 to 4-fold more cell association of EGa1-L compared to untargeted liposomes. These differences in cell association mediated by EGa1 were consistent with the results of studies described in **Chapter 3**.

To determine whether the EGa1-AG538-L could effectively inhibit activation of EGFR and IGF-1R signaling, a panel of tumor cell lines with varying EGFR and IGF-1R expression levels was exposed to the nanobullets. The panel of human tumor

cell lines consisted of the head and neck squamous cell carcinoma (SCC) line 14C, the epidermoid SCC line A431, the alveolar basal epithelial adenocarcinoma line A549 and the breast adenocarcinoma line MB-468. In all four cell lines, both EGa1-L and EGa1-AG538-L strongly inhibited or even completely blocked activation of substrate-induced EGFR signaling highlighting the powerful antagonistic effect of EGa1. Only EGa1-AG538-L were able to inhibit activation of IGF-1R signaling in the 14C and A431 cells indicating efficient cytosolic delivery of AG538. In contrast, nanobullet treatment did not alter phosphorylated levels of IGF-1R in A549 and MB-468 cells indicating that the cellular processing of EGa1-AG538-L by MB-468 and A549 occurs in a different manner than in 14C and A431 cells. In A549 cells, lower expression of EGFR compared to the other cell lines may prevent sufficient uptake of EGa1-AG538-L for AG538-mediated inhibition of IGF-1R phosphorylation. However, the expression level in MB-468 cells is comparable to 14C and A431 cells, suggesting inefficient liposomal uptake or inadequate cytosolic localization of AG538 in MB-468 cells.
The effects of nanobullet treatment on the inhibition of proliferation and survival pathways downstream of EGFR and IGF-1R were evaluated by phospho-specific WB of key mediators Akt and Erk 1/2 (p44/p42 MAPK). Nanobullet-induced blockade of EGFR and IGF-1R activation in 14C and A431 cells resulted in inhibition of Akt and Erk 1/2 activation. At the same time, Akt and Erk 1/2 phosphorylation levels in A549 and MDA-468 cells were unaffected indicating that obstruction of EGFR and IGF-1R activation is necessary for efficient inhibition of downstream proliferation and survival pathways in these tumor cells. Anti-tumor efficacy of nanobullet treatment *in vitro* was assessed by proliferation assays on the same panel of tumor cell lines. EGa1-AG538-L efficiently reduced total 14C and A431 cell numbers in a dose-dependent manner corresponding to the sensitivity of phosphorylation inhibition of the molecular targeted pathways. At the same time, nanobullet treatment of A549 and MB-468 cells induced only partial anti-proliferative effects. Taken together, the proliferation assay results correlated well with the ability of the nanobullets to induce effective molecular inhibition of cell proliferation and survival pathway activation. These results emphasize that inhibition of a single growth factor receptor pathway is not sufficient to effectively inhibit tumor cell proliferation due to activation of compensatory pathways and crosstalk induced activation of downstream effectors in these cells.

In this particular case, we focused on EGFR and IGF-1R crosstalk. At the same time, crosstalk between EGFR and other growth factor receptor signaling pathways such as the hepatocyte growth factor receptor (HGFR or c-Met) signaling has been implicated as a compensatory mechanism for tumor cells [21]. A549 cells,

additionally, bear a mutation in the K-RAS gene which can activate the Akt pathway and impair treatment with EGFR inhibitors [22]. MB-468 cells have amplificated EGFR and loss of the PTEN tumor suppressor protein also resulting in activation of Akt signaling [23]. The limited responses of both A549 and MB-468 cells *in vitro* might reveal the strong activity of compensatory pathways in these cells.
The 14C and MDA-468 cell lines were implanted in mice to investigate if nanobullet-induced anti-tumor effects *in vivo* correlate with cytotoxicity results and inhibition of targeted molecular pathways.
EGa1-AG538-L significantly inhibited tumor growth more effectively compared to controls in the fast-growing 14C xenograft model, corresponding to the strong *in vitro* response pattern to nanobullet exposure. In the slow-growing MB-468 model representative of a medium *in vitro* response pattern, nanobullet treatment did not cause significant tumor growth reduction when compared to controls. Taken together, nanobullet-induced inhibition of cell proliferation and survival pathway activation in the investigated cell lines was highly predictive of anti-tumor efficacy *in vitro* and *in vivo*.

The results described in **Chapter 3** and **Chapter 4** demonstrate the feasibility of developing a targeted nanomedicine for the molecular inhibition of multiple molecular pathways in tumor cells. Inhibition of proliferation and survival pathway activation correlated well with anti-tumor effects, producing limited *in vitro* and *in vivo* efficacy on MB-468 cells and good therapeutic effects in 14C cells. These results underline the importance of pathway profiling of tumor tissue before molecular targeted therapy to maximize the chance of therapeutic success. Even so, frequent dosing (once every other day) of the nanobullets was necessary to inhibit tumor growth in 14C xenografts. To improve anti-tumor effects, it may be required to increase the dose of AG538 encapsulated in the liposomes. Another possibility is to load multi-targeted kinase inhibitors, such as sunitinib, to inhibit multiple molecular pathways in the cell. The risk of side-effects, inherently associated with the use of kinase inhibitors with broad activity may be limited in this formulation as a result of the specific target cell delivery by the Nb-liposomes. It may be further diminished by using a sunitinib analogue that is unable to pass cellular membranes on its own requiring an effective delivery platform to reach the tumor cell cytoplasm. The versatile Nb-liposome platform is readily adjustable allowing conjugation of Nbs directed at different molecular targets and the incorporation of a broad range of therapeutic molecules.

Different nanobullet platforms for combination treatment of cancer have recently been reported. For example, anti-EGFR Nb crosslinked albumin-nanoparticles

loaded with a sunitinib analogue effectively inhibited tumor cell proliferation [24]. Anti-EGFR polymeric micelles based on poly(ethylene glycol)-b-poly[N-(2-hydroxypropyl) methacrylamide-lactate] loaded with doxorubicin markedly inhibited tumor growth in xenograft models and prolonged survival compared to controls [10]. In an exciting novel active targeting approach, mice bearing intracranial glioblastoma tumors received treatment with tumoritropic stem cells releasing cytotoxic anti-EGFR Nb-immunoconjugates. Treatment prevented tumor outgrowth and markedly increased survival [25].

As the Nb repertoire directed at cancer targets is rapidly growing, the feasibility to produce cost-effective and efficacious nanomedicines for combination treatment or imaging is increasing. Experience with Nbs is increasing as the first Nb-based therapeutics are undergoing clinical evaluation [26-27]. Combined with the clinical studies on targeted nanomedicines, it may facilitate the transition of nanobullets towards clinical reality.

3. Anti-cancer therapy by inhibition of angiogenesis

Malignant transformation and subsequent uncontrollable growth of cells eventually results in the development of a small tumor. During this stage, the formation of new blood vessels from pre-existing ones, a process know as angiogenesis, has to be initiated to overcome limiting concentrations of nutrients and oxygen. Since the discovery in the 1970s that angiogenesis is vital for tumor development [28], tumor angiogenesis has become an attractive target for anti-cancer treatment. Efforts to better understand the molecular mechanisms and key mediators involved in tumor angiogenesis resulted in the approval of several angiogenesis inhibitors in the last decade such as the mAb bevacizumab and the multi-target KI sunitinib and sorafenib [29-30]. These inhibitors primarily aim at interfering with vascular endothelial growth factor (VEGF)-induced signaling. Although many other angiogenic signaling cascades have been unraveled in recent years, stimulation of endothelial cells (EC) by VEGF via its cognate tyrosine kinase receptor family (VEGFR) remains one of the critical events in angiogenesis [29]. However, clinical VEGF-targeted therapy has elicited at best modest and even conflicting effects. As is observed with the molecular inhibitors directed at growth factor receptor pathways in tumor cells, tumor resistance develops also against this EC pathway and tumors eventually progress [31]. In addition, anti-angiogenic therapy might induce more invasive and metastatic tumor phenotypes as it reduces the hospitality of the primary tumor site [32-33]. As a result, there is a demand for innovative or combinatorial approaches that more effectively inhibit angiogenesis and subsequent tumor growth and metastasis. In ECs, VEGF-mediated VEGFR-2 activation can stimulate the Rho GTPase signaling cascade. Rho GTPases are small proteins that function as molecular switches in the cell. Rho GTPases and

their regulatory and effectors proteins are crucial regulators of cellular processes such as cytoskeleton dynamics, vesicle trafficking, membrane transport and transcription factor activity [34]. In **Chapter 5** the role of Rho proteins in tumor angiogenesis and invasion is outlined. Rho GTPases are often indispensable for processes that contribute to angiogenesis such as amplified vascular permeability, degradation of the basement membrane, enhanced cell migration, increased cell proliferation and lumen formation. In addition, Rho proteins have been implicated in tumor cell migration, invasion and even metastasis. Notably, mutations in Rho GTPases have seldomly been observed (only recently a Rac1 mutation melanoma was reported [35]). Taken together, Rho GTPases are an attractive target for anticancer treatment. Strategies to interfere with Rho GTPase signaling include the use of small inhibitors for Rho GTPases or effector/regulator proteins, post-translational modification inhibitors such as statins or bisphosphonates and RNAi-mediated approaches.
Such an approach is described in **Chapter 6**, where the role of the Rho GTPase Rac1 in tumor angiogenesis and growth is investigated with an RNAi approach. Rac1 has been implicated in being the predominant Rho GTPase responsible for VEGF-induced angiogenesis [36] and serves as an appealing target for anti-cancer therapy. Efficient knockdown of Rac1 in human ECs was achieved by transient transfection with anti-Rac1 siRNA (siRac1). Functional angiogenesis assays demonstrated that silencing of Rac1 inhibited VEGF-mediated EC tube formation, migration, invasion and proliferation *in vitro.* Moreover, treatment of mice bearing VEGF-supplemented Matrigel plugs with siRac1 resulted in reduced blood vessel formation when compared to treatment with control siRNA (siNS). Importantly, intratumoral treatment of mice bearing highly vascularized Neuro2A tumors with siRac1 almost completely blocked the outgrowth of tumors compared to saline and siNS treatments. The anti-tumor effect of siRac1 treatment seemed to be predominantly caused by anti-angiogenic effects mediated via ECs. In our studies we did not observe a combined inhibition of angiogenesis and tumor cell proliferation to be responsible for the anti-tumor effects. However, in a similar study siRNA-induced knockdown of the Rho GTPase RhoA resulted in breast cancer xenograft tumor growth inhibition where dual effects in ECs and tumor cells appeared to be involved [37]. Most recently, Rho GTPases have been implicated in the formation, loading and shedding of microvesicles (MV) by cancer cells [38]. Shedding of MV by cancer cells is a method for communication and sharing of cell contents, which can substantially influence tumor development [39]. Moreover, Rho GTPase signaling has been implicated in facilitating elevated metabolism necessary for cancer cells to progress [40]. These reports, studies that implicate aberrant Rho GTPase signaling in tumor angiogenesis and proliferation and our observations taken together confirm interference with these cellular regulators a rational and attractive approach for more

effective (combination) therapy of cancer.

4. Conclusions

To date, cancer remains the leading cause of death in the world. Extensive research efforts have resulted in the introduction of nanomedicines and molecular inhibitors to the arsenal of anti-cancer strategies. Concurrently, increased understanding of the underlying molecular mechanisms of processes such as tumor development, angiogenesis and metastatic spread has rendered cancer treatment more efficacious.

This thesis has addressed two approaches for anti-cancer therapy using innovative techniques. The first approach involved the development of an actively-targeted nanomedicine for the direct inhibition of tumor cell proliferation. The second approach concerns indirect inhibition of tumor growth by RNAi-mediated obstruction of tumor angiogenesis.

In the first approach we have encapsulated an anti-IGF-1R kinase inhibitor in liposomes that were subsequently equipped with anti-EGFR Nbs for the anti-cancer combination therapy. These loaded Nb-liposomes or Nanobullets could effectively inhibit the activation of both EGFR and IGF-1R signaling in tumor cells. Inhibition of cell proliferation and survival pathways on a molecular level predicted the cytotoxic efficacy of the nanobullets in a panel of tumor cell lines *in vitro*. In human xenograft models in mice, nanobullet-induced anti-tumor effects corresponded with the cytotoxicity observed in the respective cell line. An interesting challenge for future studies is the determination of the combination of therapeutic strategies that is most efficacious for the treatment of a specific indication. It may even be applied to combinations between drug and targeting ligand that form the basis for a personalized anti-cancer strategy.

For the second approach we have employed an RNAi-mediated approach to specifically silence a gene which encodes a protein essential for tumor angiogenesis. Knockdown of the Rho GTPase Rac1 with specific siRNAs significantly decreased the ability of human ECs to transform into an angiogenic phenotype. In addition, siRac1 treatment inhibited angiogenesis and tumor growth in mice. The essential role of Rho GTPases including their regulator and effector proteins in a plethora of cellular processes that contribute to tumor development makes this signaling cascade a valid target to augment current cancer treatment. However, as Rho GTPases are ubiquitously expressed and involved in many cellular household functions, it is highly likely that targeted inhibition of these proteins at only at the site of disease is crucial. An actively-targeted nanomedicine, similar to the CALAA-01 formulation, that is able to selectively deliver the, otherwise ineffective, siRNA to the cytoplasm of target cells would be an important step towards clinical application of this strategy.

This thesis has demonstrated valuable innovative strategies to improve existing anti-cancer therapy. This knowledge, together with the information from the first active-

targeted nanomedicines currently in clinical trials, the data from targeted delivery of siRNA in humans and the increased understanding of molecular mechanisms that underlie cancer development and progression combined with improved treatment and diagnosis may lay the foundations for a future where certain types of cancer are no longer considered lethal but chronic diseases.

References

1. Barenholz, Y., Doxil® - the first FDA-approved nano-drug: lessons learned, J Control Release, 160 (2012) 117-134.
2. Svenson, S., Clinical translation of nanomedicines, Curr Opin Solid St M, 16 (2012) 287-294.
3. Etheridge, M.L., Campbell, S.A., Erdman, A.G., Haynes, C.L., Wolf, S.M., McCullough, J., The big picture on nanomedicine: the state of investigational and approved nanomedicine products, Nanomedicine, 9 (2013) 1-14.
4. Matsumura, Y., Maeda, H., A new concept for macromolecular therapeutics in cancer chemotherapy: mechanism of tumoritropic accumulation of proteins and the antitumor agent smancs, Cancer Res, 46 (1986) 6387-6392.
5. Fang, J., Nakamura, H., Maeda, H., The EPR effect: Unique features of tumor blood vessels for drug delivery, factors involved, and limitations and augmentation of the effect, Adv Drug Deliv Rev, 63 (2011) 136-151.
6. Lammers, T., Kiessling, F., Hennink, W.E., Storm, G., Drug targeting to tumors: principles, pitfalls and (pre-) clinical progress, J Control Release, 161 (2012) 175-187.
7. Davis, M.E., Zuckerman, J.E., Choi, C.H., Seligson, D., Tolcher, A., Alabi, C.A., Yen, Y., Heidel, J.D., Ribas, A., Evidence of RNAi in humans from systemically administered siRNA via targeted nanoparticles, Nature, 464 (2010) 1067-1070.
8. Gordon, E.M., Hall, F.L., The 'timely' development of Rexin-G: first targeted injectable gene vector (review), Int J Oncol, 35 (2009) 229-238.
9. Mamot, C., Ritschard, R., Wicki, A., Kung, W., Schuller, J., Herrmann, R., Rochlitz, C., Immunoliposomal delivery of doxorubicin can overcome multidrug resistance mechanisms in EGFR-overexpressing tumor cells, J Drug Target, 20 (2012) 422-432.
10. Talelli, M., Oliveira, S., Rijcken, C.J., Pieters, E.H., Etrych, T., Ulbrich, K., van Nostrum, R.C., Storm, G., Hennink, W.E., Lammers, T., Intrinsically active nanobody-modified polymeric micelles for tumor-targeted combination therapy, Biomaterials, 34 (2013) 1255-1260.
11. Schiffelers, R.M., Koning, G.A., ten Hagen, T.L., Fens, M.H., Schraa, A.J., Janssen, A.P., Kok, R.J., Molema, G., Storm, G., Anti-tumor efficacy of tumor vasculature-targeted liposomal doxorubicin, J Control Release, 91 (2003) 115-122.
12. Murphy, E.A., Majeti, B.K., Barnes, L.A., Makale, M., Weis, S.M., Lutu-Fuga, K., Wrasidlo, W., Cheresh, D.A., Nanoparticle-mediated drug delivery to tumor vasculature suppresses metastasis, Proc Natl Acad Sci U S A, 105 (2008) 9343-9348.
13. Yarden, Y., Pines, G., The ERBB network: at last, cancer therapy meets systems biology, Nat Rev Cancer, 12 (2012) 553-563.
14. Gao, G., Ren, S., Li, A., Xu, J., Xu, Q., Su, C., Guo, J., Deng, Q., Zhou, C., Epidermal growth factor receptor-tyrosine kinase inhibitor therapy is effective as first-line treatment of advanced non-small-cell lung cancer with mutated EGFR: A meta-analysis from six phase III randomized controlled trials, Int J Cancer, 131 (2012) E822-829.
15. Petrelli, F., Borgonovo, K., Cabiddu, M., Barni, S., Efficacy of EGFR tyrosine kinase inhibitors in patients with EGFR-mutated non-small-cell lung cancer: a meta-analysis of 13 randomized trials, Clin Lung Cancer, 13 (2012) 107-114.
16. Wheeler, D.L., Dunn, E.F., Harari, P.M., Understanding resistance to EGFR inhibitors-

impact on future treatment strategies, Nat Rev Clin Oncol, 7 (2010) 493-507.
17. Pollak, M., The insulin and insulin-like growth factor receptor family in neoplasia: an update, Nat Rev Cancer, 12 (2012) 159-169.
18. van der Veeken, J., Oliveira, S., Schiffelers, R.M., Storm, G., van Bergen En Henegouwen, P.M., Roovers, R.C., Crosstalk between epidermal growth factor receptor- and insulin-like growth factor-1 receptor signaling: implications for cancer therapy, Curr Cancer Drug Targets, 9 (2009) 748-760.
19. Hofman, E.G., Ruonala, M.O., Bader, A.N., van den Heuvel, D., Voortman, J., Roovers, R.C., Verkleij, A.J., Gerritsen, H.C., van Bergen En Henegouwen, P.M., EGF induces coalescence of different lipid rafts, J Cell Sci, 121 (2008) 2519-2528.
20. Oliveira, S., Schiffelers, R.M., van der Veeken, J., van der Meel, R., Vongpromek, R., van Bergen En Henegouwen, P.M., Storm, G., Roovers, R.C., Downregulation of EGFR by a novel multivalent nanobody-liposome platform, J Control Release, 145 (2010) 165-175.
21. Zhang, Y.W., Staal, B., Essenburg, C., Su, Y., Kang, L., West, R., Kaufman, D., Dekoning, T., Eagleson, B., Buchanan, S.G., Vande Woude, G.F., MET kinase inhibitor SGX523 synergizes with epidermal growth factor receptor inhibitor erlotinib in a hepatocyte growth factor-dependent fashion to suppress carcinoma growth, Cancer Res, 70 (2010) 6880-6890.
22. Choi, E.J., Ryu, Y.K., Kim, S.Y., Wu, H.G., Kim, J.S., Kim, I.H., Kim, I.A., Targeting epidermal growth factor receptor-associated signaling pathways in non-small cell lung cancer cells: implication in radiation response, Mol Cancer Res, 8 (2010) 1027-1036.
23. She, Q.B., Solit, D.B., Ye, Q., O'Reilly, K.E., Lobo, J., Rosen, N., The BAD protein integrates survival signaling by EGFR/MAPK and PI3K/Akt kinase pathways in PTEN-deficient tumor cells, Cancer Cell, 8 (2005) 287-297.
24. Altintas, I., Heukers, R., van der Meel, R., Lacombe, M., Amidi, M., van Bergen En Henegouwen, P.M., Hennink, W.E., Schiffelers, R.M., Kok, R.J., Nanobody-albumin nanoparticles (NANAPs) for the delivery of a multikinase inhibitor 17864 to EGFR overexpressing tumor cells, J Control Release, 165 (2013) 110-118.
25. van de Water, J.A., Bagci-Onder, T., Agarwal, A.S., Wakimoto, H., Roovers, R.C., Zhu, Y., Kasmieh, R., Bhere, D., Van Bergen en Henegouwen, P.M., Shah, K., Therapeutic stem cells expressing variants of EGFR-specific nanobodies have antitumor effects, Proc Natl Acad Sci U S A, 109 (2012) 16642-16647.
26. Bartunek, J., Barbato, E., Heyndrickx, G., Vanderheyden, M., Wijns, W., Holz, J.B., Novel Antiplatelet Agents: ALX-0081, a Nanobody Directed towards von Willebrand Factor, J Cardiovasc Transl Res, (2013).
27. Ablynx N.V., Ablynx's product portfolio, http://www.ablynx.com/en/research-development/pipeline/, Retrieved 25-02-2013.
28. Folkman, J., Tumor angiogenesis: therapeutic implications, N Engl J Med, 285 (1971) 1182-1186.
29. Carmeliet, P., Jain, R.K., Molecular mechanisms and clinical applications of angiogenesis, Nature, 473 (2011) 298-307.
30. Weis, S.M., Cheresh, D.A., Tumor angiogenesis: molecular pathways and therapeutic targets, Nat Med, 17 (2011) 1359-1370.
31. Bergers, G., Hanahan, D., Modes of resistance to anti-angiogenic therapy, Nat Rev Cancer, 8 (2008) 592-603.
32. Ebos, J.M., Lee, C.R., Cruz-Munoz, W., Bjarnason, G.A., Christensen, J.G., Kerbel, R.S., Accelerated metastasis after short-term treatment with a potent inhibitor of tumor angiogenesis, Cancer Cell, 15 (2009) 232-239.
33. Paez-Ribes, M., Allen, E., Hudock, J., Takeda, T., Okuyama, H., Vinals, F., Inoue, M., Bergers, G., Hanahan, D., Casanovas, O., Antiangiogenic therapy elicits malignant progression of tumors to increased local invasion and distant metastasis, Cancer Cell, 15 (2009) 220-231.
34. Heasman, S.J., Ridley, A.J., Mammalian Rho GTPases: new insights into their functions from in vivo studies, Nat Rev Mol Cell Biol, 9 (2008) 690-701.

35. Krauthammer, M., Kong, Y., Ha, B.H., Evans, P., Bacchiocchi, A., McCusker, J.P., Cheng, E., Davis, M.J., Goh, G., Choi, M., Ariyan, S., Narayan, D., Dutton-Regester, K., Capatana, A., Holman, E.C., Bosenberg, M., Sznol, M., Kluger, H.M., Brash, D.E., Stern, D.F., Materin, M.A., Lo, R.S., Mane, S., Ma, S., Kidd, K.K., Hayward, N.K., Lifton, R.P., Schlessinger, J., Boggon, T.J., Halaban, R., Exome sequencing identifies recurrent somatic RAC1 mutations in melanoma, Nat Genet, 44 (2012) 1006-1014.
36. Fryer, B.H., Field, J., Rho, Rac, Pak and angiogenesis: old roles and newly identified responsibilities in endothelial cells, Cancer Lett, 229 (2005) 13-23.
37. Pille, J.Y., Li, H., Blot, E., Bertrand, J.R., Pritchard, L.L., Opolon, P., Maksimenko, A., Lu, H., Vannier, J.P., Soria, J., Malvy, C., Soria, C., Intravenous delivery of anti-RhoA small interfering RNA loaded in nanoparticles of chitosan in mice: safety and efficacy in xenografted aggressive breast cancer, Hum Gene Ther, 17 (2006) 1019-1026.
38. Li, B., Antonyak, M.A., Zhang, J., Cerione, R.A., RhoA triggers a specific signaling pathway that generates transforming microvesicles in cancer cells, Oncogene, 31 (2012) 4740-4749.
39. Antonyak, M.A., Wilson, K.F., Cerione, R.A., R(h)oads to microvesicles, Small GTPases, 3 (2012) 219-224.
40. Wilson, K.F., Erickson, J.W., Antonyak, M.A., Cerione, R.A., Rho GTPases and their roles in cancer metabolism, Trends Mol Med, 19 (2013) 74-82.

Appendices
Nederlandse samenvatting voor niet-ingewijden

1. Doelgerichte aflevering van antikanker medicijnen

Kanker is een verzamelnaam voor verschillende complexe aandoeningen die allemaal gekenmerkt worden door abnormale en ongereguleerde celgroei. Kanker is de belangrijkste doodsoorzaak in de wereld en verantwoordelijk voor 7.6 miljoen sterfgevallen in 2008 (13% van het totaal). Hoewel door onderzoek steeds beter wordt begrepen welke factoren een rol spelen bij de verandering van een 'normale' cel in een kankercel, blijft het lastig om te bepalen wanneer dit gebeurt. Kankertherapie is erop gericht om kankercellen te doden en tegelijkertijd zo min mogelijk schade aan te richten in gezonde delen van het lichaam. De effectiviteit van kankertherapie is afhankelijk van het stadium van de ziekte ten tijde van de diagnose en is vooral gebaseerd op (een combinatie van) chirurgische verwijdering van de tumor, bestraling (radiotherapie) en chemotherapie.

Chemotherapeutica verhinderen de celdeling van snel delende cellen zoals tumor cellen. Echter, doordat het geneesmiddel zich over het hele lichaam verdeelt, worden ook andere snel delende cellen aangevallen zoals cellen in het beenmerg, maag-darmstelsel en haar follikels. Dit kan voor ernstige ongewenste bijwerkingen zorgen die de toepassing van deze therapie beperken.

In de laatste decennia is de kennis over de cellulaire factoren die een belangrijke rol spelen bij de ontwikkeling van een tumor enorm toegenomen. Dit heeft geresulteerd in de ontwikkeling van antikanker medicijnen die selectiever tumoren aanvallen dan de hierboven genoemde conventionele therapieën. Door de toename in specificiteit is de balans tussen effectiviteit en toxiciteit (therapeutische index) van deze nieuwe klasse medicijnen veel gunstiger. Toch verdelen ook deze geneesmiddelen zich over het gehele lichaam na orale of intraveneuze toediening, en dus kan de toepassing van deze remmers verder worden verbeterd door de ophoping in zieke weefsels (tumor) te vergroten en zo tegelijkertijd de blootstelling van gezonde weefsels te verminderen. De strategie die wordt gebruikt om dit te bereiken wordt *'Targeted Drug Delivery'* genoemd, wat zich in het Nederlands laat vertalen tot *'doelgerichte afgifte van geneesmiddelen'*. Doelgerichte afgifte van geneesmiddelen kan worden gerealiseerd door ze te verpakken in dragersystemen. Deze dragersystemen zijn zeer kleine deeltjes met een afmeting van 50 – 400 nanometer. Ter vergelijking, 1 nanometer is 1.000.000 x kleiner dan een millimeter en de doorsnede van een dragersysteem is ongeveer 1.000 x zo klein als de doorsnede van een menselijke haar. Dragersystemen die beladen zijn met een geneesmiddel worden *'Nanomedicijnen'* genoemd.

Nanomedicijnen worden veelal intraveneus toegediend en kunnen vervolgens circuleren in de bloedbaan omdat de bloedvatwand in gezonde weefsels niet doorlaatbaar is voor deeltjes van deze grootte. Tegelijkertijd worden de bloedvaten van tumoren juist gekenmerkt door een verhoogde doorlaatbaarheid, waardoor nanomedicijnen uit de bloedbaan kunnen treden, zich kunnen ophopen in de tumor

en het antikanker medicijn aan de tumorcellen kunnen afgeven. Naast de bloedvaten is het drainagesysteem (lymfevatenstelsel) in tumoren meestal slecht ontwikkeld waardoor de opgehoopte nanomedicijnen in een tumor niet effectief afgevoerd worden. Het verpakken van een antikanker medicijn in een dragersysteem met als doel een grotere hoeveelheid van het geneesmiddel in de tumor te krijgen wordt *'Passieve Targeting (passief richten)'* genoemd (Fig. 1). De effectiviteit en selectiviteit van deze strategie kan worden verbeterd door het oppervlak van het nanomedicijn uit te rusten met *'targeting liganden'*. Deze targeting liganden herkennen specifieke eiwitten (*'receptoren'*) op het oppervlak van tumorcellen en zorgen voor een verbeterde hechting en opname van het nanomedicijn in de cellen. Het hechten van targeting liganden aan nanomedicijnen wordt *'Actieve Targeting (actief richten)'* genoemd (Fig. 1).

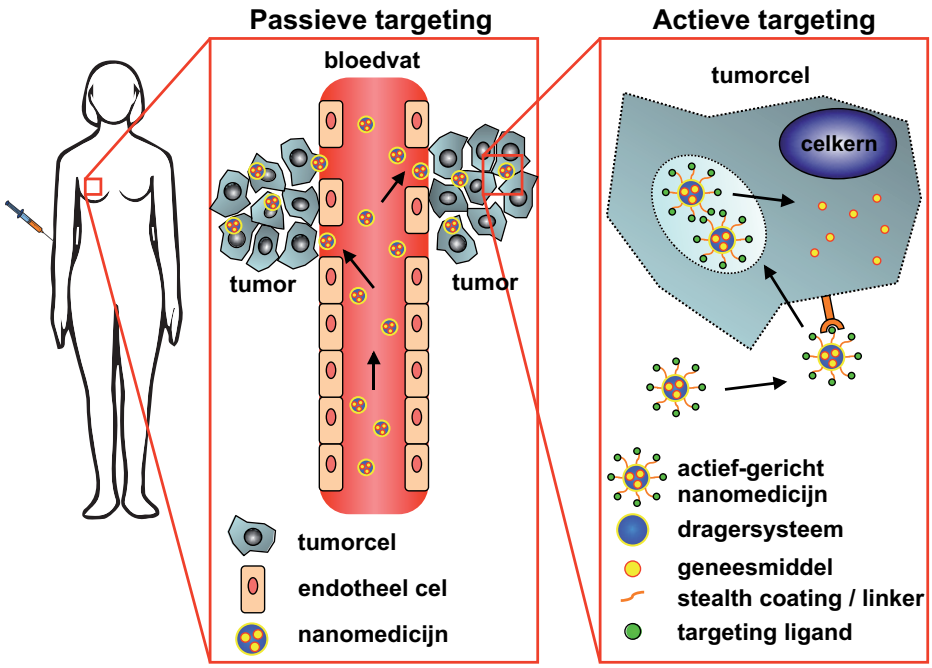

Figuur 1. Doelgerichte afgifte van nanomedicijnen in tumoren na intraveneuze toediening. Passieve targeting wordt bereikt doordat de bloedvaten van tumoren doorlaatbaar zijn voor nanomedicijnen die zich daardoor kunnen ophopen in de tumor. Actieve targeting wordt gerealiseerd door nanomedicijnen uit te rusten met targeting liganden die tumorcellen herkennen en zo de specificiteit en de opname van nanomedicijnen in tumorcellen vergroten.

Het eerste antikankernanomedicijn (Doxil®/Caelyx) werd bijna 20 jaar geleden goedgekeurd voor therapie en wordt sindsdien gebruikt in de kliniek. Het verpakken van het geneesmiddel doxorubicine in een lang-circulerend dragersysteem zorgde

voor gelijke en soms verbeterde therapeutische activiteit in vergelijking met het 'onverpakt' toegediende geneesmiddel. Bovendien werd de schade aan het hart, een ongewenste bijwerking van doxorubicine, flink verminderd door het toe te dienen in dit dragersysteem. Sindsdien zijn verschillende antikankernanomedicijnen goedgekeurd voor klinisch gebruik. Er wordt geschat dat er ongeveer 250 nanomedicijnen in verschillende stadia van ontwikkeling zijn, waarvan verreweg de meeste voor de behandeling van kanker.

Vrijwel alle antikankernanomedicijnen die momenteel goedgekeurd zijn, kunnen worden beschouwd als *passief gerichte nanomedicijnen (PGNM)*. Deze nanomedicijnen maken vooral gebruik van het feit dat ze lang in het lichaam circuleren en ophopen in de tumor vanwege de doorlaatbaarheid van de bloedvaten in tumoren. Ondanks dat het aanbrengen van targeting liganden de effectiviteit van nanomedicijnen kan verbeteren, zijn er op dit moment geen *actief gerichte nanomedicijnen (AGNM)* goedgekeurd voor gebruik in de kliniek. De status van 12 AGNM die momenteel worden getest in klinische trials is beschreven in **Hoofdstuk 2**. Uit de beschikbare literatuur die de (pre)klinische studies van de AGNM beschrijft, blijkt dat:

- AGNM effectief en veilig zijn in preklinische diermodellen,
- Het merendeel van de AGNM ontwikkeld wordt voor de behandeling van kanker,
- De bijdrage van targeting liganden aan de effectiviteit van nanomedicijnen nog niet onomstotelijk bewezen is,
- Targeting liganden vaak niet zorgen voor een verhoogde ophoping van het nanomedicijn in het doelweefsel (bijvoorbeeld een tumor), maar wel voordelig kunnen zijn met betrekking tot opname van het nanomedicijn in de doelcel en retentie in het doelweefsel.

Ondanks dat verbeterde inzichten in de interacties van AGNM met eiwitten en cellen na toediening in het menselijk lichaam nodig zijn om een effectieve vertaalslag naar de kliniek te realiseren, zijn er veelbelovende toekomstperspectieven voor AGNM. Zo kunnen actieve targeting strategieën toegepast worden voor het afleveren van geneesmiddelen die niet of slecht in staat zijn om cellulaire membranen te passeren, de behandeling van resistente tumoren, het aanvallen van de bloedvaten van de tumor of het ontwikkelen van specifiek gerichte vaccins.

2. Tumorgerichte Nanokogels voor antikanker therapie

De *epidermal growth factor receptor (EGFR)* is een receptoreiwit dat in hoge mate voorkomt op het celoppervlak van verschillende soorten tumoren. Zodra de juiste *groeifactor* bij de cel arriveert en na binding EGFR activeert, worden er belangrijke cellulaire signaalroutes aangezet die ervoor zorgen dat een tumorcel kan groeien en zo bijdragen aan de ontwikkeling van een tumor. De belangrijke rol van EGFR in

kanker heeft geleid tot de ontwikkeling van geneesmiddelen die specifiek EGFR blokkeren en zo de activering van cellulaire groei signaalroutes remt. Ondanks dat antikanker therapie met specifieke EGFR-remmers initieel zeer effectief is, is een tumor in staat om na verloop van tijd verder te groeien door het optreden van resistentie tegen de behandeling. Dit kan komen doordat een tumorcel zijn genetische code aanpast of ervoor zorgt dat andere eiwitten dan EGFR op het cel oppervlak cellulaire groei signaalroutes aanzetten. In beide gevallen wordt de tumor ongevoelig voor EGFR-gerichte therapie.

Eén van de eiwitten op het celoppervlak waarvan in de literatuur is beschreven dat het door tumoren kan worden gebruikt als 'omleiding' indien EGFR geblokkeerd is, heet de *insulin-growth factor 1 receptor (IGF-1R)*. Net als EGFR, kan geactiveerd IGF-1R cellulaire signaalroutes aanzetten die belangrijk zijn voor de groei en deling van een tumorcel.

In **Hoofdstuk 3** is getracht om de groei van tumorcellen te remmen door EGFR en IGF-1R tegelijkertijd te blokkeren en zo te voorkomen dat cellulaire groei- en overleving signaalroutes in tumorcellen worden aangezet. Hiervoor hebben wij een tweevoudig-actief AGNM of *Nanokogel* ontwikkeld die zowel EGFR als IGF-1R activering blokkeert (Fig. 2).

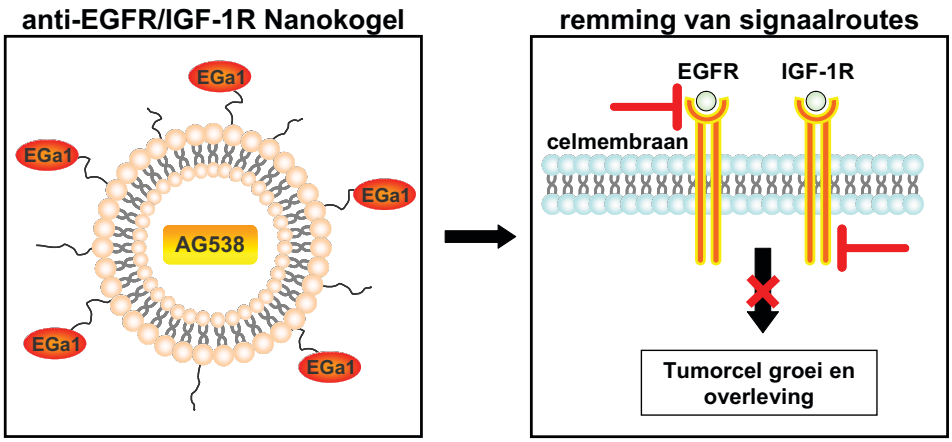

Figuur 2. De anti-EGFR/IGF-1R Nanokogel is een lang-circulerend actief gericht nanomedicijn. Het is geladen met een IGF-1R remmer (AG538) en uitgerust met targeting liganden (EGa1 nanobodies) die EGFR op het celoppervlak herkennen. Naast het vergroten van de specificiteit hebben de anti-EGFR nanobodies ook een EGFR-remmende functie. Het gelijktijdig blokkeren van EGFR en IGF-1R activering zorgt voor een effectieve remming van groei- en overlevingsignaalroutes in de tumorcel.

Het dragersysteem dat als basis dient voor de Nanokogel is een *liposoom*. Liposomen zijn de meest gebruikte dragersystemen voor doelgerichte aflevering van medicijnen. Een liposoom is een kunstmatig geproduceerd deeltje dat bestaat uit een door een

membraan omgeven *waterige inhoud*. De architectuur van het liposomale membraan lijkt op dat van een cel. De waterige inhoud van de Nanokogel is geladen met de anti-IGF-1R remmer *AG538*, die het gedeelte van IGF-1R blokkeert aan de binnenkant van de cel, en zo het aanzetten van signaalroutes remt. Aan het oppervlak van de Nanokogel zijn anti-EGFR *nanobodies (EGa1)* gehecht, die ervoor zorgen dat de Nanokogel gericht wordt naar tumorcellen die veel EGFR op hun oppervlak hebben. Tevens blokkeren de anti-EGFR nanobodies het gedeelte van EGFR aan de buitenkant van de cel, en voorkomen hiermee de activering van EGFR door binding van een groeifactor. Nanobodies zijn kleine stukjes *antilichaam* en kunnen zo worden ontwikkeld, dat ze zeer specifiek aan een bepaald eiwit binden. Hierdoor zijn nanobodies uitermate geschikt voor gebruik als targeting ligand.

De resultaten in **Hoofdstuk 3** laten zien dat anti-EGFR Nanokogels beter aan EGFR-positieve hoofd-hals tumorcellen binden, en beter door deze cellen werden opgenomen in vergelijk met liposomen zonder anti-EGFR nanobodies op het oppervlak. Ook waren cellen zonder EGFR op het oppervlak niet in staat om liposomen met of zonder nanobodies op te nemen. Dit betekent dat de opname van de anti-EGFR Nanokogels in EGFR-positieve tumorcellen wordt veroorzaakt door de anti-EGFR nanobodies op het oppervlak van de liposomen. Blootstelling van EGFR-positieve tumorcellen aan anti-EGFR Nanokogels geladen met AG538 zorgde voor een remming van zowel EGFR als IGF-1R activering in de cellen. Ook waren de Nanokogels in staat om de groei van tumorcellen sterk te remmen.

In **Hoofdstuk 4** is de toepasbaarheid van de anti-EGFR/IGF-1R Nanokogels als nanomedicijn verder onderzocht. Dit is gedaan door te onderzoeken of de Nanokogels in staat waren om in vier verschillende humane tumorcellijnen groei- en overlevingsignaalroutes te remmen (*moleculair*) en wat het effect hiervan was op de groei van de tumorcellen (*cellulair, in vitro*). Vervolgens is getest of systemische behandeling met anti-EGFR/IGF-1R Nanokogels tumorgroei in muizen kon remmen (*in vivo*). De cellijnen verschilden van elkaar in hoeveelheid EGFR en IGF-1R op het celoppervlak en bestonden uit de volgende tumortypen: hoofd-halsepitheel (14C), huidepitheel (A431), longepitheel (A549) en borst (MB-468). In alle vier de cellijnen resulteerde blootstelling aan de anti-EGFR/IGF-1R Nanokogels tot een blokkade van EGFR activering. Daarentegen zorgde behandeling met Nanokogels alleen voor een effectieve blokkade van IGF-1R activering in 14C en A431 cellen en niet in A549 en MB-468 cellen. Om de activering van IGF-1R te remmen dient de anti-IGF-1R kinase remmer AG538 afgeleverd te worden in de tumorcellen door de Nanokogel. Het is mogelijk dat de opname en verwerking van de Nanokogels door 14C en A431 cellen wel efficiënt verloopt, maar dat dit niet het geval is in A549 en MB-468 cellen en dat daardoor geen remmend effect van de kinase remmer kon worden waargenomen. Naast EGFR en IGF-1R, is ook bepaald wat de

gevolgen van behandeling met Nanokogels zijn voor de activering van twee eiwitten (Akt en ERK 1/2) die een belangrijke rol spelen in de groei en overleving van de onderzochte tumorcellijnen. Hieruit bleek dat alleen in 14C en A431 cellen, waarin Nanokogelblootstelling leidde tot remming van EGFR en IGF-1R, ook de activering van Akt en ERK 1/2 geremd werd. Tegelijkertijd zorgde Nanokogelbehandeling in A549 en MB-468 cellen alleen voor een blokkering van EGFR activering en niet voor een remming van Akt en ERK1/2 activering. Dit betekent dat in de vier onderzochte tumor cellijnen zowel EGFR als IGF-1R activering geblokkeerd moet worden om een efficiënte remming van groei en overlevingsignaalroutes te veroorzaken.
Dezelfde tumorcellijnen werden gebruikt om te bepalen of een behandeling met anti-EGFR/IGF-1R Nanokogels een effect had op de groei van de cellen in vitro. Het bleek dat de Nanokogels op een concentratie-afhankelijke manier de groei van zowel 14C als A431 cellen remde. Tegelijkertijd zorgde Nanobullet behandeling alleen voor een gedeeltelijk remmend effect in A549 en MB-468 cellen. De remming van celgroei veroorzaakt door behandeling met Nanokogels correleerde met het vermogen van het nanomedicijn om belangrijke cellulaire groei en overleving te blokkeren.
Tenslotte werden zowel humane 14C en MB-468 tumorcellen onderhuids in muizen aangebracht waarna tumoren zich ontwikkelden. Vervolgens werden de muizen systemisch behandeld met anti-EGFR/IGF1R Nanokogels om te onderzoeken of het anti-tumor effect in vivo correspondeerde met de effecten geobserveerd in de cellen. In het snel groeiende 14C model zorgde behandeling met Nanokogels voor een significante remming van tumorgroei in vergelijk met controle behandelingen. In het langzaam groeiende MB-468 model zorgde de behandeling met Nanokogels niet voor een significant anti-tumor effect in vergelijk met controle behandelingen.
Uit deze resultaten blijkt dat Nanokogel-geïnduceerde remming van cellulaire groei- en overlevingsignaalroutes in de onderzochte cellijnen voorspellend was voor het anti-tumor effect in vitro en in vivo.
De gezamenlijke resultaten uit **Hoofdstuk 3** en **Hoofdstuk 4** laten zien dat het mogelijk is om een AGNM te ontwikkelen voor het blokkeren van meerdere signaalroutes in tumorcellen en de daarmee gepaard gaande anti-tumor effecten. Het blijkt dat hoewel alle onderzochte cellijnen EGFR en IGF-1R op het oppervlak hebben, dit niet voorspellend is voor het anti-tumor effect veroorzaakt door de Nanobullets. Het kan zijn dat in de tumorcellijnen die een gemiddeld responsepatroon lieten zien, veranderingen in de genetische code van de cellen ervoor zorgen dat de behandeling met Nanokogels minder effectief is. Ook kan het zijn dat er naast EGFR en IGF-1R nog andere eiwitten op het oppervlak van de cellen bijdragen aan het aanzetten van groei- en overlevingsignaalroutes.
Een manier om de anti-tumor effecten van de Nanokogels te verbeteren is om de

hoeveelheid geladen kinase remmer AG538 te verhogen. Ook kan gekozen worden voor een multi-target kinase remmer zoals sunitinib of een ander soort geneesmiddel, zoals een chemotherapeuticum. Daarnaast kunnen ook nanobodies gebruikt worden die andere eiwitten op tumorcellen herkennen, zoals HER2.
Naast liposomen zijn er ook nog andere dragersystemen die benut kunnen worden voor het ontwikkelen van Nanokogels zoals nanodeeltjes gebaseerd op albumine of synthetische polymeren.
De ontwikkeling van Nanokogels voor de behandeling van kanker staat nog in de kinderschoenen. Desalniettemin worden de eerste nanobody-gebaseerde geneesmiddelen momenteel getest in klinische trials. Gecombineerd met de klinische trials met AGNM beschreven in **Hoofdstuk 2** zou dit kunnen leiden tot het toepassen van Nanokogels voor de behandeling van patiënten.

3. Anti-kanker therapie door het remmen van tumor-angiogenese

De transformatie van een gewone cel naar een kwaadaardige cel die zich ongecontroleerd blijft delen, leidt uiteindelijk tot de ontwikkeling van een kleine tumor. Als deze kleine tumoren verder willen groeien, dienen ze aan de toegenomen vraag van zuurstof en voedingstoffen te voldoen door de vorming van nieuwe bloedvaten vanuit bestaande vaten te stimuleren. Dit proces wordt angiogenese genoemd. Sinds de ontdekking dat angiogenese cruciaal is voor de ontwikkeling van solide tumoren, is het remmen van dit proces een aantrekkelijke strategie geworden voor een effectieve behandeling van kanker.
Wetenschappelijk onderzoek naar belangrijke signaalroutes en eiwitten in de *endotheel cellen (ECs)* verantwoordelijk voor angiogenese, heeft geleid tot de goedkeuring van een aantal angiogenese remmers in het afgelopen decennium. Deze remmers zijn vooral gericht op het blokkeren van *vascular endothelial growth factor (VEGF)*-geactiveerde cellulaire signaalroutes. Ondanks dat er meerdere angiogenese signaalroutes zijn ontrafeld in de laatste paar jaar, is de door tumorcellen uitgescheiden VEGF dat ECs activeert via de *VEGF-receptor (VEGFR)* één van de meest cruciale gebeurtenissen in tumor-angiogenese. Het blijkt echter dat therapie gericht op het remmen van VEGF-gestimuleerde signaalroutes bescheiden klinische resultaten oplevert. Net zoals in het geval van specifieke remmers van receptoreiwitten op tumorcellen, ontwikkelt een tumor ook resistentie tegen specifieke angiogenese remmers en kunnen tumoren uiteindelijk verder groeien. Het is zelfs zo dat anti-angiogenese therapie ervoor kan zorgen dat tumoren zich sneller verspreiden omdat het de omgeving van de primaire tumor minder gastvrij maakt. Er is daarom vraag naar innovatieve of combinatie strategieën die effectief tumor-angiogenese en eventuele tumorgroei en uitzaaiing (*metastasering*) effectiever remmen. In ECs, VEGF-gestimuleerde activering van VEGFR-2 kan leiden tot het aanzetten van de *Rho GTPase* signaal route. Rho

GTPases zijn kleine eiwitten die functioneren als kleine schakelaars in de cel. Ze zijn betrokken bij verschillende processen in de cel zoals transport van eiwitten door de cel, celbeweging en celdeling. In **Hoofdstuk 5** is de rol van Rho GTPases in tumor-angiogenese en invasiviteit beschreven. Rho GTPases zijn veelal onmisbaar voor processen in ECs die bijdragen aan angiogenese zoals doorlaatbaarheid van de bloedvatwand, afbraak van de extracellulaire matrix, celmigratie, celgroei en de vorming van het bloedvat. Verder is beschreven dat Rho eiwitten zijn betrokken bij tumorcel migratie, invasiviteit en uitzaaiing. Rho GTPases zijn dus een aantrekkelijk doelwit van processen in ECs en tumorcellen die bijdragen aan de ontwikkeling van de tumor. Strategieën die Rho GTPase signaalroutes remmen bestaan uit het gebruik van specifieke Rho eiwitremmers, het gebruik van statines en bisfosfonaten en *RNA interferentie (RNAi)*.

Een voorbeeld van een dergelijke methode is beschreven in **Hoofdstuk 6**, waarin de rol van de Rho GTPase *Rac1* in tumor-angiogenese en groei is onderzocht met een RNAi strategie.

Normaal gesproken wordt de genetische code van een cel (DNA) eerst overgeschreven (*transcriptie*) naar boodschapper RNA. Het boodschapper RNA verlaat de celkern waarna het vertaald (*translatie*) wordt in een functioneel eiwit. Bij RNAi wordt het de vertaling van boodschapper RNA naar functionele eiwitten geblokkeerd door kleine stukjes RNA (*siRNA*). RNAi wordt door cellen gebruikt als afweer tegen virussen, maar is ook een genregulatie mechanisme. Het proces kan worden gebruikt voor het remmen van de productie van praktisch ieder eiwit, door het introduceren van synthetische siRNA in een cel.

Het is beschreven dat Rac1 de voornaamste Rho GTPase is, betrokken bij VEGF-gemedieerde angiogenese en vormt daarom een interessant doelwit voor antikanker therapie. Effectieve remming van de Rac1 eiwitproductie (*knockdown*) in humane ECs kon worden bereikt door het introduceren van anti-Rac1 siRNA (*siRac1*). De knockdown van Rac1 in ECs zorgde ervoor dat de cellen minder goed in staat waren om VEGF-gestimuleerde processen te ondergaan die bijdragen aan angiogenese zoals het vormen van cellulaire uitlopers, celmigratie, celgroei en celinvasie *in vitro*. Behandeling met siRac1 remde de aanmaak van bloedvaten in muizen in vergelijking met controle siRNA (*siNS*) behandeling. Tenslotte resulteerde een behandeling van tumordragende muizen met intratumorale injecties van siRac1 tot een significant anti-tumoreffect in vergelijk met siNS controle behandelingen. Het bleek dat het remmen van de tumorgroei vooral werd veroorzaakt door verminderde tumor-angiogenese, en niet door het remmen van tumorcelgroei.

Recentelijk is beschreven dat Rho GTPases betrokken zijn bij het uitscheiden van kleine blaasjes (*microvesicles*) door tumorcellen, die een rol spelen in de communicatie en de uitwisseling van materiaal tussen cellen. Ook zijn Rho GTPases betrokken bij

de het faciliteren van het verhoogde metabolisme van tumorcellen wat nodig is voor de cellen om te groeien.
De grote hoeveelheid literatuur die laat zien dat afwijkende cellulaire Rho GTPase signalering betrokken is bij tumor-angiogenese en groei en de observaties in **Hoofdstuk 6** samen genomen, bevestigen dat het remmen van deze cellulaire schakelaars een rationele en attractieve strategie is voor een meer effectieve (combinatie) therapie voor de behandeling van kanker.

4. Conclusies

Momenteel blijft kanker de belangrijkste doodsoorzaak in de wereld. Intensief wetenschappelijk onderzoek heeft geleid tot de toevoeging van nanomedicijnen en selectieve remmers aan het arsenaal van antikankerstrategieën.
In dit proefschrift staan de resultaten beschreven van twee innovatieve methoden voor de behandeling van kanker. De eerste strategie omvat de ontwikkeling van een AGNM voor de directe remming van tumorcelgroei. De tweede strategie bestaat uit de remming van tumorgroei door een RNAi-gemedieerde obstructie van tumor-angiogenese.
In de eerste strategie is een anti-IGF-1R kinase remmer geladen in liposomen die zijn uitgerust met anti-EGFR nanobodies voor gerichte antikankercombinatietherapie. Behandeling met deze AGNM of Nanokogel zorgde voor een remming van EGFR en IGF-1R signalering in tumor cellen. Remming van cellulaire groei- en overlevingsignaalroutes in tumorcellen was voorspellend voor het anti-tumor effect van Nanokogel behandeling *in vitro* en *in vivo*. Een interessante uitdaging voor toekomstige studies met Nanokogels is het vinden van de meest effectieve AGNM samenstelling (dragersysteem, nanobody, geneesmiddel) voor de behandeling van een specifieke indicatie. In de toekomst zouden de combinaties van intrinsiek actieve targeting liganden en antikankergeneesmiddelen de basis kunnen vormen voor een persoonlijke antikankerbehandeling waaraan de specifieke moleculaire samenstelling van de tumor ten grondslag ligt.
In de tweede strategie is RNAi toegepast om de productie van een specifiek eiwit te remmen, dat essentieel is voor tumor-angiogenese. Knockdown van de Rho GTPase Rac1 verminderde het vermogen van humane ECs om zich te veranderen in een angiogene cel. Verder zorgde behandeling met siRac1 voor een remming van angiogenese en tumorgroei in muizen. De belangrijke rol van Rho GTPases in cellulaire processen die bijdragen aan de ontwikkeling van een tumor maakt deze cellulaire signaalroute tot een geldig doelwit om bestaande behandeling van kanker te verbeteren. Rho GTPases komen echter in iedere cel voor en zijn onmisbaar voor veel 'huishoud' functies. Het is zeer waarschijnlijk dat het gericht remmen van deze eiwitten alleen dient plaats te vinden in zieke weefsels. Een AGNM dat in staat is om

het anders inactieve siRNA, selectief af te leveren in doelcellen zou een enorme stap richting de klinische toepassing van RNAi zijn.
Dit proefschrift heeft waardevolle innovatieve strategieën beschreven voor het verbeteren van bestaande antikankertherapieën. Deze kennis, samen met de informatie van de eerste AGNM in klinische trials, data van gerichte aflevering van siRNA in mensen en meer kennis van mechanismen die ten grondslag liggen aan de ontwikkeling en voortschrijding van kanker, in combinatie met een verbeterde behandeling en diagnose, kan de basis vormen voor een toekomst waar bepaalde vormen van kanker niet langer worden beschouwd als een dodelijke maar chronische ziekte.

Appendices
Curriculum vitae

Curriculum Vitae

Roy van der Meel was born on June 24th 1984 in Sliedrecht, The Netherlands. After graduating from secondary school at the Johan de Witt Gymnasium in Dordrecht, he started the Bachelor's program Biomedical Sciences at Utrecht University in 2003. In 2006, he started the Master's program Drug Innovation at Utrecht University. During this Master's, he performed a 9-month research project under the supervision of Dr. Sabrina Oliveira and Dr. Raymond M. Schiffelers at the department of Pharmaceutics at Utrecht University, focusing on the development of targeted lipoplexes for inhibition of angiogenesis. After this, he performed a 9-month research project under the supervision of Dr. Raymond M. Schiffelers, Dr. Annette T. Byrne and Prof. Dr. William M. Gallagher at the UCD Conway Institute at University College Dublin, Ireland, during which he screened Rho GTPases as therapeutic targets for inhibition of angiogenesis. In 2009, Roy obtained his Master's degree *cum laude* and started a PhD project at the department of Pharmaceutics at Utrecht University supervised by Prof. Dr. Gert Storm, Prof. Dr. Wim E. Hennink, Dr. Robbert J. Kok and Dr. Raymond M. Schiffelers. During his work as a PhD candidate, Roy explored several targeted strategies to inhibit tumor growth and angiogenesis for the treatment of cancer of which the results are presented in this thesis.

Appendices
List of publications

List of publications from this thesis

R. van der Meel[*], L.J.C. Vehmeijer[*], R.J. Kok, G. Storm, E.V.B. van Gaal. Actively-targeted nanomedicines in the clinic: current status. *Submitted for publication*
[*] *These authors contributed equally to this work*

R. van der Meel, S. Oliveira, I. Altintaş, R. Heukers, E.H.E Pieters, P.M.P. van Bergen en Henegouwen, G. Storm, W.E. Hennink, R.J. Kok, R.M. Schiffelers. Inhibition of cell survival pathways *in vitro* by targeted anti-EGFR/IGF-1R Nanobullets predicts anti-tumor efficacy. *Submitted for publication*

R. van der Meel, S. Oliveira, I. Altintaş, R. Haselberg, J. van der Veeken, R.C. Roovers, P.M.P. van Bergen en Henegouwen, G. Storm, W.E. Hennink, R.M. Schiffelers, R.J. Kok. Tumor-targeted Nanobullets: Anti-EGFR nanobody-liposomes loaded with anti-IGF-1R kinase inhibitor for cancer treatment. J Control Release. 2012 Apr 30;159(2):281-289

P. Vader[*], **R. van der Meel**[*], M.H. Symons, M.H.A.M Fens, E.H.E. Pieters, K.J. Wilschut, G. Storm, M. Jarzabek, W.M. Gallagher, R.M. Schiffelers, A.T. Byrne. Examining the role of Rac1 in tumor angiogenesis and growth: a clinically relevant RNAi-mediated approach. Angiogenesis. 2011 Dec;14(4):457-466
[*] *These authors contributed equally to this work*

R. van der Meel, M.H. Symons, R. Kudernatsch, R.J. Kok, R.M. Schiffelers, G. Storm, W.M. Gallagher, A.T. Byrne. The VEGF/Rho GTPase signalling pathway: A promising target for anti-angiogenic/anti-invasion therapy. Drug Discov Today. 2011 Mar;16(5-6):219-228.

Other publications

I. Altintaş, M. Roest, E. Al-Awwadi, L. Novo, **R. van der Meel**, L. van Bloois, W.E. Hennink, T.C. van Holten, R.J. Kok, R.M. Schiffelers. Evaluation of the haemocompatibility of nanoparticulate systems by platelet activation assays. *Manuscript in preparation*

I. Altintaş, R. Heukers, **R. van der Meel**, M. Lacombe, M. Amidi, P.M.P van Bergen en Henegouwen, W.E. Hennink, R.M. Schiffelers, R.J. Kok. Nanobody-albumin nanoparticles (NANAPs) for the delivery of a multikinase inhibitor 17864 to EGFR overexpressing tumor cells. J Control Release. 2012 Nov 16;165(2):110-118

P. Vader, B.J. Crielaard, S.M. van Dommelen, **R. van der Meel**, G. Storm, R.M. Schiffelers. Targeted Delivery of small interfering RNA to angiogenic endothelial cells with liposome-polycation-DAN particles. J Control Release. 2012 Jun 10; 160(2):211-216

M. Talelli, C.J. Rijcken, S. Oliveira, **R. van der Meel**, P.M. van Bergen en Henegouwen, T. Lammers, C.F. van Nostrum, G. Storm. W. E. Hennink. Nanobody-shell functionalized thermosensitive core-crosslinked polymeric micelles for active drug targeting. J Control Release. 2011 Apr 30;151(2):183-92.

S. Oliveira, R.M. Schiffelers, J. van der Veeken, **R. van der Meel**, R. Vongpromek, P.M.P. van Bergen en Henegouwen, G. Storm, R.C. Roovers. Downregulation of EGFR by a novel multivalent nanobody-liposome platform. J Control Release. 2010 Jul 14;145(2):165-175.

R. van der Meel, W.M. Gallagher, S. Oliveira, A.E. O'Connor, R.M. Schiffelers, A.T. Byrne. Recent advances in molecular imaging biomarkers in cancer: application of bench to bedside technologies. Drug Discov Today. 2010 Feb;15(3-4):102-114.

N. de Jonge, M.J. Goumans, D. Lips, R. Hassink, E.J. Vlug, **R. van der Meel**, C.D. Emmerson, J. Nijman, L. de Windt, P.A. Doevendans. Controlling cardiomycocyte survival. Novartis Found Symp. 2006;274:41-51; discussion 51-57, 152-155, 272-276

Selected abstracts

R. van der Meel, S. Oliveira, I. Altintaş, R. Haselberg, J. van der Veeken, R.C. Roovers, P.M.P. van Bergen en Henegouwen, G. Storm, W.E. Hennink, R.M. Schiffelers, R.J. Kok. Tumor-targeted Nanobullets for Anti-Cancer Combination Therapy. Poster presentation at the 24th EORTC-NCI-AACR Symposium on Molecular Targets and Cancer Therapeutics, Dublin, Ireland, November 2012.

R. van der Meel, S. Oliveira, I. Altintaş, R. Haselberg, J. van der Veeken, R.C. Roovers, P.M.P. van Bergen en Henegouwen, G. Storm, W.E. Hennink, R.M. Schiffelers, R.J. Kok. Nanobullets: A tumor-targeted Nanomedicine for Anti-Cancer Combination Therapy. Poster presentation at the Meeting of the Belgian-Dutch Biopharmaceutical Society, Utrecht, The Netherlands, November 2012.

R. van der Meel, S. Oliveira, I. Altintaş, R. Haselberg, J. van der Veeken, R.C. Roovers, P.M.P. van Bergen en Henegouwen, G. Storm, W.E. Hennink, R.M. Schiffelers, R.J. Kok. Tumor-targeted Nanobullets: Anti-EGFR nanobody-liposomes loaded with anti-IGF-1R kinase inhibitor for cancer treatment. Oral presentation at the 6th Nanomedicine in Oncology Workshop, Berder Island, France, September 2012

R. van der Meel, S. Oliveira, I. Altintaş, R. Haselberg, J. van der Veeken, R.C. Roovers, P.M.P. van Bergen en Henegouwen, G. Storm, W.E. Hennink, R.M. Schiffelers, R.J. Kok. Tumor-targeted Nanobullets: Anti-EGFR nanobody-liposomes loaded with anti-IGF-1R kinase inhibitor for cancer treatment. Poster presentation at the 39th Annual Meeting & Exposition of the Controlled Release Society, Québec City, Canada, July 2012

R. van der Meel, S. Oliveira, I. Altintaş, R. Haselberg, J. van der Veeken, R.C. Roovers, P.M.P. van Bergen en Henegouwen, G. Storm, W.E. Hennink, R.M. Schiffelers, R.J. Kok. Tumor-targeted Nanobullets: Anti-EGFR nanobody-liposomes loaded with anti-IGF-1R kinase inhibitor for cancer treatment. Poster presentation at the 13th FIGON Dutch Medicine Days, Lunteren, The Netherlands, October 2011

P. Vader, **R. van der Meel**, M.H. Symons , M.H.A.M Fens, E. Pieters, K.J. Wilschut, G. Storm, W.M. Gallagher, R.M. Schiffelers, A.T. Byrne. RNA Interference-mediated silencing of Rac1 inhibits angiogenesis and tumor growth. Poster presentation at the 4th International Meeting on Angiogenesis, Amsterdam, The Netherlands, March 2011

R. van der Meel, S. Oliveira, J. van der Veeken, R.C. Roovers, P.M.P. van Bergen en Henegouwen, G. Storm, R.J. Kok, R.M. Schiffelers. Kinase-inhibitor loaded nanobody coupled liposomes for cancer treatment. Poster presentation at the 1st Symposium on Single Domain Antibodies, Ghent, Belgium, October 2010

R. van der Meel, S. Oliveira, J. van der Veeken, R.C. Roovers, P.M.P. van Bergen en Henegouwen, G. Storm, R.J. Kok, R.M. Schiffelers. Nanobody coupled liposomes for downregulation of EGFR. Oral presentation at the 20th Mountain/Sea Liposome Workshop, Ameland, The Netherlands, September 2009

Appendices
Dankwoord / Acknowledgements

"Slowly walking down the hall, faster than a cannonball."

Oasis - Champagne Supernova, 1996

All good things come to an end and so does my PhD project. It's amazing how fast four years can pass. The completion of this thesis wouldn't have been possible without the support of some great people that I've met over the years. I've made an attempt to thank all of you here but please keep in mind that my gratitude reaches far beyond these few words on paper.

I was very lucky to have a supervising team consisting of four extraordinary people with their own specific expertises and input. Thank all of you that I could always walk into your office when I had a question or needed advice.

Beste Wim, geachte promotor, ik heb bijzonder veel respect voor jou. Je werkt ongelooflijk hard, bent altijd recht voor z'n raap, bent voetballiefhebber en lust graag een sappie op z'n tijd. Kortom: alle kenmerken van een Feyenoord supporter :-) (bedankt voor m'n nieuwe mok!). Ontzettend bedankt voor alle nuttige discussies tijdens werkbesprekingen en het kritisch doornemen van alle manuscripten. Ook bedankt voor het lachen tijdens alle borrels, de CRS en natuurlijk voor de filosofie lessen op vrijdagmiddag.

Beste Gert, geachte promotor, hoewel je minder betrokken was bij de dagelijkse begeleiding heb je zeker voor een belangrijk deel bijgedragen aan dit proefschrift. Bedankt voor het doornemen van alle artikelen, je hulpvolle suggesties bij het schrijven en die Snelle Jelles tijdens het werk 's avonds.

Beste Ray, geachte co-promotor, je loopt als een rode draad door mijn pas korte carrière. Eerst als stagebegeleider, toen als co-promotor en nu als baas. Bedankt voor je positieve kijk op ieder resultaat, je enthousiasme, waardevolle suggesties, alle hulp bij het schrijven en natuurlijk je gezelligheid. Ik waardeer enorm alle kansen die je me hebt gegeven en hoop dat we nog lang blijven samenwerken.

Beste Robbert Jan, geachte co-promotor, ondanks dat je het zowel thuis als op het werk ontzettend druk hebt, maakte je tijd voor mij als dat nodig was. Ik ben het vaakst jouw kamer ingelopen als ik hulp of advies nodig had. Dankjewel voor je suggesties tijdens werkbesprekingen en het opzetten van experimenten.

In addition to my daily supervisors, I was fortunate to collaborate with great people from the Netherlands and abroad without whom this thesis could have not have been realized. Thank you all for your helpful input and good times in and outside the lab!

Dear Annette, I consider you as my third co-promotor and I want to thank you for giving me the chance to study in Dublin for a year. It was a great experience for me both inside and outside the lab (sláinte)! I am very happy we continued our collaboration when I started my PhD project. Our joint efforts have resulted in three scientific publications, of which two have been included as a chapter in this thesis. In regard to this work, I would also like to thank Prof. Liam Gallagher from the Cancer Biology and Therapeutics Lab at University College Dublin and Dr. Marc Symons from the Feinstein Institute for Medical Research.

Dear Sabrina, I remember when I first walked in Z-513 as a bachelor student to do a short internship with you. I can't believe we are now seven years and five joint scientific publications later. Thank you for your patience, guidance and all the fun ouside the lab! I wish you all the best and hope we maintain our collaboration and friendship for a long time. Obrigado por tudo!

Beste Paul, dankjewel voor jouw biologische insteek in het Nanobullet project. Ik heb jouw suggesties en commentaar op alle manuscripten maar ook onze fijne gesprekken over het skiën erg op prijs gesteld!

Dear Rob H., Laurens, Rob R., Joris and Robert, thank you for your valuable contributions. Without you this thesis would have been much thinner!

A PhD student without paranymphs is like drinking beer while sitting on a wonky barstool: it's a lot easier with the proper support…

Dear Işil, you started your project half a year after me and when we moved from the Went to the DDW we really started working together. I'm really happy that you are the second Nanobullet PhD student in the department! I have great respect for you as a person and how you paved your own path during this project. It is not always easy to have so many supervisors with different suggestions…Thank you for all your help, advice, suggestions during meetings and of course all the fun we had outside of work! I wish you the best of the luck the coming few months and before you know it it's October! You're a good friend and I'm very happy you're my paranymph!

Beste Jim, ik ben heel erg blij dat jij ook in Utrecht woont! Ondanks dat jij het de afgelopen jaren druk had met afstuderen, een baan zoeken en natuurlijk Gabrielle, bleef er genoeg tijd over om een happie of sappies (het blijft er nooit bij eentje) te doen. Ik was waarschijnlijk al lang opgehouden met voetballen in Papendrecht als wij niet bijna elke week samen een treintje zouden pakken. Bedankt voor alle hilarische

weekendjes met de boys, het voetbalteam en met pa, en alle gezellige avondjes met de meiden erbij. Dankjewel dat je zo'n goede broer en vriend bent, en dat ik altijd op je kan rekenen (zelfs als ik verdwaald ben). Ik ben ontzettend trots en blij dat jij mijn paranimf bent! Gabrielle, dankjewel voor al jouw gezelligheid, dat we altijd de auto kunnen lenen en dat je het beste in Jim naar boven haalt!

Dear fellow Nanobullet colleagues, Işil, Raimond and Remko, cheers for the help and collaboration in the lab and the nice dinners and drinks outside the lab. Good luck finishing your theses!

One of the reasons why the last four years have flown by is the great working environment at Biopharmacy. I want to thank all of you for your help in the lab and the good times during borrels, BBQ's, lab days, X-mas dinners and conferences!

First of all, I would have been lost without the support of Biopharmacy's well respected technicians. These people are always there to help you out regardless if you cause infections in the cell culture lab, paint a lab black by nearly blowing up an autoclave, ruin a high speed centrifuge rotor, forget to remove covers of plates when measuring on the plate reader or perform other random acts of stupidity...Ik heb waarschijnlijk nergens zo veel tijd doorgebracht als in het celkweek lab en ben daarom veel dank verschuldigd aan alle bazen van de ML-II: Roel (ouwe köttbullar), later Kim, en tenslotte Joep. Op een goede tweede plek qua tijdsbesteding komen de dierenstallen in het Went. Ebel, ontzettend bedankt voor alle hulp, flexibiliteit en input bij alle *in vivo* experimenten. Zonder jou waren deze nooit mogelijk geweest. Ik wil ook graag Willemiek, Hans Sturkenboom en alle andere mensen die hebben meegeholpen bij deze experimenten bedanken. Louis, bedankt voor alle hulp en advies bij het bereiden van liposomen. Mies, bedankt voor de introductie in de wondere wereld van de HPLC, en voor een onvergetelijke labdag. Jij bent de meest sexy breteldrager in een kano!

De eerste twee jaar van mijn promotie onderzoek heeft zich afgespeeld in het legendarische lab Z-513 in het Went gebouw. Mijn labmaatjes daar zorgden voor zo'n fijne werksfeer dat die eerste twee jaar omvlogen waarna we verhuisden naar het DDW.

Lieve Emmy, als labmanager was jij verantwoordelijk voor alles wat er in Z-513 gebeurde en die rol heb jij met verve vervuld. Vanwege uiteenlopende projecten hebben we niet veel samengewerkt maar we hadden genoeg gemene delers (kinase remmers, co-promotor) om te bespreken onder het genot van een bakkie. Buiten

het lab hebben we heel veel gelachen! En als jij begint met lachen is er geen houden meer aan…Bedankt voor alle gezelligheid tijdens borrels, etentjes, Koninginnedagen, voetbal kijken en nog veel meer. Nooit gedacht dat professionele party starters in zo'n formaat kwamen. Ik ben blij dat je nog regelmatig bij Biofarmacie over de vloer komt want die grote blauwe kijkers zorgen altijd voor een lach op m'n gezicht. Wanneer gaan we Pieter en Stella in Oxford bezoeken?

Pieter, fijne gozer, jij bent een van de redenen waarom mijn project een vliegende start had. Ondanks dat we nogal van elkaar verschillen, vulden we elkaar prima aan en hadden we een uitstekende samenwerking. Ray zei na afloop van jouw promotie over ons: "Wie had ooit gedacht dat de meest onwaarschijnlijke combinatie zo'n synergistisch effect kon hebben?" Ik heb veel van je opgestoken, zowel in het lab als persoonlijk. Je blijft altijd rustig, ziet van ieder resultaat de positieve kant (hoewel dat een aantal keer flink op de proef is gesteld) en je houdt van aanpakken. Ik ben erg trots dat ik jou paranimf mocht zijn en heel erg blij dat ik erbij was toen Stella en jij jullie eeuwige liefde aan elkaar verklaarden! Het zou zo maar kunnen dat we binnenkort weer samenwerken en ik kijk er nu al naar uit. Dankjewel voor alle hulp en je vriendschap!

I had the chance to supervise a few highly motivated master students. Dear Shima, Marius and Amr, I learned a lot from supervising you and I hope you learned a lot from me too. More importantly, I hope you had fun during the internship and it has made you decide to stay in research. Thank you for your help!

Beste Karlijn en Marcel, naast een fijne samenwerking in het lab met als resultaat een prima paper, hebben jullie ons ook buiten het werk veel geholpen. Bedankt voor de trip naar Dublin voordat ik daar een jaar ging studeren, en alle hulp bij de verhuizing zodat we van jullie nestje ons nestje konden maken!

Dear Maria and Bart, thank you for help in the lab in the lab whenever I had liposome or *in vivo* study questions. Also thank you for all the nice discussions and talks we had while enjoying a drink or two. I want to thank you the most for letting us stay with you in NYC last summer even though you had just moved in one week earlier. I had the best time and laughed so much while exploring the city, enjoying the sunshine, having drinks and ending up in karaoke bars. I'm really glad I got to know you and I'm sure we'll see each other again!

Beste Markus, onze projecten zijn zeer verschillend maar toch hebben we elkaar soms kunnen assisteren in de celkweek of bij het WBen. Ik denk dat wij op een

vergelijkbare manier tegen onze PhD projecten en het onderzoek aankijken. Je bent een ontzettend goede gast en ik heb bewondering voor hoe jij je doel om een postdoc positie te bemachtigen nagestreefd en bereikt hebt. Dankjewel voor alle gezelligheid tijdens de ontelbare keren dat wij een sappie genuttigd hebben. Nog veel meer bedankt voor de onvergetelijke trip afgelopen zomer! Naast dat er gewerkt moest worden op de CRS, heb ik verschrikkelijk veel gelachen tijdens onze uitstapjes in Quebec City en NYC. Ik wens je veel succes met het afmaken van je boekje en een hele mooie dag in september met jouw Claire. We zien elkaar aan de andere kant van de plas!

Thank you to everyone who started in 2009: Işil, Markus, Afrouz, Negar, Erik T., Audrey, Filis, Luis, Sylvia, Peter, Grzegorz, Neda, and Kimberly. Good luck finishing up!
Thank you to all the people that showed how to succesfully defend a thesis: Hajar, Marina, Pieter, Emmy, Amir G(azelle), Bart, Maria, Inge, Amir V. (cheers for choosing me as your paranymph!), Marcel, Karlijn, Joris, Ellen, Ethlinn, Rolf, Niels, Joost, Albert G., Stefan, Maarten, Twan, Frank, Roberta, Melody and Laura.
Thank you to those who started more recently: Kristel, Merel, Burçin, Forever Yang, Sima, Mazda, Shima, Farshad, Erik O., Anna, Louann, Yinan, Dandan, Reka, Iris, Mohadeseh, Mernoosh, Susan, Sander and Andhyk.
Thank you to the boys and girls at Cristal Delivery: Cristianne, Ethlinn (cheers for the nice collaboration on the review!), Anne, Paul, Martin, Gert and Rachel.
And thank you to all the others: Steffen, Enrico, Herre, René, Huub, Herman, Daan, Maryam, Vera, Eduardo, Anastasia, Meriem, Abdul, Naushad, Georgi, Sytze, Niels, Jos, Fransisco (huevo suave), Tina, Oil, Orn, Francesca, Kohei, de dames en heren van het onderwijs, Barbara, Lidija and Frits.

Peter en Sert, bedankt voor alle praktische hulp en het gedogen van alle Biofarmacie borrels en BBQ's.

I'd like to thank all the sponsors, whose kind contributions have made printing of this thesis possible.

My elevated PhD project-induced stress levels were fortunately often and effectively reduced by trained professionals during social gatherings in the Netherlands and abroad. Cheers to all of you who I raised a glass with during the last four years, you know who you are!

Eén illuster gezelschap heren wil ik in het bijzonder bedanken. Beste Ed, Frits, Mario,

Jordi, Wes en Joep oftewel de RN, ondanks dat we inmiddels wat meer verspreid wonen en het ontzettend druk hebben met allerlei andere dingen, is het één groot feest als wij bij elkaar komen. Dankzij jullie was het niet moeilijk om het onderzoek soms even compleet uit m'n hoofd te zetten en te ontspannen. Ontzettend bedankt voor de gezelligheid, het vele lachen, het oprapen en de vloeibare weekenden in uithoeken van Nederland! Natuurlijk gaat mijn dank ook uit naar jullie meiden! Joep, een hele dikke dankjewel voor het ontwerpen van de cover! Loot, dankjewel voor het kritisch doorlezen van de NL samenvatting.

Elf jaar geleden hadden een aantal mensen (waaronder ik) het briljante idee om een vriendenteam op te richten. Er zijn nog weinig spelers van het originele team over maar Drechtstreek 5 is een begrip binnen de club vanwege het voetbal en vooral vanwege de gezelligheid. Iets om trots op te zijn. Mannen, bedankt voor alle dingen die we samen hebben meegemaakt tijdens wedstrijden, de derde helft, toernooien, weekenden weg en bruiloften! En hou op met mij wodka te voeren…

Ook de beste mannen van Voorwaarts 4 wil ik graag bedanken voor hun gezelligheid en voor het tolereren van mijn onnuttige geschreeuw.

Finally I'd like to thank my family. Because of them I've been able to take advantage of every opportunity that crossed my path!

Lieve tante Coby, toen ik begon met het onderzoek vond ik het vooral heel interessant. Dankzij jou heeft het een diepere betekenis gekregen. Tot ooit.

Liebe Irene, dankeschön fe ois wos du de letztn 5 johr fe de Anna und fe mi tu host. Jeds moi boid ma zu dia kemman, is wia hoam kemma! Danke fe de supa nette Zeit, egal ob Weihnachtn, Silvesta, Fosching, Toifest, fes guade Essn und Gedränke (Schnapsä), schifohn gea und dass i iaz - dank dia - wia a „Meister" Plafonds roin ku! Bleib so wia du bist und i hob di lieb! Liebe Theresa, liebe Eva und lieber Niels, dass Österreich a zwoate Heimat is, kimb a durch ench. I mecht ench a bedankn fe encha Unterstützung und bearige Zeit a de letztn poor Johr! I hob ench lieb!

Lieve Ma en Kees, dat woorden niet kunnen beschrijven hoe dankbaar ik ben is vooral op jullie van toepassing. Heel erg bedankt dat wij het eerste jaar bij jullie mochten wonen en voor alle support tijdens en na de verhuizing naar Utrecht. Ook nadat we in Utrecht woonden stonden jullie voor ons klaar als dat nodig was. Bedankt voor alle gezellige avondjes, babysitten van de kat en de afgelopen keer dat we naar Oostenrijk zijn gegaan. Sorry dat het zo laat werd die laatste avond… Ma,

dankjewel dat ik je altijd kan bellen als er iets is en dat ik nog steeds mag blijven slapen als de voetbal zaterdag iets te gezellig wordt…Kees, dankjewel dat Anna zich door jou meteen thuis voelde en voor het doen van ontelbare klusjes. Sorry dat we door de douchebak heen zijn gezakt…Ik hou van jullie!

Lieve Pa en Dimphy, dankjulliewel voor alle hulp en steun de afgelopen jaren. Jullie hebben ook flink bijgedragen aan onze verhuizing naar Utrecht. Dimph, dankjewel voor alle etentjes en borrels onder de rivier die steevast gezellig waren! Pa, vanwege jouw werk begrijp jij waarschijnlijk het best van iedereen wat ik de afgelopen jaren heb gedaan. Ik hoop dat je trots bent! Samen naar Oostenrijk rijden om te skiën en het weekend in Barcelona met Jim zijn dingen die ik nooit meer vergeet. Doe het een beetje rustig aan zodat we dat soort dingen nog vaker kunnen doen. Dankjewel dat ook jij er altijd voor mij bent als het nodig is. Ik hou van jullie!

Mei liabste Anna, I glab du hedst da nia denkt, dass es so lafn wead wias iatz is, wia mia ins vua meara wia fünf Johr kenna gleant hom… du host dei Lem mid deina Familie und mid deine Freunde in Österreich aufgem und bist mid mia noch Hollond zochn. I hob greasstn Respekt wia schnö du di eigleb host im Kaskopflond. A wenns ned oewei leicht gwesn is, bin i echt frua, dasst miatkemma bist nach Holland. Des beste vo mein Tog is Hoamkemma zu dia und realisian, dass i pures Glück mid dia hob. I ku ma a Lem ohne di echt ned vuastön, und kus kam dawortn, dass ma insa naxts Abenteuer midanond dalem. I lieb di mid mein gonzn Herzn x!